Final Technical Report

Award number:
DE-SC0018142

Awarding Institution:
The City College of New York (CCNY) at the City University of New York (CUNY)

Project Title:
Accelerating Biomimetic Solar - Energy Harvesting: Mapping the Interaction Landscape of Plasmonic-Excitonic Hybrid Nanosystems

Project Period Dates:
09/15/2017 – 09/14/2021

PI's Name:
Dorthe M. Eisele
Assistant Professor

Executive Summary.

In general, excitonic and plasmonic nanoscale materials in close proximity show high potential for significant breakthroughs in energy related materials research. The interactions between these two kinds of materials result in coupled optical transitions (plexcitons), distinct from those of both the individual exciton and plasmon as well as from those of the sum of their constituents (synergistic effects). By linking together materials-research and physical-research approaches, this project contributes to a concerted approach on nanomaterials energy research. The project's overall goal is to accelerate the development of well-defined plexcitonic model systems consisting of carefully engineered plasmonic and excitonic nanomaterial— essential for both gaining a fundamental understanding of plexcitonic nanomaterials and the development of novel design principles for biomimetic solar energy harvesting. During the 3-year project period and the terminal renewal with limited support for a 12-month period, we successfully synthesized and characterized (1) a robust excitonic nanomaterial and (2) a library of plasmonic nanoparticles as well as developed (3) a microfluidic platform for homogenous nanosynthesis as summarized below:

(1) Robust Excitonic Nanomaterial. Supramolecular assemblies are Nature's most successful material system for solar energy harvesting. However, photovoltaic devices based on artificial supramolecular assemblies continue to be stymied by disappointing efficiencies and poor stability. The conceptual failure may lie in current solar cell architectures, which rely on solidifying supramolecular assemblies as an ensemble into a solid matrix, neglecting the intrinsic fragility of the assemblies' internal structure, thus disrupting or even destroying their delicate optoelectronic properties, that is, delicate Frenkel excitonic properties. Supramolecular assemblies may finally serve as usable light harvesting material systems for solar energy conversion technologies, only if they meet the following criteria: (a) Stability, that is, the fragile structure including its delicate Frenkel excitonic character needs to be stable, (b) Robustness, that is, resistant against elevated and fluctuating temperatures, and (c) Viability for device integration, that is, capable of being immobilized onto solid substrates. Here, by developing a nanocomposite via a tunable, cage-like scaffold design, we successfully provided stable supramolecular nanocomposites, that inhabit robust Frenkel excitons despite harming environmental conditions such as extreme heat stress.

(2) Library of Plasmonic Nanoparticles. Naturally, current models describing plasmonic hybrid quantum states—plasmonic hybridizations—parallel those developed for molecular orbitals, equating individual plasmonic nanostructures with "*atoms*" and the plasmonic nanoassemblies with "*molecules*." In analogy to organic synthesis, a suitably robust fabrication method would allow for "*atom-like*" manipulation of "*molecule-like*" plasmonic nanoassemblies; of high value for next-generation energy nanotechnologies. Despite this frequent comparison, current plasmonic nanoassembly fabrication methods favor top-down templating over wet-chemical synthesis, however, achieving precise control over nanostructure's geometry and surface characteristics remain an art and a scientific challenge. The conceptual failure may lie in the current wet-chemical synthesis paradigm, as it relies on the accessibility of a *multi-dimensional* synthesis parameter space through limited, rather *one-dimensional* synthesis procedures by employing step-by-step approaches. Solution-based nanoarchitectonics for rational design of precisely built plasmonic nanoassemblies via solution-based fabrication may finally be possible only if *multi-dimensional* syntheses approaches are available that allow for comprehensive control over the plasmonic nanomaterials' (a) Structural Properties and (b) Surface Properties. Here, by developing an innovative multidimensional 1,3-propanediol based polyol synthesis, we successfully provided control over the plasmonic building-block's geometry (size and shape) together with its surface characteristics. Our results present a critical step toward the vision of a "*periodic table-like*" system for plasmonic materials based on straightforward wet-chemical syntheses for energy nanotechnologies. Developing deliberate modifications on this synthesis, we generated a library of plasmonic nanostructures covering the vast parameter space—opening the door for fundamental investigation of plexcitonic model systems.

(3) *Microfluidic Platform for Homogenous Nanosynthesis.* Control over structural properties of plexcitonic nanocomposites remains a challenge due to current limitations in nanosynthesis techniques. Slight variations in nanostructure's geometry impact their optoelectronic properties, demanding precise synthesis beyond the capabilities of solution-based (batch) synthesis processes. In contrast, the small, confined liquid volumes used in microfluidics—a reaction technique where the manipulation of fluids takes place in channels with dimensions of tens of micrometers—allows for homogenous synthesis conditions, providing excellent control of the reaction and, as a result, of the materials' geopmetry and composition. However, thus far, the majority of plexcitonic systems has been developed via batch synthesis. Here, by successfully developing a two-channel microreactor, our microfluidic-supported synthesis approach combines the advantages of both microfluidics and batch platforms, allowing for precise spatio-temporal control over all synthesis parameters opening the possibility for homogenous nanosythnesis of well-defined plexcitonic model systems.

Accepted Manuscripts.

The 3-year project period and the terminal renewal with limited support for a 12-month period allowed for an orderly conclusion of the project to completion and publication. For the terminal renewal, the requested funding supported postdoctoral researcher Dr. Nikunjkumar Visaveliya, who completed the proposed

(i) microfluidics device design and fabrication as well as

(ii) development of microfluidic synthesis procedures for size and shape controlled nanostructures.

Products in peer reviewed journals: 2

***** *indicates Corresponding Authorship*
[+] *indicates PhD candidates*
[UG] *indicates Undergraduate (UG) Researchers*

DOE-CCNY1

Visaveliya, N.R., St. Peter [UG], L., Leo [UG], K., Khatoon [UG], F., Xu [UG], J., Chan [UG], C., Mikhailova [UG], T., Bedzeti [UG], V., Kapadia [UG], A., Carbery, W.P., Ng[+], K., and Eisele*, D.M. *"Microfluidic-Supported Synthesis of Anisotropic Polyvinyl Methacrylate Nanoparticles via Interfacial Agents."*

***ACS Polymer Chemistry* (2022) 13, 4625.** [IF 5.58]

- *Cover Article.*
- *Paper has been selected as the 'Best Paper of the Month' in Polymer Chemistry (August 2022).*

DOE-QUEENS1

Ng[+], K. , Webster[+], M., Carbery, W.P., Visaveliya, N., Gaikwad[+], P., Jang, S., Kretzschmar, I., and Eisele*, D.M. *"Robust Frenkel excitons in heat stressed supramolecular nanocomposites enabled by tunable cage-like scaffolding."*

***Nature Chemistry* (2020) 12, 1157-1164.** [IF 24.27]

(first submission July 2019; published in November 2020)

- *CCNY'S PRESS RELEASE available online*

Patents: none

Acknowledgment of Federal Support and Disclaimer.

This work was prepared as an account of work sponsored by an agency of the United States Government. Neither the United States Government nor any agency thereof, nor any of their employees, nor any of their contractors, subcontractors or their employees, makes any warranty, express or implied, or assumes any legal liability or responsibility for the accuracy, completeness, or any third partys use or the results of such use of any information, apparatus, product, or process disclosed, or represents that its use would not infringe privately owned rights. Reference herein to any specific commercial product, process, or service by trade name, trademark, manufacturer, or otherwise, does not necessarily constitute or imply its endorsement, recommendation, or favoring by the United States Government or any agency thereof or its contractors or subcontractors. The views and opinions of authors expressed herein do not necessarily state or reflect those of the United States Government or any agency thereof, its contractors or subcontractors.

Project Overview and Objectives.

Excitonic and plasmonic nanoscale systems in close proximity show high potential for significant breakthroughs in materials research. The interactions between these two kinds of nanostructures result in coupled optical transitions (plexcitons) having novel properties distinct from those of both excitons and plasmons. Among these properties, particularly promising are plasmonic enhancement of excitonic transitions, tunability of resonance energies at plasmonic hot spots for photocatalysis, and enforced directionality of excitation energy transport. The pivotal next step for exploiting the full potential of these promising hybrid materials is to gain a fundamental understanding of their complex plexcitonic properties.

Overall, the proposed research aims to contribute to a basic understanding of plasmon-exciton interactions in nanoscale systems. Such understanding is essential to enable the controlled tuning of the hybrid system's optoelectronic properties. Such principles may lead to new technologies, such as photovoltaic and photocatalytic devices with improved functionality, utilizing unique characteristics of coupled plasmon-exciton systems, such as excitation enhancement effects, directed and enhanced energy transport, and enforced interfacial charge extraction. This project aims to contribute towards the vision to devise new design principles for solar energy harvesting materials – and beyond.

In contrast to recent research efforts, this project aims for a concerted treatment of hybrid nanosystems by bringing together both *Materials Research* and *Physical Research* approaches; by uniting *Synthesis*, *Experimental Investigation*, and *Theoretical Modeling* of well-defined plasmonic-excitonic model systems. These three phases provide an iterative workflow to zero in on the most fundamental relationships between the nanomaterial's composition and its optoelectronic properties:

PHASE I: *iteratively refine synthetic methods to synthesize well-defined model system;*

PHASE II: *experimental characterization and analysis;*

PHASE III: *fundamental theoretical understanding of plasmon-exciton interactions.*

While taking a distinct approach to the material synthesis, our research builds upon the classic *Plasmon-centric assembly Approach* (**Figure 1A**). The major goal of Project PHASE I has been to develop a *Nanoconjugation Approach* (**Figure 1B**) for the synthesis of Hybrid Plexcitonic Model Systems: both components—the excitonic system and the plasmonic system—are treated on an even footing: in solution, the two components are synthesized separately, then functionalized by a spacer material and finally electrostatically linked with one another (**Figure 1C**).

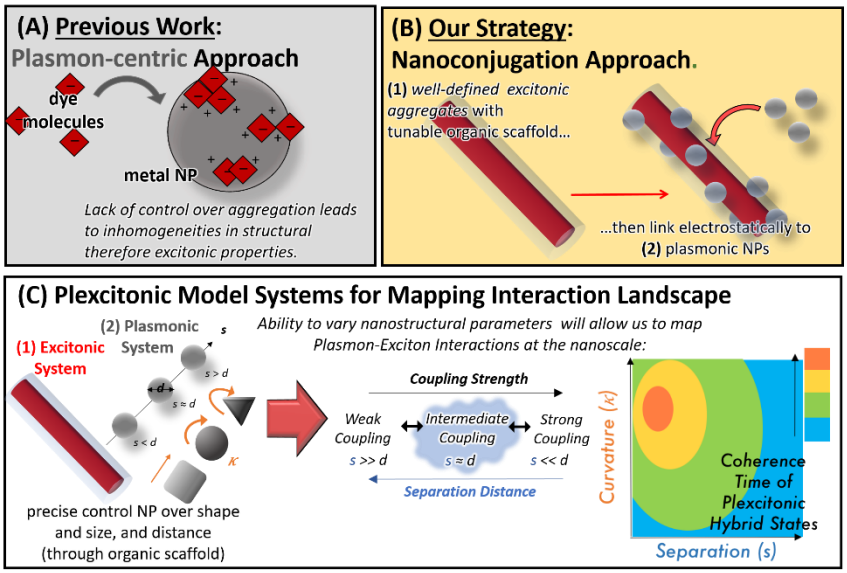

Figure 1: Illustration of classic Plasmon-centric approach and our Nanoconjugation approach.

Key Results.

The 3-year project period and the terminal renewal with limited support for a 12-month period allowed for an orderly conclusion of the project concerning PHASE I. We successfully synthesized and characterized (Key Result #1) a robust excitonic nanomaterial and (Key Result #2) a library of plasmonic nanoparticles as well as developed (Key Result #3) a microfluidic platform for homogenous nanosynthesis as summarized further below.

Key Result #1: Robust Excitonic Nanomaterial

We finalized research activities concerning the proposed excitonic nanosystem. This system consists of a well-defined supramolecular nanotube scaffolded with transparent, non-excitonic materials to mimic both, the natural light-harvesting antennae as well as the protective role of the protein environment found in the natural photosynthetic complexes (**Figure 2**). Our work lead to a publication in the 2020 December issue of NATURE CHEMISTRY.

Scaffolded Supramolecular Nanotubess: Exciton *Delocalization Maintained upon Encapsulation.* The collective optical properties, *i.e.*, large red-shift, and intense, narrow absorption and emission, of both natural and artificial supramolecular LH materials are determined by the ultrafast formation and subsequent transport of highly delocalized excitons. To assess whether our in situ encapsulation strategy has preserved these LHNTs' exciton delocalization – which are largely obscured in steady-state spectra – we utilize broadband femtosecond transient absorption (TA) spectroscopy and compare the pump-probe peak separations of LHNTs before and after scaffolding. We utilize broadband femtosecond transient absorption (TA) spectroscopy and analyzed the pump-probe peak separations of LHNTs before and after scaffolding, verifying that our in situ encapsulation strategy has preserved these LHNTs' exciton delocalization, which are largely obscured in steady-state spectra.

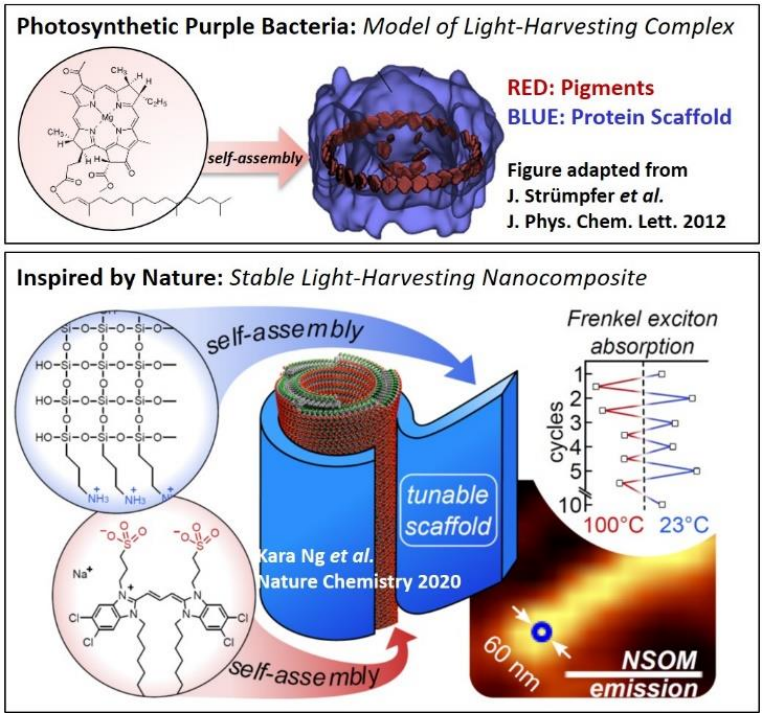

Figure 2: Robust Excitons in Scaffolded Supramolecular Assemblies

Scaffolded Supramolecular Nanotubes Upon Heat-Stress: *Robust Excitonic Character.* As artificial supramolecular assemblies consist of weakly, non-covalently bound molecules, it is unsurprising that supramolecular structure, thus the excitonic character, of artificial LH assemblies are easily destroyed under mildly elevated temperatures. Through analysis of exciton transitions in the absorption and emission of scaffolded LHNTs, we demonstrated – for the first time – that through *in situ* encapsulation, excitons in a weakly-bound supramolecular structure can be made remarkably robust against extreme thermal fluctuations.

Details about our work are available in

Ng[+], K. , Webster[+], M., Carbery, W.P., Visaveliya, N., Gaikwad[+], P., Jang, S., Kretzschmar, I., and Eisele*, D.M. *"Robust Frenkel excitons in heat stressed supramolecular nanocomposites enabled by tunable cage-like scaffolding."*
***Nature Chemistry* (2020) 12, 1157-1164.**

Key Result #1: Library of Plasmonic Nanoparticles

We developed methods for well-defined nanostructure synthesis (**Figure 3**), providing access to a diverse library of plasmonic nanostructures with (a) morphology-controlled core-shell metal nanoparticles (*e.g.* Au@Ag, Au@Ag@Au, *etc*.) with tuned size, plasmon shift, and surface property tunability (see detailed result description below) as well as with (b) controlled shape *e.g.* triangular prism, nanocube, pentagonal, hexagonal, octagonal, and elongated rods of different aspect ratios. Specifically, with our work, we demonstrate proof-of-concept for giving full access to the *multi-dimensional* synthesis parameter space via successfully utilizing 1,3-propanediol as an innovative mediating solvent. With our 1,3-propanediol-based polyol synthesis, we provide a critical step toward the vision of a "*periodic table-like*" system for plasmonic building-blocks based on straightforward wet-chemical syntheses allowing the control over:

Structural Properties: *Plasmonic Building-block's Geometry*. we successfully synthesized homogenous silver nanostructures with unique geometries that each share a synthetic route that branches out from ***one*** common starting point along three main axes: silver salt concentration, reducing agent, & interfacial agent chain length.

Surface Properties: *Plasmonic Building-block Surface Characteristics.* for our synthesis, we developed a layer-by-layer surface modification using charged polyelectrolytes to control the nanostructure surface charge and developed a metal-catalyzed metal deposition technique to create nanoassemblies with ligand-free surfaces.

Plasmonic Nanoassembly: *Showcasing Silver-based Nanoassemblies.* enabled by our platform, we demonstrated the straightforward nanoassembly process for a prototype plasmonic nanoassembly with ligand-free surface functionalization by showcasing silver-based nanoassemblies.

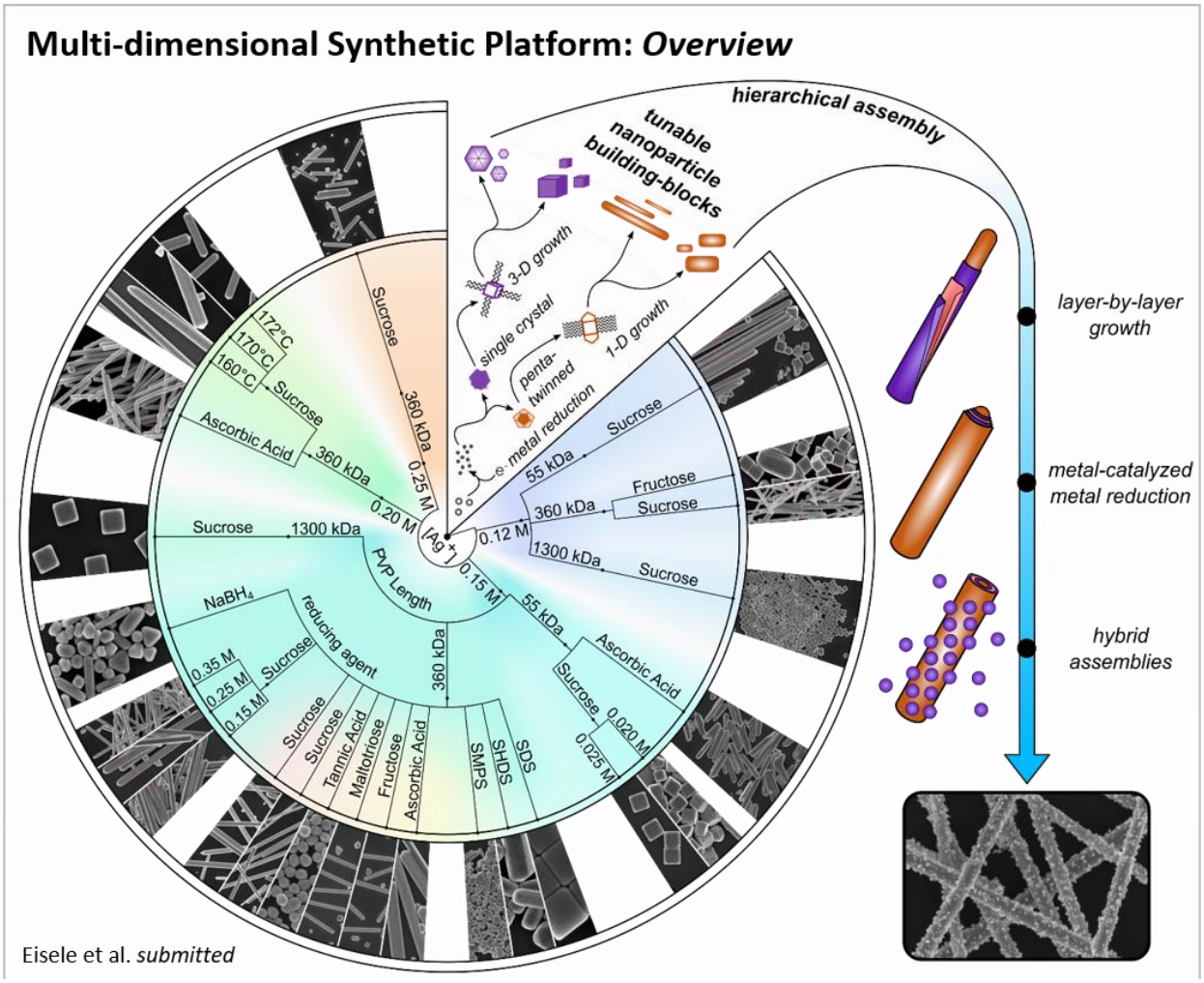

Figure 3: Multi-dimensional Framework for a Comprehensive Control of Plasmonic Building-block Properties. Schematic illustrates multi-dimensional synthesis' parameter space allowing for comprehensive control of silver nanostructure characteristics through innovative multi-dimensional 1,3-

As our work is not published yet (currently under peer-review), detailed results are available below. References are available in APPEDIX I and extensive Supporting Information in APPENDIX II of this report.

I N T R O D U C T I O N. The electronic coupling between plasmonic nanostructures (plasmonic building blocks) that are close-packed within a plasmonic nanoassembly results in collective phenomena—collective plasmonic hybrid quantum states[1-4]—leading to order-of-magnitude increases in electric field enhancements of the kind necessary for high-sensitivity molecular sensing experiments.[5] The ability to tune these hybrid quantum states, however, depends on the ability to comprehensively control the (i) plasmonic nanostructure's geometry[6-8] and (ii) its surface characteristics[9] as well as (iii) its arrangement within the plasmonic nanoassembly.[10-12] Naturally, models describing plasmonic hybridization[1, 13] parallel those developed for molecular orbitals, equating individual nanostructures with "atoms" and plasmonic nanoassemblies with "molecules."[10, 14] In analogy to organic synthesis, a suitably robust fabrication method would allow for "atom-like" manipulation of "molecule-like" plasmonic nanoassemblies.[1, 15, 16]

Despite this frequent comparison, however, current fabrication methods for plasmonic nanoassemblies favor top-down templating methods over wet-chemical syntheses.[17] Of these, the use of DNA as a template scaffold[14, 18] for arranging pre-synthesized plasmonic building-blocks,[10, 19-21] and metal-organic framework[22] approaches that preferentially stabilize the otherwise kinetically unfavorable nanoassemblies, seem most promising. By contrast, "molecule-like" fabrication approaches involving straightforward wet-chemical syntheses that do not require external templating agents have been largely ignored due to their focus on optimization along a single synthesis parameter, *i.e.*, on a synthesis paradigm that relies on rather one-dimensional synthesis procedures.[23] Recent efforts using wet-chemical synthesis, including the well-established polyol syntheses, have demonstrated impressive progress towards the synthesis of gold and silver nanostructures with certain geometries, or certain sizes, or certain surface characteristics.[6, 24-27] Still, the comprehensive control over nanostructures geometries together with the control over their surface characteristics—a necessary innovation towards empowering solution-based nanoarchitectonics for the rational design of higher-order nanostructures such as plasmonic nanoassemblies[28-30]—remains an art and scientific challenge.

R E S U L T S A N D D I S C U S S I O N

We address these limitations by developing a solution-based, polyol platform that provides access to the complete multi-dimensional parameter space of plasmonic nanostructure synthesis (**Fig. 3**). In polyol processes[31], the solvent—such as commonly used ethylene glycol[25, 32]—serves two critical purposes: as the reaction mediator and as the reducing agent that facilitates nanostructure nucleation.[33-36] We discovered that 1,3-propanediol can be used as an innovative mediating solvent, facilitating the development of a multi-dimensional platform towards a "molecule-like" framework for plasmonic nanoassemblies. Specifically, with our 1,3-propanediol-based polyol synthesis (**Methods**), we give full access to the multi-dimensional synthesis parameter space allowing for comprehensive control of the plasmonic nanostructure geometry as well as surface characteristic, and showcasing silver-based nanoassemblies with ligand-free surface functionalization (**Fig. 3).**

PLASMONIC BUILDING-BLOCK GEOMETRIES.

Using our polyol platform, encompassing the full complexity of the multi-dimensional synthesis parameter space, we successfully synthesized over 200 silver nanostructure building block samples with geometries, for example, ranging from nanorods, nanobars, and nanocubes, to multifaceted particles (**Fig. 3, Supplementary Fig. S1-5, Supplementary Table S1-33**). Each of these unique geometries share a synthetic route that branches out from *one* common starting point along three main axes: silver salt concentration, reducing agent identity, and interfacial agent chain length (**Supplemementary Chapter 2-5, Supplementary Table S1**). Taken together, these critical parameters (i) define the nucleated character of the nanostructures, *i.e.*, control whether they are based on single-crystal nucleii or nucleii with multiple twin boundaries,[11, 37, 38] (ii) control the nanostructure growth,[6] and (iii) affect a given sample's polydispersity. We observ that the silver salt concentration affects the geometry of the resultant plasmonic nanostructure less than the reducing agent identity or the chain length of the interfacial agent. Instead, appropriate concentrations of silver salt ensures high standards of homogeneity across the polyol platform. As silver salt we employ silver nitrate $AgNO_3$, which is the most commonly used salt in silver nanostructure syntheses.[6, 25]

For example, the first branching point of the polyol platform involves dissolving between 0.12 M and 0.25 M of $AgNO_3$ into the mediating solvent 1,3-propanediol and heating the solution to between 165°C and 175°C. This increased temperature relative to other well-established polyol syntheses possible through the higher boiling point of 1,3-propanediol of 214°C, and since the overall reductive capability of polyol solvents are temperature-dependent, the nucleation process in our polyol platform is greatly accelerated. This fast reduction of $AgNO_3$ limits the inhomogeneity caused by random aggregation and common stacking faults during the initial nucleation of silver nanostructures, however, the rapid dissolution interferes with the subsequent growth kinetics, and by extension, the resultant properties of the nanostructures. To remedy this, shortly after $AgNO_3$ insertion and addition of an interfacial agent, an external reducing agent is added.

The external reagent allows for precise control over the nucleation environment and subsequent nanostructure growth. Most importantly, decoupling the dual role of 1,3-propanediol as both reducing agent and mediating solvent allows for the incorporation of a broad variety of external reducing agents able to tune the individual properties of the silver nanostructures. All substances that demonstrated reducing ability in this report are called "external reducing agents" and can be grouped into four main categories: (i) carbohydrates, *e.g.*, sucrose or fructose, (ii) organic molecules, *e.g.*, tannic acid or ascorbic acid, (iii) additional salts, *e.g.*, sodium hydroxide, and (iv) surfactants, *e.g.*, sodium dodecyl sulfate (SDS) and sodium hexadecyl sulfate (SHDS). By altering the reducing agent identity, a broad variety of silver nanostructure geometries are made available (**Supplementary Section 2**) and examples are diplayed via representative scanning electron microscopy (SEM) images in **Fig. 4** of four common geometries, including nanorods, nanobars, nanocubes, and multifaceted nanoparticles.

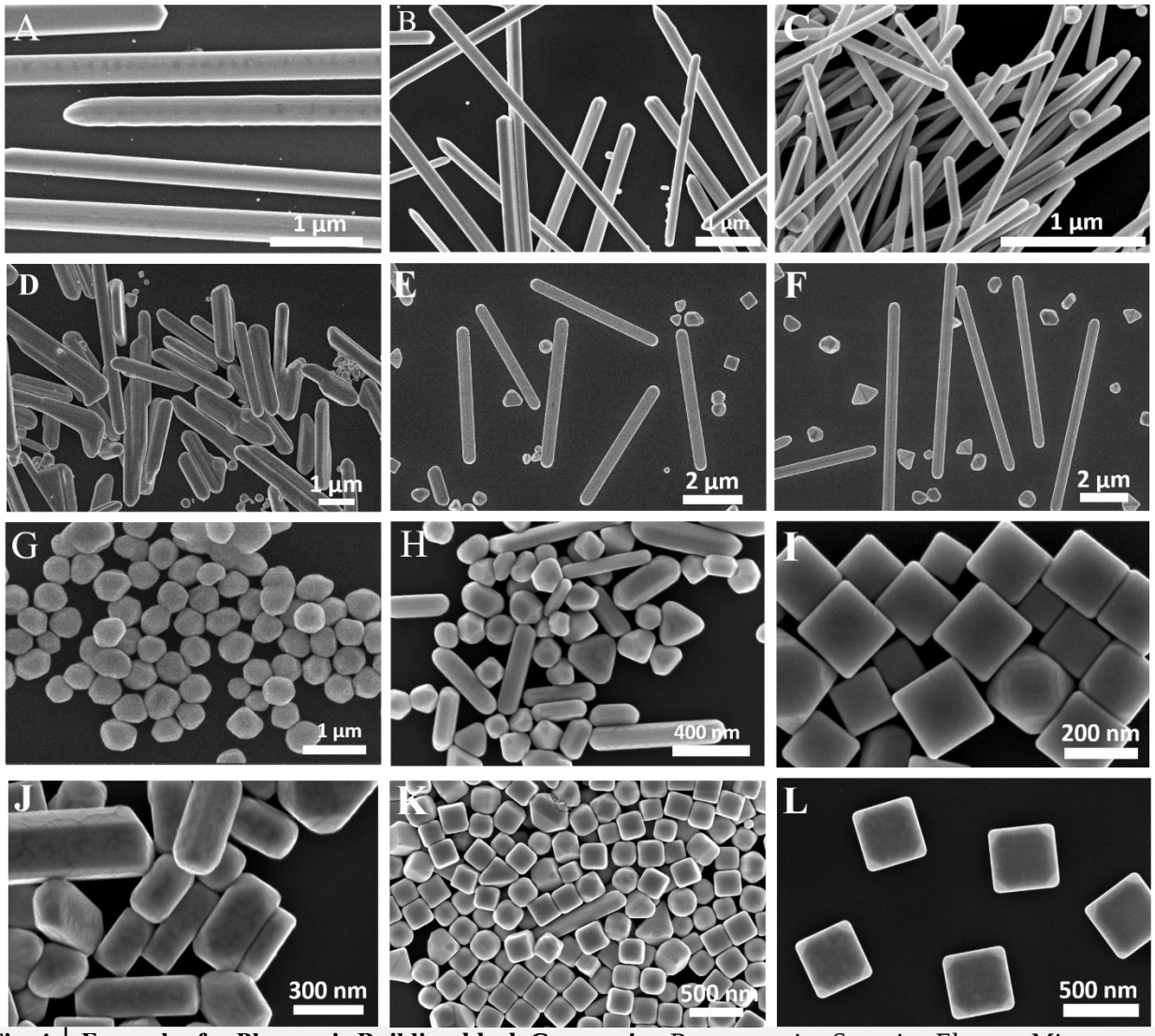

Fig. 4 | Examples for Plasmonic Building-block Geometries. Representative Scanning Electron Microscopy (SEM) images display examples for obtained silver nanostructure geometries: **(A)** Silver nanorods formed by 0.2 M $AgNO_3$, 0.35 M PVP-360,000, and 0.02 M sucrose at 160 °C. **(B)** Silver nanorods formation by 0.15 M $AgNO_3$ and 0.35 M PVP-360,000 together with 0.02 M sucrose at 170 °C. **(C)** Silver nanorods formed by 0.2 M $AgNO_3$, 0.35 M PVP-360,000, and 0.1 M ascorbic acid at 160 °C. **(D)** Overgrown silver nanorods formation by 0.15 M $AgNO_3$ and 0.35 M PVP-55,000. together with 0.15 M ascorbic acid at 170 °C. **(E-F)** Silver nanorods of different length and diameter from the effect of different carbohydrates; 0.15 M $AgNO_3$ and 0.35 M PVP-360,000 together with **(E)** 0.02 M fructose and **(F)** 0.02 M maltotriose at 167 °C. **(G)** Multifaceted silver nanoparticles and **(H)** silver nanostructures with diverse geometries at 0.15 M $AgNO_3$ and 0.35 M PVP-360,000 together with **(G)** 0.04 M tannic acid and **(H)** 0.02 M sodium borohydride at 170 °C, respectively. **(I)** Sharp-cornered silver nanocubes formation by 0.15 M $AgNO_3$ and 0.35 M PVP-360,000 together with 0.1 M Sodium dodecyl sulfonate (SDS) at 170 °C. **(J)** Formation of silver nanobars by addition of surface-active agent 0.1 M sodium 1-hexadecanesulfonate (SHDS) together with 0.15 M $AgNO_3$ and 0.35 M PVP-360,000 at 170 °C. **(K)** Silver nanocubes formation by 0.12 M $AgNO_3$ and 0.35 M PVP-1,300,000 together with 0.02 M sucrose at 170 °C. **(L)** Formation of silver nanocubes at high molecular weighed 0.35 M PVP-1,300,000 together with 0.15 M $AgNO_3$ and 0.02 M sucrose at 170 °C.

Surprisingly, while widely used in biochemistry related applications, we discovered that sucrose can be employed as a mild reducing agent for silver nanorods with almost 100% yield (**Fig. 4A-B**, and **Supplementary**

Table S5). The addition of sucrose during the reaction results in a slower nucleation process, may likely eliminate the random growth that can occur for smaller nuclei. Similar to sucrose, the utilization of ascorbic acid as an external reducing agent also form the the nanorods as shown in **Fig. 4C-D**. The aspect ratio of the silver nanorod was strongly dependent on the reducing agent concentration (**Supplementary Table S31)**. In addition, we found that the strength of the reducing agent can also be used to modify the nanorod's aspect ratio (**Supplementary Table S8-12**): fructose, for example, resulted in nanorods with a length and diameter of 6µm ± 0.9µm and 420nm ± 22nm, respectively, while the usage of maltotriose resulted in nanorods with a length of 11µm ± 2.2µm and a diameter of 470nm ± 18nm (**Fig. 4E-F** and **Supplementary Table S11-12**). In contrast, the reducing agent tannic acid produced multifaceted nanoparticles as shown in **Fig. 4G.** This suggests that the reducing agent's molecular structure, specifically its so-called structural bulkiness, may also impact the nanostructure's geometry (**Supplementary Fig. S6**). Sodium borohydride was the strongest reducing agent used in this report and, as expected, its inclusion lead to nanostructures with mixed geometries (**Fig. 4H**) as the nucleation process proceeded far too rapidly to overcome random growth. Additional salts such as sodium hydroxide (NaOH) facilitated the formation of mixed geometries with larger population of relatively thinner nanorods (**Supplementary Table S20**). In contrast, the addition of molecular surfactants such as sodium dodecyl sulfate (SDS) or sodium hexadecyl sulfate (SHDS) accelerated the formation of nanocubes (**Fig. 4I**) and nanobars (**Fig. 4J**), respectively. Boradly speaking, our approach allows for the manipulation of the environemnt at the early stages of nanostructure nucleation, which allows for early biasing towards a specific nanostructure geometry. Reducing agent strength and concentration remain key factors, however, our work also reveals that the structure of the reducing agent itself as well as the addition of NaOH, SDS, or SHDS, provide early direction along a specific synthetic pathway within a larger polyol platform.[39]

While the addition of an external reducing agent biases the geometry of the nanostructure during the nucleation stage, we found that the subsequent addition of an interfacial agent—here polyvinylpyrrolidone (PVP) with chain lengths of 55,000, 360,000, and 1,300,000 (molecular weight)—may passivate certain sides of the early nanostructure (low-energy facets) and directs the nanostructure growth (**Supplementary Section 3**, **Supplementary Table S13-16**). This mechanism was also suggested by previous work.[40, 41] Quasi-spherical shaped nanostructures are considered thermodynamically favorable because they have geometries with the lowest possible surface energy. Therefore, to achieve thermodynamically unfavorable, non-spherical geometries such as nanorods or nanocubes, the growth kinetics of a geometry-biased seed nanostructure must be carefully controlled. We found that nanostructures with high yield (98%) can be synthesized by using a specific PVP concentration of 0.35M PVP. Within a series of synthetic reactions using sucrose as the reducing agent, our results suggest that PVP with a low molecular weight such as 55,000 selectively directs the growth of the nanostructures into a nanocube-like shape together with a smaller population of nanorods (**Supplementary Table S14**). Specifically, using PVP with an intermediate molecular weight such as 360,000 results in the formation of nanorods (**Supplementary Table S6**). Using higher molecular weight PVP such as 1,300,000, however, reveals completely changed growth kinetics, likely due to the suppression of twin-boundary nucleation in favor of single-crystal type nanostructures such as uniform nanocubes (**Fig. 4K-2L**). In general, PVP is a dynamic interfacial agent, continuously adsorbing and desorbing during an ongoing chemical reaction that allows incoming free silver atoms to participate in the nanostructure growth.[25, 37, 41, 42]

PLASMONIC BUILDING-BLOCK SURFACE CHARACTERISTICS.

With our 1,3-propanediol-based polyol synthesis, we give full access to the multi-dimensional synthesis parameter space allowing not only for comprehensive control of the plasmonic building blocks geometry but also for subsequent control over their surface characteristics. The latter is key for two aspects. Firstly, control over the individual nanostructure's surface charge is a prerequisite for plasmonic nanoassemblies based on electrostatic interactions between the plasmonic building blocks.[43] Secondly, in particular for sensing applications, surface ligands can significantly hinder the detection ability of external compounds such as biological or chemical substances.[5] Thus, plasmonic building-blocks with ligand-free surfaces are key for plasmonic nanoassemblies that may find use in sensing applications like colorimetric sensing[44] and enhanced spectroscopic detection.[5, 45] To provide control over both the surface charge and character, we (1) adopted a layer-by-layer surface modification[46] using charged polyelectrolytes to control the nanostructure surface charge

and (2) developed a metal-catalyzed metal deposition technique to create nanoassemblies with ligand-free surfaces.

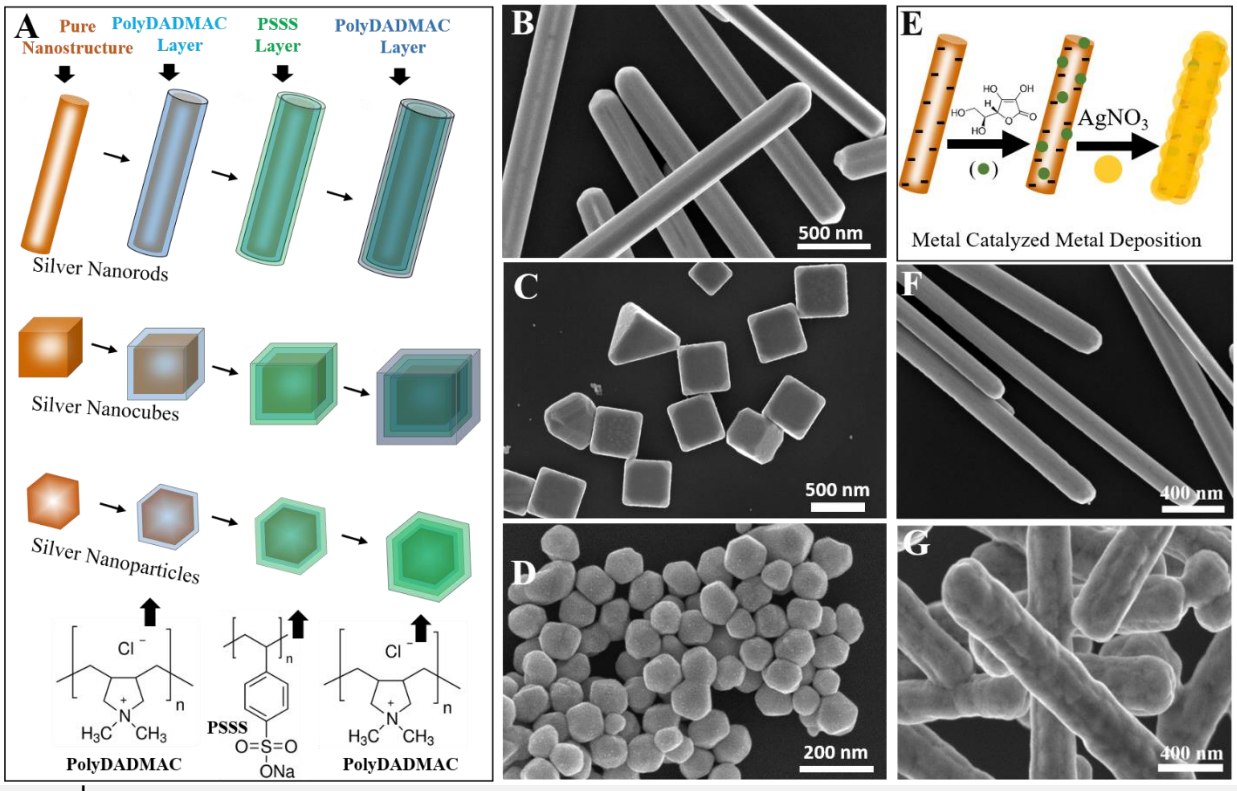

Fig. 5 | Plasmonic Building-block Surface Characteristics. (A) Illustration of the layer-by-layer surface modifications of silver nanostructures with alternatively charged polyelectrolytes **(**cationic-anionic-cationic). **(B-D)** Representative SEM images of the silver nanostructures with functionalized surfaces where three layers of the alternatively charged polyelectrolytes were applied on the pure silver nanostructure: **(B)** silver rods, **(C)** silver cubes, and **(D)** silver particles. **(E)** Illustration of our metal-catalyzed metal deposition technique applied to the surface of silver nanorods. Representative SEM images of **(F)** silver nanorods synthesized by using 0.02 M sucrose as a reducing agent and **(G)** after applying our metal-catalyzed metal deposition technique for ligand-free nanostructure surfaces.

Firstly, to control the nanostructure's surface charge, we transfer a layer-by-layer technique that is commonly applied on two-dimensional surfaces[46, 47] to our colloidal nanostructures (**Fig. 5A**). We apply up to three consecutive layers of alternatively charged polyelectrolytes through electrostatic interaction on the nanostructures' surface (**Supplementary Fig. S7**). Initially, the surface charge of isolated, untreated nanorods, for example, can be inferred from the zeta potential and shows a negative value of -13.6 mV ± 3.5mV (**Supplementary Table S32**). A positively charged polydiallyldimethyl ammonium bromide (PolyDADMAC) layer (**Fig. 5A**) is systematically applied onto the surface of, for example, nanorods, nanocubes, or multifaceted nanoparticles (**Fig. 5B-D**). The surface functionalization of the nanorods by 0.8 wt% cationic polyelectrolyte polyDADMAC yields a strongly positive zeta potential value (+78mV ± 7mV, **Supplementary Fig. S8**). A second polyelectrolyte layer composed of anionic polystyrene sodium sulfonate (PSSS) is applied onto the cationic surface of these nanorods and yields a negative zeta potential value of -48mV ± 4.8mV (**Supplementary Fig. S8**). In this way, the desired number of alternative layers of charged polyelectrolytes can straightforwardly be applied to the nanostructure by which the electrical charges, both type, and density, as well as the surface functional groups of interest, can be tailored elegantly. Secondly, to achieve nanostructures with ligand-free surfaces, we developed a metal-catalyzed metal enforcement approach (**Fig. 5E**), where the nanostructure itself acts as a catalyst for the formation and growth of silver layers in the presence of external reducing agents. The

formation of ligand-free silver layers is realized by addition of $AgNO_3$ in the presence of ascorbic acid, where the silver layer formation depends on the concentration of both ascorbic acid and $AgNO_3$ similar to the initial reduction of the silver nanostructures (**Supplementary Fig. S9).** A representative selection of nanorods before and after metal-catalyzed metal deposition are displayed in **Fig. 5F** and **Fig. 5G**, respectively.

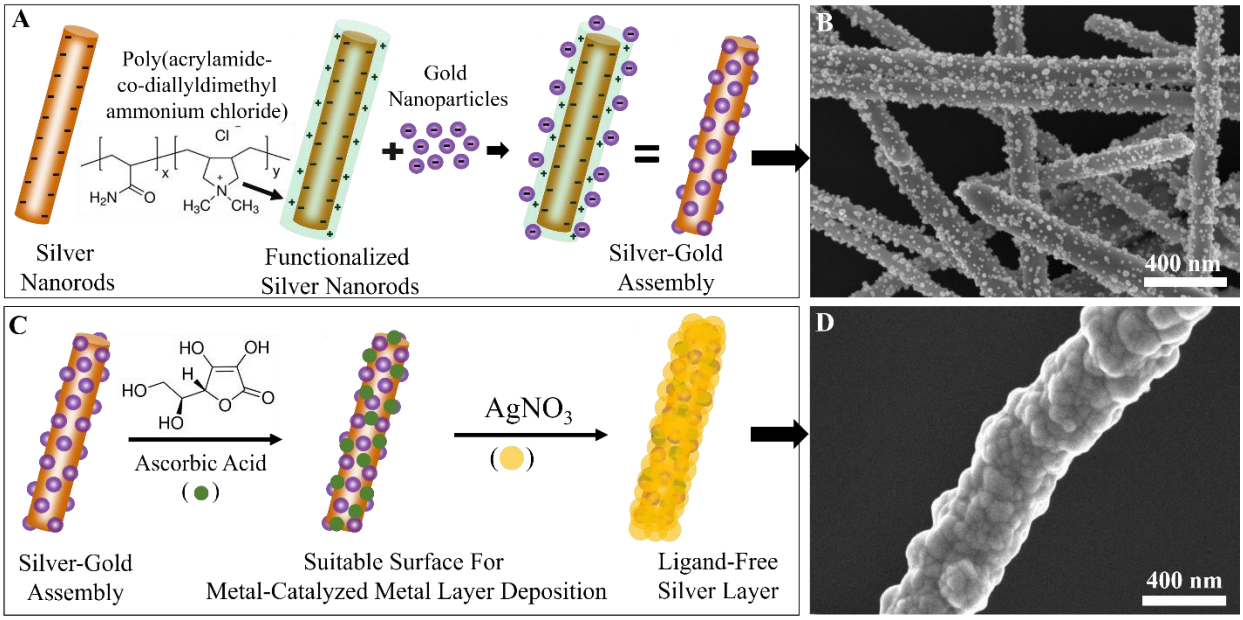

Fig 6: Proof-of-concept for Solution-based Plasmonic Nanoassembling by Showcasing Silver-based Nanoassemblies with Ligand-free Surface Functionalization. (A) To guide the assembly process, we modified the surface of our anionic silver nanorods with a cationic polyelectrolyte poly(AAm-co-DADMAC) (Method, Supplementary Section 9) followed by the addition of separately synthesized anionic gold nanoparticles (Method). **(B)** representative SEM image shows the systematic uptake of gold nanoparticles by the surface of silver nanorods without any secondary gold-gold nanoparticle agglomeration, *i.e.*, gold nanoparticle are distributed over the entire silver nanorod surface. **(C)** of the ligand-free metal layer deposition on the silver-gold nanoassembling structure via metal-catalyzed metal deposition process **(D)** shown via respresentative SEM image.

SOLUTION-BASED PLASMONIC NANOASSEMBLING.

The first generation of the silver nanostructures synthesized using the 1,3-propanediol platform were between the nano- and micro-scale. While additional experimentation along the branches of the polyol platform will likely yield particles of diverse scales, the mesoscopic nanorods in particular provide an opportunity to demonstrate the straightforward nanoassembly process enabled by our robust platform for nanostructure syntheses. Taking our cue from the needs of sensing applications, we design a proof-of-concept nanoassembly incorporating a silver-gold hybrid structure with a large surface area (**Fig. 6**). To guide the assembly process,[48, 49] we modified the surface of our anionic silver nanorods with a cationic polyelectrolyte poly(acrylamide-co-diallyldimethylammonium chloride) (poly(AAm-co-DADMAC)) (**Fig. 6A**) followed by the addition of separately synthesized anionic gold nanoparticles.[50] In complement with electrostatic interactions between opposite surface charges, the silver-gold assemblies are also selective to specific types of molecular surface functionalization (**Supplementary Fig. S11, SI Table S29-33)**. With the surface functionalization of silver rods by poly(AAm-co-DADMAC), we observe a consistent uptake of gold nanoparticles by the surface of silver nanorods without observation of secondary gold-gold nanostructure agglomeration within the solution (**Fig. 6A, Supplementary Fig. S11-12)**: indeed, the gold nanoparticles are distributed over the entire silver -nanorod surface (**Fig. 6B**). Next, plasmonic nanoassemblies with ligand-free outer surfaces are synthesized by applying ligand-free metallic layer on the gold-silver assembly *via* our metal-catalyzed metal layer deposition (**Fig. 6C-D**). Here, as described above and illustrated in **Fig. 5E**, the silver-gold nanoassemblies act as the catalyst for further growth of silver layer in the presence of external reducing agents and form the surfactant-free, metal-

coated nanoassembly that holds the potential to serve as promising substrates for SERS sensing and catalysis applications.

CONCLUSIONS AND OUTLOOK

The concept of a "periodic table-like" system for plasmonic building-blocks that is based on straightforward wet-chemical syntheses will allow envisioning rational design of plasmonic nanoassemblies via an elegant "atom-like" manipulation of "molecule-like" nanoassemblies. However, fabrication approaches involving straightforward wet-chemical syntheses that do not require external templating agents have been largely ignored due to their focus on a synthesis paradigm that relies on rather one-dimensional synthesis procedures. By successfully utilizing 1,3-propanediol as an innovative mediating solvent, our multi-dimensional polyol synthesis provides a critical step toward a "periodic table-like" system allowing the systematic control of plasmonic building-block geometries as well as surface characteristics. Finally, we show how our approach can be utilized for colloidal solution-based fabrication of plasmonic nanoassemblies with ligand-free surface functionalization by showcasing silver-based nanoassemblies. Our results open the door for solution-based nanoarchitectonics approaches to finally leverage their advantages over top-down materials fabrication toward rationally designed interfacial plasmonic nanoassemblies.

METHODS

***Polyol synthesis of silver nanostructures*:** The reaction flask was filled with 5 mL of "as received" 1,3-propanediol (Sigma Aldrich, 98%) and subsequently heated to 170 °C for 1 hour at a stirring rate of 500 rpm. Afterwards, three main reactants (all dissolved in 1,3-propanediol) were simultaneously added dropwise within 8 minutes: 3 ml 0.15 M silver nitrate ($AgNO_3$) (≥99.0%, ACS Reagents, Sigma-Aldrich), 3 ml 0.35 M polyvinylpyrrolidone (PVP) (360,000 molecular weight, Sigma-Aldrich), and 1 ml 0.02 M sucrose (≥99.5% (GC), BioXtra, Sigma-Aldrich) as an external reducing agent. Newera syringe pumps (http://www.syringepump.com) were used for the precise addition of reactants. External reducing agents accelerate the reaction rate where reaction progress depends on the type, concentration, and molecular structure of reducing agents. For geometry-controlled nanostructures, therefore, various external reducing agents (ascorbic acid, tannic acid, sodium borohydride, sucrose, maltotriose, and fructose) were used. Nanostructure geometry depends not only on the reducing agents but also on the concentration and molecular weight of PVP, molecular surfactants (sodium dodecyl sulfate and sodium hexadecyl sulfate), and ionic additives (NaOH and CsOH). Three different molecular-weighed PVP (55,000, 360,000, and 1,300,000) were used with varying concentrations between 0.15 M and 0.45 M (repeating unit concentration). Detailed description in Supplementary Section 1.

Surface characteristics of nanostructures building blocks: Various anionic and cationic charged polyelectrolytes were applied through electrostatic interactions on the surface of obtained nanostructures (nanorods, nanocubes, multi-faceted nanoparticles, and nanobars) in a multi-layered fashion. The surfaces of pure nanostructures are negatively charged (measured zeta potential -13.6 mV ± 1.8 mV); therefore, the first layer is applied through electrostatic interaction by 0.8% cationic poly(diallyldimethylammoniumbromide) (polyDADMAC) (average Mw 200,000-350,000, Sigma-Aldrich). Similarly, the second and third layers were applied by 0.4% anionic poly(styrene sodium sulfonate) (PSSS) (average Mw ~1,000,000, Sigma-Aldrich) and 0.8% cationic polyDADMAC (average Mw 400,000-500,000, Sigma Aldrich), respectively.

Plasmonic nanoassembly: For a model electrostatic plasmonic assemblies, primarily, silver nanorods have been functionalized with 0.8 % cationic poly(acrylamide-co-diallyldimethylammonium chloride) (poly(AAm-co-DADMAC)) by adding 1 mL poly(AAm-co-DADMAC) to 150 µL of silver nanorods dispersion at room temperature under stirring. Afterward, three repeated washing cycles were applied with ultrapure water to remove the unreacted polyelectrolyte molecules, and finally, nanorods were re-dispersed in pure water. For silver-gold nanoassembling, gold nanoparticles were prepared following the synthesis protocol from ref[50]. Briefly, 20 ml of 1.2 mM of gold chloride (99%, Sigma-Aldrich) were heated at boiling temperature and subsequently, 2 ml of 1% trisodium citrate dihydrate (>99%, Sigma-Aldrich) were added to the boiling gold chloride solution. Within two minutes, color has been changed from light yellow to dark red indicating the formation of gold nanoparticles. Later, freshly prepared citrate-capped anionic gold nanoparticles were mixed with poly(AAm-co-DADMAC)-functionalized silver nanorods under the stirring condition in a 1:2 (silver:gold) solution ratio. Because of the strong surface charge, the solution changed its color to dark purple immediately

upon the addition of gold nanoparticles indicating the successful assembling reaction. After the silver-gold assembling, an additional metal layer was deposited on its surface to obtain a ligand-free metal surface useful for potential catalysis and sensing applications. Initially, 150 µL 0.1 M ascorbic acid solution was added to 100 µL dispersion of silver-gold nanoassembly, and then 150 µL $AgNO_3$ solution has been added under a strong stirring condition at room temperature. Upon deposition of the metal layer, the color becomes dark brown (reaction time is less than 10 seconds). For all the experiments, all chemicals were used as received without further purification.

***Sample Characterization*:** The surface charge of the nanostructures after their layer-by-layer surface modification was measured using zeta potential measurement in the Malvern Zetasizer instrument (Zetasizer Nano Series: Nano ZS). A 1/20 dilution of silver nanostructures filled in the zeta potential cell (Malvern: DTS1070) and measured zeta potential at room temperature with 1/100 runs for three repeated measurement cycles. Scanning Electron Microscope (SEM) was used to obtain particle images. Nanostructures were washed with ultrapure water to completely remove the impurities and 1,3-propanediol solvent. Three cycles of centrifuge at 11,000 RPM speed for 12 minutes were applied for the washing process. Afterward, a 1/25 dilution of 10 µL water dispersion of nanostructures were deposited on the 500 nm thick washed silicon chip, allowing the natural evaporation of water at room temperature. The nanostructures were adsorbed to the silicon chip after drying and, afterward, brought it to the SEM chamber for imaging. Imaging was taken at 5 KV voltage and 25 PA current.

Key Result #1: Microfluidic Platform for Homogenous Nanosynthesis

Control over structural properties of plexcitonic nanocomposites remains a challenge due to current limitations in nanosynthesis techniques. Slight variations in nanostructure's geometry impact their optoelectronic properties, demanding precise synthesis beyond the capabilities of solution-based (batch) synthesis processes. In contrast, the small, confined liquid volumes used in microfluidics—a reaction technique where the manipulation of fluids takes place in channels with dimensions of tens of micrometers—allows for homogenous synthesis conditions, providing excellent control of the reaction and, as a result, of the materials' geopmetry and composition. However, thus far, the majority of plexcitonic systems has been developed via batch synthesis.

While having progress on batch synthesis on excitonic and plasmonic systems (see above, Key Result #1 and Key Result #2), we developed a two-channel microreactor and our microfluidic platform was installed successfully by realizing the proof-of-principle synthesis via a semi-microfluidics approach: polymer nanoparticles of different size, shape, assembly and composition were synthesized (**Figure 7**). Our microfluidic-supported synthesis approach combines the advantages of both microfluidics and batch platforms, allowing for precise spatio-temporal control over all synthesis parameters opening the possibility for homogenous nanosythnesis of well-defined plexcitonic model systems.

Details about our work are available in

Visaveliya, N.R., St. Peter [UG], L., Leo [UG], K., Khatoon [UG], F., Xu [UG], J., Chan [UG], C., Mikhailova [UG], T., Bedzeti [UG], V., Kapadia [UG], A., Carbery, W.P., Ng^{+}, K., and Eisele*, D.M. *"Microfluidic-Supported Synthesis of Anisotropic Polyvinyl Methacrylate Nanoparticles via Interfacial Agents."*
***ACS Polymer Chemistry* (2022) 13, 4625.**

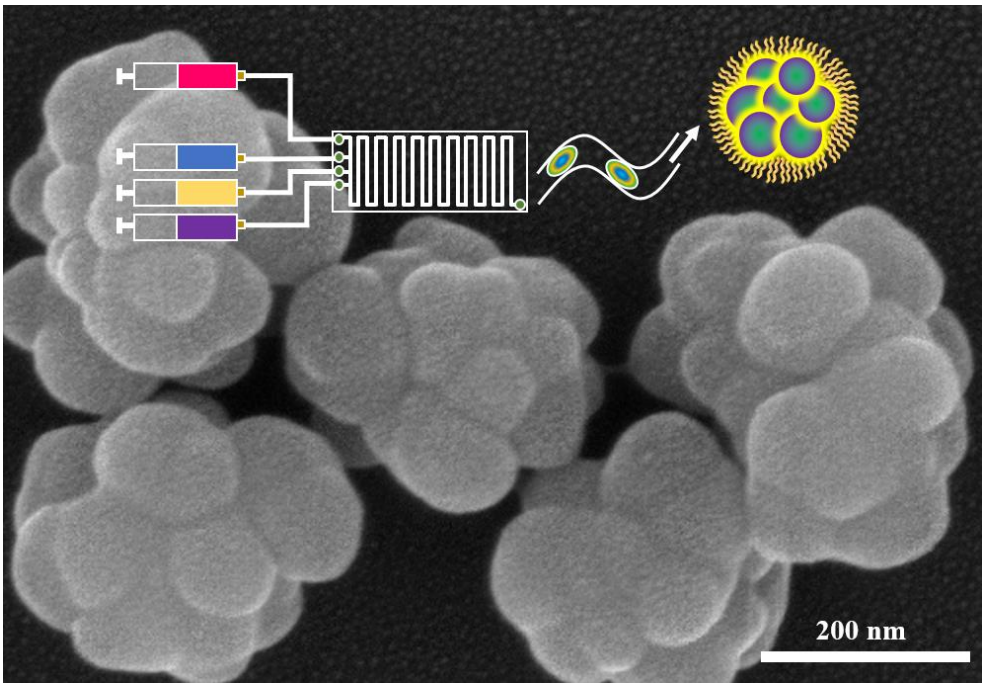

Figure 7: By combining the advantages of microfluidics and bulk batch synthesis, Eisele and coworkers at The City College at The City University of New York developed a single-step, microfluidic-supported synthesis for anisotropic polyvinyl methacrylate (PVMA) polymer nanoparticles with dimensions ranging from 200 nm to 50 nm. ***Cover Art, Visaveliya, N.R et al. Polymer Chemistry 2022.***

Appendix II: References

1. Halas, N.J., Lal, S., Chang, W.-S., Link, S. & Nordlander, P. Plasmons in Strongly Coupled Metallic Nanostructures. *Chem. Rev.* **111**, 3913-3961 (2011).
2. Li, J. et al. Hierarchical Assembly of Plasmonic Nanoparticle Heterodimer Arrays with Tunable Sub-5 nm Nanogaps. *Nano Lett.* **19**, 4314-4320 (2019).
3. Wu, X. et al. Environmentally responsive plasmonic nanoassemblies for biosensing. *Chem. Soc. Rev.* **47**, 4677-4696 (2018).
4. Yu, H., Peng, Y., Yang, Y. & Li, Z.-Y. Plasmon-enhanced light–matter interactions and applications. *Npj Comput. Mater.* **5**, 45 (2019).
5. Anker, J.N. et al. Biosensing with plasmonic nanosensors. *Nat. Mater.* **7**, 442-453 (2008).
6. Xia, Y., Xiong, Y., Lim, B. & Skrabalak, S.E. Shape-Controlled Synthesis of Metal Nanocrystals: Simple Chemistry Meets Complex Physics? *Angew. Chem. Int. Ed.* **48**, 60-103 (2009).
7. Seeman, N.C. & Sleiman, H.F. DNA nanotechnology. *Nat. Rev. Mater.* **3**, 17068 (2017).
8. Edwardson, T.G.W., Lau, K.L., Bousmail, D., Serpell, C.J. & Sleiman, H.F. Transfer of molecular recognition information from DNA nanostructures to gold nanoparticles. *Nat. Chem.* **8**, 162-170 (2016).
9. Yao, G. et al. Programming nanoparticle valence bonds with single-stranded DNA encoders. *Nat. Mater.* **19**, 781-788 (2020).
10. Fan, J.A. et al. Self-Assembled Plasmonic Nanoparticle Clusters. *Science* **328**, 1135-1138 (2010).
11. Molleman, B. & Hiemstra, T. Size and shape dependency of the surface energy of metallic nanoparticles: unifying the atomic and thermodynamic approaches. *Phys. Chem. Chem. Phys.* **20**, 20575-20587 (2018).
12. Ha, M. et al. Multicomponent Plasmonic Nanoparticles: From Heterostructured Nanoparticles to Colloidal Composite Nanostructures. *Chem. Rev.* **119**, 12208-12278 (2019).
13. Schirato, A. et al. Transient optical symmetry breaking for ultrafast broadband dichroism in plasmonic metasurfaces. *Nat. Photonics* **14**, 723-727 (2020).
14. Tan, S.J., Campolongo, M.J., Luo, D. & Cheng, W. Building plasmonic nanostructures with DNA. *Nat. Nanotechnol.* **6**, 268-276 (2011).
15. Aldaye, F.A. & Sleiman, H.F. Sequential Self-Assembly of a DNA Hexagon as a Template for the Organization of Gold Nanoparticles. *Angew. Chem. Int. Ed.* **45**, 2204-2209 (2006).
16. Sun, S. et al. Valence-programmable nanoparticle architectures. *Nat. Commun.* **11**, 2279 (2020).
17. Zhang, H., Kinnear, C. & Mulvaney, P. Fabrication of Single-Nanocrystal Arrays. *Adv. Mater.* **32**, 1904551 (2020).

18. Lin, Q.-Y. et al. Building superlattices from individual nanoparticles via template-confined DNA-mediated assembly. *Science* **359**, 669-672 (2018).

19. Fan, J.A. et al. DNA-Enabled Self-Assembly of Plasmonic Nanoclusters. *Nano Lett.* **11**, 4859-4864 (2011).

20. Eisele, D.M. et al. Utilizing redox-chemistry to elucidate the nature of exciton transitions in supramolecular dye nanotubes. *Nat. Chem.* **4**, 655-62 (2012).

21. Ng, K. et al. Frenkel excitons in heat-stressed supramolecular nanocomposites enabled by tunable cage-like scaffolding. *Nat. Chem.* **12**, 1157-1164 (2020).

22. Grommet, A.B., Feller, M. & Klajn, R. Chemical reactivity under nanoconfinement. *Nat. Nanotechnol.* **15**, 256-271 (2020).

23. Du, J.S. et al. Galvanic Transformation Dynamics in Heterostructured Nanoparticles. *Adv. Funct. Mater.* **31**, 2105866 (2021).

24. Fiévet, F. et al. The polyol process: a unique method for easy access to metal nanoparticles with tailored sizes, shapes and compositions. *Chem. Soc. Rev.* **47**, 5187-5233 (2018).

25. Sun, Y.G., Yin, Y.D., Mayers, B.T., Herricks, T. & Xia, Y.N. Uniform silver nanowires synthesis by reducing AgNO3 with ethylene glycol in the presence of seeds and poly(vinyl pyrrolidone). *Chem. Mater.***14**, 4736-4745 (2002).

26. Lu, F. et al. Unusual packing of soft-shelled nanocubes. *Sci. Adv.* **5**, eaaw2399 (2019).

27. Li, Q. et al. Structural distortion and electron redistribution in dual-emitting gold nanoclusters. *Nat. Commun.* **11**, 2897 (2020).

28. Hendricks, M.P., Campos, M.P., Cleveland, G.T., Jen-La Plante, I. & Owen, J.S. NANOMATERIALS. A tunable library of substituted thiourea precursors to metal sulfide nanocrystals. *Science* **348**, 1226-30 (2015).

29. Jayant, K. et al. Targeted intracellular voltage recordings from dendritic spines using quantum-dot-coated nanopipettes. *Nat. Nanotechnol.* **12**, 335-342 (2017).

30. Zhou, L. et al. Hot carrier multiplication in plasmonic photocatalysis. *Proc. Natl. Acad. Sci.* **118**, e2022109118 (2021).

31. Dong, H., Chen, Y.C. & Feldmann, C. Polyol synthesis of nanoparticles: status and options regarding metals, oxides, chalcogenides, and non-metal elements. *Green Chem.* **17**, 4107-4132 (2015).

32. Biacchi, A.J. & Schaak, R.E. The Solvent Matters: Kinetic versus Thermodynamic Shape Control in the Polyol Synthesis of Rhodium Nanoparticles. *ACS Nano* **5**, 8089-8099 (2011).

33. Ducrot, É., He, M., Yi, G.-R. & Pine, D.J. Colloidal alloys with preassembled clusters and spheres. *Nat. Mater.* **16**, 652-657 (2017).

34. Liu, M. et al. Two-Dimensional (2D) or Quasi-2D Superstructures from DNA-Coated Colloidal Particles. *Angew. Chem. Int. Ed.* **60**, 5744-5748 (2021).

35. Wang, S. et al. The emergence of valency in colloidal crystals through electron equivalents. *Nat. Mater.* (2022) doi.org/10.1038/s41563-021-01170-5.

36. Nagaoka, Y. et al. Superstructures generated from truncated tetrahedral quantum dots. *Nature* **561**, 378-382 (2018).

37. Liz-Marzán, L.M. & Grzelczak, M. Growing anisotropic crystals at the nanoscale. *Science* **356**, 1120-1121 (2017).

38. Wu, Z., Yang, S. & Wu, W. Shape control of inorganic nanoparticles from solution. *Nanoscale* **8**, 1237-1259 (2016).

39. Chen, Z., Balankura, T., Fichthorn, K.A. & Rioux, R.M. Revisiting the Polyol Synthesis of Silver Nanostructures: Role of Chloride in Nanocube Formation. *ACS Nano* **13**, 1849-1860 (2019).

40. Heuer-Jungemann, A. et al. The Role of Ligands in the Chemical Synthesis and Applications of Inorganic Nanoparticles. *Chem. Rev.* **119**, 4819-4880 (2019).

41. Koczkur, K.M., Mourdikoudis, S., Polavarapu, L. & Skrabalak, S.E. Polyvinylpyrrolidone (PVP) in nanoparticle synthesis. *Dalton Trans.* **44**, 17883-17905 (2015).

42. Al-Johani, H. et al. The structure and binding mode of citrate in the stabilization of gold nanoparticles. *Nat. Chem.* **9**, 890-895 (2017).

43. Nie, Z., Petukhova, A. & Kumacheva, E. Properties and emerging applications of self-assembled structures made from inorganic nanoparticles. *Nat. Nanotechnol.* **5**, 15-25 (2010).

44. Reinhard, I., Miller, K., Diepenheim, G., Cantrell, K. & Hall, W.P. Nanoparticle Design Rules for Colorimetric Plasmonic Sensors. *ACS Appl. Nano Mater.* **3**, 4342-4350 (2020).

45. Howes, P.D., Chandrawati, R. & Stevens, M.M. Colloidal nanoparticles as advanced biological sensors. *Science* **346** (2014).

46. Decher, G. Fuzzy nanoassemblies: Toward layered polymeric multicomposites. *Science* **277**, 1232-1237 (1997).

47. Budy, S.M., Hamilton, D.J., Cai, Y., Knowles, M.K. & Reed, S.M. Polymer mediated layer-by-layer assembly of different shaped gold nanoparticles. *J. Colloid Interface Sci.* **487**, 336-347 (2017).

48. Zhang, Y., Lu, F., Yager, K.G., van der Lelie, D. & Gang, O. A general strategy for the DNA-mediated self-assembly of functional nanoparticles into heterogeneous systems. *Nat. Nanotechnol.* **8**, 865-72 (2013).

49. Tian, Y. et al. Ordered three-dimensional nanomaterials using DNA-prescribed and valence-controlled material voxels. *Nat. Mater.* **19**, 789-796 (2020).

50. Kimling, J. et al. Turkevich Method for Gold Nanoparticle Synthesis Revisited. *J. Phys. Chem. B* **110**, 15700-15707 (2006).

Appendix II: Supplementary Information

Multi-dimensional Synthesis for Plasmonic Silver-based Nanoassemblies

Table of Contents

1. Multi-dimensional Synthesis Parameter Space: *1,3-Propanediol Mediated Polyol Synthesis*

Background and Significance: *Solution-based Fabrication of Colloidal Metal Nanostructures.* In general, wet-chemical fabrication approaches for geometry-controlled colloidal metal nanostructures rely on pre-synthesized nanoclusters, so-called nanoparticle seeds. Unfortunately, as these seed-mediated approaches require subsequent synthesis protocols—multi-step syntheses—they favor self-aggregation processes leading to undesirable inhomogeneities in nanostructure growth. These challenges prompted the development of single-step synthesis protocols that do not require the use of pre-synthesized nanoparticle seeds. Meanwhile, after more than 30 years of research and development, single-step polyol syntheses have emerged as the most successful platform to fabricate colloidal metallic nanostructures with well-defined geometries and surface characteristics. However, towards a rational "molecule-like" design of plasmonic nanoassemblies for next-generation nanotechnological devices, straightforward wet-chemical syntheses methods have been largely ignored due to their lack of comprehensive control over the individual nanostructure's materials properties as well as over their packing within the nanoassembly.

Limitations of Current Synthesis Paradigm: *One-dimensional Synthesis Procedures.* While polyol syntheses offer many advantages—low cost, ease of use, and very importantly, already proven scalability for industrial applications—their limitations stem from the current synthesis paradigm relying on one-dimensional synthesis procedures. Current polyol syntheses follow a restricted one-dimensional reaction path within the multi-dimensional synthesis parameter space, which include synthesis parameters such as (i) temperature, (ii) metal salt concentration, (iii) reducing agent identity and (iv) its concentration, (v) interfacial agent molecular weight and (vi) its concentration. As a result, current polyol syntheses are restricted to ***one*** specific nanostructure geometry with ***one*** specific surface characteristic. However, a rational design of plasmonic nanoassemblies requires a fundamental change—a paradigm shift—of current solution-based engineering strategies to access the entire multi-dimensional synthesis parameter space of metal nanostructure synthesis. Here, we report on the development of an innovative multi-dimensional polyol synthesis, which implements flexible reaction paths elegantly evolving from the same base starting point. Indeed, with our polyol synthesis, we provide full access to the multi-dimensional synthesis parameter space allowing for ***unrestrained*** tuning of both nanostructure geometries and surface characteristics; a platform towards envisioning "molecule-like" engineering for plasmonic nanoassemblies.

Innovative Mediating Solvent: *1,3-propanediol.* In previous polyol syntheses, the commonly used reaction mediator is ethylene glycol, which also serves as the reducing agent facilitating the nucleation process of the geometry-controlled formation of metal nanostructure.[1] We discovered that 1,3-propanediol can be used as an innovative mediating solvent for polyol syntheses. We found that 1,3-propanediol allows decoupling the mediating solvent from the reducing agent, which enabled us to utilize novel external reducing agents and provided access to the entire multi-dimensional synthesis parameter space. We hypothesize that the 1,3-propanediol likely accelerates the nucleation process, thereby extending favorable reaction yield and structural homogeneity (of nanostructures within the solution) towards a wide variety of nanostructure geometries (more diverse geometries). Using 1,3-propanediol as an innovative mediating solvent we were able to develop a multi-dimensional 1,3-propanediol-based polyol synthesis allowing fabrication of fully tunable silver nanostructures.

1,3-Propanediol-based Polyol Synthesis: *Protocols for Ag Nanostructure Synthesis.* With our 1,3-propanediol-based polyol platform, we give full access to the multi-dimensional synthesis parameter space allowing for comprehensive control of the plasmonic nanostructure geometry ranging from nanorods, nanocube, nanobars to nanoparticles as illustrated in **Supplementary Figure S1** as well as for control of

their surface characteristics. In the following, a blueprint—basic synthesis method—of 1,3-propanediol mediated polyol synthesis is outlined.

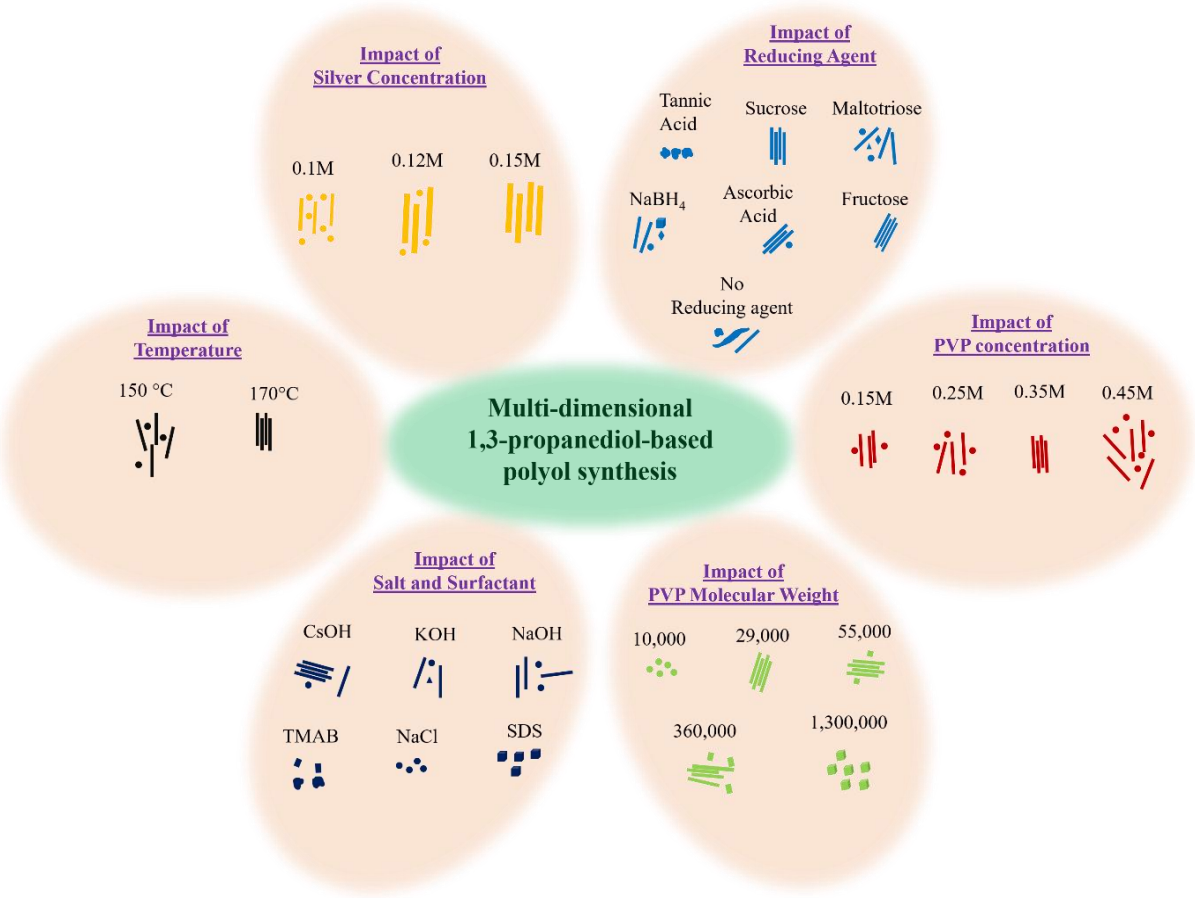

Supplementary Figure S2: Schematic Overview of Ag Nanostructure's Geometries. 1,3-propanediol-based polyol platform that gives full access to the multi-dimensional synthesis parameter space allowing for comprehensive control of the plasmonic nanostructure geometry ranging from nanorods, nanocubes, nanobars to nanoparticles. The impact of various key reactants on the formation of silver nanostructures has been depicted in this schematic overview Figure. Top left-wing—Impact of silver concentration: Three different silver concentrations (0.1M, 0.12M, and 0.15M) were highlighted, and underneath the cartoons of the nanostructures were drawn that obtained during the use of specific silver concentrations mentioned above (**Supplementary Table S27**). Top right-wing—Impact of reducing agent: Six different reducing agents (tannic acid, sucrose, maltotriose, sodium borohydride, ascorbic acid, and fructose) are highlighted and one additional reaction condition is also mentioned where no external reducing agent was used. The cartoons of the obtained silver nanostructures during the use of a specific type of reducing agent are shown in this wing. Tannic acid plays the main role during the polyol synthesis because only silver nanoparticles were obtained during its use where no other geometries such as nanorods, nanobars, and nanocubes were obtained (**Supplementary Table S2**). Sucrose and other carbohydrates such as maltotriose and fructose play an important role during the polyol synthesis because their presence allows the formation of nanorod geometry of the silver nanostructures (**Supplementary Table S10-S12, Supplementary Table 27; Supplementary Figure S17-S21**). Ascorbic acid also plays an important role as a mild reducing agent that allows the formation of silver nanorods (**Supplementary Table S3 and Supplementary Figure S7**). Sodium borohydride is a strong reducing agent that allows the formation of silver nanostructures rapidly with mixed geometries (**Supplementary Figure S9**). Right-wing—Impact of concentration of interfacial agent PVP: Four different repeating unit concentrations of PVP (0.15M, 0.25M, 0.35M, and 0.45M) were used during the different reactions (**Supplementary Table S27**). The cartoons of the obtained silver nanostructures during a specific concentration of PVP are shown in this wing. Bottom right-wing—Impact of molecular weight of PVP on the formation of silver nanostructures: Five different molecular weight of PVP

(10,000, 29,000, 55,000, 360,000, 1,300,000) were used during various reactions (**Supplementary Table S27**). Bottom left-wing—Impact of various salt and surfactant on the formation of silver nanostructures: Six different additives (cesium hydroxide, potassium hydroxide, sodium hydroxide, sodium dodecyl sulfate, sodium chloride, and trimethylammonium bromide) was used and the obtained nanostructures' cartoons are shown underneath. Left-wing—Impact of temperature: Two different temperatures (150°C and 170°C) were used.

General Protocol. Initially, a round bottom flask (25 mL capacity) was filled with 5 mL of "as received" 1,3-propanediol (Sigma Aldrich, 98%) and subsequently heated to 170 °C for one hour (1h) via oil bath under continuous stirring (~500 rpm). After 1h of continuous heating and stirring, all three reactants were added to the flask: metal salt ($AgNO_3$ with varying concentrations), interfacial agent (polyvinylpyrrolidone-PVP with varying molecular weight), and external reducing agents (either ascorbic acid, or tannic acid, or sodium borohydride, or sucrose, or maltotriose, or fructose). The reactants were dissolved in 1,3-propanediol solvent (room temperature) and each loaded into a plastic syringe (size of syringe: 5 mL). While the metal salt and interfacial agent each was dissolved in 3 mL (fixed volume) of 1,3-propanediol, the external reducing agent was dissolved in 1 mL (fixed volume) of 1,3-propanediol. With fixed volume, the concentration of reactants has been varied according to a specific protocol for specific Ag nanostructure synthesis (concentrations can be found **Supplementary Tables S1-S27**). Importantly, all three reactants were added simultaneously (drop-by-drop) over 7 min by continuous stirring at reaction temperature as listed in **Supplementary Tables S1-S27**. An overview of reaction parameters is given in **Supplementary Figure S2**.

For example. To synthesize Ag nanorods with a length of 28 μm ± 6 μm and a diameter of 521 nm ± 20 nm (as displayed in Table S3), we filled 3 mL of 0.15 M $AgNO_3$, 3 mL of 0.35 M PVP-360,000 MW, and 1 mL of 0.1 M ascorbic acid each into a separate syringe. all three reactants were added simultaneously (drop-by-drop) over 7 min by continuous stirring at the reaction temperature of 170°C.

Syringe Pumps. In all synthesis protocols, the three syringes were fixed in a digital syringe pump for precise and simultaneous dropwise addition of all three reactants into the round bottom reaction flask for a time window of 7 min total.

Color Changes During Reaction. As the reactants are added, the color of the solution changes from colorless to light yellow indicating the formation of smaller silver clusters. Meanwhile, small amounts of reaction volumes (300 μL) are collected at different time intervals to allow for real-time analysis of the nanoparticle growth. The reaction proceeds for 1 hour at the specific reaction temperature. The color of the reaction solution at the end of the reaction has appeared as yellowish grey.

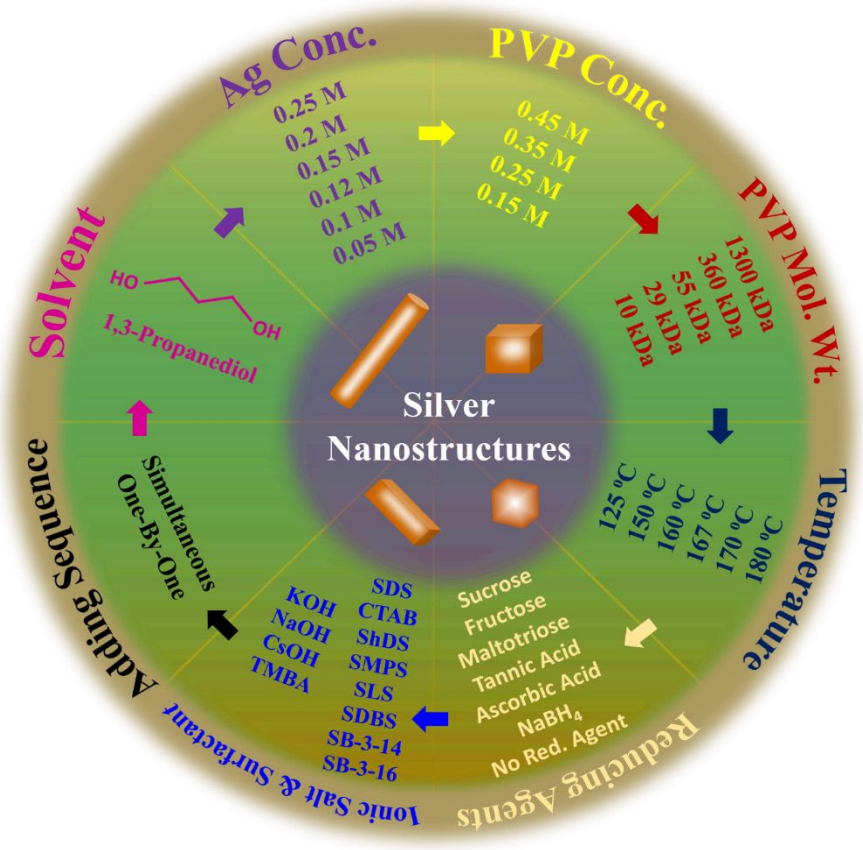

Supplementary Figure S2: Synthesis Parameter Landscape. The complete parameter landscape of the reactants used during the 1,3-propanediol-based synthesis platform for the formation of geometry-controlled silver nanostructures. This schematic Figure shows all reactants were used during different reaction conditions for the formation of geometry-controlled silver nanostructures. The arrows marked in the circle that connects one slice with the other indicate different reactants are interdependent with each other during the polyol synthesis for the formation of geometry-controlled silver nanostructures. That means that one set of reactants *e.g.*, 0.15M $AgNO_3$, 0.35 PVP-360,000, 0.01M sucrose, and 170°C forms the silver nanorods, and other geometry obtained with another set of reactants. Six different concentrations of $AgNO_3$, four different PVP concentrations, five different molecular weights of PVP, six different temperatures, six different reducing agents, and twelve different additives were altered during 200 different reaction conditions. The reactants were added in two different manners: (i) all reactants were added dropwise in 7 min in a simultaneous manner means one drop of $AgNO_3$, next drop of PVP, next drop of external reducing agent, afterward again one drop of $AgNO_3$, next drop of PVP, next drop of an external reducing agent. (ii) all reactants were added dropwise in 7 min in a one-by-one manner means the first full solution of $AgNO_3$ was added dropwise, then PVP solution added in the reaction dropwise, then reducing agent solution added dropwise.

Characterization: *Scanning Electron Microscopy*

The synthesized geometry-controlled silver nanostructures during different reaction conditions were characterized by scanning electron microscopy (SEM) (FEI Helios Nanolab 660 FIB-SEM instrument). First of all, silver nanostructures were washed with double distilled water to remove the impurities and unreacted reactants. Three rounds of centrifugation has been applied at the speed of 11,000 RPM for 12 minutes each during the washing process. Once the nanostructures have been washed, it was diluted with double distilled water (1/25 dilution). The diluted dispersion of the silver nanostructures has been,

afterward, deposited on the clean silicon wafer (500 nm thick, 1 square centimeter diameter). Evaporation of the water has been allowed naturally at room temperature. After the evaporation of water, the silver nanostructures were adsorbed to the silicon surface. Silicon chip later brought into the SEM vacuum chamber and SEM imaging has been captured at 5 KV voltage and 25 PA current.

All obtained SEM images are shown in **Figure 2** of the main manuscript, and all supporting SEM images and their data analysis are provided in **Supplementary Figure S4-S37**. Different reaction conditions are provided in **Supplementary Table S1-S27**. All results listed in the main manuscript and supplementary files were chosen based on the reproducibility of reaction conditions. During the data analysis, multiple SEM images were analyzed, and their details are provided in the captions of all Tables. Representative SEM images and their data analysis are shown here.

Data Analysis *via ImageJ Software:*

ImageJ software has been used to analyze SEM images. For data analysis, a particular SEM image of interest has been selected on the software page and the scalebar icon was applied for specifying the exact diameter at five different places in one nanorod. In this way, the uniformity of the rod can be identified with its standard deviation as shown in **Supplementary Table S1.** Similarly, the diameter of eight different rods in one SEM image has been measured to specify the uniformity of various rods in a single SEM image (**Supplementary Figure S5).** In this manner, all SEM images of various silver nanostructures presented in our manuscript and Supplementary file has been analyzed through ImageJ software.

The data analysis of the synthesized silver nanostructures during the utilization of various external reducing agents, various concentrations of PVP of different molecular weights, and various salts and surfactants are provided in **Supplementary Table S1-S30** and **Supplementary Figure S4-S35.** In all the tables, full reaction conditions, key responsible reactants, diameter and length homogeneity with their standard deviations, and a special note for particular geometry mentioned in the respective tables are provided.

2. Plasmonic Building-block Geometries: *Impact of Reducing Agents on Nanostructure's Geometry*

In the polyol synthesis, the solvent acts as a reaction medium but at the same time a mild reducing agent. Most of the conventional polyol syntheses have been performed by using ethylene glycol as a solvent that also acted as a reducing agent. Hence, the addition of the external reducing agents has been avoided. The advantage of this approach without an external reducing agent has been to proceed with reaction very slowly and allowing the formation of metal nanostructures. However, the major disadvantage is the smaller nanostructures quickly aggregate randomly if even slight changes in the reaction environment are realized. This concern has motivated us to use selected external agents in the innovative 1,3-propanediol polyol synthesis to systematically accelerate the rate of reactions.

The purpose of the addition of external reducing agents during 1,3-propanediol-based polyol synthesis is to speed up the reduction process. We have used a series of external reducing agents based on their strength (weak reducing agent such as sucrose and ascorbic acid to a strong reducing agent such as sodium borohydride). We found that sucrose is playing a key role in the formation of nanorod geometry of silver nanostructures. Similarly, another mild reducing agent ascorbic acid with its concentration in the range between 0.1 M and 0.2 M allows the formation of silver nanorods of tunable aspect ratio (**Supplementary Table S27**). Besides, tannic acid allows the formation of multi-faceted nanoparticles without any other geometries such as cubes and rods. Also, in our work, we found that a strong reducing agent (sodium borohydride) allows the formation of silver nanostructures of mixed geometries (**Supplementary Table S4**). **Supplementary Figure S3** represents the role of a specific type of external reducing agent in the formation of the respective geometry of the silver nanostructures.

In our work, we have mainly focused on four types of external reducing agents: sucrose, ascorbic acid, tannic acid, and sodium borohydride. The presence of sucrose and ascorbic acid in the reaction forms the nanorod geometry, tannic acid is solely responsible for the formation of silver nanoparticles, and silver nanostructures with mixed geometries were obtained during the use of strong reducing agent sodium borohydride. **Supplementary Figure S3** shows key reducing agents and the resultant geometry of the nanostructures during their use.

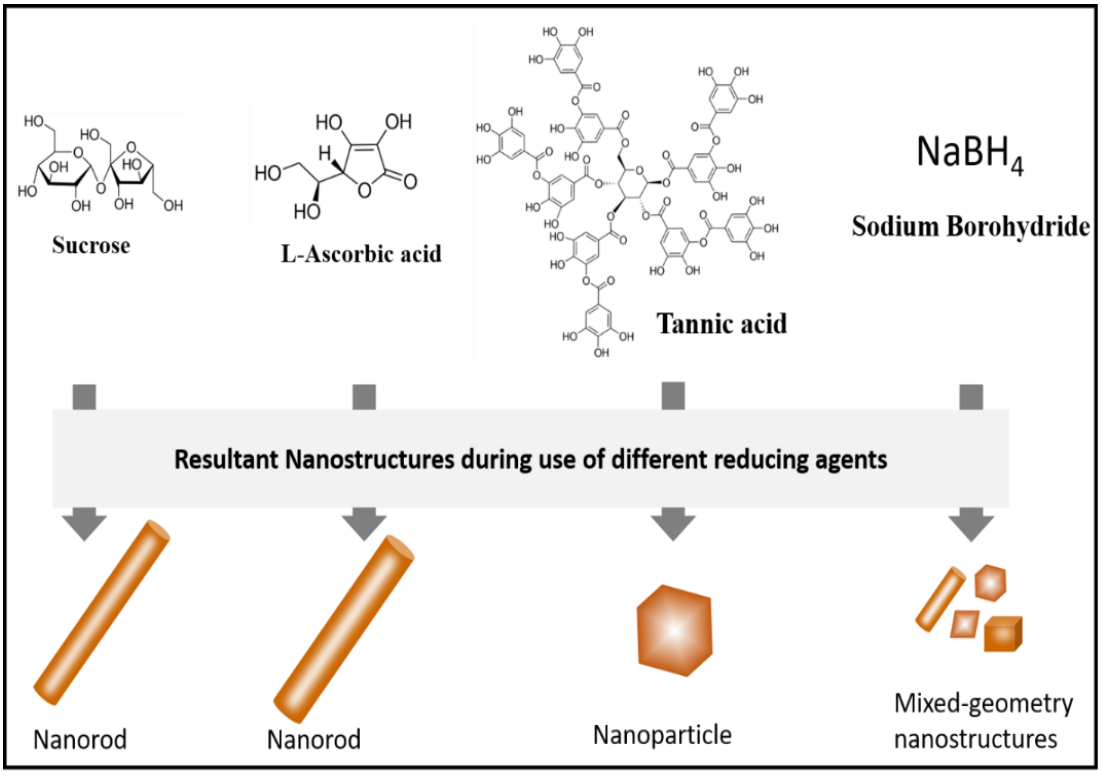

Supplementary Figure S3: Overview of External Reducing Agents and Resulting Ag Nanostructure Geometry. Role of the specific type of reducing agent during the formation of resultant geometry of silver nanostructure. The molecular structure of the reducing shown here, and the resultant geometry of the silver nanostructures are highlighted in this Figure. Silver nanorods were obtained when sucrose and ascorbic acid were used in the reaction. Silver nanoparticles were obtained when tannic acid was used as an external reducing agent. Mixed geometries of the silver nanostructures were obtained when sodium borohydride was used. Full details of various reaction conditions and utilization of external reducing agents are summarized in **Supplementary Table 27.**

In this chapter, data analysis of the silver nanostructures obtained by using various reducing agents is provided. Higher and lower magnified representative SEM images of the silver nanostructures are provided with full details in their captions. Data analysis of the SEM images has been performed by software ImageJ.

Supplementary Table S1: Silver Nanostructures with Nanorod Geometry. Data mentioned in this Table has been analyzed by software ImageJ from the SEM image shown in **Supplementary Figure S5A**. The diameter of the 8 different rods was measured and their average size (length and diameter) is provided in this Table with their standard deviation. The length of the 50 different rods from 10 different SEM images of the same sample has been measured by software ImageJ and their average length with standard deviation is provided in this Table. Furthermore, the diameter at 5 different positions of a single rod #2 (**Supplementary Figure S5A)** has been measured through ImageJ software and its average diameter with standard deviation is written in this Table for identifying the diameter homogeneity of the individual rod. Three representative SEM images at different magnifications are shown in **Supplementary Figure S4 below**.

Geometry	**Rods**
Average Size (Length and Diameter) (with Standard Deviation)	Length: 16 µm ± 2.5 µm Diameter: 214 nm ± 14 nm
Diameter Homogeneity (Individual Rod labeled #2 as shown in **Supplementary Figure S5A)**	211 nm ± 16 nm
Key Responsible Reactant	0.02 M Sucrose
Full Reaction Condition	Pure 1,3-Propanediol (5 mL) 0.15 M $AgNO_3$ (3mL) 0.35 M PVP-360,000 MW (3mL) 0.02 M Sucrose (1 mL) Temp: 170°C
Note	Pure 1,3-propanediol was heated at 170 °C for 90 minutes followed by the dropwise addition of reactants within 8 minutes. The reaction ran for 100 minutes judging from the first addition of $AgNO_3$ to the reaction solution. The color of the solution was a yellowish-grey at the end of the reaction.

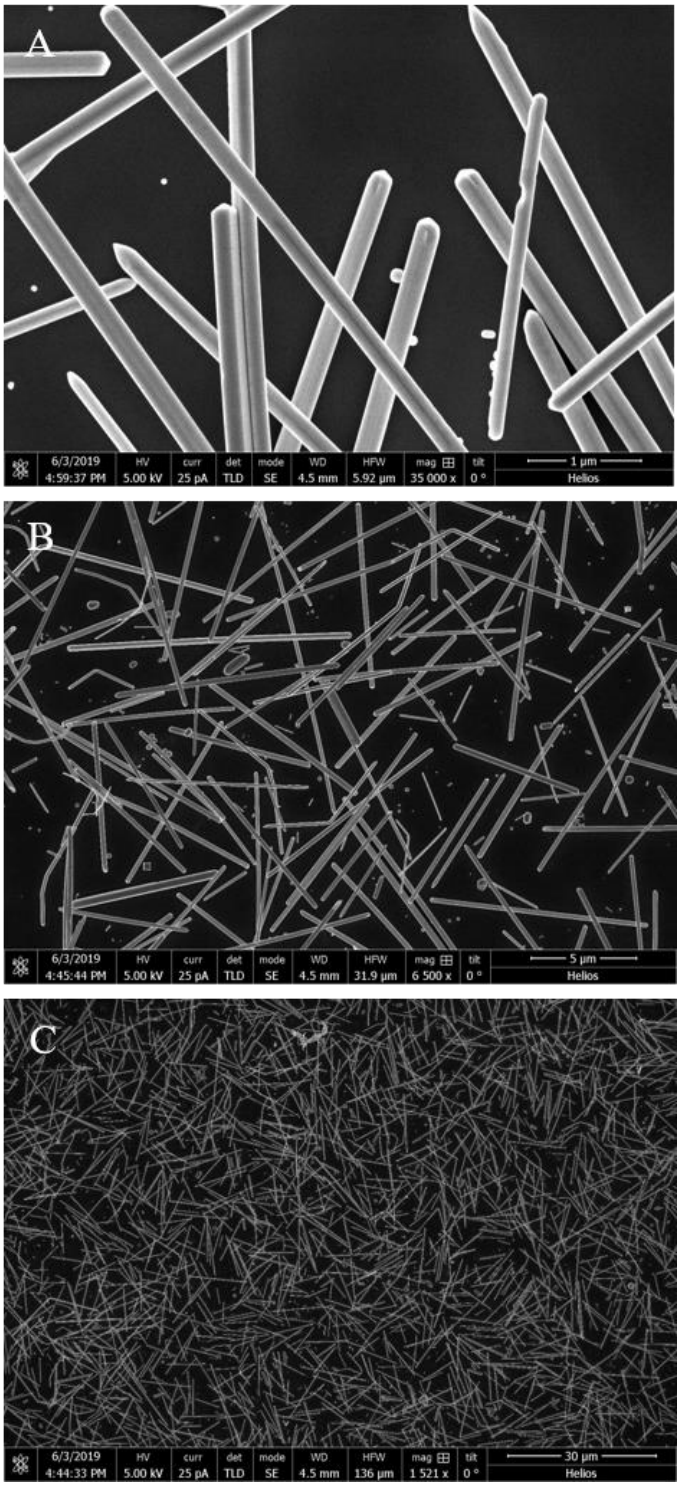

Supplementary Figure S4. (A-C) Three Representative SEM images of Silver Nanostructures with Nanorod Geometry at Three Different Magnifications. The full reaction condition for the silver nanostructures shown in this Figure is provided in **Supplementary Table S1** above. Also, the data analysis for these SEM images was performed by software ImageJ that is shown in **Supplementary Figure S5B-C** below, and their average value with their standard deviation is mentioned in **Supplementary Table S1** above.

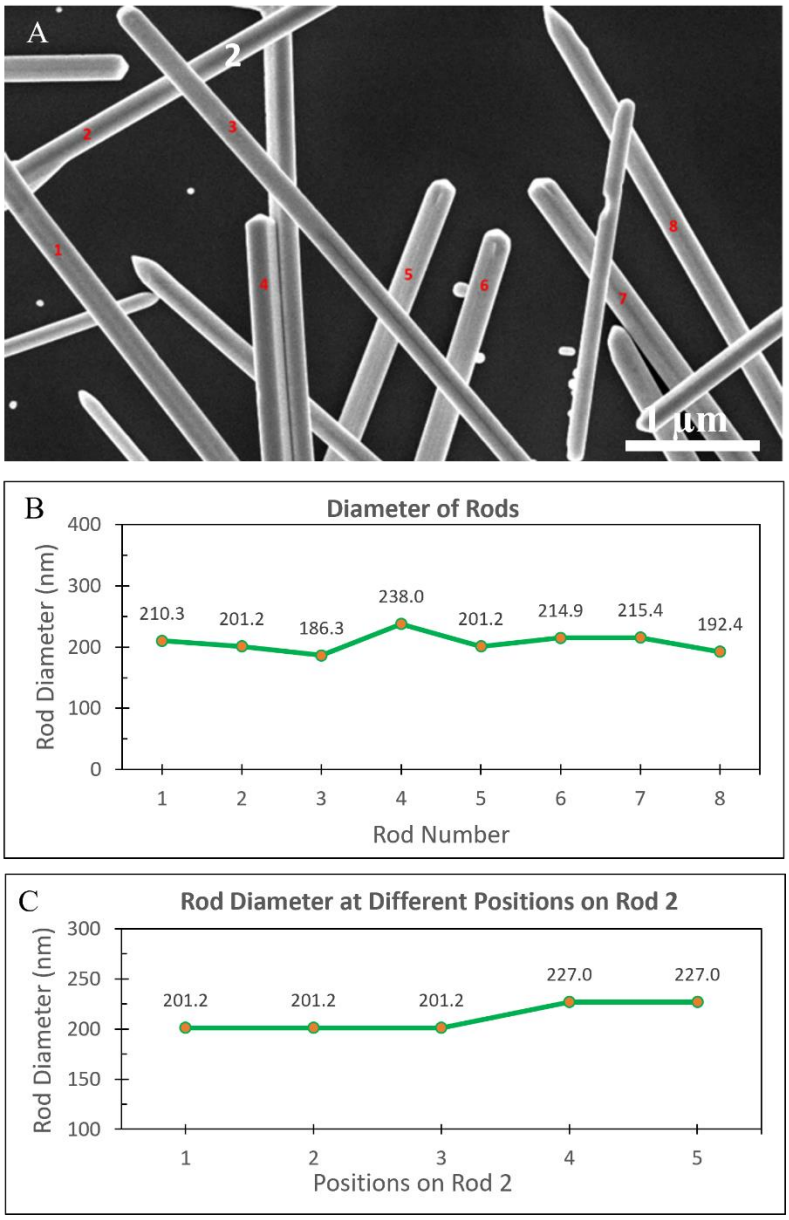

Supplementary Figure S5. (A) Representative SEM image of Silver Nanostructures with Nanorod Geometry obtained during the reaction condition provided in **Supplementary Table S1** above. (B) The diameter of 8 different rods marked in (A) measured by software ImageJ. (C) The diameter of rod #2 marked in (A) at five different positions measured by software ImageJ.

Supplementary Table S2: Multi-faceted Silver Nanoparticles. Data mentioned in this Table has been analyzed during the SEM characterization by using the imaging software of the FEI Helios Nanolab 660 FIB-SEM. Three different SEM images of the same reaction sample are shown in **Supplementary Figure S6**. The diameter of 50 different nanoparticles from 3 different SEM images shown in **Supplementary Figure S6** was measured and their average value with standard deviation is provided in this Table. Also, the diameter of a single nanoparticle at five different positions marked with * in **Supplementary Figure S6A** has been measured.

Geometry	**Multi-Faceted Nanoparticles**
Average Nanoparticle Size (with Std. Deviation)	Size: 85 nm ± 20 nm
Homogeneity of individual nanoparticle (marked* in the image shown in **Supplementary Figure S6A**; dimensions measured at 5 different positions**)**	Size: 82 nm ± 7 nm
Key Responsible Reactant	0.04 M Tannic Acid
Full reaction Condition:	Pure 1,3-Propanediol (5 mL) 0.15 M $AgNO_3$ (3mL) 0.35 M PVP-360,000 MW (3mL) 0.04 M Tannic Acid (1 mL) Temp: 170°C
Note	Pure 1,3-propanediol was heated to 170 °C for 90 minutes followed by the dropwise addition of reactants within 6 minutes. The reaction ran for 60 minutes judging from the first addition of $AgNO_3$ to the reaction solution. The color of the solution was dark brown at the end of the reaction.

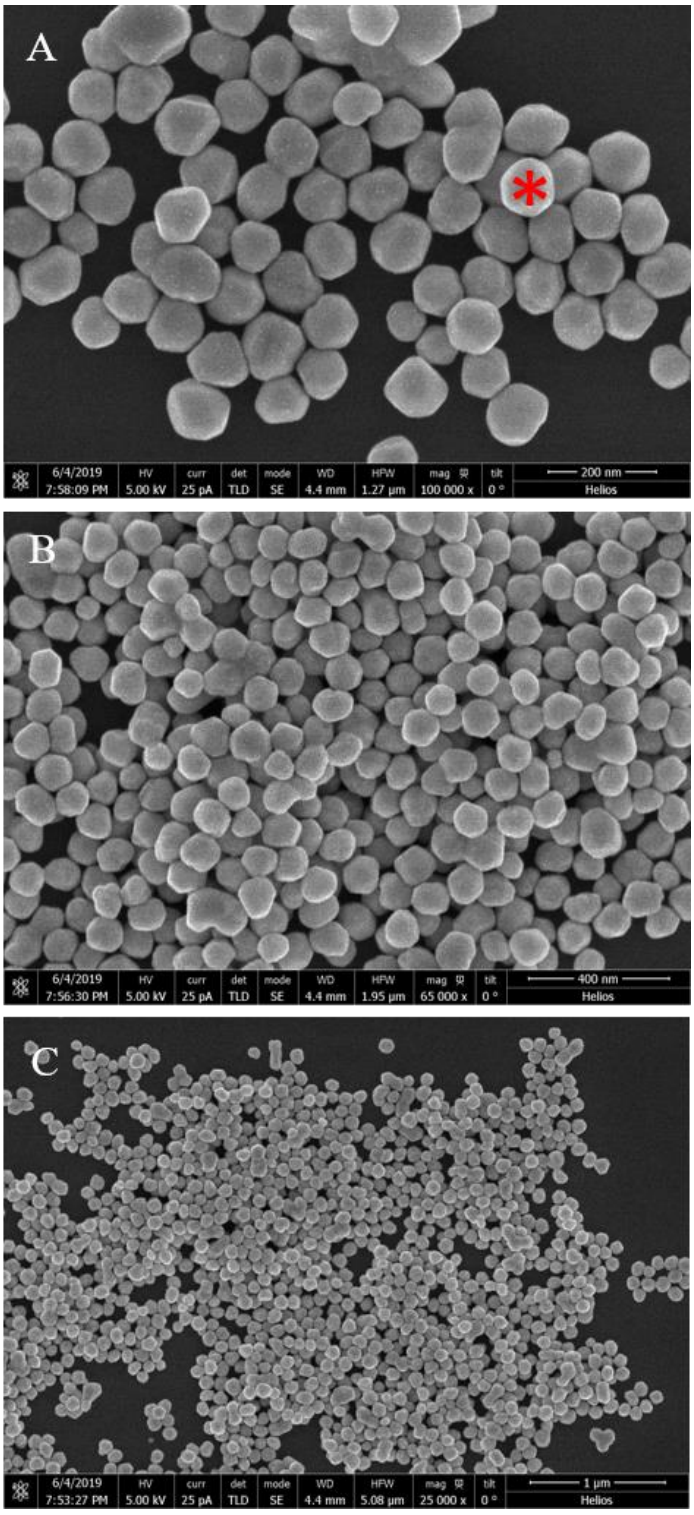

Supplementary Figure S6. (A-C) Three Representative SEM images of Silver Nanoparticles at Three Different Magnifications. The full reaction condition for the silver nanoparticles shown in this Figure is provided in **Supplementary Table S2** above. Also, the data analysis for these SEM images was performed during the SEM characterization and their average size together with standard deviation is mentioned in **Supplementary Table S2** above.

Supplementary Table S3: Silver Nanostructures with Nanorod Geometry. Data mentioned in this Table has been analyzed by software ImageJ from the SEM image shown in **Supplementary Figure S8A**. The diameter of the 4 different rods was measured and their average size (length and diameter) is provided in this Table with their standard deviation. The length of the 50 different rods from 10 different SEM images of the same sample has been measured by software ImageJ and their average length with standard deviation is provided in this Table. Furthermore, the diameter at 10 different positions of a single rod #4 (**Supplementary Figure S8A)** has been measured through ImageJ software and its average diameter with standard deviation is written in this Table for identifying the diameter homogeneity of the individual rod. Three representative SEM images at different magnifications are shown in **Supplementary Figure S7 below**.

Geometry	**Rods**
Average Size (Length and Diameter) (With Std. Deviation)	Length: 8 µm ± 3 µm Diameter: 521 nm ± 20 nm
Diameter Homogeneity (Single Rod #4 as shown in **Supplementary Figure S8A)**	502 nm ± 8.2 nm
Key Responsible Reactant	0.1 M Ascorbic Acid
Full Reaction Condition	Pure 1,3-Propanediol (5 mL) 0.15 M $AgNO_3$ (3mL) 0.35 M PVP-360,000 MW (3mL) 0.1 M Ascorbic Acid (1 mL) Temp: 170°C
Note	Pure 1,3-propanediol was heated to 170 °C for 90 minutes followed by the dropwise addition of reactants within 7 minutes. The reaction ran for 70 minutes judging from the first addition of $AgNO_3$ to the reaction solution. The color of the solution was a yellowish grey at the end of the reaction.

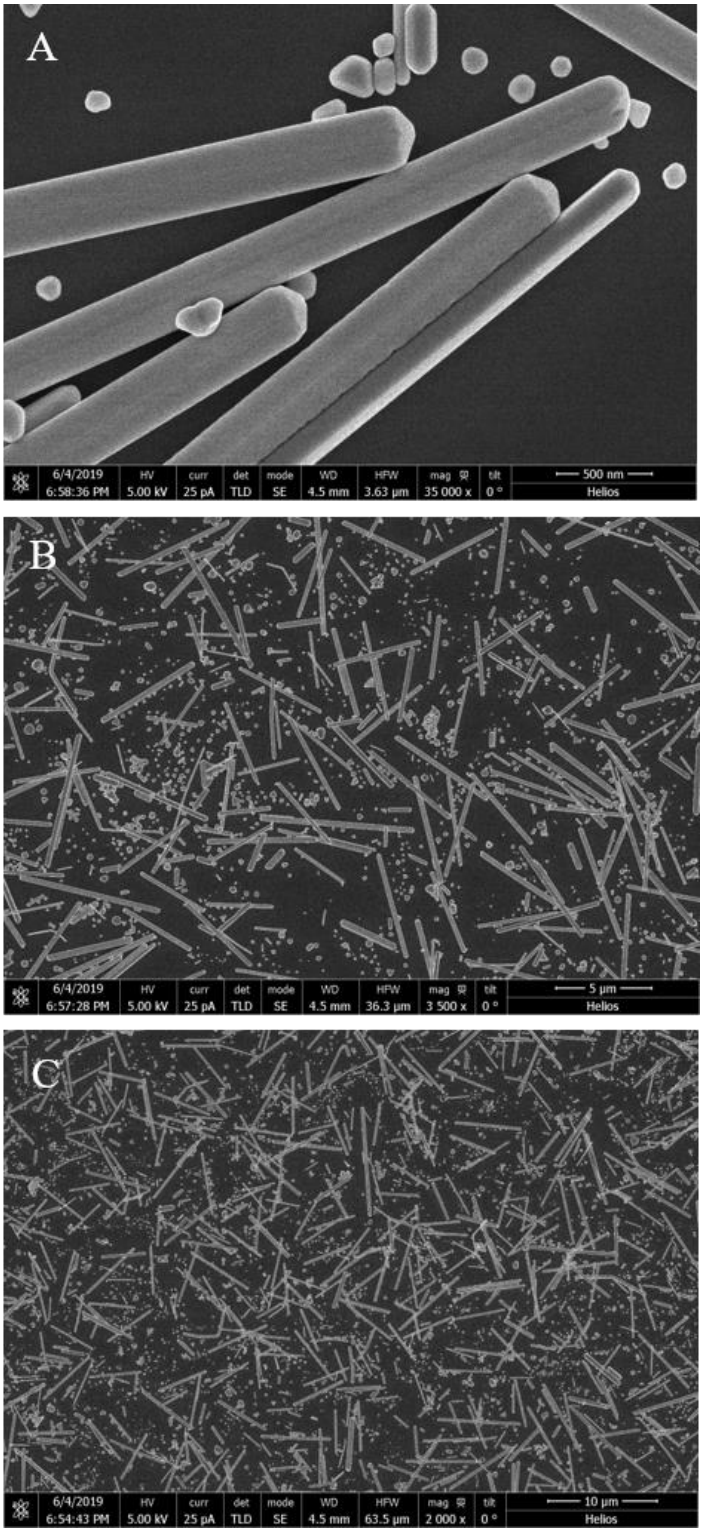

Supplementary Figure S7. (A-C) Three Representative SEM images of Silver Nanostructures with Nanorod Geometry at Three Different Magnifications. The full reaction condition for the silver nanostructures shown in this Figure is provided in **Supplementary Table S3** above. Also, the data analysis for these SEM images was performed by software ImageJ that is shown in **Supplementary Figure S8B-C** below, and their average value with their standard deviation is mentioned in **Supplementary Table S3** above.

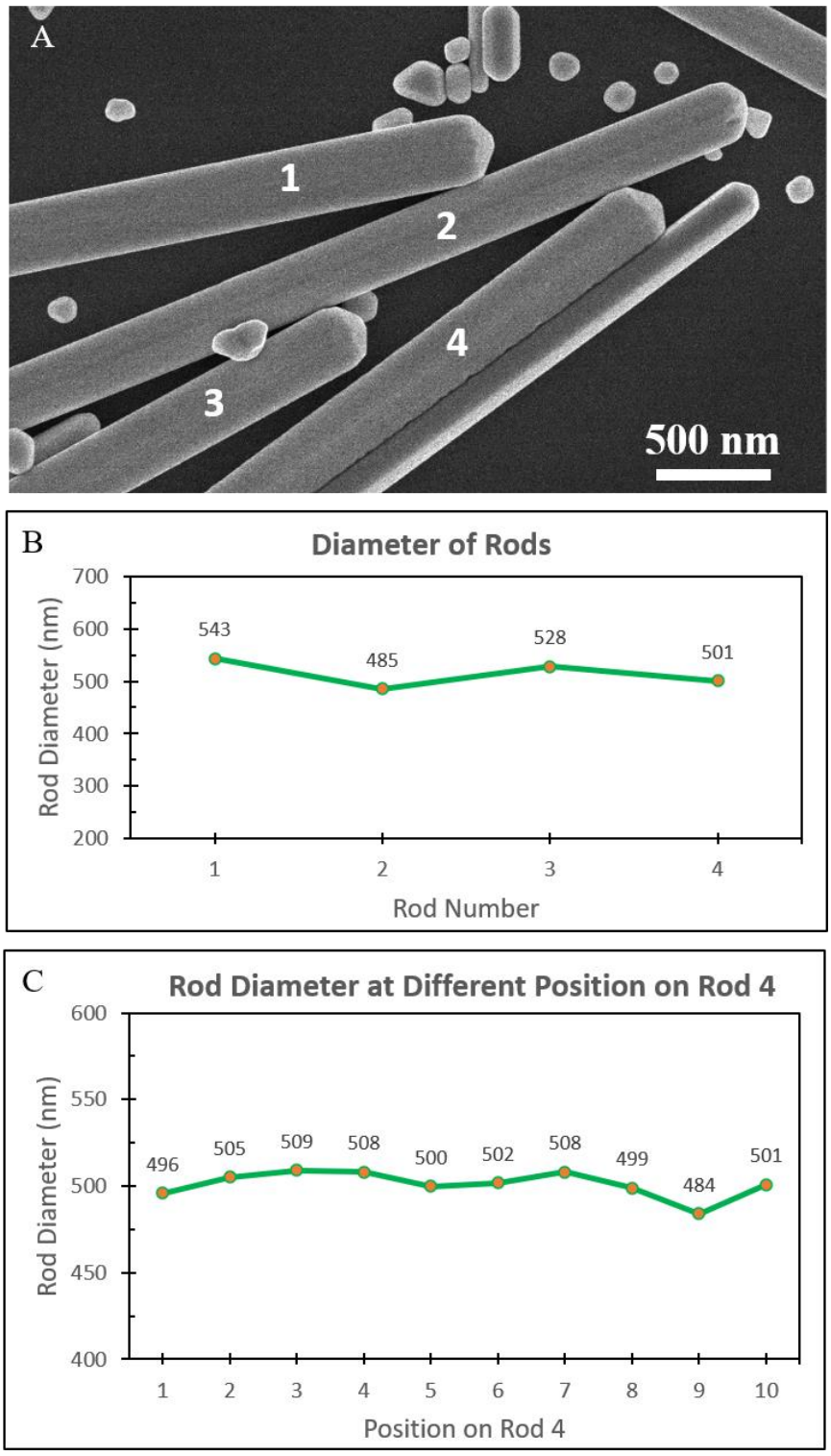

Supplementary Figure S8. (A) Representative SEM image of Silver Nanostructures with Nanorod Geometry obtained during the reaction condition provided in **Supplementary Table S3** above. (B) The diameter of 4 different rods marked in (A) measured by software ImageJ. (C) The diameter of rod #4 marked in (A) at 10 different positions measured by software ImageJ.

Supplementary Table S4: Silver Nanostructures with Nanoparticles and Nanorods (Mix-geometry). Data mentioned in this Table has been analyzed during the SEM characterization by using the imaging software of the FEI Helios Nanolab 660 FIB-SEM. Three different SEM images of the same reaction sample are shown in **Supplementary Figure S9**. The diameter of 50 different nanostructures (25 nanoparticles + 25 nanorods) from 3 different SEM images shown in **Supplementary Figure S9** was measured and their average value with standard deviation is provided in this Table. Also, the diameter of a single nanorod at five different positions marked with * in **Supplementary Figure S9A** has been measured.

Geometry	**Nanorods + Nanoparticles**
Average Size (With Std. Deviation)	Average Rod Length: 450 nm ± 60 nm Average Rod Diameter: 155 nm ± 35 nm Average Particle Size: 180 nm ± 60 nm
Diameter Homogeneity (Single Rod) (marked* in the image shown in **Supplementary Figure S9A**; diameter measured at 5 different positions)	140 nm ± 16 nm
Key Responsible Reactant	0.02 M $NaBH_4$
Full Reaction Condition	Pure 1,3-Propanediol (5 mL) 0.15 M $AgNO_3$ (3mL) 0.35 M PVP-360,000 MW (3mL) 0.02 M $NaBH_4$ (1 mL) Temp: 170°C
Note	Pure 1,3-propanediol was heated to 170 °C for 90 minutes followed by the dropwise addition of reactants within 4 minutes. The reaction ran for 30 minutes judging from the first addition of $AgNO_3$ to the reaction solution. The color of the solution was a greenish-grey at the end of the reaction.

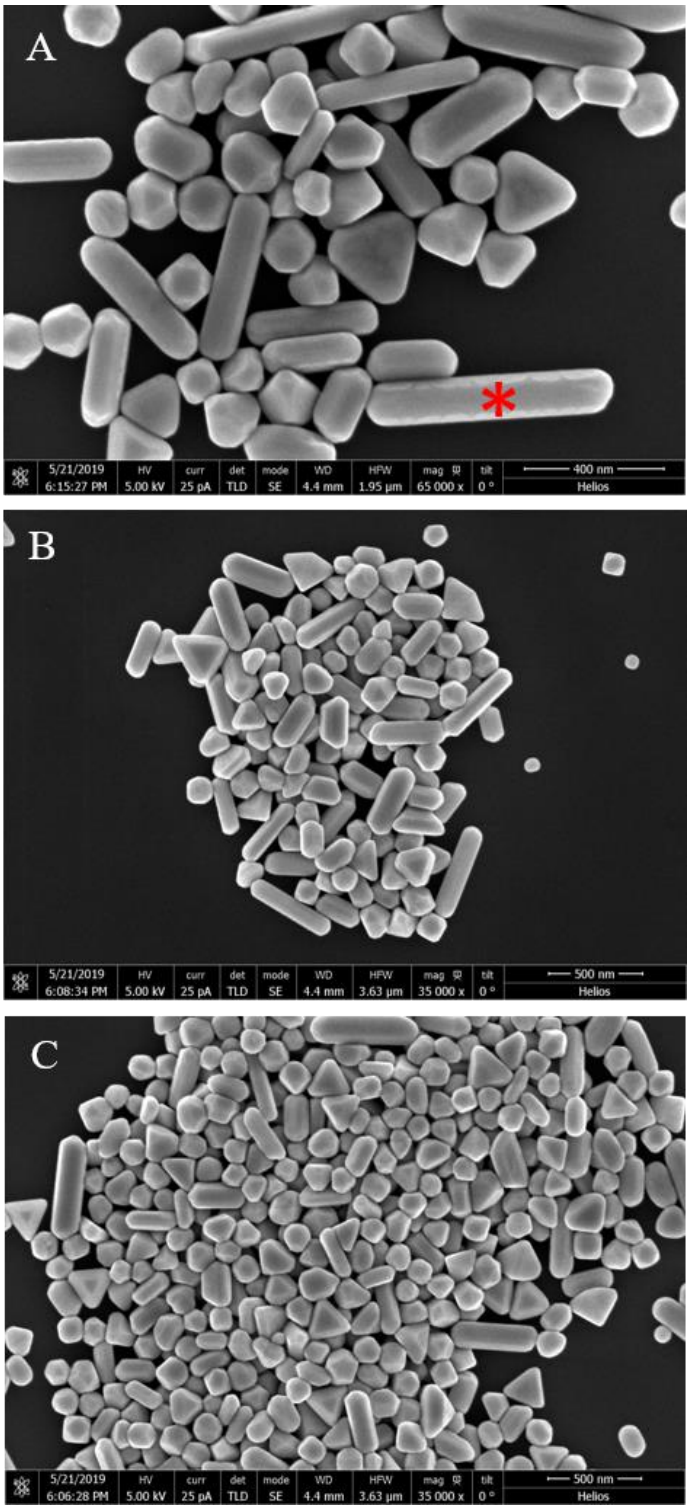

Supplementary Figure S9. (A-C) Three Representative SEM images of Silver Nanostructures at Three Different Magnifications. The full reaction condition for the silver nanostructures shown in this Figure is provided in **Supplementary Table S4** above. Also, the data analysis for these SEM images was performed during the SEM characterization and their average size together with standard deviation is mentioned in **Supplementary Table S4** above.

Supplementary Table S5: Silver Nanostructures with Nanorod Geometry. Data mentioned in this Table has been analyzed by software ImageJ from the SEM image shown in **Supplementary Figure S11A**. The diameter of the 4 different rods was measured and their average size (length and diameter) is provided in this Table with their standard deviation. The length of the 50 different rods from 10 different SEM images of the same sample has been measured by software ImageJ and their average length with standard deviation is provided in this Table. Furthermore, the diameter at 10 different positions of a single rod #1 (**Supplementary Figure S11A)** has been measured through ImageJ software and its average diameter with standard deviation is written in this Table for identifying the diameter homogeneity of the individual rod. Two representative SEM images at different magnifications are shown in **Supplementary Figure S10 below**.

Geometry	**Rods**
Average Size (Length + Diameter) (With Std. Deviation)	Length: 22 µm ± 8 µm Diameter: 316 nm ± 41 nm
Diameter Homogeneity (Single Rod #1 as shown in **Supplementary Figure S11A)**	327 nm ± 8 nm
Key Responsible Reactant	0.02 M Sucrose 0.2 M Silver Nitrate
Full Reaction Condition	Pure 1,3-Propanediol (5 mL) 0.2 M $AgNO_3$ (3mL) 0.35 M PVP-360,000 MW (3mL) 0.02 M Sucrose (1 mL) Temp: 160°C
Note	Pure 1,3-propanediol was heated to 160 °C for 90 minutes followed by the dropwise addition of reactants within 7 minutes. The reaction ran for 90 minutes judging from the first addition of $AgNO_3$ to the reaction solution. The color of the solution was a yellowish grey (dark) at the end of the reaction.

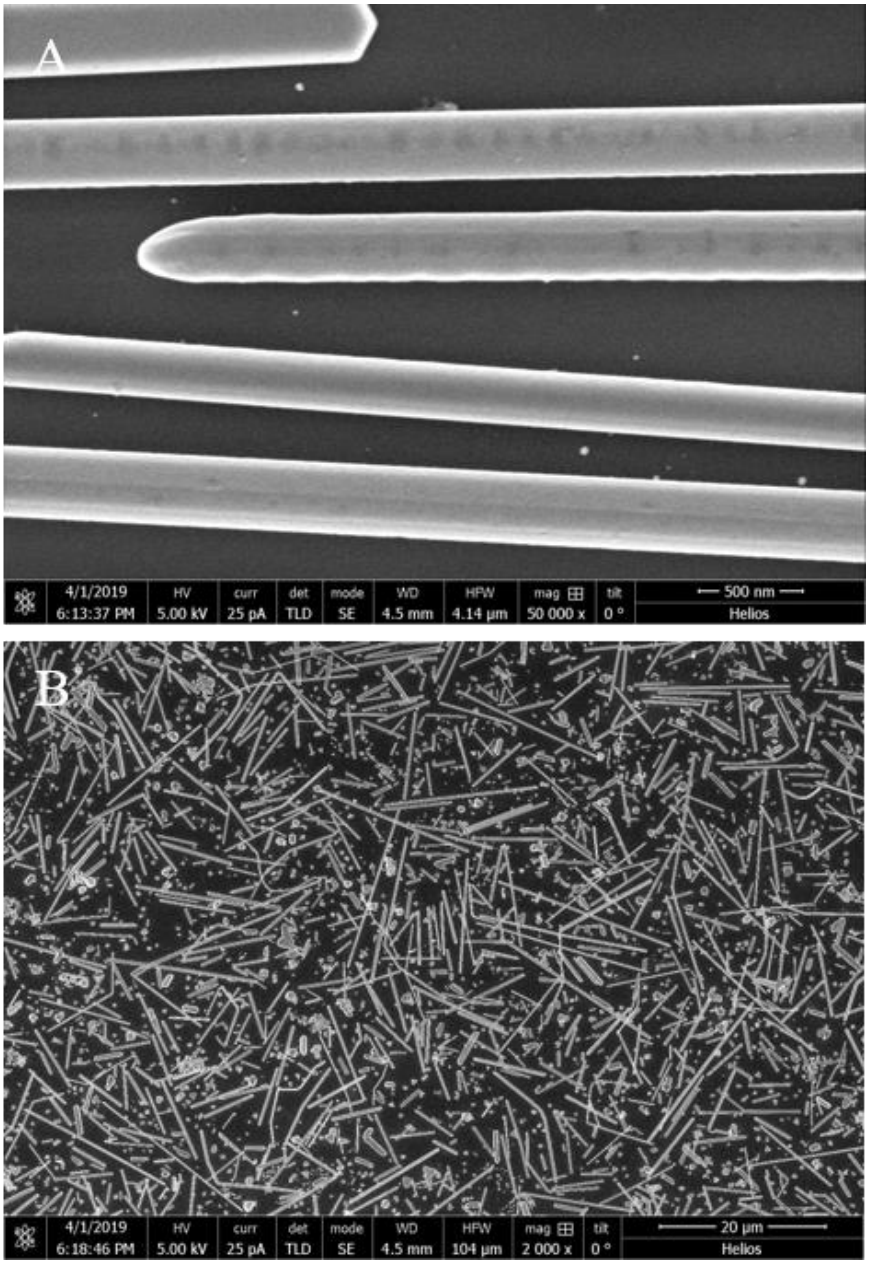

Supplementary Figure S10. (A-C) Two Representative SEM images of Silver Nanostructures with Nanorod Geometry at Two Different Magnifications. The full reaction condition for the silver nanostructures shown in this Figure is provided in **Supplementary Table S5** above. Also, the data analysis for these SEM images was performed by software ImageJ that is shown in **Supplementary Figure S11B-C** below, and their average value with their standard deviation is mentioned in **Supplementary Table S5** above.

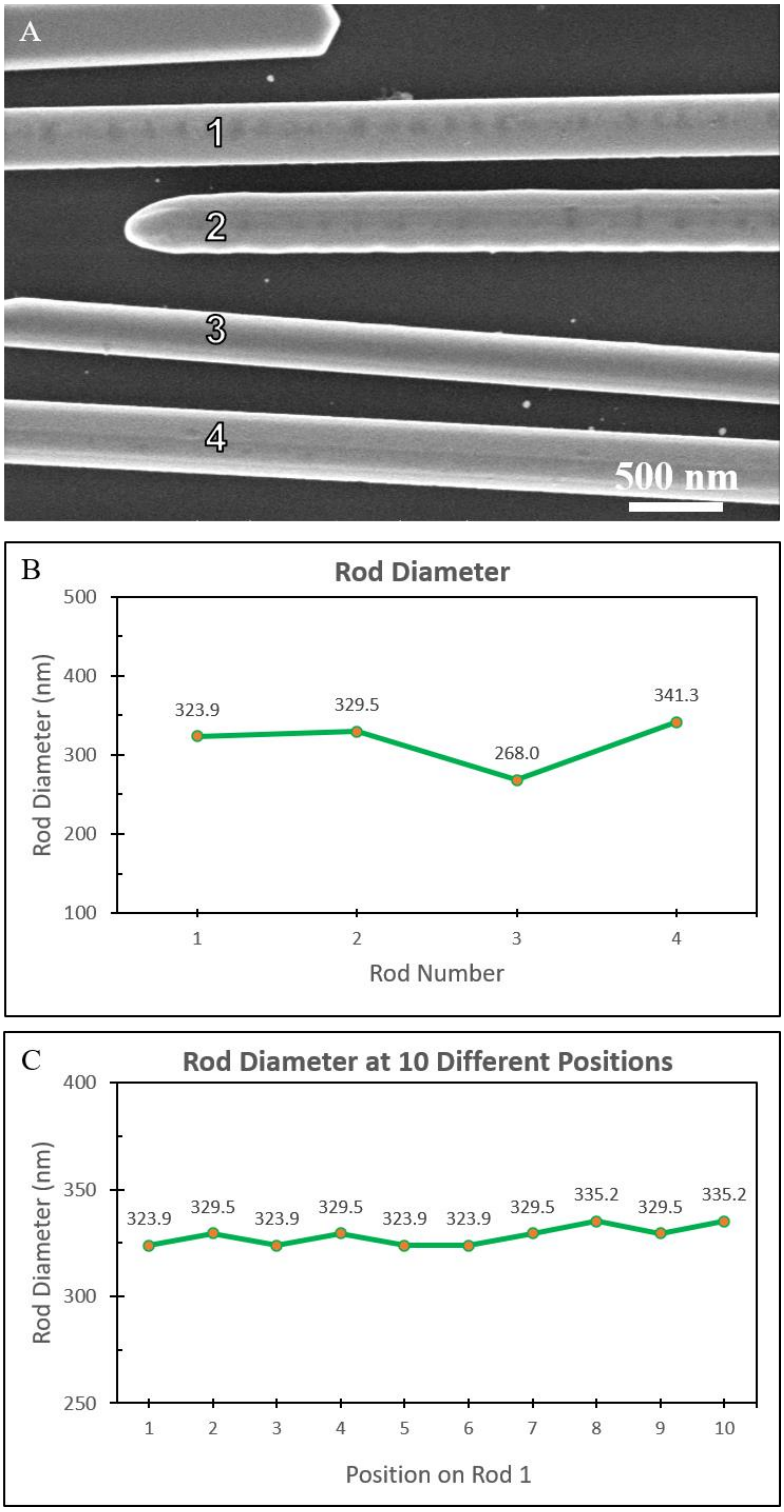

Supplementary Figure S11. (A) Representative SEM image of Silver Nanostructures with Nanorod Geometry obtained during the reaction condition provided in **Supplementary Table S5** above. (B) The diameter of 4 different rods marked in (A) measured by software ImageJ. (C) The diameter of rod #1 marked in (A) at 10 different positions measured by software ImageJ.

Supplementary Table S6: Silver Nanostructures with Nanorod Geometry. Data mentioned in this Table has been analyzed by software ImageJ from the SEM image shown in **Supplementary Figure S13A**. The diameter of the 6 different rods was measured and their average size (length and diameter) is provided in this Table with their standard deviation. The length of the 50 different rods from 10 different SEM images of the same sample has been measured by software ImageJ and their average length with standard deviation is provided in this Table. Furthermore, the diameter at 10 different positions of a single rod #6 (**Supplementary Figure S13A)** has been measured through ImageJ software and its average diameter with standard deviation is written in this Table for identifying the diameter homogeneity of the individual rod. Three representative SEM images at different magnifications are shown in **Supplementary Figure S12 below**.

Geometry	**Rods**
Average Size (Length and Diameter) (With Std. Deviation)	Average Length: 3.0 µm ± 0.8 µm Average Diameter: 80 nm ± 9 nm
Diameter Homogeneity (Single Rod #6 as shown in **Supplementary Figure S13A)**	90 nm ± 4.2 nm
Key Responsible Reactant	0.1 M Ascorbic Acid 0.2 M Silver Nitrate
Full Reaction Condition	Pure 1,3-Propanediol (5 mL) 0.2 M $AgNO_3$ (3mL) 0.35 M PVP-360,000 MW (3mL) 0.1 M Ascorbic Acid (1 mL) Temp: 160°C
Note	Pure 1,3-propanediol was heated to 160 °C for 90 minutes followed by the dropwise addition of reactants within 8 minutes. The reaction ran for 90 minutes judging from the first addition of $AgNO_3$ to the reaction solution. The color of the solution was a dark yellowish grey at the end of the reaction.

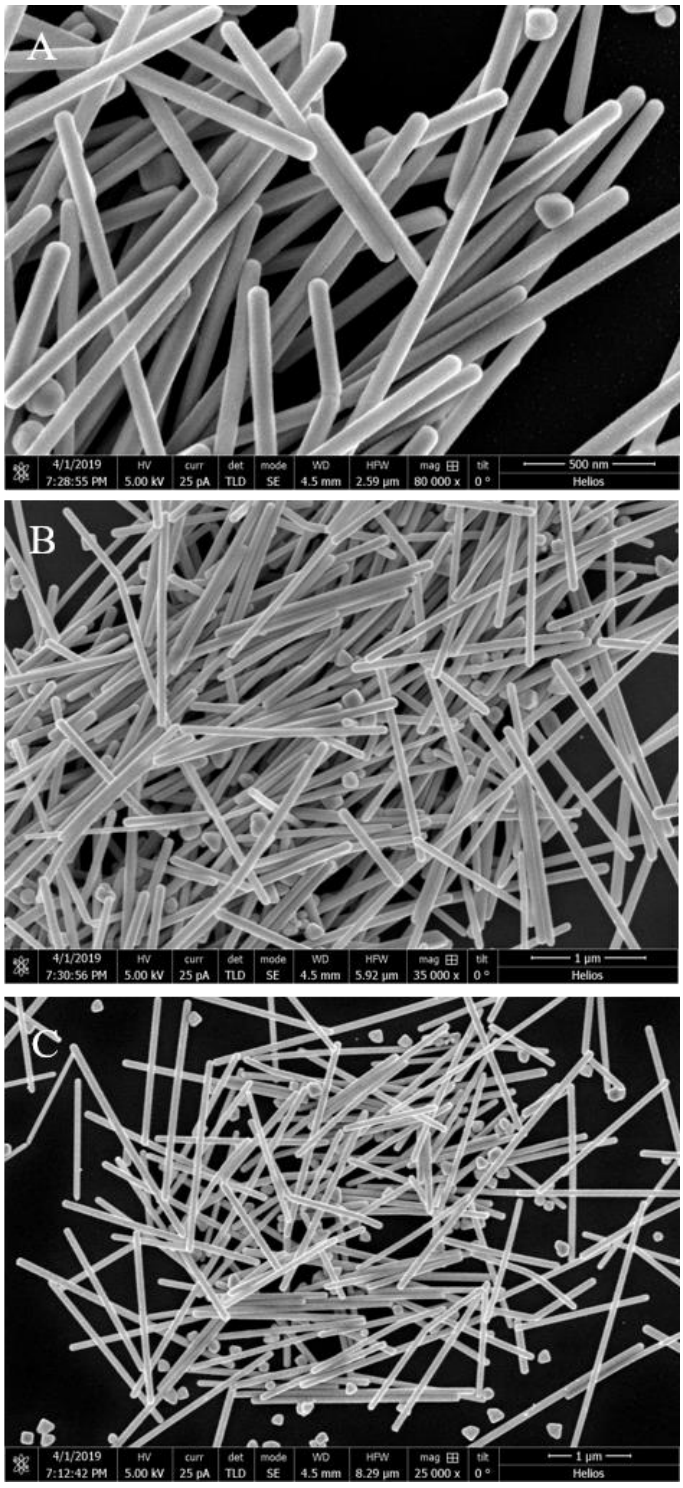

Supplementary Figure S12. (A-C) Three Representative SEM images of Silver Nanostructures with Nanorod Geometry at Three Different Magnifications. The full reaction condition for the silver nanostructures shown in this Figure is provided in **Supplementary Table S6** above. Also, the data analysis for these SEM images was performed by software ImageJ that is shown in **Supplementary Figure S13B-C** below, and their average value with their standard deviation is mentioned in **Supplementary Table S6** above.

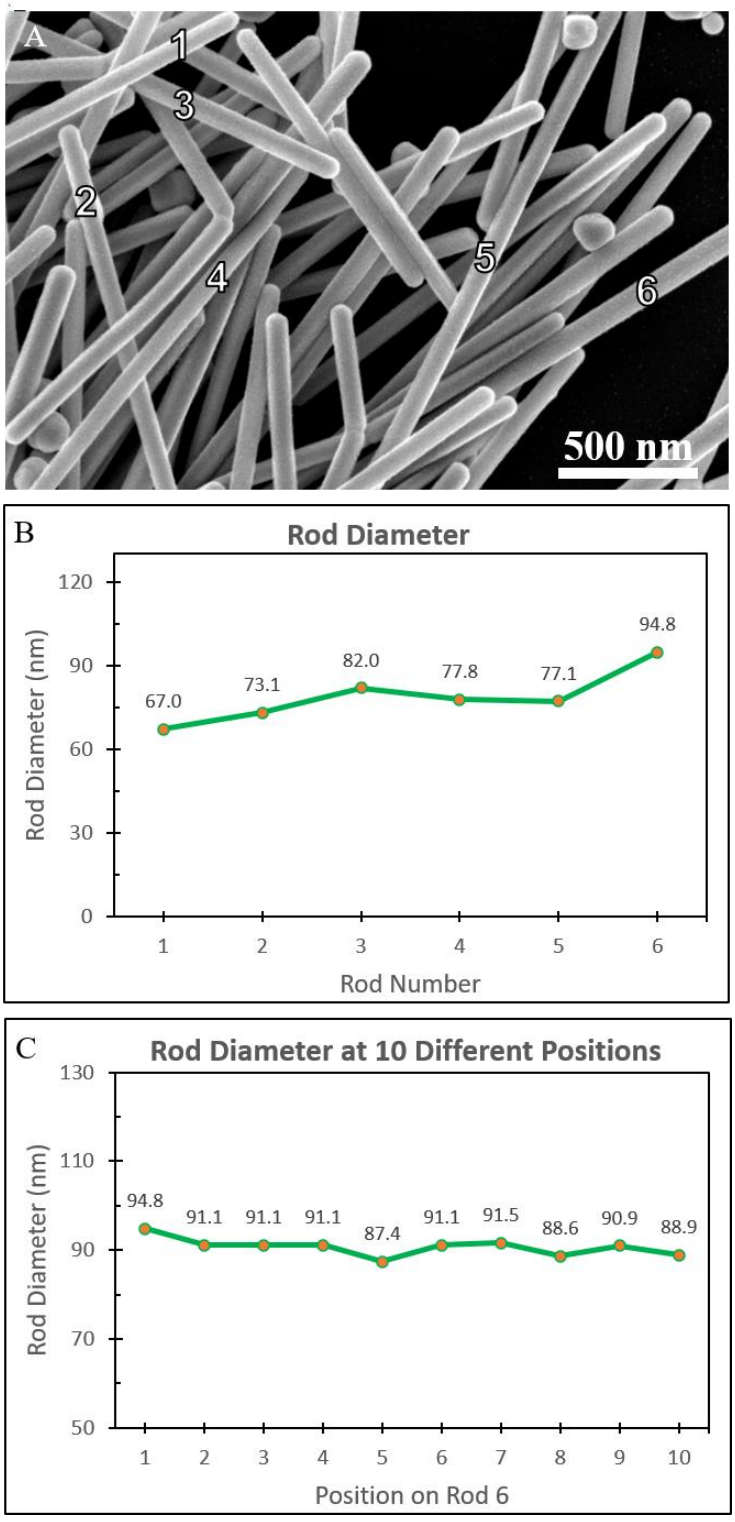

Supplementary Figure S13. (A) Representative SEM image of Silver Nanostructures with Nanorod Geometry obtained during the reaction condition provided in **Supplementary Table S6** above. (B) The diameter of 6 different rods marked in (A) measured by software ImageJ. (C) The diameter of rod #6 marked in (A) at 10 different positions measured by software ImageJ.

Supplementary Table S7: Silver Nanostructures with Nanorod Geometry. Data mentioned in this Table has been analyzed by software ImageJ from the SEM image shown in **Supplementary Figure S14A**. The diameter of the 4 different rods was measured and their average size (length and diameter) is provided in this Table with their standard deviation. The length of the 50 different rods from 10 different SEM images of the same sample has been measured by software ImageJ and their average length with standard deviation is provided in this Table. Furthermore, the diameter at 5 different positions of a single rod #3 (**Supplementary Figure S14A)** has been measured through ImageJ software and its average diameter with standard deviation is written in this Table for identifying the diameter homogeneity of the individual rod.

Geometry	**Rods**
Average Size (Length and Diameter) (With Std. Deviation)	Average Length: 3.6 µm ± 2.2 µm Average Diameter: 430 nm ± 45 nm
Diameter Homogeneity (Single Rod #3 as shown in **Supplementary Figure S14A)**	371 nm ± 41 nm
Key Responsible Reactant	0.15 M Ascorbic Acid 0.15 M Silver Nitrate
Full Reaction Condition	Pure 1,3-Propanediol (5 mL) 0.15 M $AgNO_3$ (3mL) 0.35 M PVP-55,000 MW (3mL) 0.15 M Ascorbic Acid (1 mL) Temp: 170°C
Note	Pure 1,3-propanediol was heated to 170 °C for 90 minutes followed by the dropwise addition of reactants within 4 minutes. The reaction ran for 35 minutes judging from the first addition of $AgNO_3$ to the reaction solution. The color of the solution was a dark greenish grey at the end of the reaction.

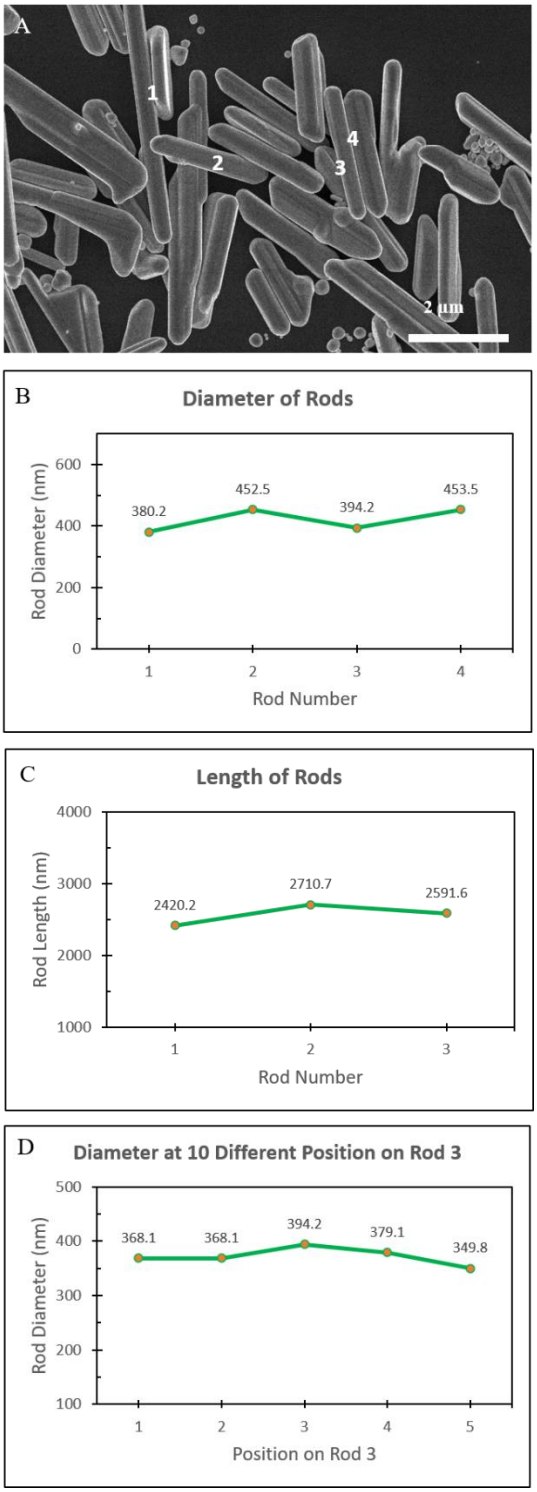

Supplementary Figure S14. (A) Representative SEM image of Silver Nanostructures with Nanorod Geometry obtained during the reaction condition provided in **Supplementary Table S7** above. (B) The diameter of 4 different rods marked in (A) measured by software ImageJ. (C) The length of 3 different rods marked in (A) measured by software ImageJ. (D) The diameter of rod #3 marked in (A) at 5 different positions measured by software ImageJ.

We found that carbohydrates are also playing roles as milder reducing agents during 1,3-propanediol-based polyol synthesis in controlling geometries of the silver nanostructures. Therefore, we have used different carbohydrates (sucrose, fructose, and maltotriose) during the syntheses. The reaction conditions by using various carbohydrates in various concentrations, data analysis, and observation during the reaction have been provided in **Supplementary Table S8-S12.**

Supplementary Table S8: Silver Nanostructures with Nanorod Geometry. Data mentioned in this Table has been analyzed by software ImageJ from the SEM image shown in **Supplementary Figure S16A**. The diameter of the 6 different rods was measured and their average size (length and diameter) is provided in this Table with their standard deviation. The length of the 50 different rods from 10 different SEM images of the same sample has been measured by software ImageJ and their average length with standard deviation is provided in this Table. Furthermore, the diameter at 10 different positions of a single rod #4 (**Supplementary Figure S16A)** has been measured through ImageJ software and its average diameter with standard deviation is written in this Table for identifying the diameter homogeneity of the individual rod. Two representative SEM images at different magnifications are shown in **Supplementary Figure S15 below**.

Geometry	**Rods**
Average Size (Length and Diameter) (With Std. Deviation)	Average Length: 16 µm ± 7 µm Diameter: 250 nm ± 42 nm
Diameter Homogeneity (Single Rod #4 as shown in **Supplementary Figure S16A)**	281 nm ± 4.6 nm
Key Responsible Reactant	0.01 M Sucrose
Full Reaction Condition	Pure 1,3-Propanediol (5 mL) 0.15 M $AgNO_3$ (3mL) 0.35 M PVP-360,000 MW (3mL) 0.01 M Sucrose (1 mL) Temp: 167°C
Note	Pure 1,3-propanediol was heated to 167 °C for 90 minutes followed by the dropwise addition of reactants within 4 minutes. The reaction ran for 70 minutes judging from the first addition of $AgNO_3$ to the reaction solution. The color of the solution was a yellowish grey at the end of the reaction.

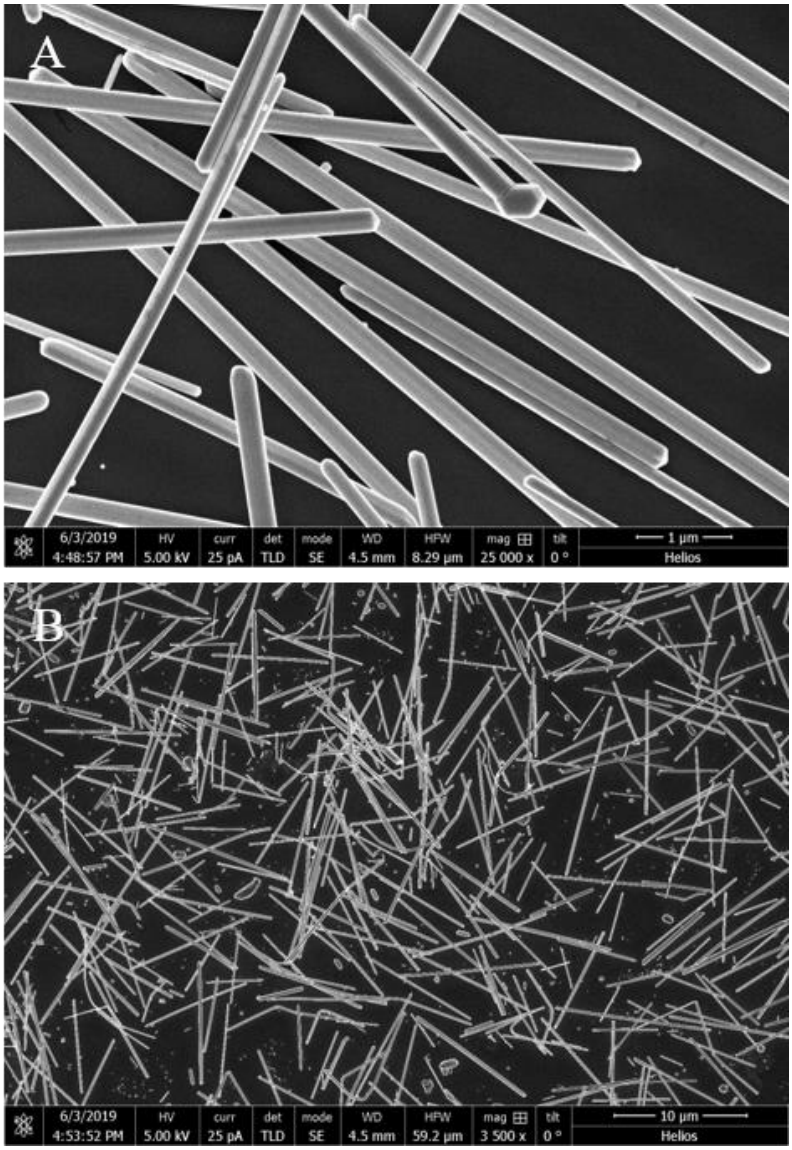

Supplementary Figure S15. (A-B) Two Representative SEM images of Silver Nanostructures with Nanorod Geometry at Two Different Magnifications. The full reaction condition for the silver nanostructures shown in this Figure is provided in **Supplementary Table S8** above. Also, the data analysis for these SEM images was performed by software ImageJ that is shown in **Supplementary Figure S16B-C** below, and their average value with their standard deviation is mentioned in **Supplementary Table S8** above.

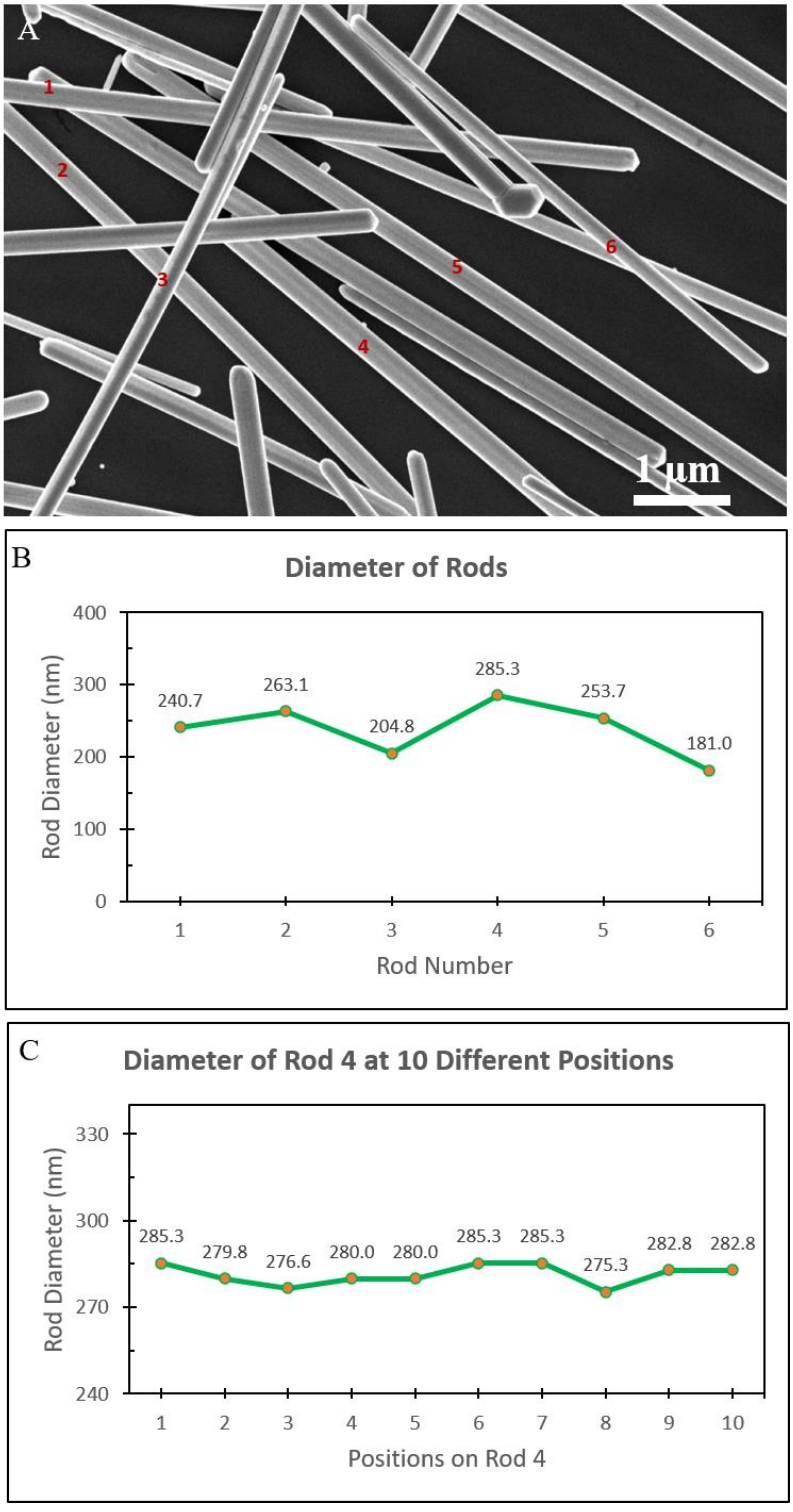

Supplementary Figure S16. (A) Representative SEM image of Silver Nanostructures with Nanorod Geometry obtained during the reaction condition provided in **Supplementary Table S8** above. (B) The diameter of 6 different rods marked in (A) measured by software ImageJ. (C) The diameter of rod #4 marked in (A) at 10 different positions measured by software ImageJ.

Supplementary Table S9: Silver Nanostructures with Nanorod Geometry. Data mentioned in this Table has been analyzed by software ImageJ from the SEM image shown in **Supplementary Figure S17A**. The diameter of the 11 different rods and length of 9 different rods was analyzed by software ImageJ and their average size (length and diameter) is provided in this Table with their standard deviation. Furthermore, the diameter at 5 different positions of a single rod #11 (**Supplementary Figure S17A)** has been measured through ImageJ software and its average diameter with standard deviation is written in this Table for identifying the diameter homogeneity of the individual rod.

Geometry	**Rods**
Average Size (Length and Diameter) (With Std. Deviation)	Average Length: 5 µm ± 1.2 µm Average Diameter: 320 nm ± 25 nm
Diameter Homogeneity (Single Rod #11 as shown in **Supplementary Figure S17A)**	309 nm ± 4.1 nm
Key Responsible Reactant	0.02 M Sucrose
Full Reaction Condition	Pure 1,3-Propanediol (5 mL) 0.12 M $AgNO_3$ (3mL) 0.35 M PVP-360,000 MW (3mL) 0.02 M Sucrose (1 mL) Temp: 170°C
Note	Pure 1,3-propanediol was heated to 170 °C for 90 minutes followed by the dropwise addition of reactants within 8 minutes. The reaction ran for 70 minutes judging from the first addition of $AgNO_3$ to the reaction solution. The color of the solution was a yellowish grey at the end of the reaction.

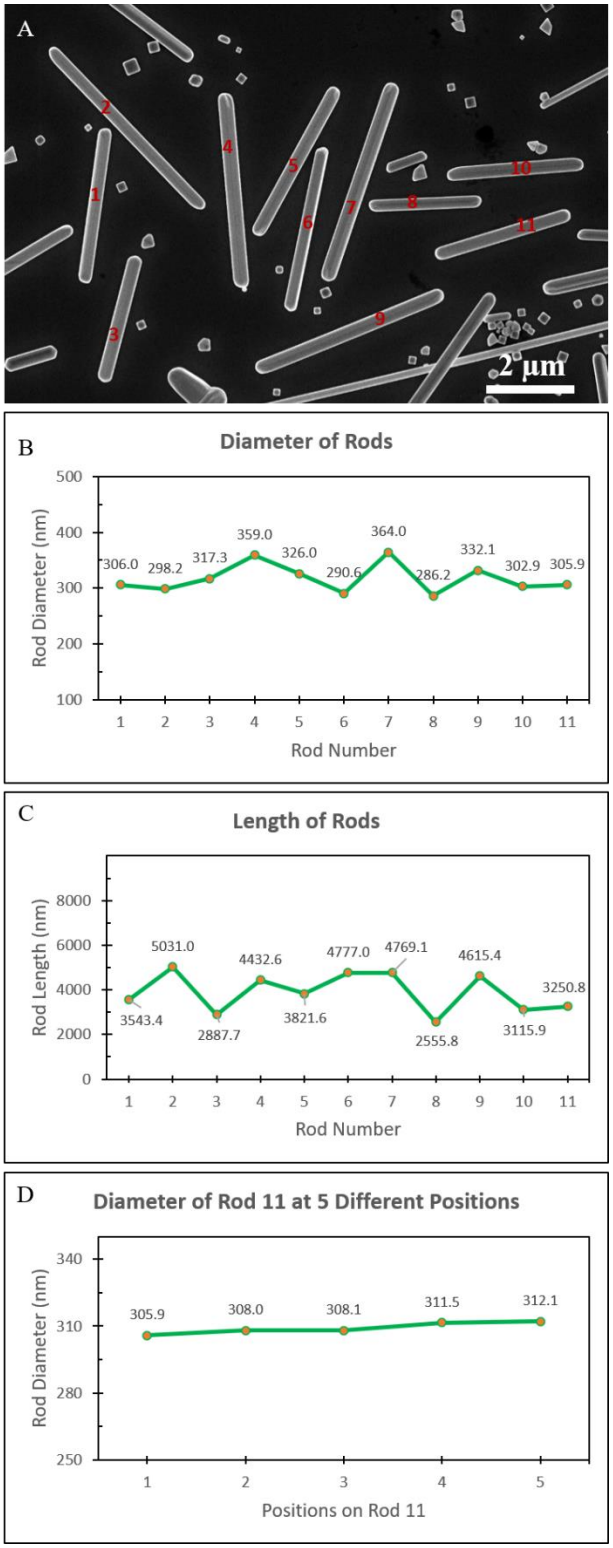

Supplementary Figure S17. (A) Representative SEM image of Silver Nanostructures with Nanorod Geometry obtained during the reaction condition provided in **Supplementary Table S9** above. (B) The diameter of 11 different rods marked in (A) was measured by software ImageJ. (C) The length of 11 different rods marked in (A) was measured by software ImageJ. (D) The diameter of rod #11 marked in (A) at 5 different positions measured by software ImageJ.

Supplementary Table S10: Silver Nanostructures with Nanorod Geometry. Data mentioned in this Table has been analyzed by software ImageJ from the SEM image shown in **Supplementary Figure S18A**. The diameter and length of the 9 different rods were analyzed by software ImageJ and their average size (length and diameter) is provided in this Table with their standard deviation. Furthermore, the diameter at 5 different positions of a single rod #9 (**Supplementary Figure S18A)** has been measured through ImageJ software and its average diameter with standard deviation is written in this Table for identifying the diameter homogeneity of the individual rod.

Geometry	**Rods**
Average Size (Length and Diameter) (With Std. Deviation)	Length: 2.5 µm ± 0.9 µm Diameter: 313 nm ± 21 nm
Diameter Homogeneity (Single Rod #9 as shown in **Supplementary Figure S18A)**	306.6 nm ± 6.9 nm
Key Responsible Reactant	0.02 M Sucrose 0.25 M $AgNO_3$
Full Reaction Condition	Pure 1,3-Propanediol (5 mL) 0.25 M $AgNO_3$ (3mL) 0.35 M PVP-360,000 MW (3mL) 0.02 M Sucrose (1 mL) Temp: 167°C
Note	Pure 1,3-propanediol was heated to 167 °C for 90 minutes followed by the dropwise addition of reactants within 9 minutes. The reaction ran for 90 minutes judging from the first addition of $AgNO_3$ to the reaction solution. The color of the solution was a yellowish grey at the end of the reaction.

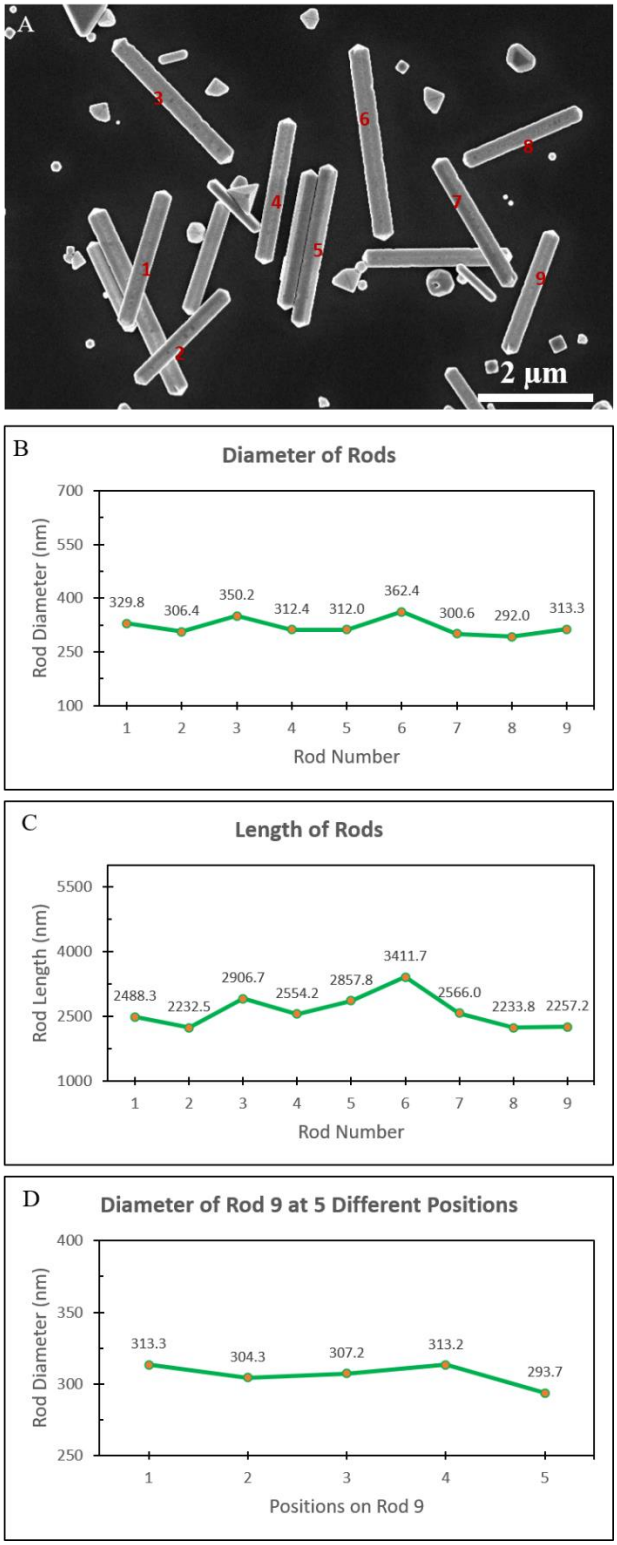

Supplementary Figure S18. (A) Representative SEM image of Silver Nanostructures with Nanorod Geometry obtained during the reaction condition provided in **Supplementary Table S10** above. (B) The diameter and (C) length of 9 different rods marked in (A) were measured by software ImageJ. (D) The diameter of rod #9 marked in (A) at 5 different positions measured by software ImageJ.

Supplementary Table S11: Silver Nanostructures with Nanorod Geometry. Data mentioned in this Table has been analyzed by software ImageJ from the SEM image shown in **Supplementary Figure S19A**. The diameter and length of the 6 different rods were analyzed by software ImageJ and their average size (length and diameter) is provided in this Table with their standard deviation. Furthermore, the diameter at 5 different positions of a single rod #4 (**Supplementary Figure S19A)** has been measured through ImageJ software and its average diameter with standard deviation is written in this Table for identifying the diameter homogeneity of the individual rod.

Geometry	**Rods**
Average Size (Length and Diameter) (With Std. Deviation)	Length: 6 µm ± 0.9 µm Diameter: 420 nm ± 22 nm
Diameter Homogeneity (Single Rod #4 as shown in **Supplementary Figure S19A)**	422.4 nm ± 6.3 nm
Key Responsible Reactant	0.02 M Fructose
Full Reaction Condition	Pure 1,3-Propanediol (5 mL) 0.15 M $AgNO_3$ (3mL) 0.35 M PVP-360,000 MW (3mL) 0.02 M Fructose (1 mL) Temp: 167°C
Note	Pure 1,3-propanediol was heated to 167 °C for 90 minutes followed by the dropwise addition of reactants within 8 minutes. The reaction ran for 90 minutes judging from the first addition of $AgNO_3$ to the reaction solution. The color of the solution was a yellowish grey at the end of the reaction.

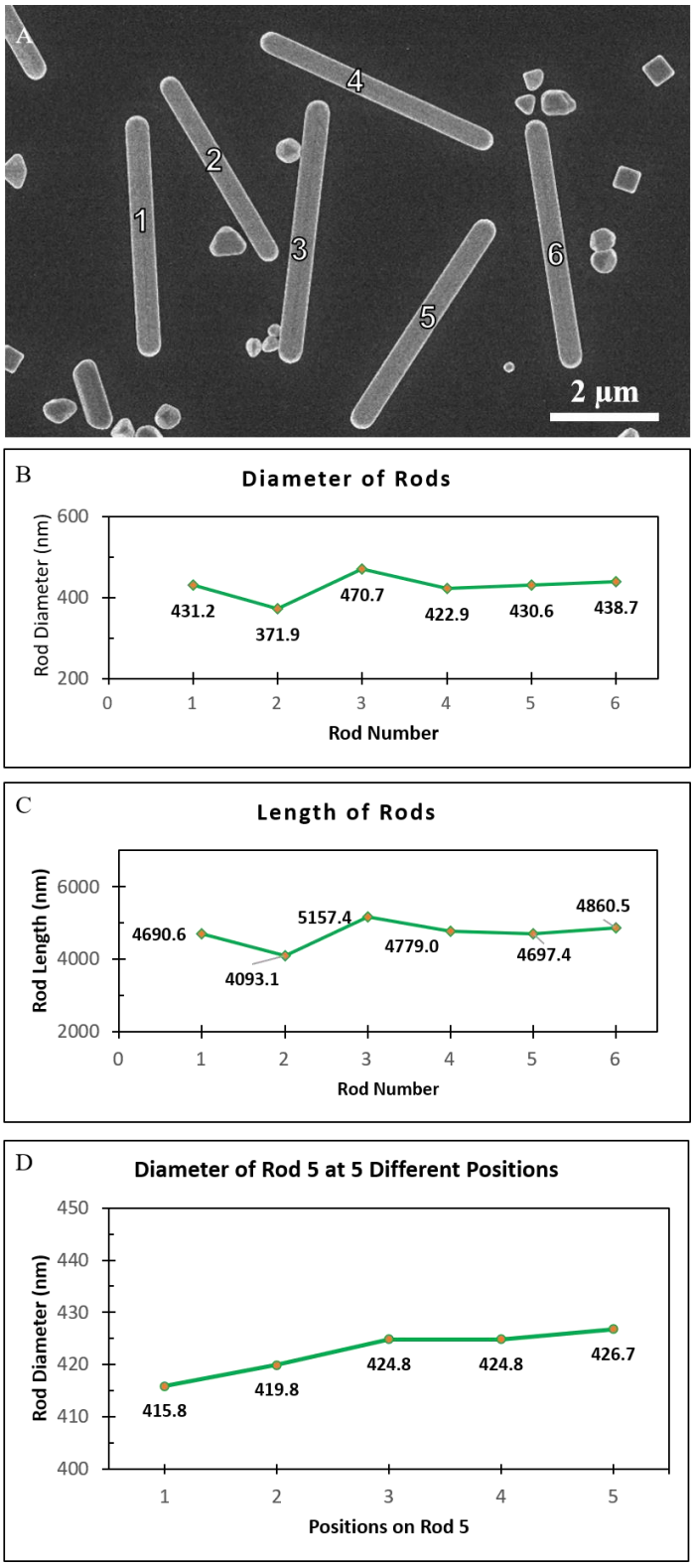

Supplementary Figure S19. (A) Representative SEM image of Silver Nanostructures with Nanorod Geometry obtained during the reaction condition provided in **Supplementary Table S11** above. (B) The diameter of 6 different rods marked in (A) was measured by software ImageJ. (C) The length of 6 different rods marked in (A) was measured by software ImageJ. (D) The diameter of rod #4 marked in (A) at 5 different positions measured by software ImageJ.

Supplementary Table S12: Silver Nanostructures with Nanorod Geometry. Data mentioned in this Table has been analyzed by software ImageJ from the SEM image shown in **Supplementary Figure S21A**. The diameter of the 5 different rods was measured and their average size (length and diameter) is provided in this Table with their standard deviation. The length of the 50 different rods from 10 different SEM images of the same sample has been measured by software ImageJ and their average length with standard deviation is provided in this Table. Furthermore, the diameter at 5 different positions of a single rod #5 (**Supplementary Figure S21A)** has been measured through ImageJ software and its average diameter with standard deviation is written in this Table for identifying the diameter homogeneity of the individual rod. Three representative SEM images at different magnifications are shown in **Supplementary Figure S20** below.

Geometry	**Rods**
Average Size (Length and Diameter) (With Std. Deviation)	Average Length: 11 µm ± 4.2 µm Diameter: 470 nm ± 18 nm
Diameter Homogeneity (Single Rod #5 as shown in **Supplementary Figure S21A)**	477 nm ± 1.8 nm
Key Responsible Reactant	0.02 M Maltotriose
Full Reaction Condition	Pure 1,3-Propanediol (5 mL) 0.15 M $AgNO_3$ (3mL) 0.35 M PVP-360,000 MW (3mL) 0.02 M Maltotriose (1 mL) Temp: 167°C
Note	Pure 1,3-propanediol was heated to 167 °C for 90 minutes followed by the dropwise addition of reactants within 8 minutes. The reaction ran for 90 minutes judging from the first addition of $AgNO_3$ to the reaction solution. The color of the solution was a yellowish grey at the end of the reaction.

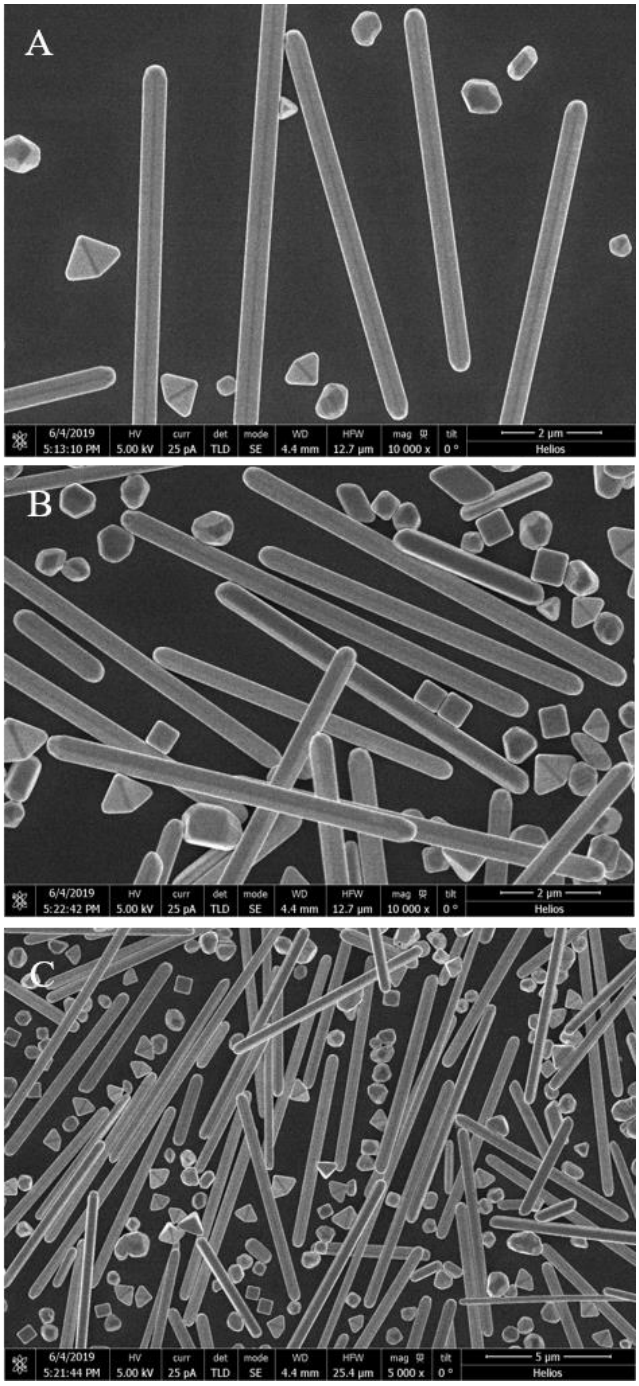

Supplementary Figure S20. (A-C) Three Representative SEM images of Silver Nanostructures with Nanorod Geometry at Three Different Magnifications. The full reaction condition for the silver nanostructures shown in this Figure is provided in **Supplementary Table S12** above. Also, the data analysis for these SEM images was performed by software ImageJ that is shown in **Supplementary Figure S21B-C** below, and their average value with their standard deviation is mentioned in **Supplementary Table S12** above.

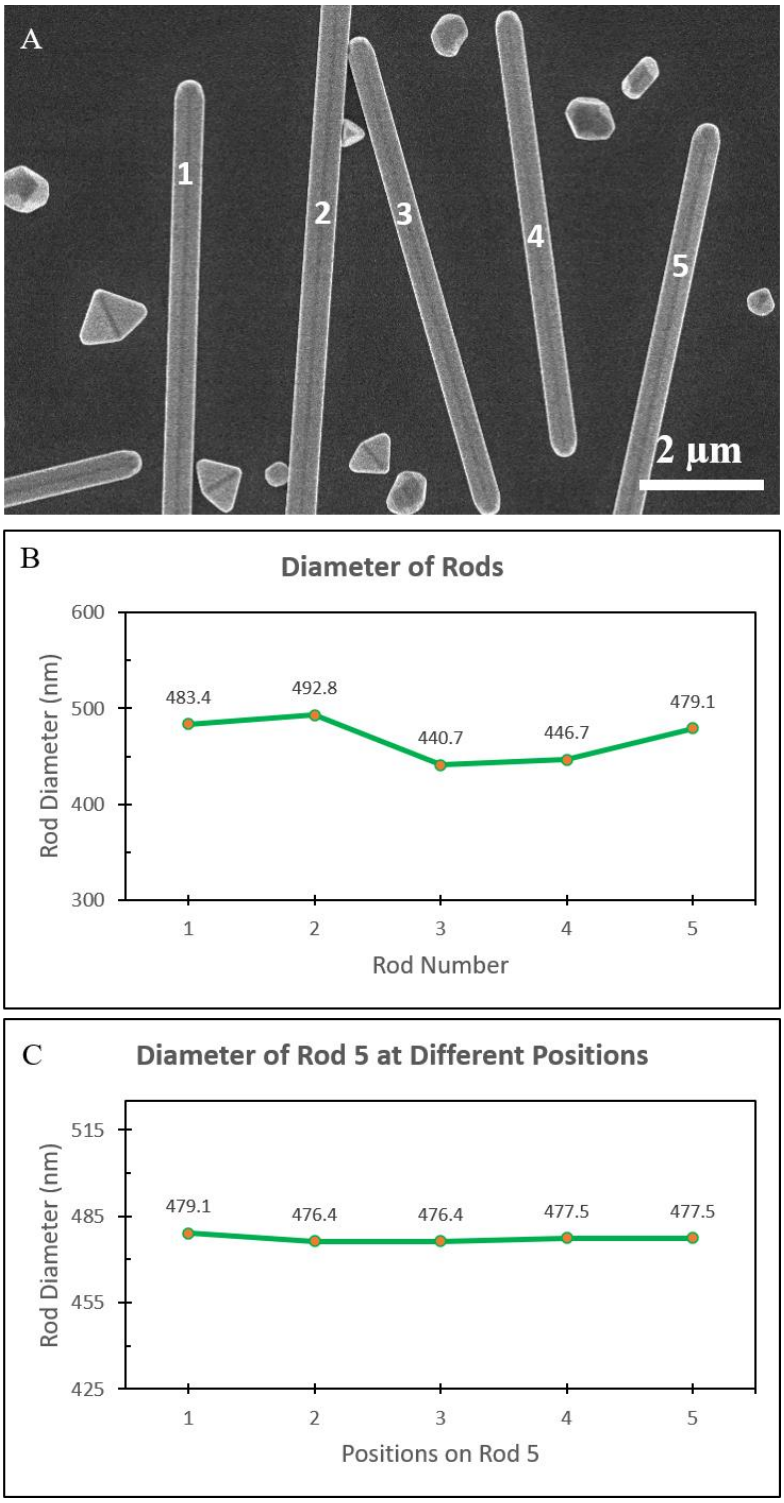

Supplementary Figure S21. (A) Representative SEM image of Silver Nanostructures with Nanorod Geometry obtained during the reaction condition provided in **Supplementary Table S12** above. (B) The diameter of 5 different rods marked in (A) was measured by software ImageJ. (C) The diameter of rod #5 marked in (A) at 5 different positions measured by software ImageJ.

3. Plasmonic Building-block Geometries: *Impact of PVP Molecular Weight on Nanostructure's Geometry*

Nanoparticles possess a high surface to volume ratio compare to their bulk counterpart.[2] For this reason, nanoparticles often aggregate to minimize the energy barrier and to achieve a more stable state.[2] An interfacial agent on the surface of the nanoparticles can instead stabilize the nanoparticles in solution and allow growth along a specific direction.[3-5] Three different molecular weights (MW) of the PVP have been used in different reactions: 55,000 MW, 360,000 MW, and 1,300,000 MW. Through our experiments, we found that the utilization of 360,000 MW PVP was key in the formation of silver nanorods and 1,300,000 MW PVP was key in the formation of silver cubes in high yield.

The results and data analysis of the silver nanostructures obtained during the addition of PVP is shown in **Supplementary Tables S13-S16.**

Supplementary Table S13: Silver Nanostructures with Nanocube Geometry. Data mentioned in this Table has been analyzed by software ImageJ from the SEM image shown in **Supplementary Figure S22A**. The diameter (side to side) and the diagonal length (corner to corner) of the 9 different cubes was measured and the average size (diameter and diagonal length) is provided in this Table with their standard deviation. Overall, the size has been measured by analyzing 50 different cubes from 10 different SEM images of the same sample by software ImageJ. Furthermore, the diameter at 5 different positions of a single cube #5 (**Supplementary Figure S22A)** has been measured through ImageJ software and its average diameter with standard deviation is written in this Table for identifying the diameter homogeneity of the individual cube.

Geometry	**Cubes**
Average Size (With Std. Deviation)	Average Diameter (Side to Side Diameter): 235 nm ± 12 nm Average Diagonal Length (Corner to Corner): 321 nm ± 20.5 nm 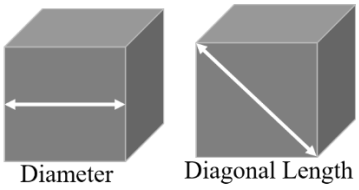
Diameter Homogeneity (Single Cube #5 as shown in **Supplementary Figure S22A)**	233 nm ± 1.9 nm
Key Responsible Reactant	0.35 M PVP1,300,000 MW 0.02 M Sucrose
Full Reaction Condition	Pure 1,3-Propanediol (5 mL) 0.12 M $AgNO_3$ (3mL) 0.35 M PVP-1,300,000 MW (3mL) 0.02 M Sucrose (1 mL) Temp: 170°C
Note	Pure 1,3-propanediol was heated to 170 °C for 90 minutes followed by the dropwise addition of reactants within 8 minutes. The reaction ran for 60 minutes judging from the first addition of $AgNO_3$ to the reaction solution. The color of the solution was a dark greenish grey at the end of the reaction.

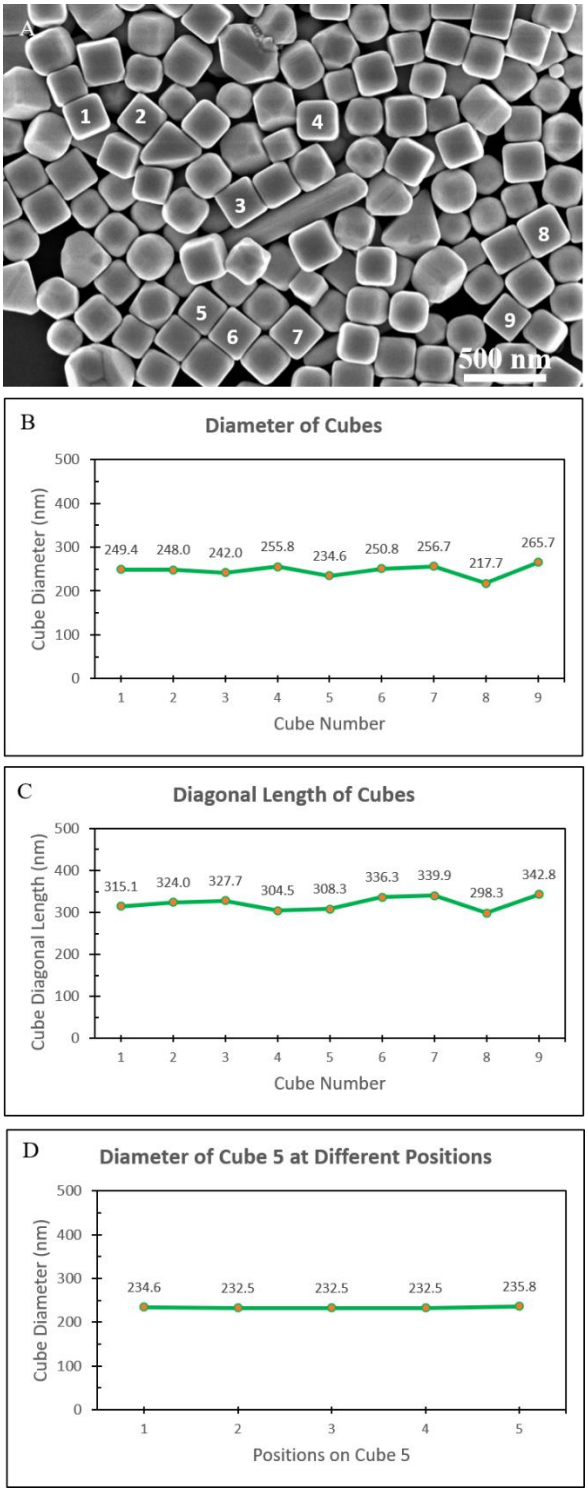

Supplementary Figure S22. (A) Representative SEM image of Silver Nanostructures with Nanocube Geometry obtained during the reaction condition provided in **Supplementary Table S13** above. (B) The diameter (side to side) and (C) diagonal length (corner to corner) of 9 different cubes marked in (A) was measured by software ImageJ. (D) The diameter of cube #5 marked in (A) at 5 different positions measured by software ImageJ.

Supplementary Table S14: Silver Nanostructures with Nanocube Geometry. Data mentioned in this Table has been analyzed by software ImageJ from the SEM image shown in **Supplementary Figure S23A**. The diameter (side to side) and the diagonal length (corner to corner) of the 6 different cubes was measured and the average size (diameter and diagonal length) is provided in this Table with their standard deviation. Overall, the size has been measured by analyzing 50 different cubes from 10 different SEM images of the same sample by software ImageJ. Furthermore, the diameter at 5 different positions of a single cube #6 (**Supplementary Figure S23A)** has been measured through ImageJ software and its average diameter with standard deviation is written in this Table for identifying the diameter homogeneity of the individual cube.

Geometry	**Cubes**
Average Size (With Std. Deviation)	Average Diameter (Side to Side Diameter): 420 nm ± 25 nm Average Diagonal Length (Corner to Corner): 559 nm ± 38.6 nm 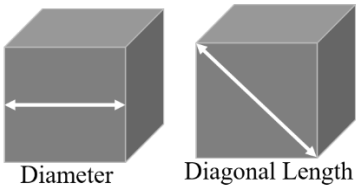
Diameter Homogeneity (Single Cube #6 as shown in **Supplementary Figure S23A)**	372 nm ± 5.2 nm
Key Responsible Reactant	0.02 M Sucrose 0.35 M PVP 55,000 MW
Full Reaction Condition	Pure 1,3-Propanediol (5 mL) 0.15 M $AgNO_3$ (3mL) 0.35 M PVP-55,000 MW (3mL) 0.02 M Sucrose (1 mL) Temp: 172°C
Note	Pure 1,3-propanediol was heated to 172 °C for 90 minutes followed by the dropwise addition of reactants within 8 minutes. The reaction ran for 90 minutes judging from the first addition of $AgNO_3$ to the reaction solution. The color of the solution was greenish-grey at the end of the reaction.

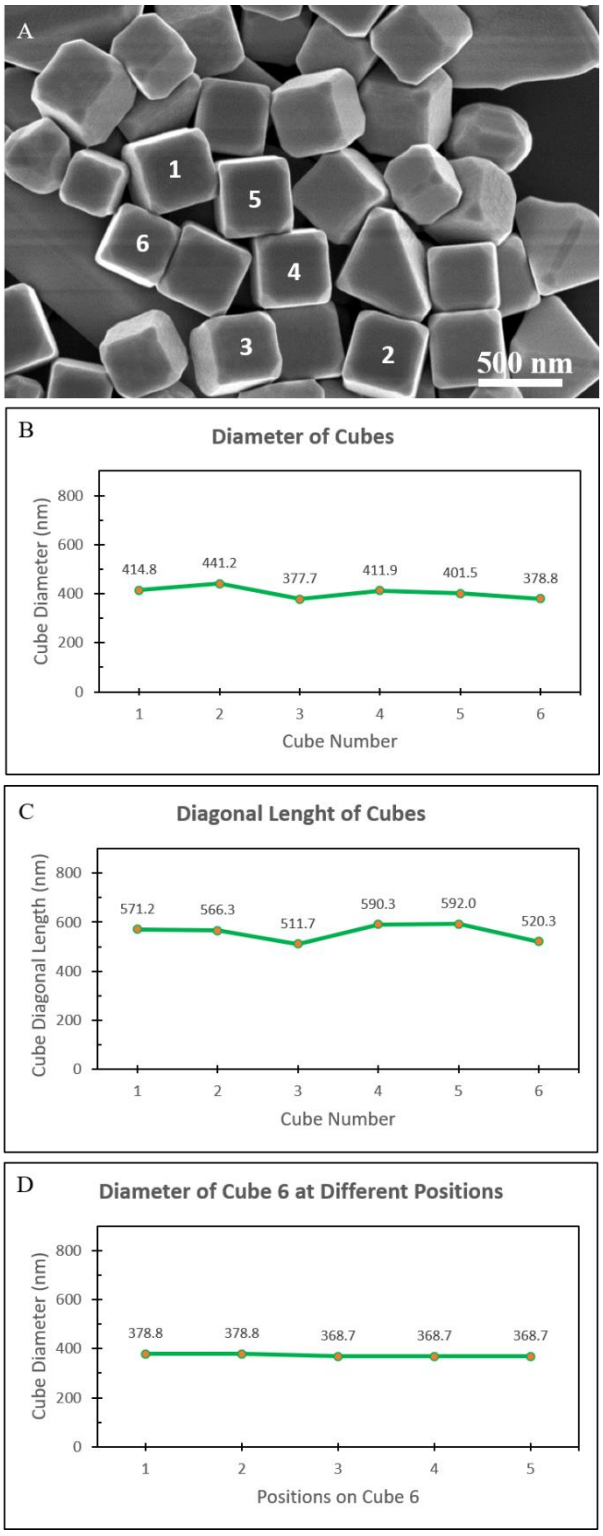

Supplementary Figure S23. (A) Representative SEM image of Silver Nanostructures with Nanocube Geometry obtained during the reaction condition provided in **Supplementary Table S14** above. (B) The diameter (side to side) and (C) diagonal length (corner to corner) of 6 different cubes marked in (A) was measured by software ImageJ. (D) The diameter of cube #6 marked in (A) at 5 different positions measured by software ImageJ.

Supplementary Table S15: Silver Nanostructures with Nanocube Geometry. Data mentioned in this Table has been analyzed by software ImageJ from the SEM image shown in **Supplementary Figure S24A**. The diameter (side to side) and the diagonal length (corner to corner) of the 4 different cubes was measured and the average size (diameter and diagonal length) is provided in this Table with their standard deviation. Overall, the size has been measured by analyzing 50 different cubes from 10 different SEM images of the same sample by software ImageJ. Furthermore, the diameter at 5 different positions of a single cube #1 (**Supplementary Figure S24A)** has been measured through ImageJ software and its average diameter with standard deviation is written in this Table for identifying the diameter homogeneity of the individual cube.

Geometry	**Cubes**
Average Size (With Std. Deviation)	Average Diameter (Side to Side Diameter): 426 nm ± 12 nm Average Diagonal Length (Corner to Corner): 567 nm ± 38.6 nm 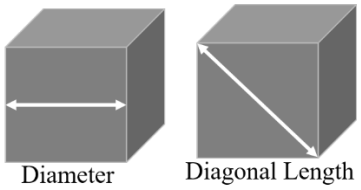
Diameter Homogeneity (Single Cube #1 as shown in **Supplementary Figure S24A)**	410.6 nm ± 4.6 nm
Key Responsible Reactant	0.35 M PVP1,300,000 MW 0.15 M $AgNO_3$
Full Reaction Condition	Pure 1,3-Propanediol (5 mL) 0.15 M $AgNO_3$ (3mL) 0.35 M PVP-1,300,000 MW (3mL) 0.02 M Sucrose (1 mL) Temp: 170°C
Note	Pure 1,3-propanediol was heated to 170 °C for 90 minutes followed by the dropwise addition of reactants within 7 minutes. The reaction ran for 120 minutes judging from the first addition of $AgNO_3$ to the reaction solution. The color of the solution was greenish-grey at the end of the reaction.

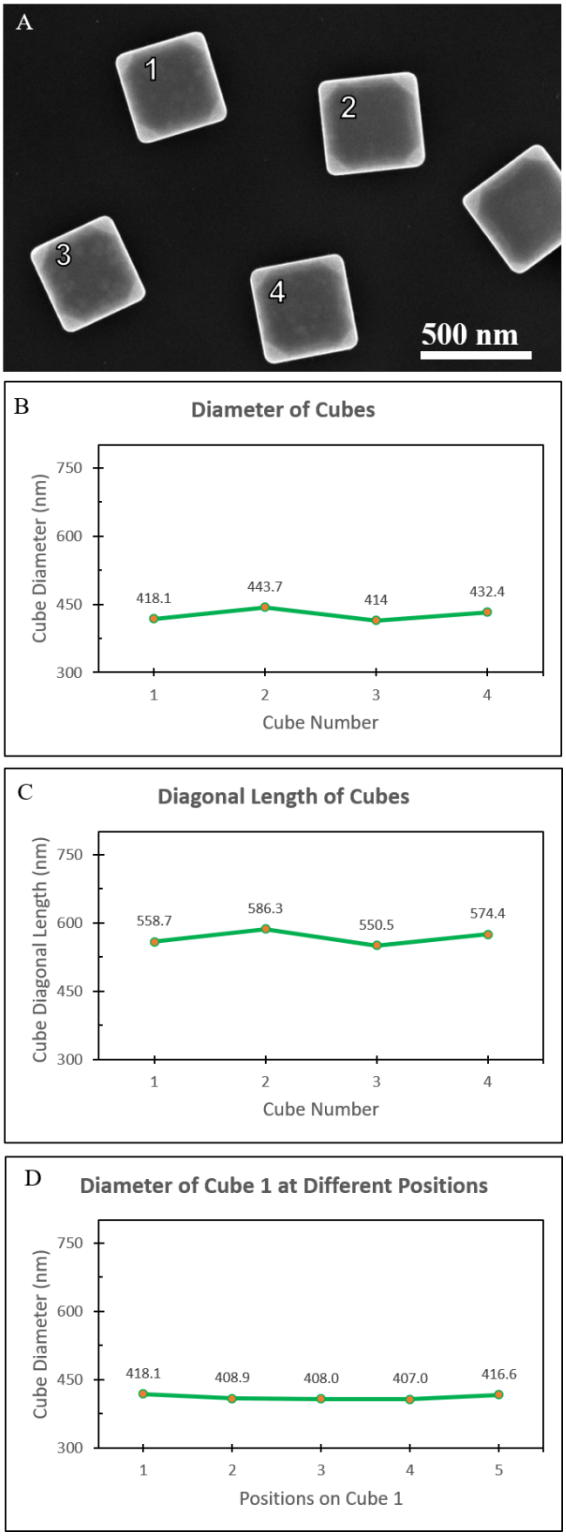

Supplementary Figure S24. (A) Representative SEM image of Silver Nanostructures with Nanocube Geometry obtained during the reaction condition provided in **Supplementary Table S15** above. (B) The diameter (side to side) and (C) diagonal length (corner to corner) of 4 different cubes marked in (A) was measured by software ImageJ. (D) The diameter of cube #1 marked in (A) at 5 different positions measured by software ImageJ.

Supplementary Table S16: Silver Nanostructures with Nanocube Geometry. Data mentioned in this Table has been analyzed by software ImageJ from the SEM image shown in **Supplementary Figure S25A**. The diameter (side to side) and the diagonal length (corner to corner) of the 5 different cubes was measured and the average size (diameter and diagonal length) is provided in this Table with their standard deviation. Overall, the size has been measured by analyzing 50 different cubes from 10 different SEM images of the same sample by software ImageJ. Furthermore, the diameter at 4 different positions of a single cube #1 (**Supplementary Figure S25A)** has been measured through ImageJ software and its average diameter with standard deviation is written in this Table for identifying the diameter homogeneity of the individual cube.

Geometry	**Cubes**
Average Size (With Std. Deviation)	Average Diameter (Side to Side Diameter): 429 nm ± 22 nm Average Diagonal Length (Corner to Corner): 573.4 nm ± 38.6 nm 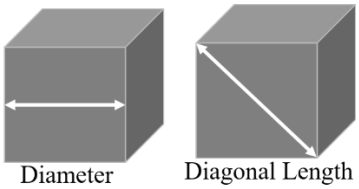
Diameter Homogeneity (Single Cube #1 as shown in **Supplementary Figure S25A)**	439 nm ± 2.2 nm
Key Responsible Reactant	0.025 M Sucrose 0.35 M PVP-55,000 MW (3mL)
Full Reaction Condition	Pure 1,3-Propanediol (5 mL) 0.15 M $AgNO_3$ (3mL) 0.35 M PVP-55,000 MW (3mL) 0.025 M Sucrose (1 mL) Temp: 165°C
Note	Pure 1,3-propanediol was heated to 165 °C for 90 minutes followed by the dropwise addition of reactants within 9 minutes. The reaction ran for 60 minutes judging from the first addition of $AgNO_3$ to the reaction solution. The color of the solution was greenish-grey at the end of the reaction.

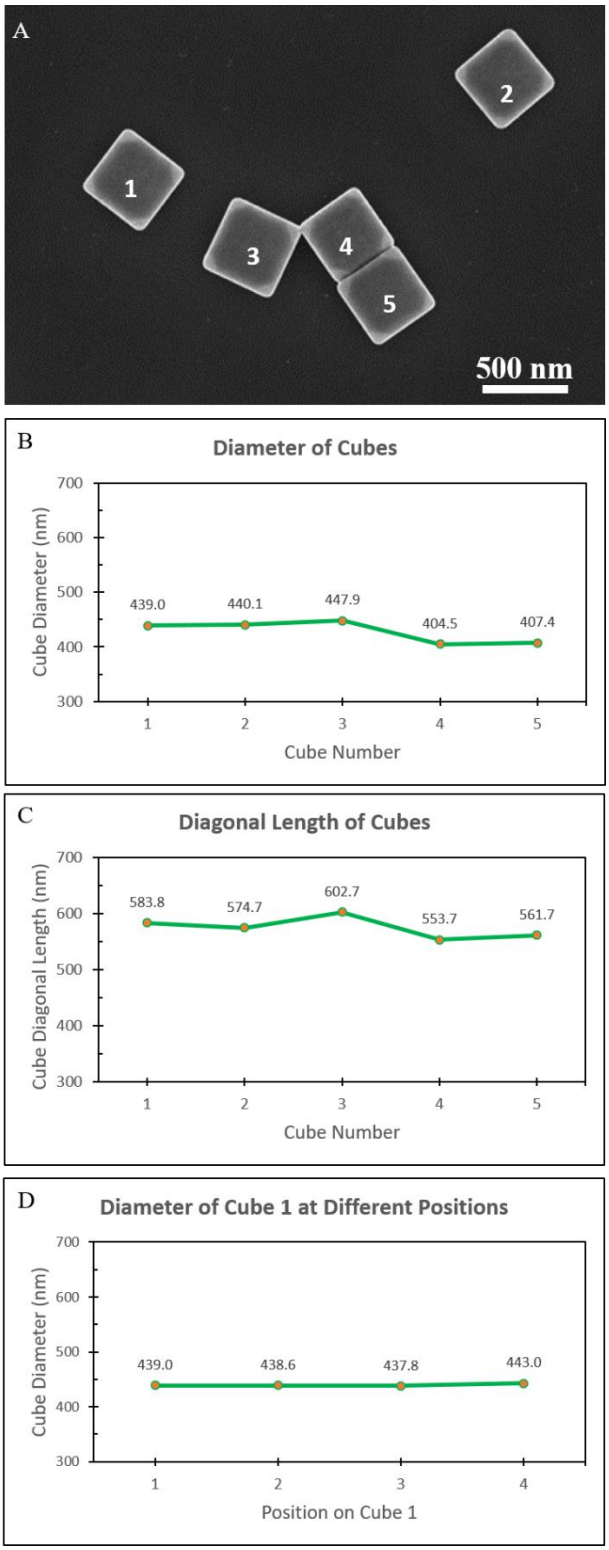

Supplementary Figure S25. (A) Representative SEM image of Silver Nanostructures with Nanocube Geometry obtained during the reaction condition provided in **Supplementary Table S16** above. (B) The diameter (side to side) and (C) diagonal length (corner to corner) of 5 different cubes marked in (A) was measured by software ImageJ. (D) The diameter of cube #1 marked in (A) at 4 different positions measured by software ImageJ.

4. Plasmonic Building-block Geometries: *Impact of Ionic Salt & Surfactants on Nanostructure's Geometry*

Charged ionic compounds play crucial roles in solvation and interfacial interactions between reactants during wet-chemical reactions.[6-8] Here, we suggest that ionic compounds accelerate the polyol reaction rate, and hence play a role similar to the external reducing agent. Ionic compounds not only enhance the rate of reaction but also provide support by adsorbing to the growing nanostructures for directing the geometries during the polyol synthesis.

We found that the addition of various ionic additives (salts and surfactants) allows controlling geometries of silver nanostructures. The utilization of 0.1 M sodium 3-mercapto-1-propanesulfonate (SMPS) was key in the formation of small rod-shaped particles with mixed geometries (**Supplementary Table S17**). On the other hand, the addition of the surfactant sodium dodecyl sulfate (SDS) supports the formation of silver nanocubes (**Supplementary Table S18)**. Similarly, another type of surfactant, sodium 1-hexadecanesulfonate (SHDS), supports the formation of silver nanobars (**Supplementary Table S19)**. The ionic salt sodium hydroxide (NaOH) allows the formation of a mixed population of rods and nanoparticles (**Supplementary Table S20)**.

Results and data analysis of the silver nanostructures during the addition of ionic salts or surfactants is shown in **Supplementary Tables S17-S20.**

Supplementary Table S17: Silver Nanostructures with Nanoparticles and Nanorods (Mix-geometry). Data mentioned in this Table has been analyzed during the SEM characterization by using the imaging software of the FEI Helios Nanolab 660 FIB-SEM. Three different SEM images of the same reaction sample are shown in **Supplementary Figure S26**. The diameter of 50 different nanostructures (25 nanoparticles + 25 nanorods) from 3 different SEM images shown in **Supplementary Figure S26** was measured and their average value with standard deviation is provided in this Table.

Geometry	**Rods + Particles**
Average Size (With Std. Deviation)	Average Rod Length: 560 nm ± 180 nm Average Rod Diameter: 108 nm ± 56 nm Average Particle size: 195 nm ± 140 nm
Key Responsible Reactant	0.1 M sodium 3-mercapto-1-propanesulfonate (SMPS)
Full Reaction Condition	Pure 1,3-Propanediol (5 mL) 0.15 M $AgNO_3$ (3mL) 0.35 M PVP-360,000 MW (3mL) 0.1 M SMPS (1 mL) Temp: 170°C
Note	Pure 1,3-propanediol was heated to 170 °C for 90 minutes followed by the dropwise addition of reactants within 5 minutes. The reaction ran for 45 minutes judging from the first addition of $AgNO_3$ to the reaction solution. The color of the solution was greenish-grey at the end of the reaction.

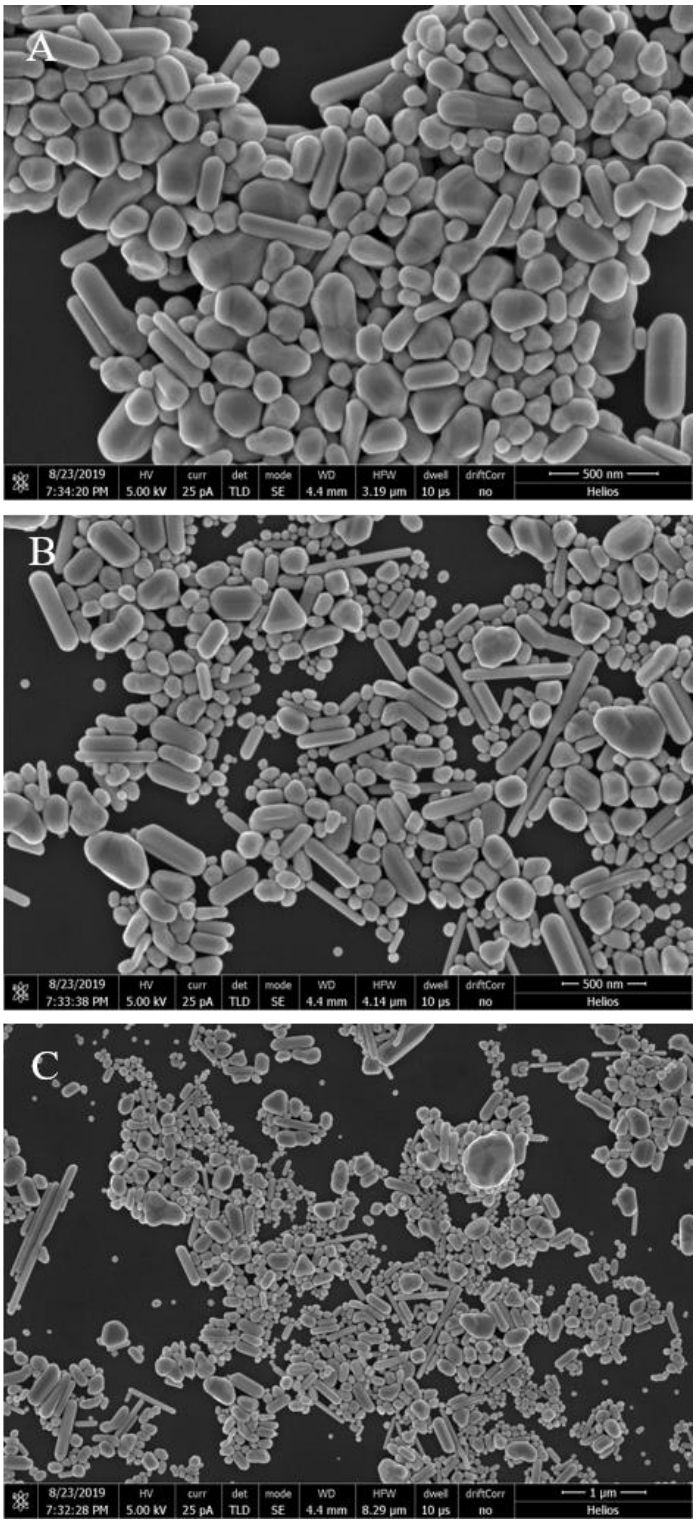

Supplementary Figure S26. (A-C) Three Representative SEM images of Silver Nanostructures at Three Different Magnifications. The full reaction condition for the silver nanostructures shown in this Figure is provided in **Supplementary Table S17** above. Also, the data analysis for these SEM images was performed during the SEM characterization, and their average size together with standard deviation is mentioned in **Supplementary Table S17** above.

Supplementary Table S18: Silver Nanostructures with Nanocube Geometry. Data mentioned in this Table has been analyzed by software ImageJ from the SEM image shown in **Supplementary Figure S27A**. The diameter (side to side) and the diagonal length (corner to corner) of the 5 different cubes was measured and the average size (diameter and diagonal length) is provided in this Table with their standard deviation. Overall, the size has been measured by analyzing 50 different cubes from 10 different SEM images of the same sample by software ImageJ. Furthermore, the diameter at 4 different positions of a single cube #1 (**Supplementary Figure S27A)** has been measured through ImageJ software and its average diameter with standard deviation is written in this Table for identifying the diameter homogeneity of the individual cube.

Geometry	**Cubes**
Average Size (With Std. Deviation)	Average Diameter (Side to Side Diameter): 191 nm ± 65 nm Average Diagonal Length (Corner to Corner): 256.8 nm ± 78.5 nm 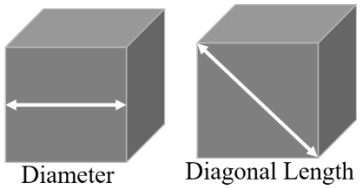
Diameter Homogeneity (Single Cube #1 as shown in **Supplementary Figure S27A)**	207 nm ± 4.9 nm
Key Responsible Reactant	0.1 M SDS
Full Reaction Condition	Pure 1,3-Propanediol (5 mL) 0.15 M $AgNO_3$ (3mL) 0.35 M PVP-360,000 MW (3mL) 0.1 M SDS (1 mL) Temp: 170°C
Note	Pure 1,3-propanediol was heated to 170 °C for 90 minutes followed by the dropwise addition of reactants within 7 minutes. The reaction ran for 30 minutes judging from the first addition of $AgNO_3$ to the reaction solution. The color of the solution was a dark greenish grey at the end of the reaction.

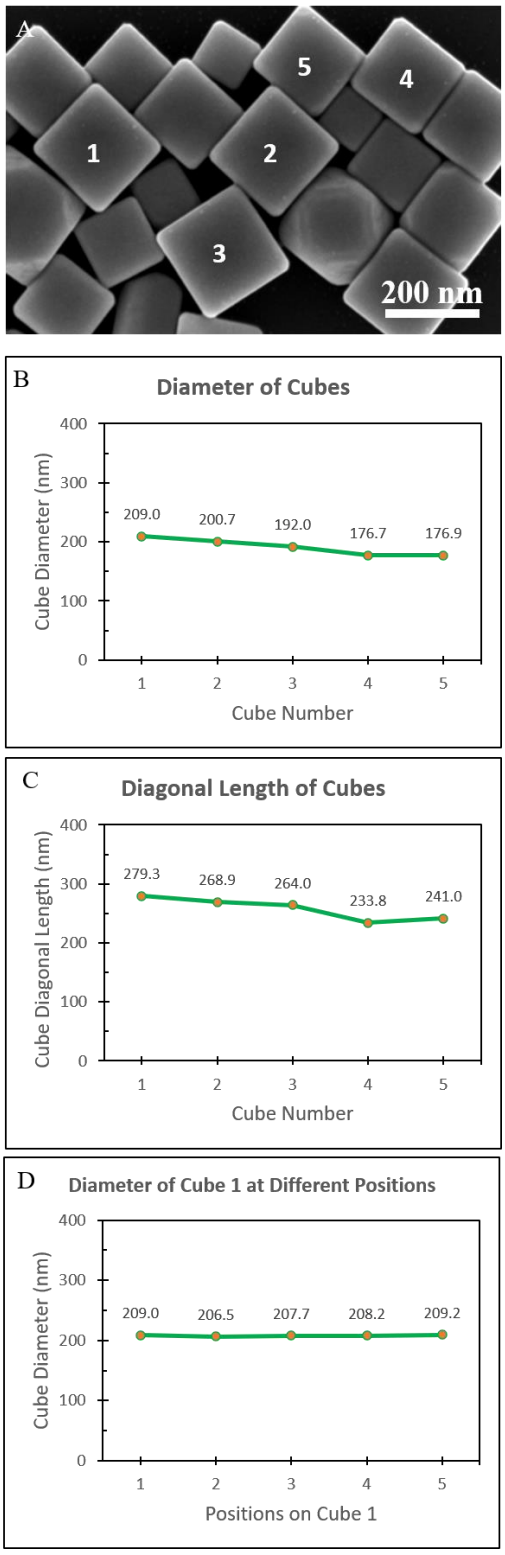

Supplementary Figure S27. (A) Representative SEM image of Silver Nanostructures with Nanocube Geometry obtained during the reaction condition provided in **Supplementary Table S18** above. (B) The diameter (side to side) and (C) diagonal length (corner to corner) of 5 different cubes marked in (A) was measured by software ImageJ. (D) The diameter of cube #1 marked in (A) at 4 different positions measured by software ImageJ.

Supplementary Table S19: Silver Nanostructures with Nanobar Geometry. Data mentioned in this Table has been analyzed during the SEM characterization by using the imaging software of the FEI Helios Nanolab 660 FIB-SEM. Three different SEM images of the same reaction sample are shown in **Supplementary Figure S28**. The diameter of 10 different nanostructures of bar geometry from 3 different SEM images shown in **Supplementary Figure S28** was measured and their average value with standard deviation is provided in this Table.

Geometry	**Bars**
Average Size (With Std. Deviation)	Average Length of Bar: 320 nm ± 125 nm Average Diameter of Bar: 172 nm ± 56 nm
Diameter Homogeneity (Single Bar) (marked* in the image shown in **Supplementary Figure S28**; diameter measured at 5 different positions)	181 nm ± 11.3 nm
Key Responsible Reactant	0.1 M SHDS
Full Reaction Condition	Pure 1,3-Propanediol (5 mL) 0.15 M $AgNO_3$ (3mL) 0.35 M PVP-360,000 MW (3mL) 0.1 M SHDS (1 mL) Temp: 170°C
Note	Pure 1,3-propanediol was heated to 170 °C for 90 minutes followed by the dropwise addition of reactants within 4 minutes. The reaction ran for 30 minutes judging from the first addition of $AgNO_3$ to the reaction solution. The color of the solution was a dark greenish grey at the end of the reaction.

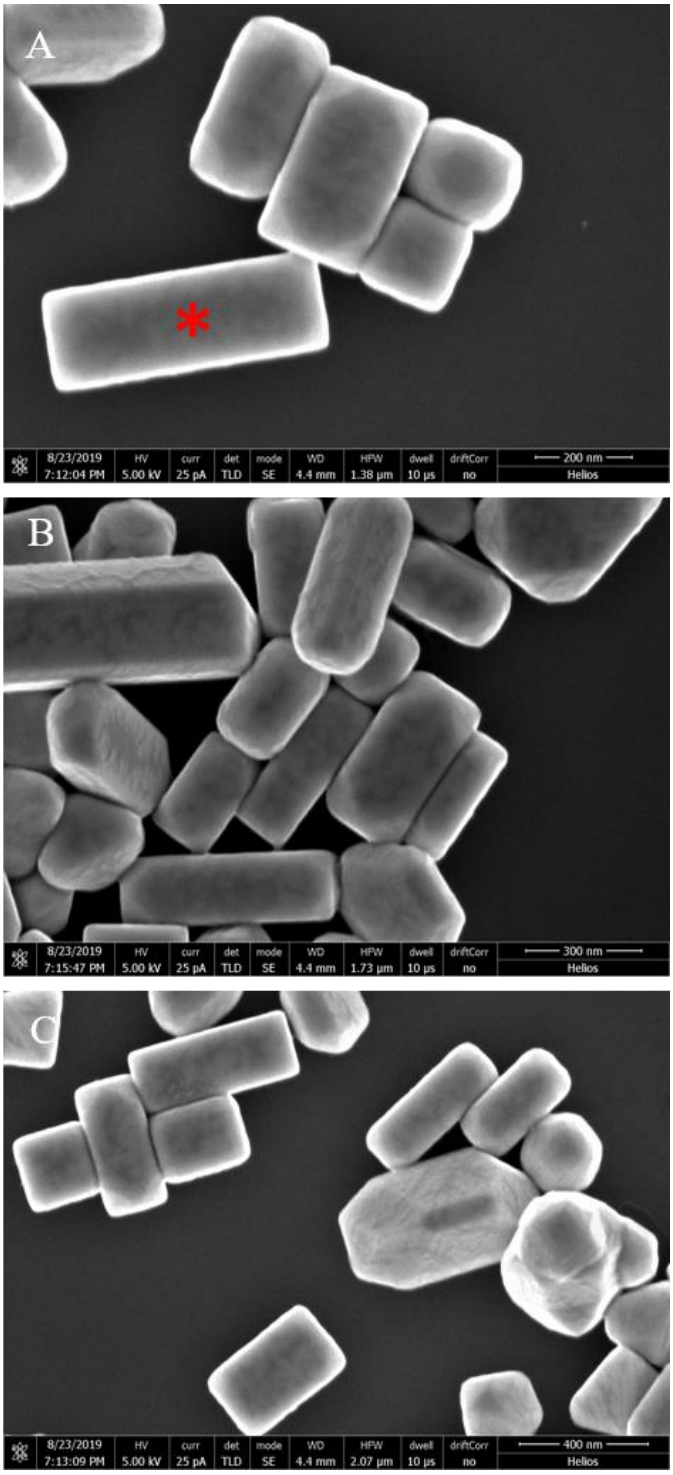

Supplementary Figure S28. (A-C) Three Representative SEM images of Silver Nanostructures of Bar Geometry at Three Different Magnifications. The full reaction condition for the silver nanostructures shown in this Figure is provided in **Supplementary Table S19** above. Also, the data analysis for these SEM images was performed during the SEM characterization, and their average size together with standard deviation is mentioned in **Supplementary Table S19** above.

Supplementary Table S20: Silver Nanostructures with Nanoparticles and Nanorods (Mix-geometry). Data mentioned in this Table has been analyzed during the SEM characterization by using the imaging software of the FEI Helios Nanolab 660 FIB-SEM. SEM image is shown in **Supplementary Figure S29**. The diameter of 10 different nanostructures (5 nanoparticles + 5 nanorods) from SEM images shown in **Supplementary Figure S29** was measured and their average value with standard deviation is provided in this Table.

Geometry	**Rods + Particles**
Average Size (With Std. Deviation)	Average Rod Length: 1.5 µm ± 800 nm Average Rod Diameter: 53 nm ± 35.5 nm Average Particle size: 120 nm ± 60 nm
Diameter Homogeneity (Single Rod) (marked* in the image shown in **Supplementary Figure S29**; diameter measured at 5 different positions)	42 nm ± 6 nm
Key Responsible Reactant	0.1 M NaOH
Full Reaction Condition	Pure 1,3-Propanediol (5 mL) 0.15 M $AgNO_3$ (3mL) 0.35 M PVP-360,000 MW (3mL) 0.1 M NaOH (1 mL) Temp: 170°C
Note	Pure 1,3-propanediol was heated to 170 °C for 90 minutes followed by the dropwise addition of reactants within 4 minutes. The reaction ran for 30 minutes judging from the first addition of $AgNO_3$ to the reaction solution. The color of the solution was a greenish-grey at the end of the reaction.

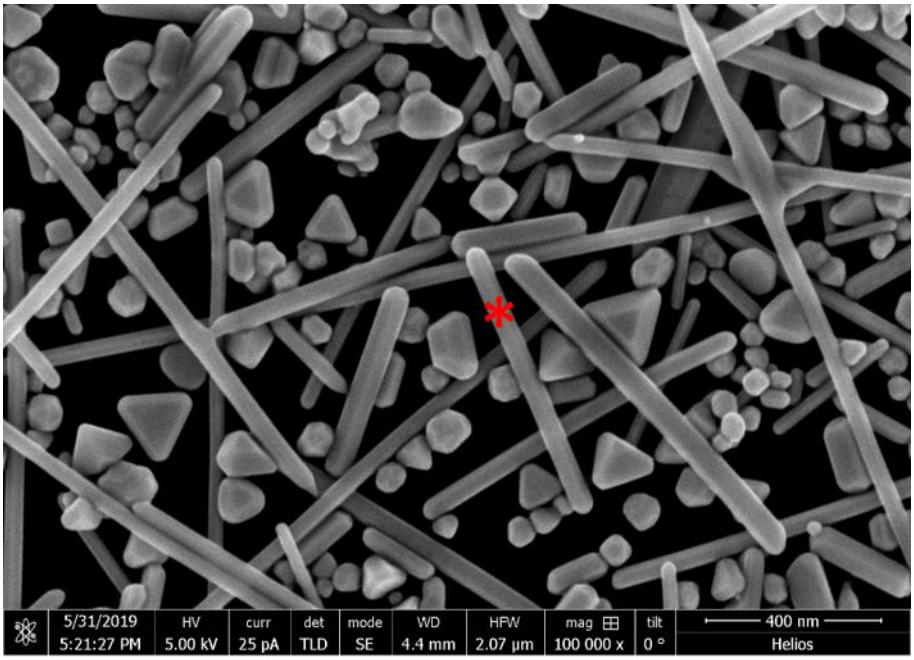

Supplementary Figure S29. A representative SEM image of Silver Nanostructures of Mixed-Geometries (Nanorod + Nanoparticles). The full reaction condition for the silver nanostructures shown in this Figure is provided in **Supplementary Table S20** above. Also, the data analysis for these SEM images was performed during the SEM characterization, and their average size together with standard deviation is mentioned in **Supplementary Table S20** above.

Overall, various reactants are playing a crucial role in the formation of various geometry-controlled silver nanostructures. We have applied around 200 reactions by using various sets of reactants to obtain the nanostructures of different geometries. In addition to the above results shown in **Supplementary Table S1-S20**, few other representative reactant combination sets with varied reaction conditions are provided below. Data analysis of different types of silver nanostructures during various reaction conditions is shown in **Supplementary Tables S21-S26.**

Supplementary Table S21: Silver Nanostructures with Nanorod Geometry. Data mentioned in this Table has been analyzed by software ImageJ from the SEM image shown in **Supplementary Figure S31A**. The diameter of the 8 different rods was measured and their average size (length and diameter) is provided in this Table with their standard deviation. The length of the 50 different rods from 10 different SEM images of the same sample has been measured by software ImageJ and their average length with standard deviation is provided in this Table. Furthermore, the diameter at 10 different positions of a single rod #6 (**Supplementary Figure S31A)** has been measured through ImageJ software and its average diameter with standard deviation is written in this Table for identifying the diameter homogeneity of the individual rod. Three representative SEM images at different magnifications are shown in **Supplementary Figure S30** below.

Geometry	**Rods**
Average Size (With Std. Deviation)	Average Length: 21 µm ± 9.5 µm Average Diameter: 336 nm ± 41 nm
Diameter Homogeneity (Single Rod #6 as shown in **Supplementary Figure S31A)**	324 nm ± 13 nm
Key Responsible Reactant	0.02 M Sucrose
Full Reaction Condition	Pure 1,3-Propanediol (5 mL) 0.12 M $AgNO_3$ (3mL) 0.35 M PVP-55,000 MW (3mL) 0.02 M Sucrose (1 mL) Temp: 170°C
Note	Pure 1,3-propanediol was heated to 170 °C for 90 minutes followed by the dropwise addition of reactants within 6 minutes. The addition of sucrose proceeded within 2 minutes. The reaction ran for 80 minutes judging from the first addition of $AgNO_3$ to the reaction solution. The color of the solution was a greenish grey at the end of the reaction.

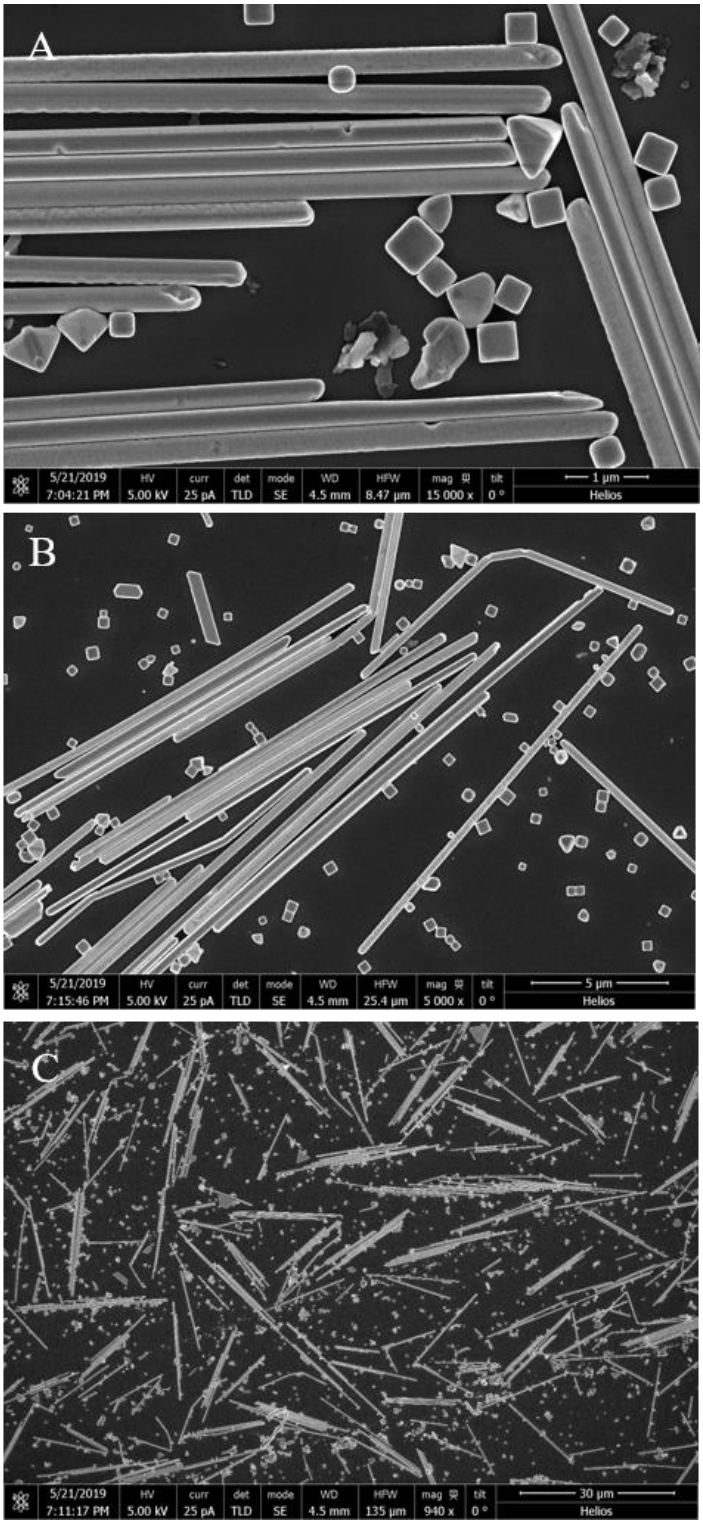

Supplementary Figure S30. (A-C) Three Representative SEM images of Silver Nanostructures with Nanorod Geometry at Three Different Magnifications. The full reaction condition for the silver nanostructures shown in this Figure is provided in **Supplementary Table S21** above. Also, the data analysis for these SEM images was performed by software ImageJ that is shown in **Supplementary Figure S31B-C** below, and their average value with their standard deviation is mentioned in **Supplementary Table S21** above.

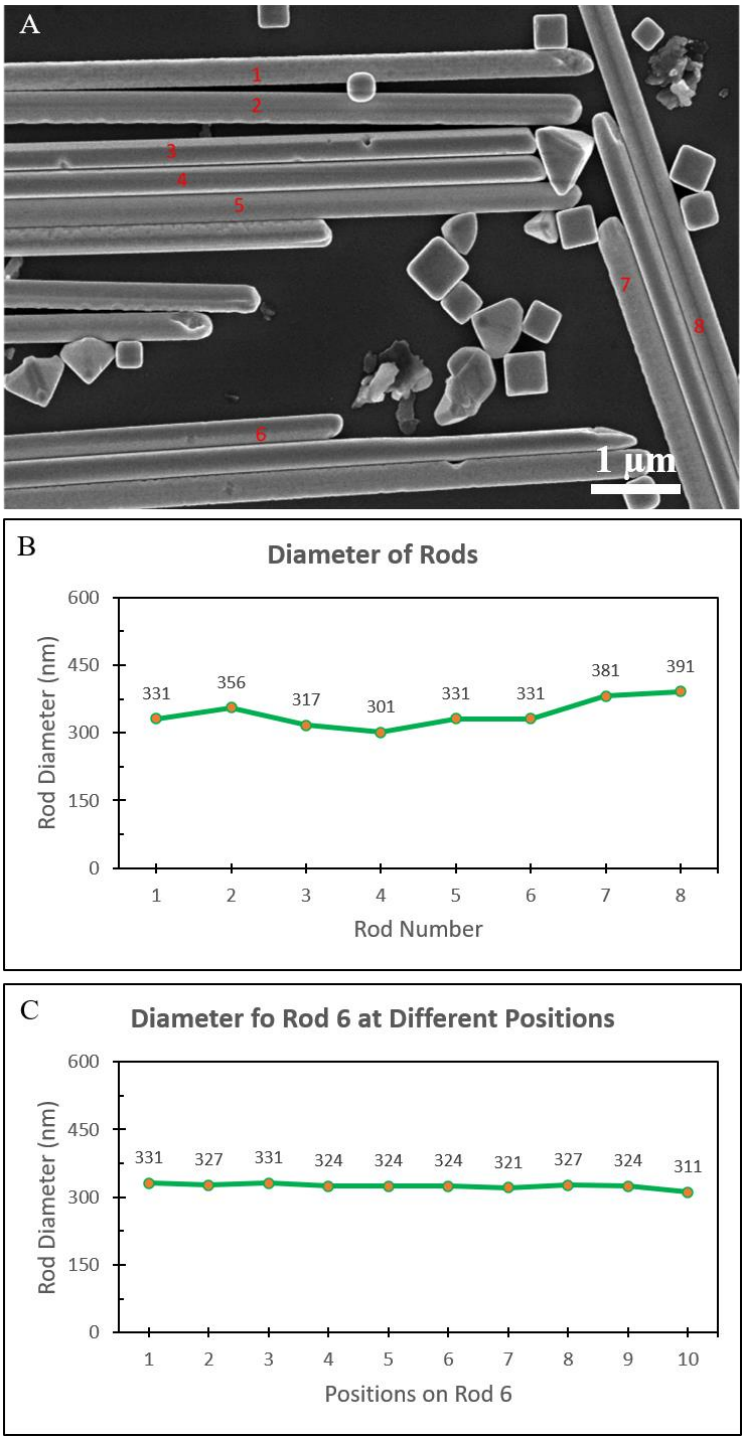

Supplementary Figure S31. (A) Representative SEM image of Silver Nanostructures with Nanorod Geometry obtained during the reaction condition provided in **Supplementary Table S21** above. (B) The diameter of 8 different rods marked in (A) was measured by software ImageJ. (C) The diameter of rod #6 marked in (A) at 10 different positions measured by software ImageJ.

Supplementary Table S22: Silver Nanostructures with Nanocube Geometry. Data mentioned in this Table has been analyzed by software ImageJ from the SEM image shown in **Supplementary Figure S32A**. The diameter (side to side) and the diagonal length (corner to corner) of the 8 different cubes was measured and the average size (diameter and diagonal length) is provided in this Table with their standard deviation. Overall, the size has been measured by analyzing 50 different cubes from 10 different SEM images of the same sample by software ImageJ. Furthermore, the diameter at 5 different positions of a single cube #1 (**Supplementary Figure S32A)** has been measured through ImageJ software and its average diameter with standard deviation is written in this Table for identifying the diameter homogeneity of the individual cube.

Geometry	**Cubes**
Average Size (With Std. Deviation)	Average Diameter (Side to Side Diameter): 252nm ± 19 nm Average Diagonal Length (Corner to Corner): 330 nm ± 21.5 nm 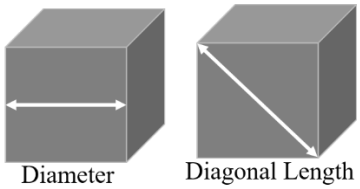
Diameter Homogeneity (Single Cube #1 as shown in **Supplementary Figure S32A)**	252.4 nm ±7.8 nm
Key Responsible Reactant	0.02 M Sucrose 0.35 M PVP1,300,000 MW
Full Reaction Condition	Pure 1,3-Propanediol (5 mL) 0.12 M $AgNO_3$ (3mL) 0.35 M PVP-1,300,000 MW (3mL) 0.02 M Sucrose (1 mL) Temp: 170°C
Note	Pure 1,3-propanediol was heated to 170 °C for 90 minutes followed by the dropwise addition of reactants within 6 minutes. The reaction ran for 60 minutes judging from the first addition of $AgNO_3$ to the reaction solution. The color of the solution was a greenish-grey at the end of the reaction.

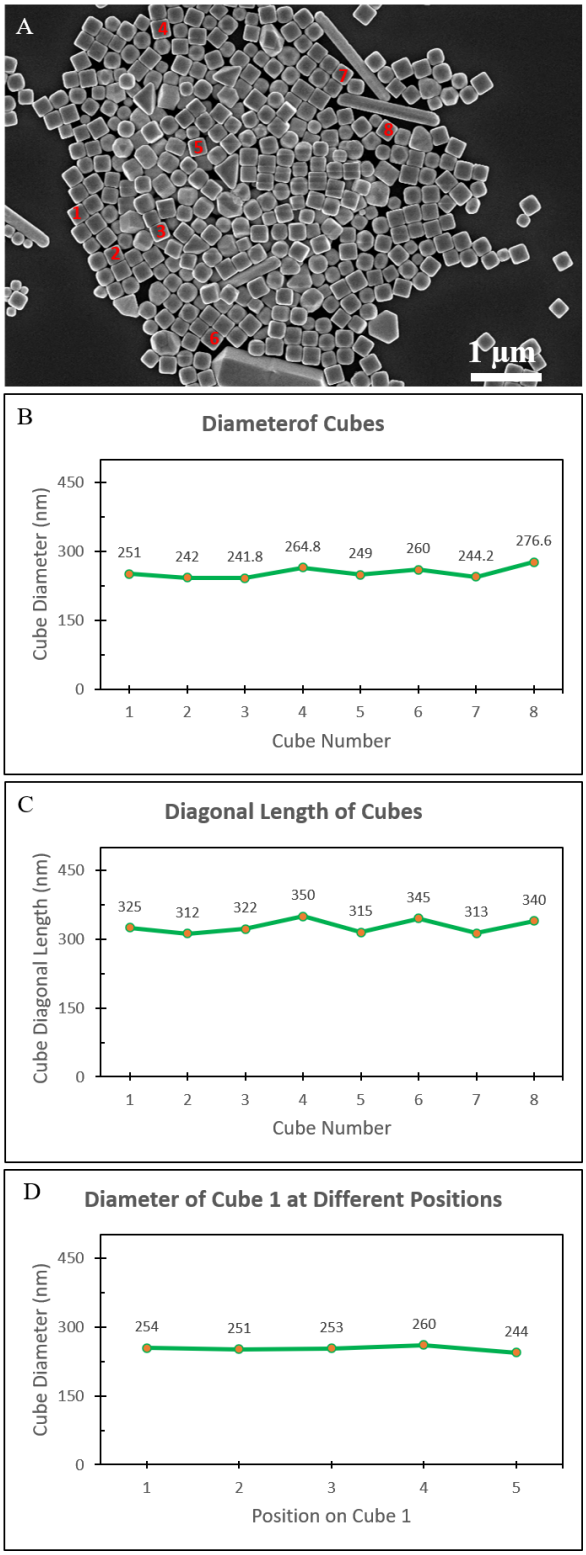

Supplementary Figure S32. (A) Representative SEM image of Silver Nanostructures with Nanocube Geometry obtained during the reaction condition provided in **Supplementary Table S22** above. (B) The diameter (side to side) and (C) diagonal length (corner to corner) of 8 different cubes marked in (A) was measured by software ImageJ. (D) The diameter of cube #1 marked in (A) at 5 different positions measured by software ImageJ.

Supplementary Table S23: Silver Nanostructures with Nanorod Geometry. Data mentioned in this Table has been analyzed by software ImageJ from the SEM image shown in **Supplementary Figure S34A**. The diameter of the 6 different rods was measured and their average size (length and diameter) is provided in this Table with their standard deviation. The length of the 50 different rods from 10 different SEM images of the same sample has been measured by software ImageJ and their average length with standard deviation is provided in this Table. Furthermore, the diameter at 10 different positions of a single rod #3 (**Supplementary Figure S34A)** has been measured through ImageJ software and its average diameter with standard deviation is written in this Table for identifying the diameter homogeneity of the individual rod. Two representative SEM images at different magnifications are shown in **Supplementary Figure S33** below.

Geometry	**Rods**
Average Size (With Std. Deviation)	Average Length: 6 µm ± 1.9 µm Average Diameter: 295 nm ± 44.5 nm
Diameter Homogeneity (Single Rod #3 as shown in **Supplementary Figure S34A)**	286 nm ±31 nm
Key Responsible Reactant	0.02 M Sucrose 0.15 M PVP 360,000 MW
Full Reaction Condition	Pure 1,3-Propanediol (5 mL) 0.15 M $AgNO_3$ (3mL) 0.15 M PVP-360,000 MW (3mL) 0.02 M Sucrose (1 mL) Temp: 170°C
Note	Pure 1,3-propanediol was heated to 170 °C for 90 minutes followed by the dropwise addition of reactants within 6 minutes. The reaction ran for 80 minutes judging from the first addition of $AgNO_3$ to the reaction solution. The color of the solution was a greenish-grey at the end of the reaction.

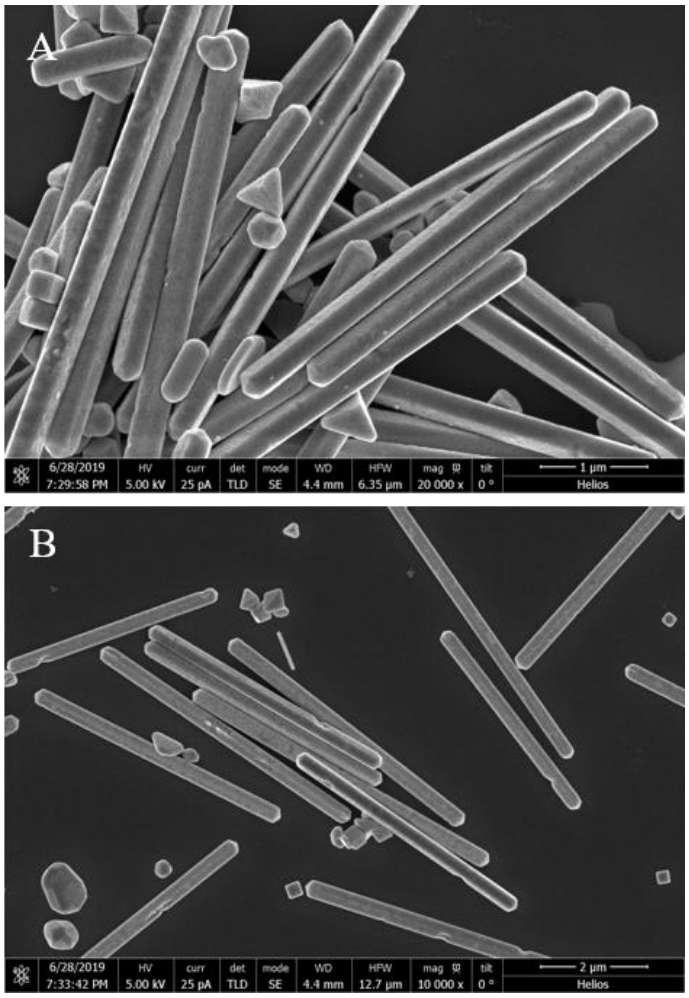

Supplementary Figure S33. (A-B) Two Representative SEM images of Silver Nanostructures with Nanorod Geometry at Two Different Magnifications. The full reaction condition for the silver nanostructures shown in this Figure is provided in **Supplementary Table S23** above. Also, the data analysis for these SEM images was performed by software ImageJ that is shown in **Supplementary Figure S34B-C** below, and their average value with their standard deviation is mentioned in **Supplementary Table S23** above.

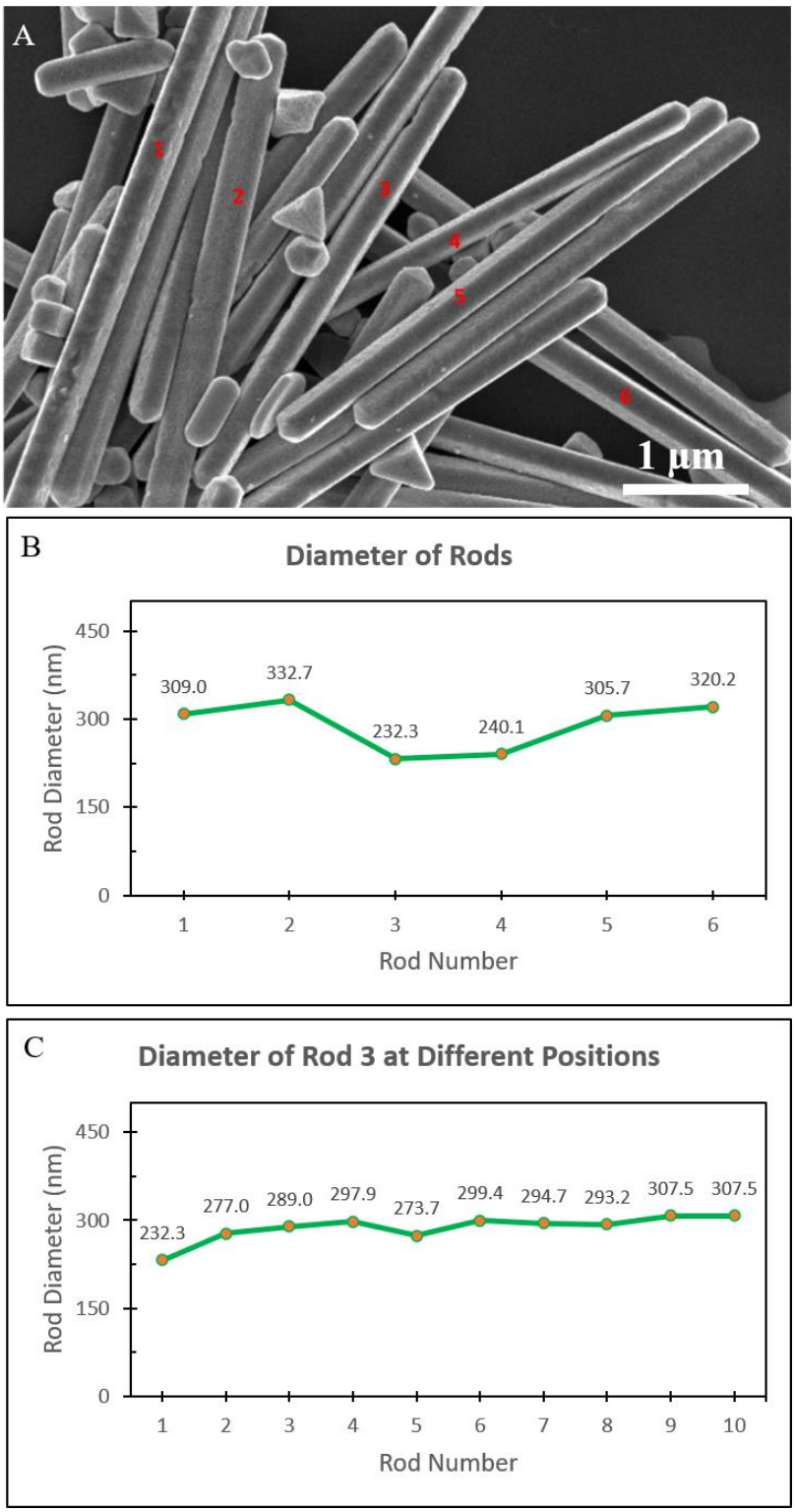

Supplementary Figure S34. (A) Representative SEM image of Silver Nanostructures with Nanorod Geometry obtained during the reaction condition provided in **Supplementary Table S21** above. (B) The diameter of 6 different rods marked in (A) was measured by software ImageJ. (C) The diameter of rod #3 marked in (A) at 10 different positions measured by software ImageJ.

Supplementary Table S24: Silver Nanostructures with Nanocube Geometry. Data mentioned in this Table has been analyzed by software ImageJ from the SEM image shown in **Supplementary Figure S35A**. The diameter (side to side) and the diagonal length (corner to corner) of the 3 different cubes was measured and the average size (diameter and diagonal length) is provided in this Table with their standard deviation. Overall, the size has been measured by analyzing 50 different cubes from 10 different SEM images of the same sample by software ImageJ. Furthermore, the diameter at 4 different positions of a single cube #1 (**Supplementary Figure S35A)** has been measured through ImageJ software and its average diameter with standard deviation is written in this Table for identifying the diameter homogeneity of the individual cube.

Geometry	**Cubes**
Average Size (With Std. Deviation)	Average Diameter (Side to Side Diameter): 207 nm ± 10 nm Average Diagonal Length (Corner to Corner): 278 nm ± 9 nm 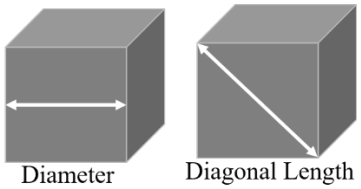
Diameter Homogeneity (Single Cube #1 as shown in **Supplementary Figure S35A)**	201 nm ± 8 nm
Key Responsible Reactant	0.1 M SDS
Full Reaction Condition	Pure 1,3-Propanediol (5 mL) 0.15 M $AgNO_3$ (3mL) 0.35 M PVP-360,000 MW (3mL) 0.1 M SDS (1 mL) Temp: 170°C
Note	Pure 1,3-propanediol was heated to 170 °C for 90 minutes followed by the dropwise addition of reactants within 3 minutes. The reaction ran for 30 minutes judging from the first addition of $AgNO_3$ to the reaction solution. The color of the solution was a dark greenish grey at the end of the reaction.

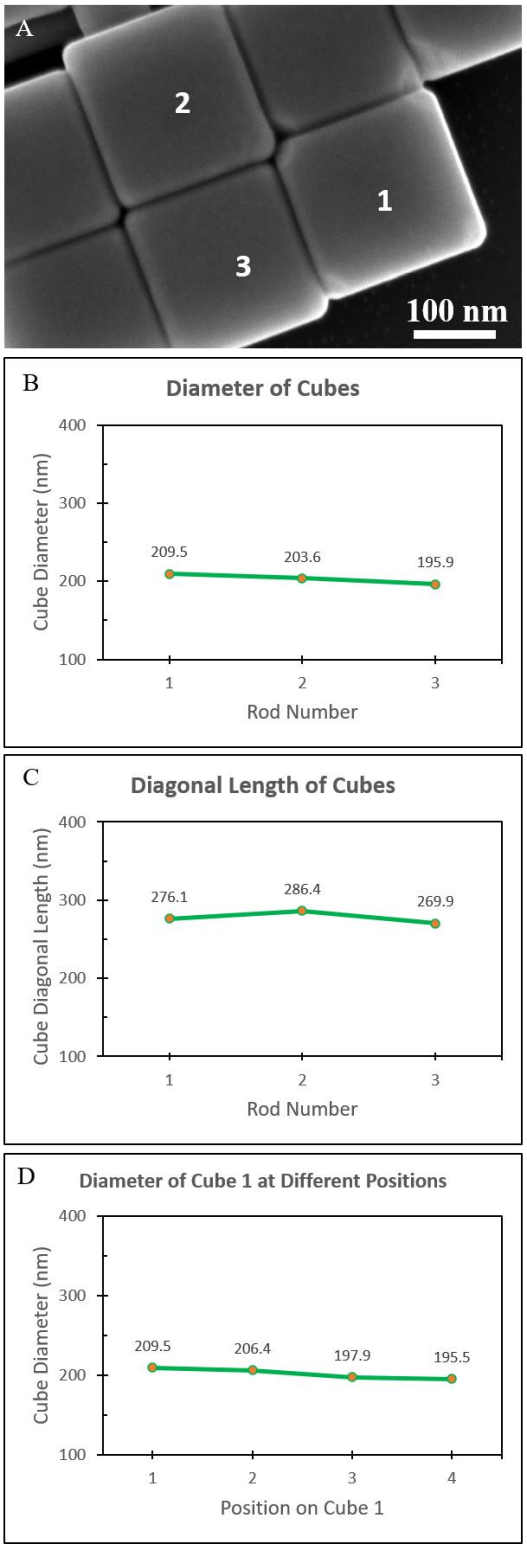

Supplementary Figure S35. (A) Representative SEM image of Silver Nanostructures with Nanocube Geometry obtained during the reaction condition provided in **Supplementary Table S24** above. (B) The diameter (side to side) and (C) diagonal length (corner to corner) of 3 different cubes marked in (A) was measured by software ImageJ. (D) The diameter of cube #1 marked in (A) at 4 different positions measured by software ImageJ.

Supplementary Table S25: Silver Nanostructures with Nanorod Geometry. Data mentioned in this Table has been analyzed by software ImageJ from the SEM image shown in **Supplementary Figure S36A**. The diameter of the 4 different rods and length of 3 different rods were measured and their average size (length and diameter) is provided in this Table with their standard deviation. The length of the 50 different rods from 10 different SEM images of the same sample has been measured by software ImageJ and their average length with standard deviation is provided in this Table. Furthermore, the diameter at 5 different positions of a single rod #2 (**Supplementary Figure S36A)** has been measured through ImageJ software and its average diameter with standard deviation is written in this Table for identifying the diameter homogeneity of the individual rod.

Geometry	**Rods**
Average Size (With Std. Deviation)	Average Length: 1.3 µm ± 0.4 µm Average Diameter: 259 nm ± 54 nm
Diameter Homogeneity (Single Rod #2 as shown in **Supplementary Figure S36A)**	326 nm ± 11 nm
Key Responsible Reactant	0.02 M Sucrose 0.2 M $AgNO_3$
Full Reaction Condition	Pure 1,3-Propanediol (5 mL) 0.2 M $AgNO_3$ (3mL) 0.35 M PVP-360,000 MW (3mL) 0.02 M Sucrose (1 mL) Temp: 172°C
Note	Pure 1,3-propanediol was heated to 172 °C for 90 minutes followed by the dropwise addition of reactants within 7 minutes. The reaction ran for 80 minutes judging from the first addition of $AgNO_3$ to the reaction solution. The color of the solution was a dark yellowish grey at the end of the reaction.

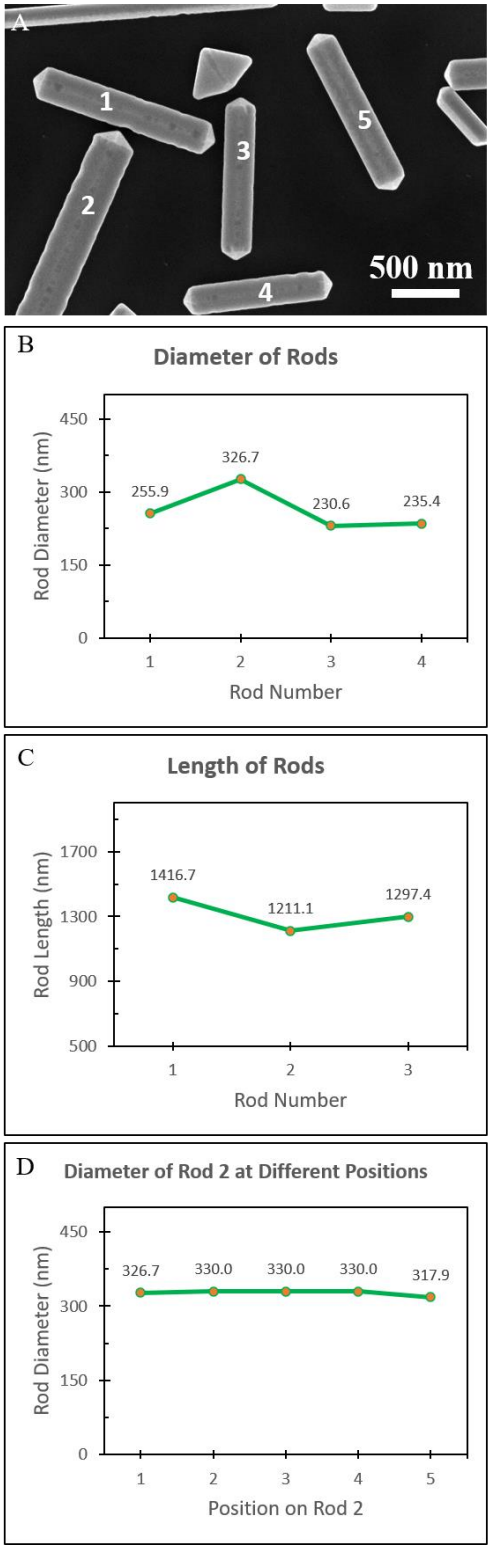

Supplementary Figure S36. (A) Representative SEM image of Silver Nanostructures with Nanorod Geometry obtained during the reaction condition provided in **Supplementary Table S25** above. (B) The diameter of 4 different rods marked in (A) was measured by software ImageJ. (C) The length of 3 different rods marked in (A) was measured by software ImageJ. (D) The diameter of rod #2 marked in (A) at 5 different positions measured by software ImageJ.

Supplementary Table S26: Silver Nanostructures with Nanorod Geometry. Data mentioned in this Table has been analyzed by software ImageJ from the SEM image shown in **Supplementary Figure S37A**. The diameter of the 4 different rods and length of 3 different rods were measured and their average size (length and diameter) is provided in this Table with their standard deviation. The length of the 50 different rods from 10 different SEM images of the same sample has been measured by software ImageJ and their average length with standard deviation is provided in this Table. Furthermore, the diameter at 5 different positions of a single rod #2 (**Supplementary Figure S37A)** has been measured through ImageJ software and its average diameter with standard deviation is written in this Table for identifying the diameter homogeneity of the individual rod.

Geometry	**Rods**
Average Size (With Std. Deviation)	Average Length: 1.61 µm ± 90 nm Average Diameter: 272 nm ± 7 nm
Diameter Homogeneity (Single Rod #2 as shown in **Supplementary Figure S37A)**	278 nm ± 10 nm
Key Responsible Reactant	0.02 M Sucrose 0.2 M $AgNO_3$
Full Reaction Condition	Pure 1,3-Propanediol (5 mL) 0.2 M $AgNO_3$ (3mL) 0.35 M PVP-360,000 MW (3mL) 0.02 M Sucrose (1 mL) Temp: 170°C
Note	P Pure 1,3-propanediol was heated to 170 °C for 90 minutes followed by the dropwise addition of reactants within 7 minutes. The reaction ran for 80 minutes judging from the first addition of $AgNO_3$ to the reaction solution. The color of the solution was a dark yellowish grey at the end of the reaction.

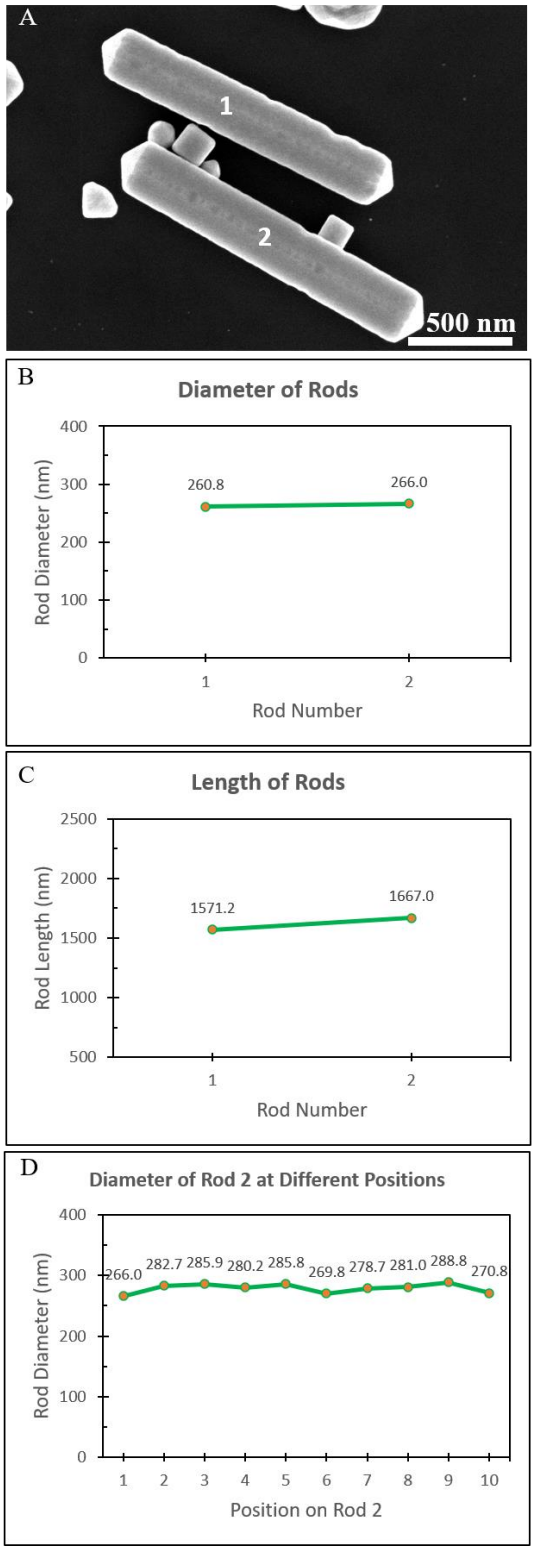

Supplementary Figure S37. (A) Representative SEM image of Silver Nanostructures with Nanorod Geometry obtained during the reaction condition provided in **Supplementary Table S26** above. (B) The diameter and (C) length of 2 different rods marked in (A) was measured by software ImageJ. (D) The diameter of rod #2 marked in (A) at 10 different positions measured by software ImageJ.

5. Plasmonic Building-block Geometries: *Overview of Nanostructure's Geometries*

Supplementary Table S27. Overview of the geometry of the silver nanostructures and their homogeneity at given reaction conditions.

Geometry	Average Size	Reaction Condition	Details
Rods	Length: 16 μm ± 2.5 μm Diameter: 214 nm ± 14 nm	Pure 1,3-Propanediol (5 mL) 0.15 M AgNO3 (3mL) 0.35 M PVP-360,000 MW (3mL) 0.02 M Sucrose (1 mL) Temp: 170°C	See Table S1
Particles	Size: 85 nm ± 20 nm	Pure 1,3-Propanediol (5 mL) 0.15 M $AgNO_3$ (3mL) 0.35 M PVP-360,000 MW (3mL) 0.04 M Tannic Acid (1 mL) Temp: 170°C	See Table S2
Rods	Length: 8 μm ± 3 μm Diameter: 521 nm ± 20 nm	Pure 1,3-Propanediol (5 mL) 0.15 M $AgNO_3$ (3mL) 0.35 M PVP-360,000 MW (3mL) 0.1 M Ascorbic Acid (1 mL) Temp: 170°C	See Table S3
Rods + Particles	Rod Length: 450 nm ± 60 nm Rod Diameter: 155 nm ± 35 nm Particle Size: 180 nm ± 60 nm	Pure 1,3-Propanediol (5 mL) 0.15 M $AgNO_3$ (3mL) 0.35 M PVP-360,000 MW (3mL) 0.02 M $NaBH_4$ (1 mL) Temp: 170°C	See Table S4
Rods	Length: 22 μm ± 8 μm Diameter: 316 nm ± 41 nm	Pure 1,3-Propanediol (5 mL) 0.2 M $AgNO_3$ (3mL) 0.35 M PVP-360,000 MW (3mL) 0.02 M Sucrose (1 mL) Temp: 160°C	See Table S5
Rods	Length: 3.0 μm ± 0.8 μm Diameter: 80 nm ± 9 nm	Pure 1,3-Propanediol (5 mL) 0.2 M $AgNO_3$ (3mL) 0.35 M PVP-360,000 MW (3mL) 0.1 M Ascorbic Acid (1 mL) Temp: 160°C	See Table S6
Rods	Length: 3.6 μm ± 2.2 μm Diameter: 430 nm ± 45 nm	Pure 1,3-Propanediol (5 mL) 0.15 M $AgNO_3$ (3mL) 0.35 M PVP-55,000 MW (3mL) 0.15 M Ascorbic Acid (1 mL) Temp: 170°C	See Table S7

Rods	Length: 16 μ m ± 7 μ m Diameter: 250 nm ± 42 nm	Pure 1,3-Propanediol (5 mL) 0.15 M $AgNO_3$ (3mL) 0.35 M PVP-360,000 MW (3mL) 0.01 M Sucrose (1 mL) Temp: 167°C	See Table S8
Rods	Length: 5 μ m ± 1.2 μ m Diameter: 320 nm ± 25 nm	Pure 1,3-Propanediol (5 mL) 0.12 M $AgNO_3$ (3mL) 0.35 M PVP-360,000 MW (3mL) 0.02 M Sucrose (1 mL) Temp: 170°C	See Table S9
Rods	Length: 2.5 μ m ± 0.9 μ m Diameter: 313 nm ± 21 nm	Pure 1,3-Propanediol (5 mL) 0.25 M $AgNO_3$ (3mL) 0.35 M PVP-360,000 MW (3mL) 0.02 M Sucrose (1 mL) Temp: 167°C	See Table S10
Rods	Length: 6 μ m ± 0.9 μ m Diameter: 420 nm ± 22 nm	Pure 1,3-Propanediol (5 mL) 0.15 M $AgNO_3$ (3mL) 0.35 M PVP-360,000 MW (3mL) 0.02 M Fructose (1 mL) Temp: 167°C	See Table S11
Rods	Length: 11 μ m ± 4.2 μ m Diameter: 470 nm ± 18 nm	Pure 1,3-Propanediol (5 mL) 0.15 M $AgNO_3$ (3mL) 0.35 M PVP-360,000 MW (3mL) 0.02 M Maltotriose (1 mL) Temp: 167°C	See table S12
Cubes	Diameter (Side to Side Diameter): 235 nm ± 12 nm Diagonal Length (Corner to Corner): 321 nm ± 20.5 nm	Pure 1,3-Propanediol (5 mL) 0.12 M $AgNO_3$ (3mL) 0.35 M PVP-1300,000 MW (3mL) 0.02 M Sucrose (1 mL) Temp: 170°C	See Table S13
Cubes	Diameter (Side to Side Diameter): 420 nm ± 25 nm Diagonal Length (Corner to Corner): 559 nm ± 38.6 nm	Pure 1,3-Propanediol (5 mL) 0.15 M AgNO3 (3mL) 0.35 M PVP-55,000 MW (3mL) 0.02 M Sucrose (1 mL) Temp: 172°C	See table S14
Cubes	Diameter (Side to Side Diameter): 426 nm ± 12 nm Diagonal Length (Corner to Corner): 567 nm ± 38.6 nm	Pure 1,3-Propanediol (5 mL) 0.15 M AgNO3 (3mL) 0.35 M PVP-1,300,000 MW (3mL) 0.02 M Sucrose (1 mL) Temp: 170°C	See Table S15
Cubes	Diameter (Side to Side Diameter):	Pure 1,3-Propanediol (5 mL)	See Table S16

	429 nm ± 22 nm Diagonal Length (Corner to Corner): 573.4 nm ± 38.6 nm	0.15 M AgNO3 (3mL) 0.35 M PVP-55,000 MW (3mL) 0.025 M Sucrose (1 mL) Temp: 165°C	
Rods + particles	Rod Length: 560 nm ± 180 nm Rod Diameter: 108 nm ± 56 nm Particle size: 195 nm ± 140 nm	Pure 1,3-Propanediol (5 mL) 0.15 M $AgNO_3$ (3mL) 0.35 M PVP-360,000 MW (3mL) 0.1 M SMPS (1 mL) Temp: 170°C	See Table S17
Cubes	Diameter (Side to Side Diameter): 191 nm ± 65 nm Diagonal Length (Corner to Corner): 256.8 nm ± 78.5 nm	Pure 1,3-Propanediol (5 mL) 0.15 M $AgNO_3$ (3mL) 0.35 M PVP-360,000 MW (3mL) 0.1 M SDS (1 mL) Temp: 170°C	See Table S18
Bars	Length of Bar: 320 nm ± 125 nm Diameter of Bar: 172 nm ± 56 nm	Pure 1,3-Propanediol (5 mL) 0.15 M $AgNO_3$ (3mL) 0.35 M PVP-360,000 MW (3mL) 0.1 M SHDS (1 mL) Temp: 170°C	See Table S19
Rods + Particles	Rod Length: 1.5 μ m ± 800 nm Rod Diameter: 53 nm ± 35.5 nm Particle size: 120 nm ± 60 nm	Pure 1,3-Propanediol (5 mL) 0.15 M AgNO3 (3mL) 0.35 M PVP-360,000 MW (3mL) 0.1 M NaOH (1 mL) Temp: 170°C	See Table S20
Rods	Average Length: 21 μ m ± 9.5 μ m Average Diameter: 336 nm ± 41 nm	Pure 1,3-Propanediol (5 mL) 0.12 M AgNO3 (3mL) 0.35 M PVP-55,000 MW (3mL) 0.02 M Sucrose (1 mL) Temp: 170°C	See Table S21
Cubes	Diameter (Side to Side Diameter): 252nm ± 19 nm Diagonal Length (Corner to Corner): 330 nm ± 21.5 nm	Pure 1,3-Propanediol (5 mL) 0.12 M $AgNO_3$ (3mL) 0.35 M PVP-1300,000 MW (3mL) 0.02 M Sucrose (1 mL) Temp: 170°C	See Table S22
Rods	Length: 6 μ m ± 1.9 μ m Diameter: 295 nm ± 44.5 nm	Pure 1,3-Propanediol (5 mL) 0.15 M $AgNO_3$ (3mL) 0.15 M PVP-360,000 MW (3mL) 0.02 M Sucrose (1 mL) Temp: 170°C	See Table S23
Cubes	Diameter (Side to Side Diameter): 207 nm ± 10 nm Diagonal Length (Corner to Corner): 278 nm ± 9 nm	Pure 1,3-Propanediol (5 mL) 0.15 M $AgNO_3$ (3mL) 0.35 M PVP-360,000 MW (3mL) 0.1 M SDS (1 mL) Temp: 170°C	See Table S24

Rods	Length: 1.3 μ m ± 0.4 μ m Diameter: 259 nm ± 54 nm	Pure 1,3-Propanediol (5 mL) 0.2 M $AgNO_3$ (3mL) 0.35 M PVP-360,000 MW (3mL) 0.02 M Sucrose (1 mL) Temp: 172°C	See Table S25
Rods	Length: 1.61 μ m ± 90 nm Diameter: 272 nm ± 7 nm	Pure 1,3-Propanediol (5 mL) 0.2 M $AgNO_3$ (3mL) 0.35 M PVP-360,000 MW (3mL) 0.02 M Sucrose (1 mL) Temp: 170°C	See Table S26

Additional nanostructures were obtained at various reaction conditions.

Supplementary Table SA: Silver Nanostructures with Nanorod Geometry. Reaction condition is provided here in this Table for the nanostructures shown in **Supplementary Figure SA** below. Four different SEM images of the same reaction sample are shown in **Supplementary Figure SA** below.

Geometry	**Nanorods**
Full Reaction Condition	Pure 1,3-Propanediol (5 mL) 0.2 M $AgNO_3$ (3mL) 0.35 M PVP-10,000 MW (3mL) 0.01M Sucrose (1 mL) Temp: 160°C
Note	Pure 1,3-propanediol was heated to 160 °C for 90 minutes followed by the dropwise addition of reactants within 7 minutes. The reaction ran for 60 minutes judging from the first addition of $AgNO_3$ to the reaction solution. The color of the solution was a dark greenish grey at the end of the reaction.

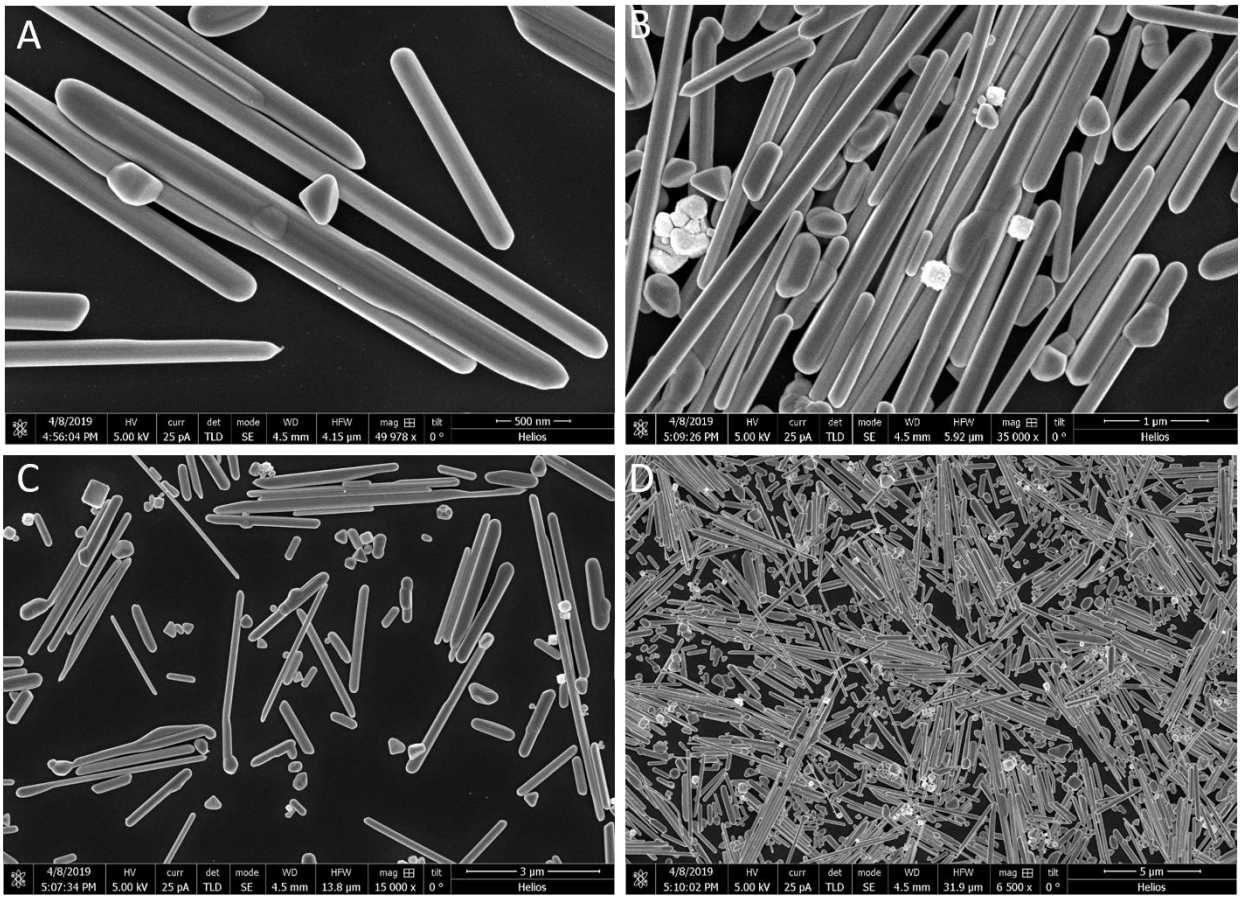

Supplementary Figure SA. (A-D) Four Representative SEM images of Silver Nanostructures with Nanorod Geometry at Four Different Magnifications. The full reaction condition for the silver nanostructures shown in this Figure is provided in **Supplementary Table SA** above.

Supplementary Table SB: Silver Nanostructures with Nanorod Geometry. Reaction condition is provided here in this Table for the nanostructures shown in **Supplementary Figure SB** below. Four different SEM images of the same reaction sample are shown in **Supplementary Figure SB** below.

Geometry	**Nanorods**
Full Reaction Condition	Pure 1,3-Propanediol (5 mL) 0.2 M $AgNO_3$ (3mL) 0.35 M PVP-29,000 MW (3mL) 0.01M Sucrose (1 mL) Temp: 160°C
Note	Pure 1,3-propanediol was heated to 160 °C for 90 minutes followed by the dropwise addition of reactants within 7 minutes. The reaction ran for 60 minutes judging from the first addition of $AgNO_3$ to the reaction solution. The color of the solution was a dark greenish grey at the end of the reaction.

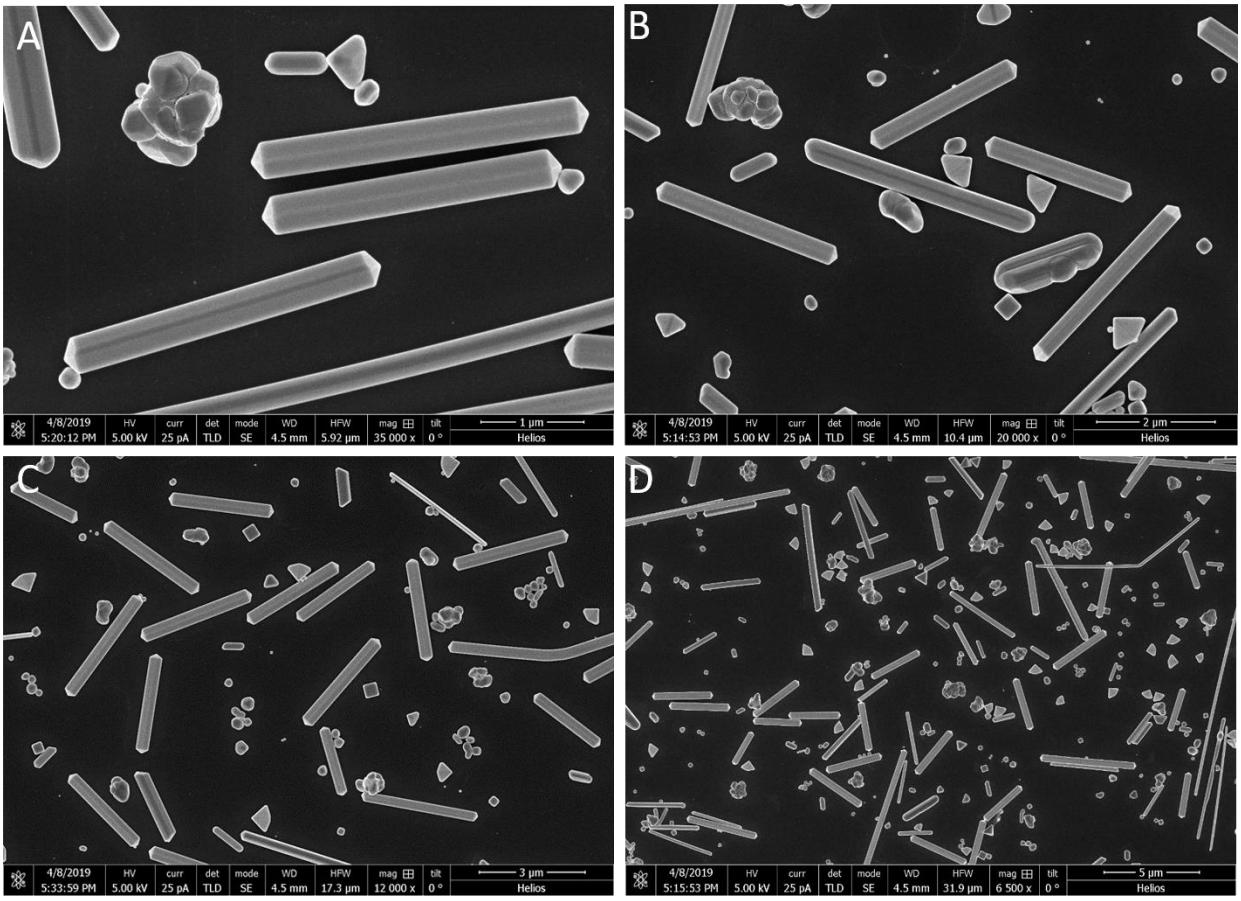

Supplementary Figure SB. (A-D) Four Representative SEM images of Silver Nanostructures with Nanorod Geometry at Four Different Magnifications. The full reaction condition for the silver nanostructures shown in this Figure is provided in **Supplementary Table SB** above.

Supplementary Table SC: Silver Nanostructures with Nanorod Geometry. Reaction condition is provided here in this Table for the nanostructures shown in **Supplementary Figure SC** below. Four different SEM images of the same reaction sample are shown in **Supplementary Figure SC** below.

Geometry	**Nanorods**
Full Reaction Condition	Pure 1,3-Propanediol (5 mL) 0.12 M $AgNO_3$ (3mL) 0.35 M PVP-360,000 MW (3mL) 0.01M Maltotriose (1 mL) 0.1 M KOH (1 mL) (After 6 hour) Temp: 131°C
Note	Pure 1,3-propanediol was heated to 131 °C for 90 minutes followed by the dropwise addition of reactants within 7 minutes. The reaction ran for 6 hours judging from the first addition of $AgNO_3$ to the reaction solution but there was no color change. Reason for longer reaction without color change is low temperature (131°C). After that, 0.1 M KOH (1 mL) was added dropwise, and immediately color of the solution changed to yellowish grey.

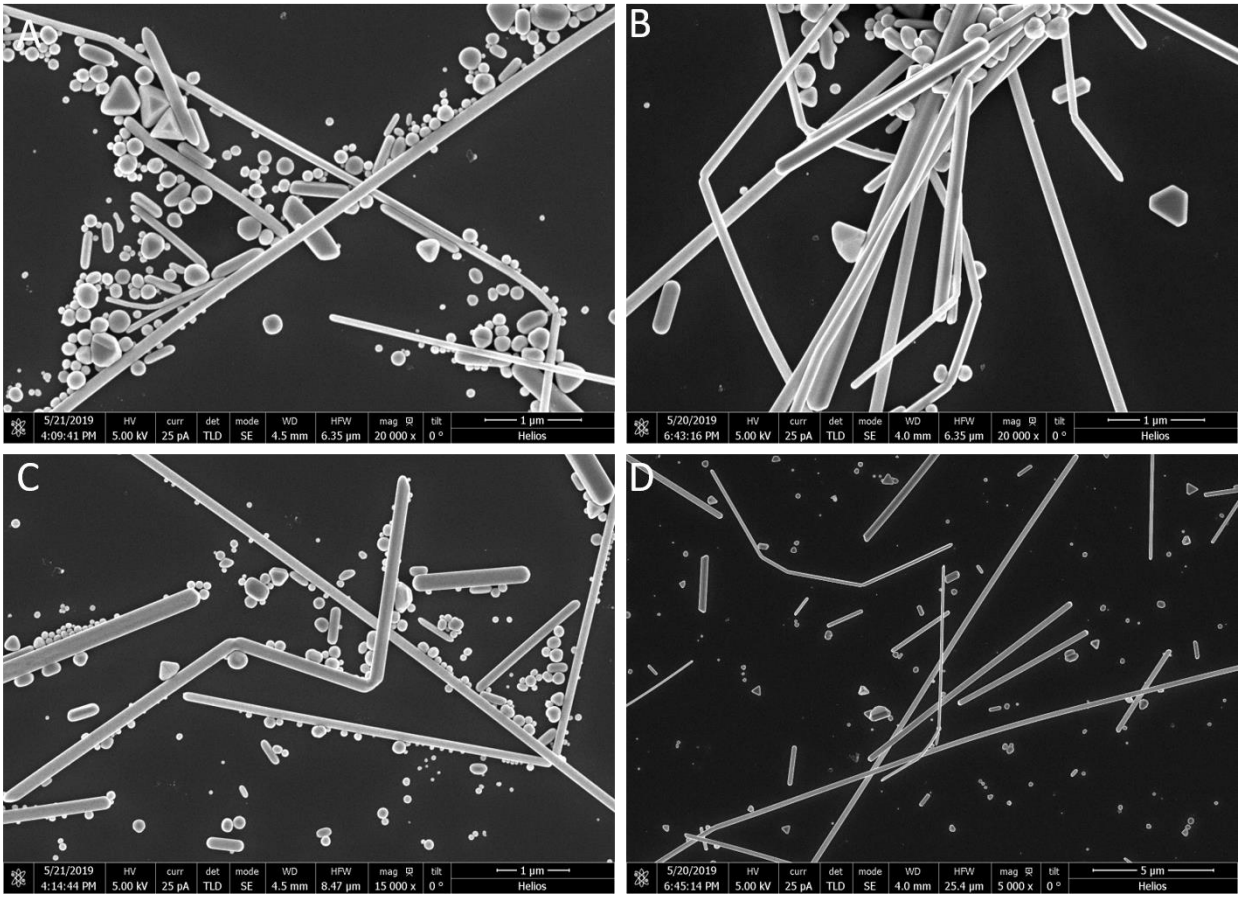

Supplementary Figure SC. (A-D) Four Representative SEM images of Silver Nanostructures with Nanorod Geometry at Four Different Magnifications. The full reaction condition for the silver nanostructures shown in this Figure is provided in **Supplementary Table SC** above.

Supplementary Table SD: Silver Nanostructures with Nanorod Geometry. Reaction condition is provided here in this Table for the nanostructures shown in **Supplementary Figure SD** below. Four different SEM images of the same reaction sample are shown in **Supplementary Figure SD** below.

Geometry	**Nanorods**
Full Reaction Condition	Pure 1,3-Propanediol (5 mL) 0.12 M $AgNO_3$ (3mL) 0.35 M PVP-360,000 MW (3mL) 0.01M Maltotriose (1 mL) 0.1 M Ascorbic Acid (1 mL) (After 6 hour) Temp: 131°C
Note	Pure 1,3-propanediol was heated to 131 °C for 90 minutes followed by the dropwise addition of reactants within 7 minutes. The reaction ran for 6 hours judging from the first addition of $AgNO_3$ to the reaction solution but there was no color change. The reason for a longer reaction without color change is the low temperature (131°C). After that, 0.1 M Ascorbic Acid (1 mL) was added dropwise, and immediately color of the solution changed to yellowish-grey.

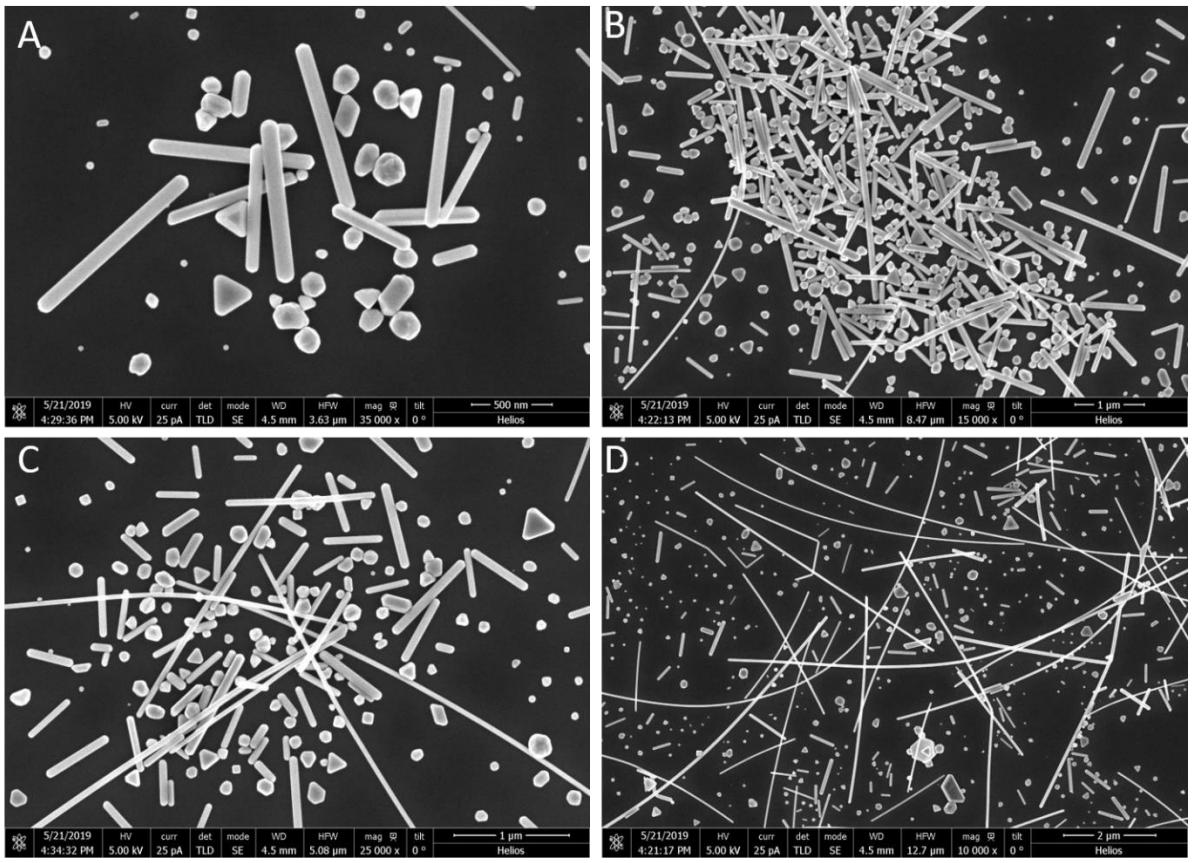

Supplementary Figure SD. (A-D) Four Representative SEM images of Silver Nanostructures with Nanorod Geometry at Four Different Magnifications. The full reaction condition for the silver nanostructures shown in this Figure is provided in **Supplementary Table SD** above.

Supplementary Table SE: Silver Nanostructures with Nanorod Geometry. Reaction condition is provided here in this Table for the nanostructures shown in **Supplementary Figure SE** below. Four different SEM images of the same reaction sample are shown in **Supplementary Figure SE** below.

Geometry	**Nanoparticles**
Full Reaction Condition	Pure 1,3-Propanediol (5 mL) 0.12 M $AgNO_3$ (3mL) 0.35 M PVP-360,000 MW (3mL) 0.01M Sucrose (1 mL) 0.01 M Tannic Acid (1 mL) (After 6 hour) Temp: 131°C
Note	Pure 1,3-propanediol was heated to 131 °C for 90 minutes followed by the dropwise addition of reactants within 7 minutes. The reaction ran for 6 hours judging from the first addition of $AgNO_3$ to the reaction solution but there was no color change. The reason for a longer reaction without color change is low temperature (131°C). After that, 0.01 M Tannic Acid (1 mL) was added dropwise, and immediately color of the solution changed to yellowish-grey.

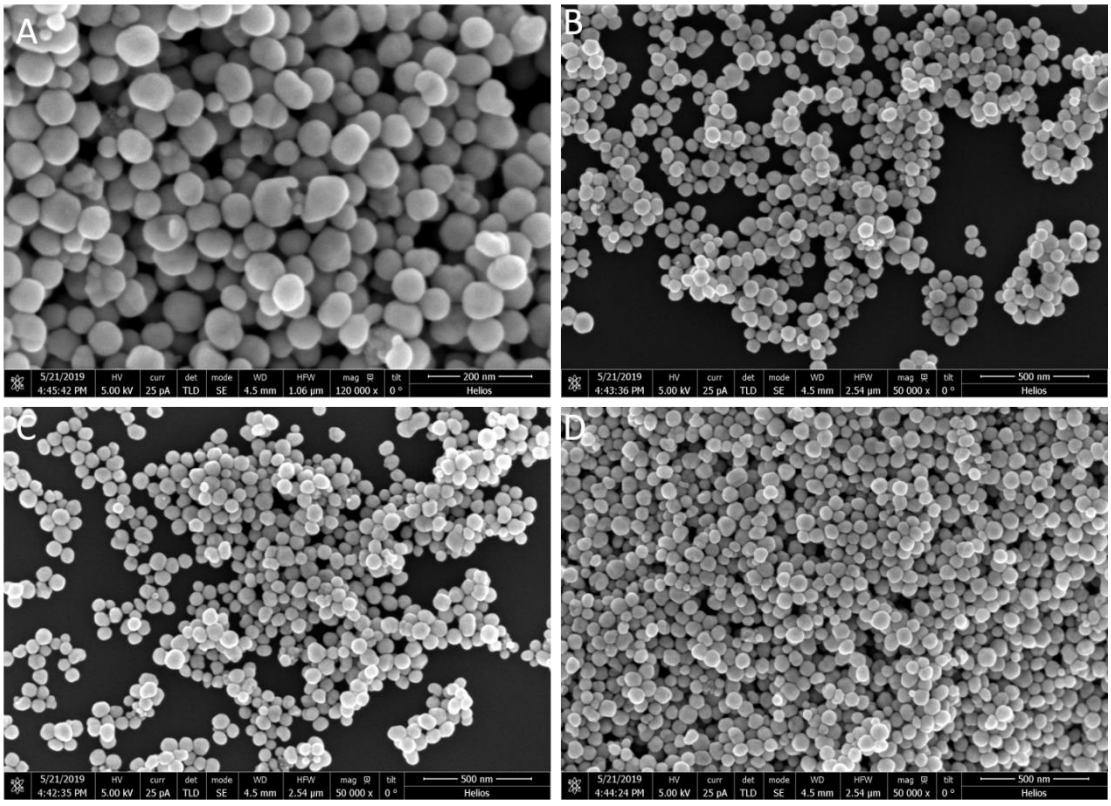

Supplementary Figure SE. (A-D) Four Representative SEM images of Silver Nanostructures with Nanoparticles Geometry at Four Different Magnifications. The full reaction condition for the silver nanostructures shown in this Figure is provided in **Supplementary Table SE** above.

Supplementary Table SF: Silver Nanostructures with Nanorod Geometry. Reaction condition is provided here in this Table for the nanostructures shown in **Supplementary Figure SF** below. Four different SEM images of the same reaction sample are shown in **Supplementary Figure SF** below.

Geometry	**Nanorods**
Full Reaction Condition	Pure 1,3-Propanediol (5 mL) 0.12 M $AgNO_3$ (3mL) 0.35 M PVP-360,000 MW (3mL) 0.01M Sucrose (1 mL) 0.1M Ascorbic Acid (1 mL) (After 6 hour) Temp: 131°C
Note	Pure 1,3-propanediol was heated to 131 °C for 90 minutes followed by the dropwise addition of reactants within 7 minutes. The reaction ran for 6 hours judging from the first addition of $AgNO_3$ to the reaction solution but there was no color change. The reason for a longer reaction without color change is the low temperature (131°C). After that, 0.1M Ascorbic Acid (1 mL) was added dropwise, and immediately color of the solution changed to yellowish-grey.

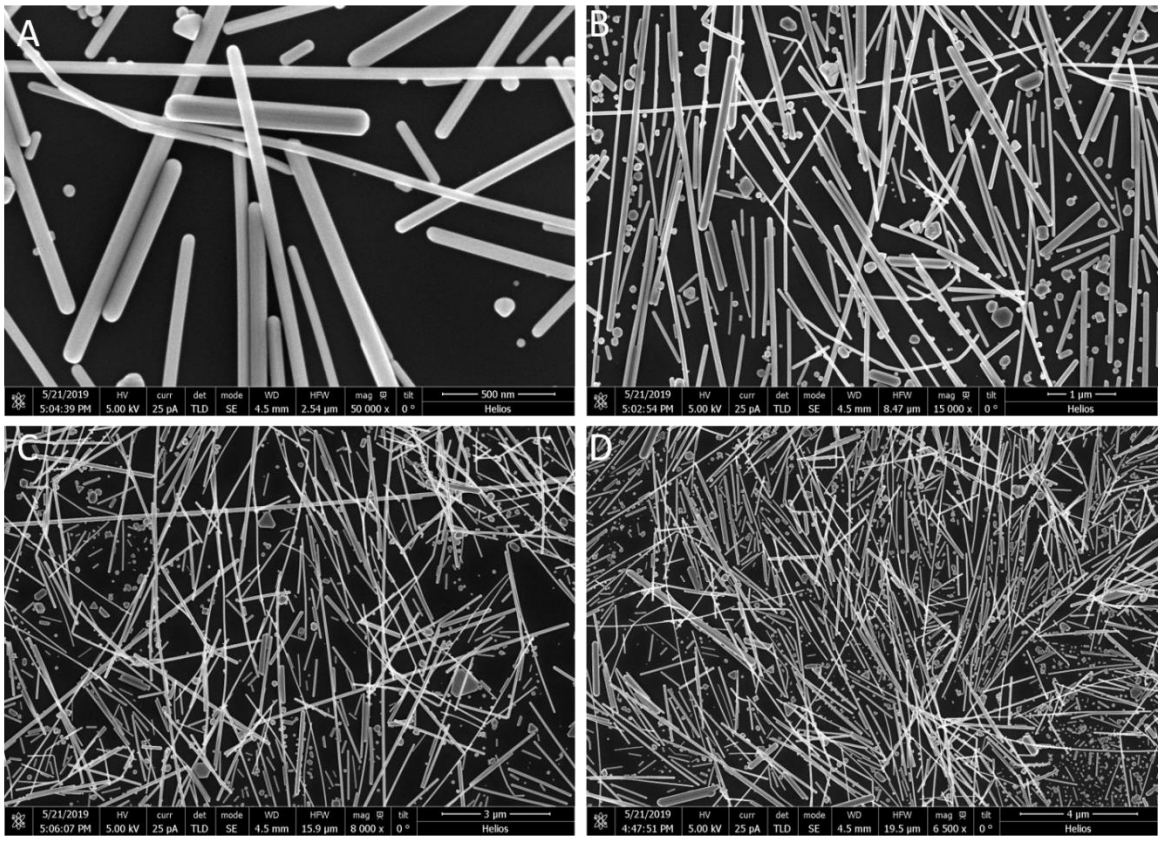

Supplementary Figure SF. (A-D) Four Representative SEM images of Silver Nanostructures with Nanorod Geometry at Four Different Magnifications. The full reaction condition for the silver nanostructures shown in this Figure is provided in **Supplementary Table SF** above.

Supplementary Table SG: Silver Nanostructures with Nanorod Geometry. Reaction condition is provided here in this Table for the nanostructures shown in **Supplementary Figure SG** below. Four different SEM images of the same reaction sample are shown in **Supplementary Figure SG** below.

Geometry	**Nanorods**
Full Reaction Condition	Pure 1,3-Propanediol (5 mL) 0.12 M $AgNO_3$ (3mL) 0.35 M PVP-360,000 MW (3mL) Temp: 131°C
Note	Pure 1,3-propanediol was heated to 131 °C for 90 minutes followed by the dropwise addition of reactants within 7 minutes. The reaction ran for 4 hours judging from the first addition of $AgNO_3$ to the reaction and color was slowly changed from yellow to dark yellowish grey (without any external reducing agents).

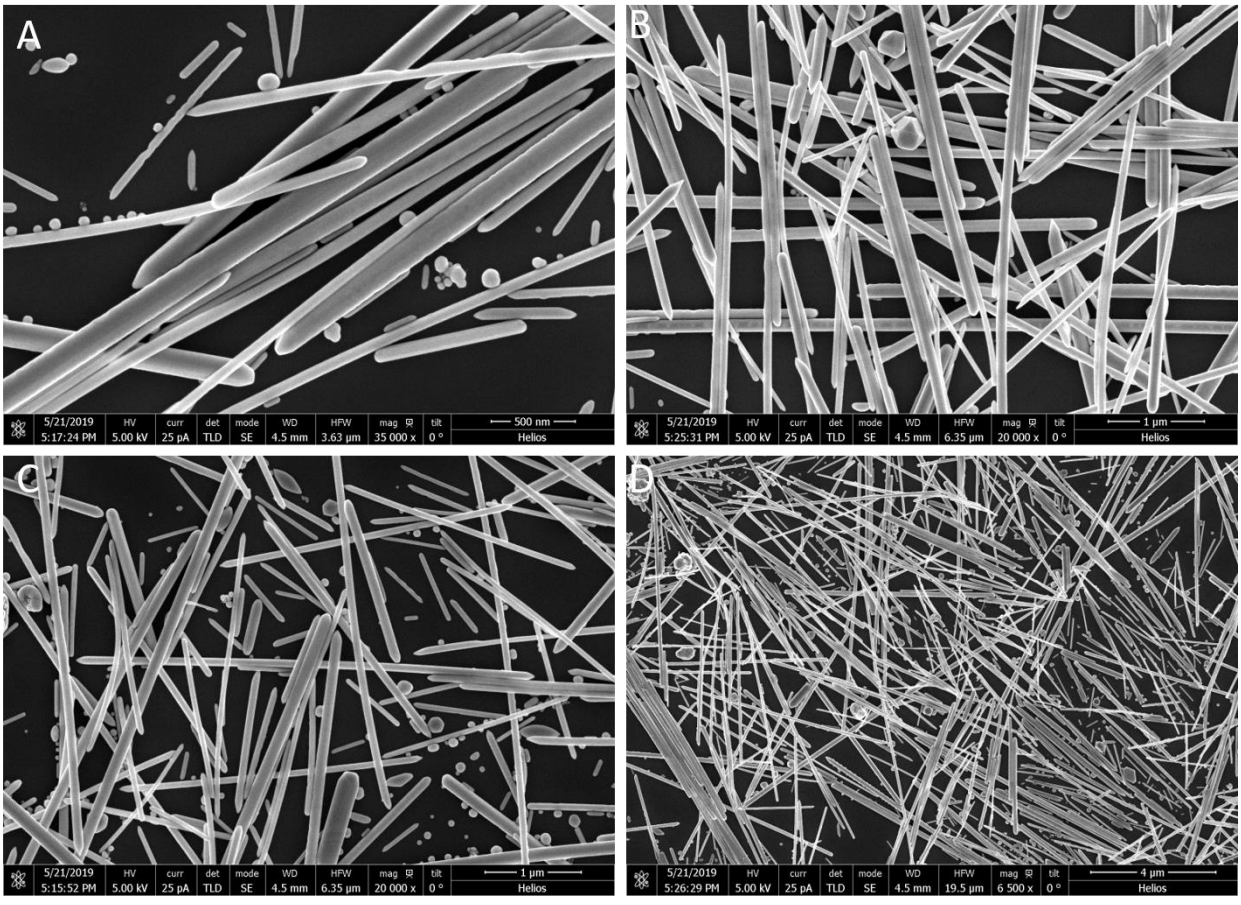

Supplementary Figure SG. (A-D) Four Representative SEM images of Silver Nanostructures with Nanorod Geometry at Four Different Magnifications. The full reaction condition for the silver nanostructures shown in this Figure is provided in **Supplementary Table SG** above.

Supplementary Table SH: Silver Nanostructures with Nanorod Geometry. Reaction condition is provided here in this Table for the nanostructures shown in **Supplementary Figure SH** below. Four different SEM images of the same reaction sample are shown in **Supplementary Figure SH** below.

Geometry	**Nanorods**
Full Reaction Condition	Pure 1,3-Propanediol (5 mL) 0.12 M $AgNO_3$ (3mL) 0.35 M PVP-360,000 MW (3mL) 0.1M Ascorbic Acid (1 mL) Temp: 131°C
Note	Pure 1,3-propanediol was heated to 131 °C for 90 minutes followed by the dropwise addition of reactants within 7 minutes. The reaction ran for 1-hour judging from the first addition of $AgNO_3$ to the reaction solution and the color was obtained yellowish-grey.

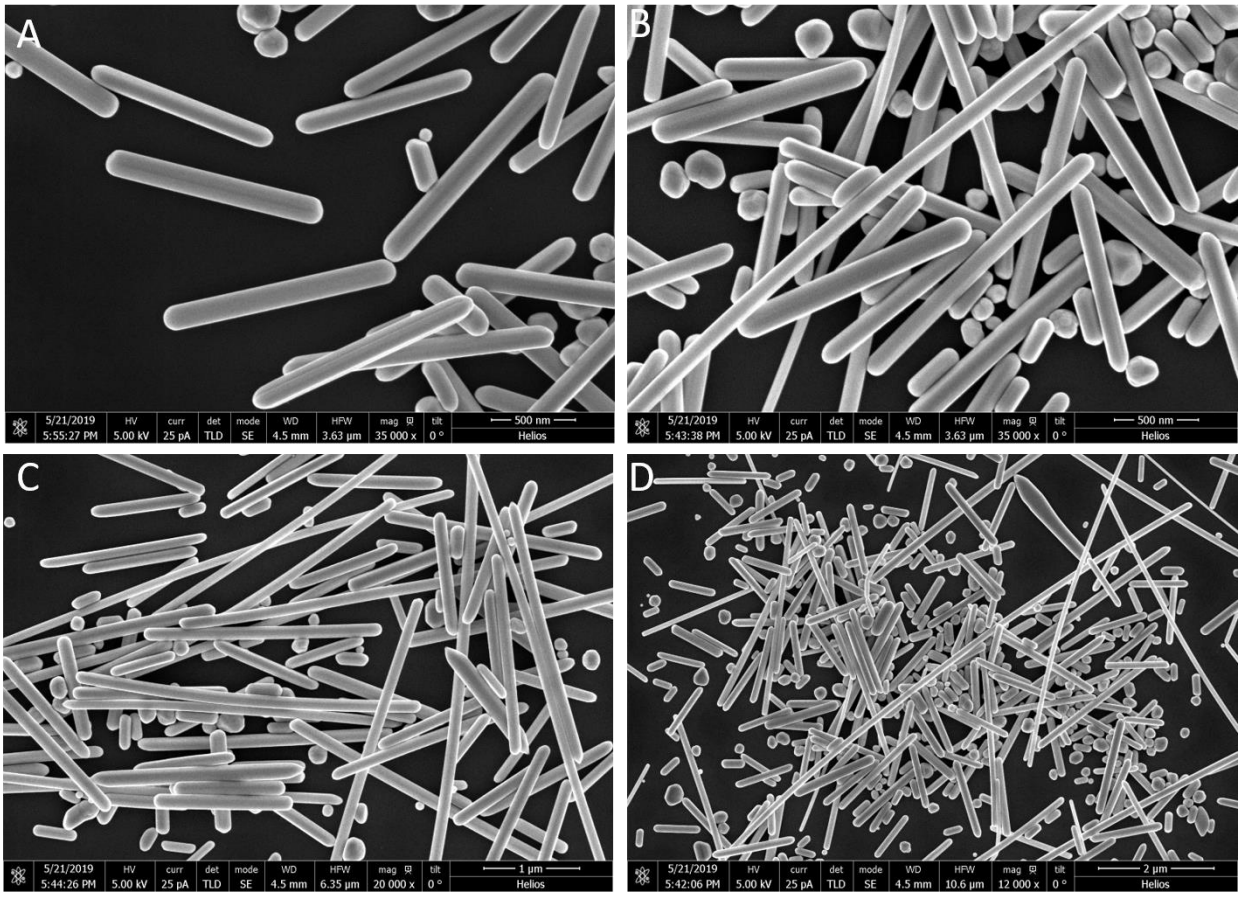

Supplementary Figure SH. (A-D) Four Representative SEM images of Silver Nanostructures with Nanorod Geometry at Four Different Magnifications. The full reaction condition for the silver nanostructures shown in this Figure is provided in **Supplementary Table SH** above.

Supplementary Table SI: Silver Nanostructures with Nanorod Geometry. Reaction condition is provided here in this Table for the nanostructures shown in **Supplementary Figure SI** below. Four different SEM images of the same reaction sample are shown in **Supplementary Figure SI** below.

Geometry	**Nanoparticles**
Full Reaction Condition	Pure 1,3-Propanediol (5 mL) 0.12 M $AgNO_3$ (3mL) 0.35 M PVP-10,000 MW (3mL) 0.02M Sucrose (1 mL) Temp: 170°C
Note	Pure 1,3-propanediol was heated to 170 °C for 90 minutes followed by the dropwise addition of reactants within 7 minutes. The reaction ran for 60 minutes judging from the first addition of $AgNO_3$ to the reaction solution. The color of the solution was a dark greenish grey at the end of the reaction.

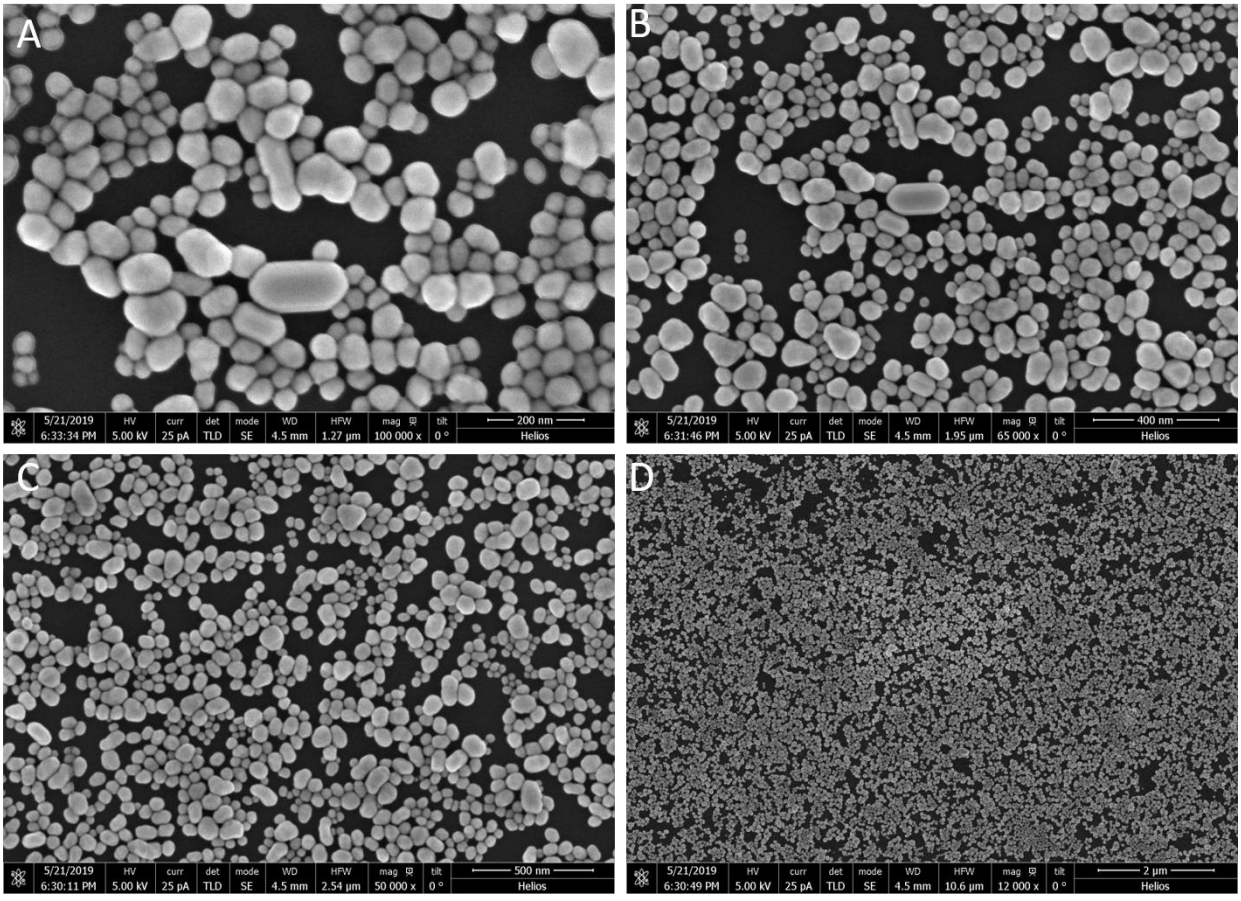

Supplementary Figure SI. (A-D) Four Representative SEM images of Silver Nanostructures with Nanoparticles Geometry at Four Different Magnifications. The full reaction condition for the silver nanostructures shown in this Figure is provided in **Supplementary Table SI** above.

Supplementary Table SJ: Silver Nanostructures with Nanorod Geometry. Reaction condition is provided here in this Table for the nanostructures shown in **Supplementary Figure SJ** below. below. Four different SEM images of the same reaction sample are shown in **Supplementary Figure SJ** below.

Geometry	**Nanorods**
Full Reaction Condition	Pure 1,3-Propanediol (5 mL) 0.12 M $AgNO_3$ (3mL) 0.35 M PVP-29,000 MW (3mL) 0.02M Sucrose (1 mL) Temp: 170°C
Note	Pure 1,3-propanediol was heated to 170 °C for 90 minutes followed by the dropwise addition of reactants within 7 minutes. The reaction ran for 60 minutes judging from the first addition of $AgNO_3$ to the reaction solution. The color of the solution was a dark greenish grey at the end of the reaction.

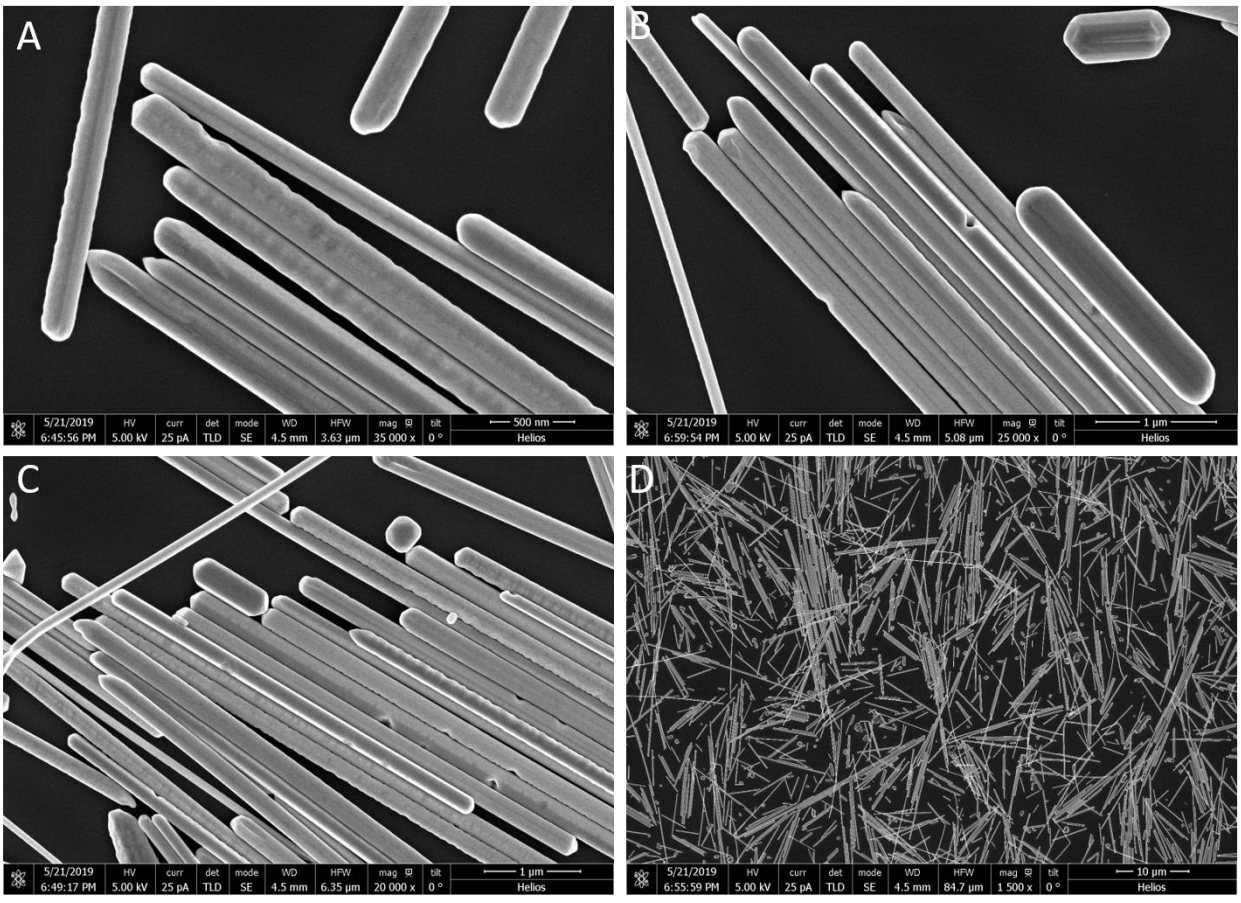

Supplementary Figure SJ. (A-D) Four Representative SEM images of Silver Nanostructures with Nanorod Geometry at Four Different Magnifications. The full reaction condition for the silver nanostructures shown in this Figure is provided in **Supplementary Table SJ** above.

Supplementary Table SK: Silver Nanostructures with Nanorod Geometry. Reaction condition is provided here in this Table for the nanostructures shown in **Supplementary Figure SK** below. Four different SEM images of the same reaction sample are shown in **Supplementary Figure SK** below.

Geometry	**Nanorods**
Full Reaction Condition	Pure 1,3-Propanediol (5 mL) 0.05 M $AgNO_3$ (3mL) 0.35 M PVP-360,000 MW (3mL) 0.01M Sucrose (1 mL) Temp: 167°C
Note	Pure 1,3-propanediol was heated to 167 °C for 90 minutes followed by the dropwise addition of reactants within 7 minutes. The reaction ran for 60 minutes judging from the first addition of $AgNO_3$ to the reaction solution. The color of the solution was a dark greenish grey at the end of the reaction.

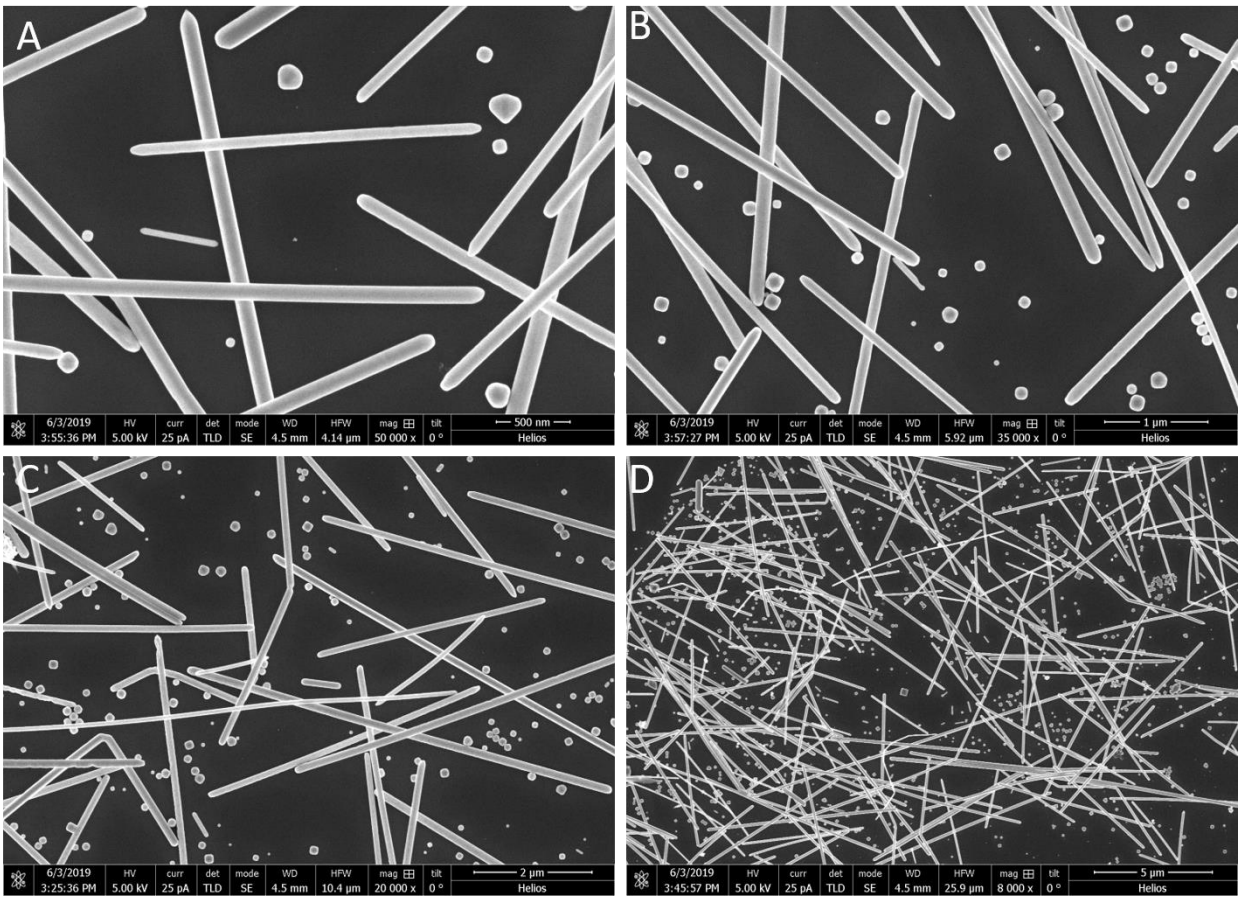

Supplementary Figure SK. (A-D) Four Representative SEM images of Silver Nanostructures with Nanorod Geometry at Four Different Magnifications. The full reaction condition for the silver nanostructures shown in this Figure is provided in **Supplementary Table SK** above.

Supplementary Table SL: Silver Nanostructures with Nanorod Geometry. Reaction condition is provided here in this Table for the nanostructures shown in **Supplementary Figure SL** below. Four different SEM images of the same reaction sample are shown in **Supplementary Figure SL** below.

Geometry	**Nanorods**
Full Reaction Condition	Pure 1,3-Propanediol (5 mL) 0.1 M $AgNO_3$ (3mL) 0.35 M PVP-360,000 MW (3mL) 0.01M Sucrose (1 mL) Temp: 167°C
Note	Pure 1,3-propanediol was heated to 167 °C for 90 minutes followed by the dropwise addition of reactants within 7 minutes. The reaction ran for 60 minutes judging from the first addition of $AgNO_3$ to the reaction solution. The color of the solution was a dark greenish grey at the end of the reaction.

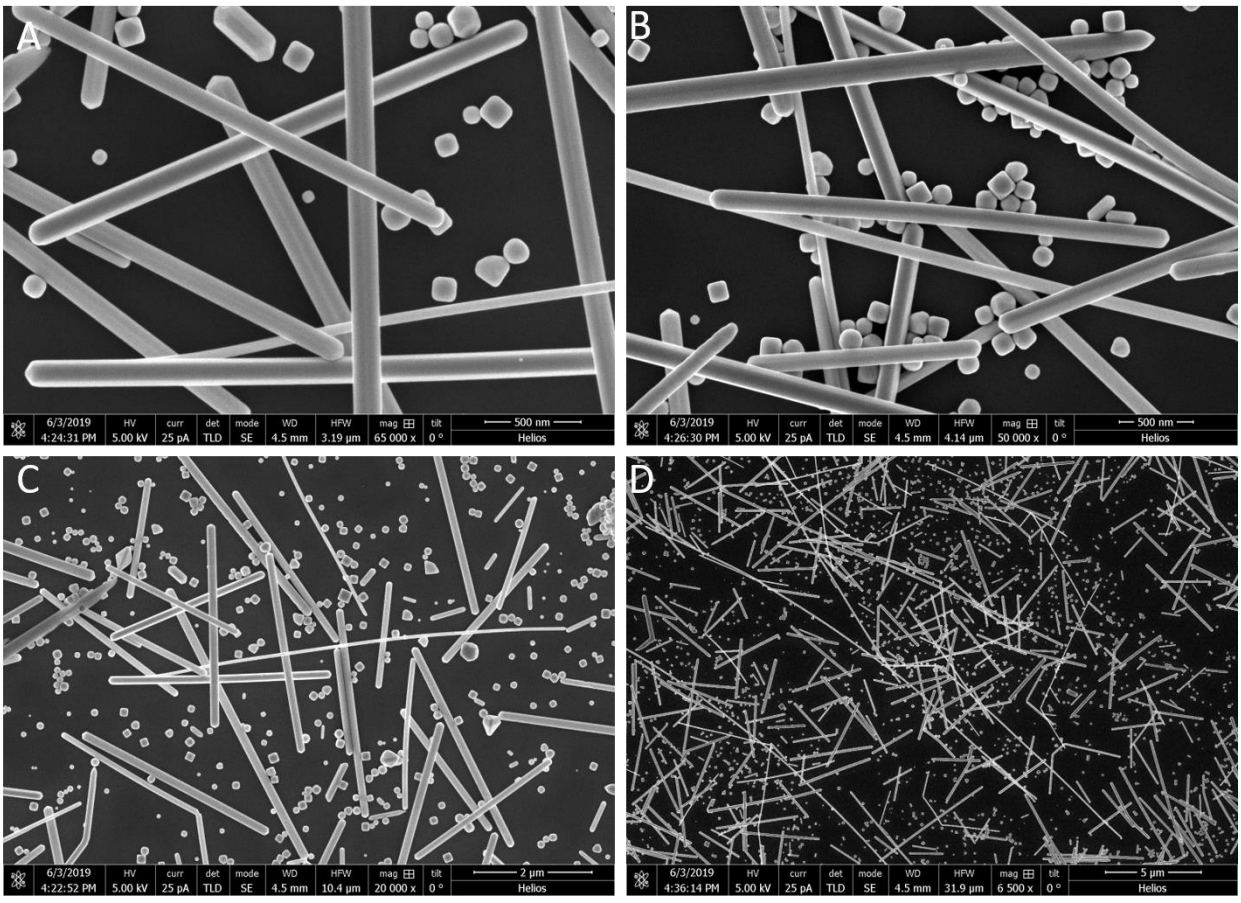

Supplementary Figure SL. (A-D) Four Representative SEM images of Silver Nanostructures with Nanorod Geometry at Four Different Magnifications. The full reaction condition for the silver nanostructures shown in this Figure is provided in **Supplementary Table SL** above.

Supplementary Table SM: Silver Nanostructures with Nanorod Geometry. Reaction condition is provided here in this Table for the nanostructures shown in **Supplementary Figure SM** below. Four different SEM images of the same reaction sample are shown in **Supplementary Figure SM** below.

Geometry	**Nanorods**
Full Reaction Condition	Pure 1,3-Propanediol (5 mL) 0.2 M $AgNO_3$ (3mL) 0.35 M PVP-360,000 MW (3mL) 0.01M Sucrose (1 mL) Temp: 167°C
Note	Pure 1,3-propanediol was heated to 167 °C for 90 minutes followed by the dropwise addition of reactants within 7 minutes. The reaction ran for 60 minutes judging from the first addition of $AgNO_3$ to the reaction solution. The color of the solution was a dark greenish grey at the end of the reaction.

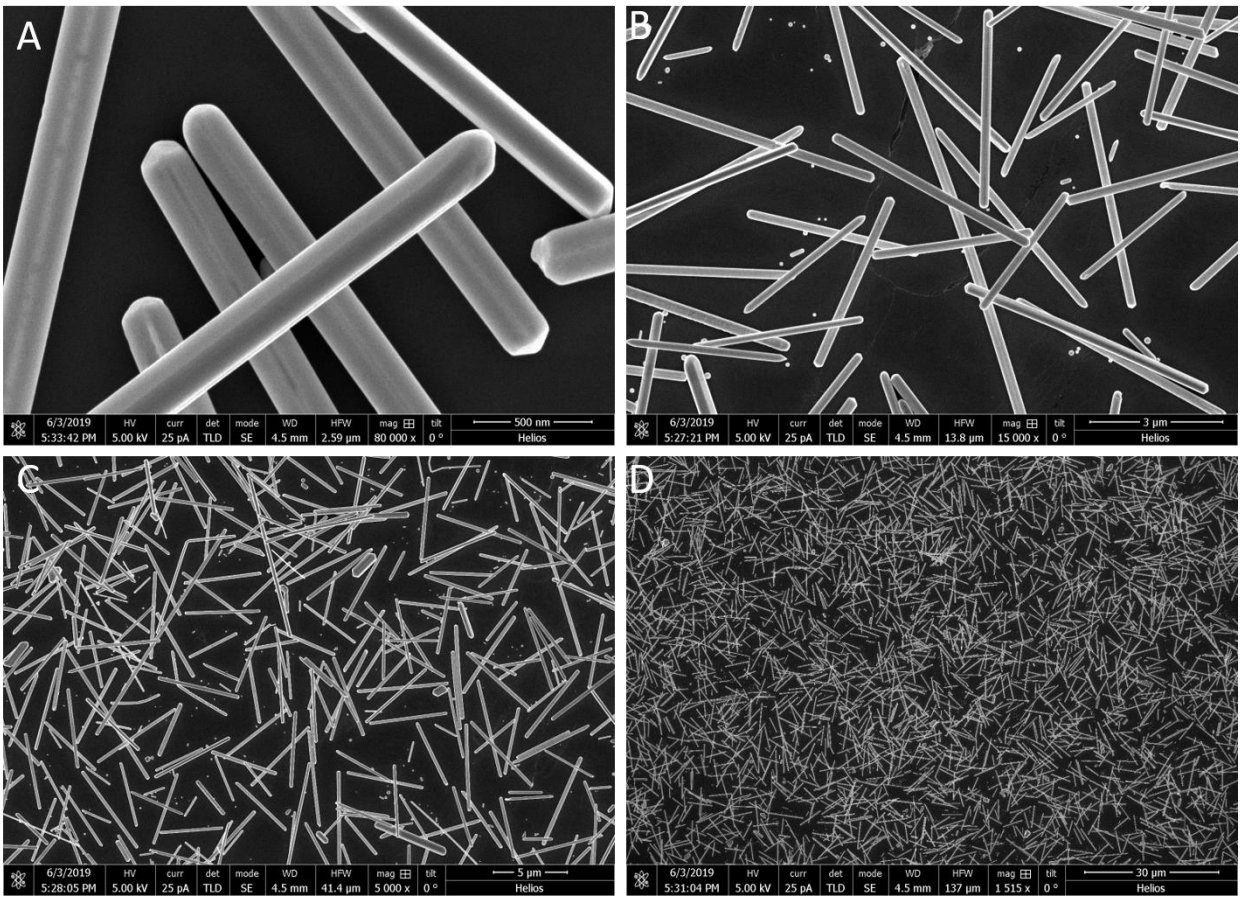

Supplementary Figure SM. (A-D) Four Representative SEM images of Silver Nanostructures with Nanorod Geometry at Four Different Magnifications. The full reaction condition for the silver nanostructures shown in this Figure is provided in **Supplementary Table SM** above.

Supplementary Table SN: Silver Nanostructures with Nanorod Geometry. Reaction condition is provided here in this Table for the nanostructures shown in **Supplementary Figure SN** below. Four different SEM images of the same reaction sample are shown in **Supplementary Figure SN** below.

Geometry	**Nanorods**
Full Reaction Condition	Pure 1,3-Propanediol (5 mL) 0.25 M $AgNO_3$ (3mL) 0.35 M PVP-360,000 MW (3mL) 0.01M Sucrose (1 mL) Temp: 167°C
Note	Pure 1,3-propanediol was heated to 167 °C for 90 minutes followed by the dropwise addition of reactants within 7 minutes. The reaction ran for 60 minutes judging from the first addition of $AgNO_3$ to the reaction solution. The color of the solution was a dark greenish grey at the end of the reaction.

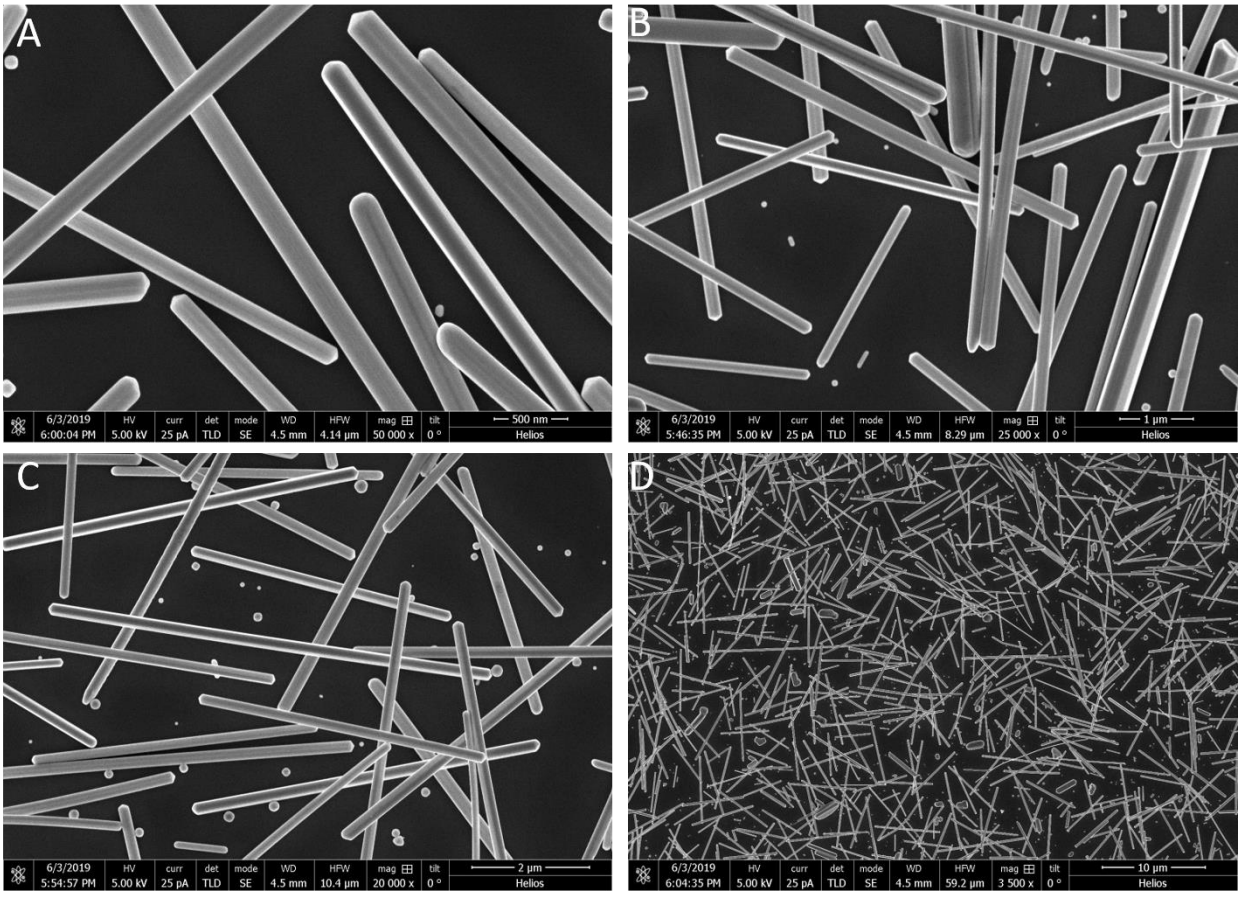

Supplementary Figure SN. (A-D) Four Representative SEM images of Silver Nanostructures with Nanorod Geometry at Four Different Magnifications. The full reaction condition for the silver nanostructures shown in this Figure is provided in **Supplementary Table SN** above.

Supplementary Table SO: Silver Nanostructures with Nanorod Geometry. Reaction condition is provided here in this Table for the nanostructures shown in **Supplementary Figure SO** below. Four different SEM images of the same reaction sample are shown in **Supplementary Figure SO** below.

Geometry	**Nanorods**
Full Reaction Condition	Pure 1,3-Propanediol (5 mL) 0.12 M $AgNO_3$ (3mL) 0.15 M PVP-360,000 MW (3mL) 0.01M Sucrose (1 mL) Temp: 167°C
Note	Pure 1,3-propanediol was heated to 167 °C for 90 minutes followed by the dropwise addition of reactants within 7 minutes. The reaction ran for 60 minutes judging from the first addition of $AgNO_3$ to the reaction solution. The color of the solution was a dark greenish grey at the end of the reaction.

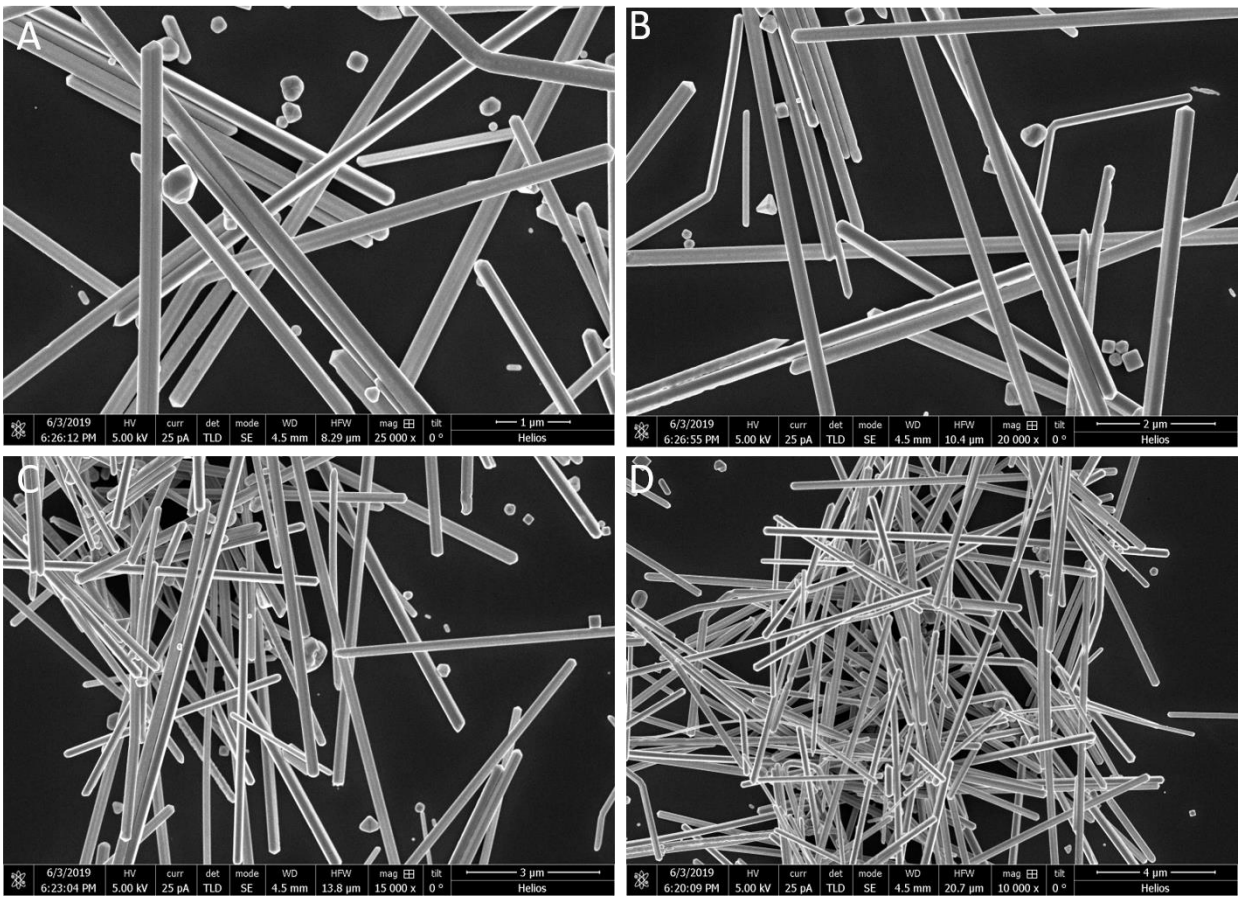

Supplementary Figure SO. (A-D) Four Representative SEM images of Silver Nanostructures with Nanorod Geometry at Four Different Magnifications. The full reaction condition for the silver nanostructures shown in this Figure is provided in **Supplementary Table SO** above.

Supplementary Table SP: Silver Nanostructures with Nanorod Geometry. Reaction condition is provided here in this Table for the nanostructures shown in **Supplementary Figure SP** below. Four different SEM images of the same reaction sample are shown in **Supplementary Figure SP** below.

Geometry	**Nanorods**
Full Reaction Condition	Pure 1,3-Propanediol (5 mL) 0.12 M $AgNO_3$ (3mL) 0.25 M PVP-360,000 MW (3mL) 0.01M Sucrose (1 mL) Temp: 167°C
Note	Pure 1,3-propanediol was heated to 167 °C for 90 minutes followed by the dropwise addition of reactants within 7 minutes. The reaction ran for 60 minutes judging from the first addition of $AgNO_3$ to the reaction solution. The color of the solution was a dark greenish grey at the end of the reaction.

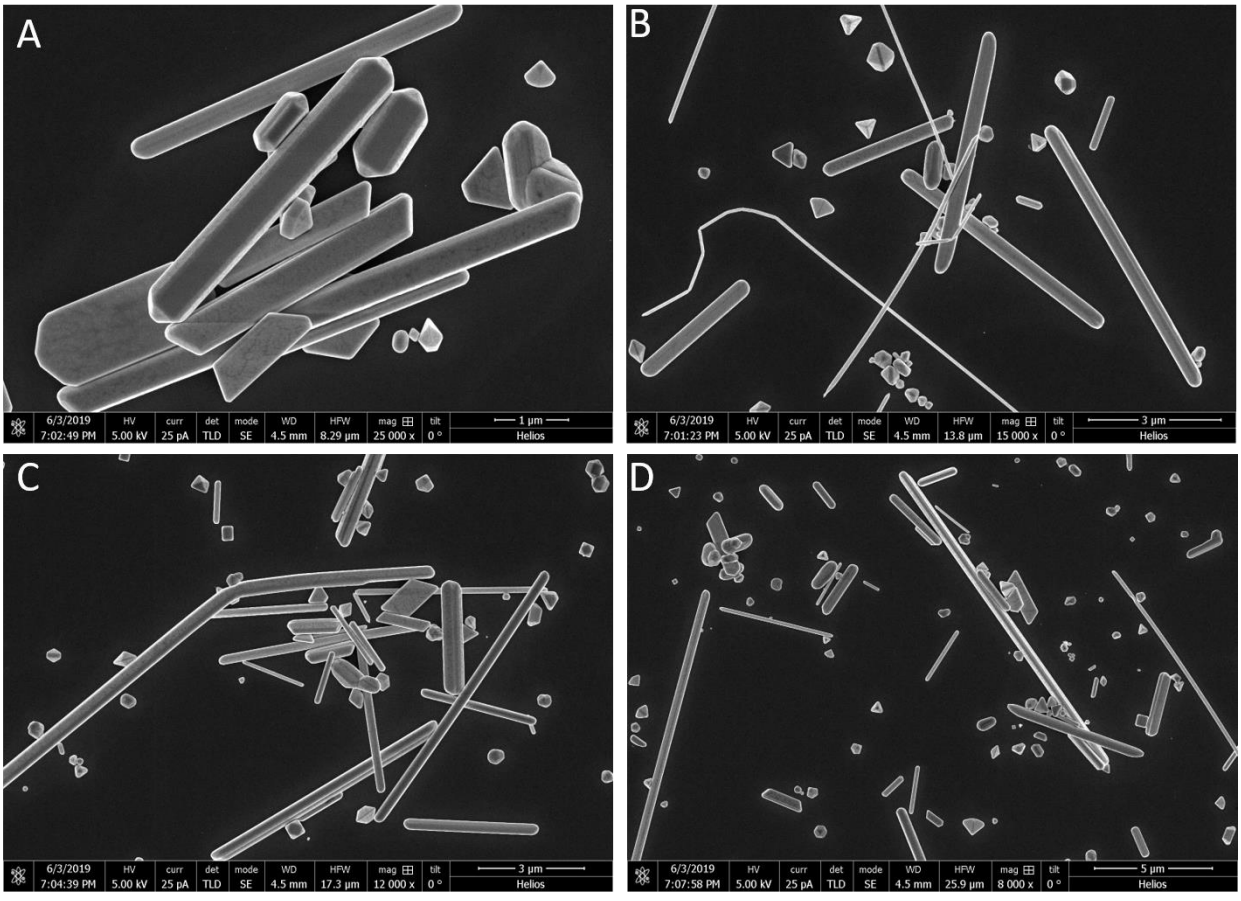

Supplementary Figure SP. (A-D) Four Representative SEM images of Silver Nanostructures with Nanorod Geometry at Four Different Magnifications. The full reaction condition for the silver nanostructures shown in this Figure is provided in **Supplementary Table SP** above.

Supplementary Table SQ: Silver Nanostructures with Nanorod Geometry. Reaction condition is provided here in this Table for the nanostructures shown in **Supplementary Figure SQ** below. Four different SEM images of the same reaction sample are shown in **Supplementary Figure SQ** below.

Geometry	**Nanorods**
Full Reaction Condition	Pure 1,3-Propanediol (5 mL) 0.12 M $AgNO_3$ (3mL) 0.45 M PVP-360,000 MW (3mL) 0.01M Sucrose (1 mL) Temp: 167°C
Note	Pure 1,3-propanediol was heated to 167 °C for 90 minutes followed by the dropwise addition of reactants within 7 minutes. The reaction ran for 60 minutes judging from the first addition of $AgNO_3$ to the reaction solution. The color of the solution was a dark greenish grey at the end of the reaction.

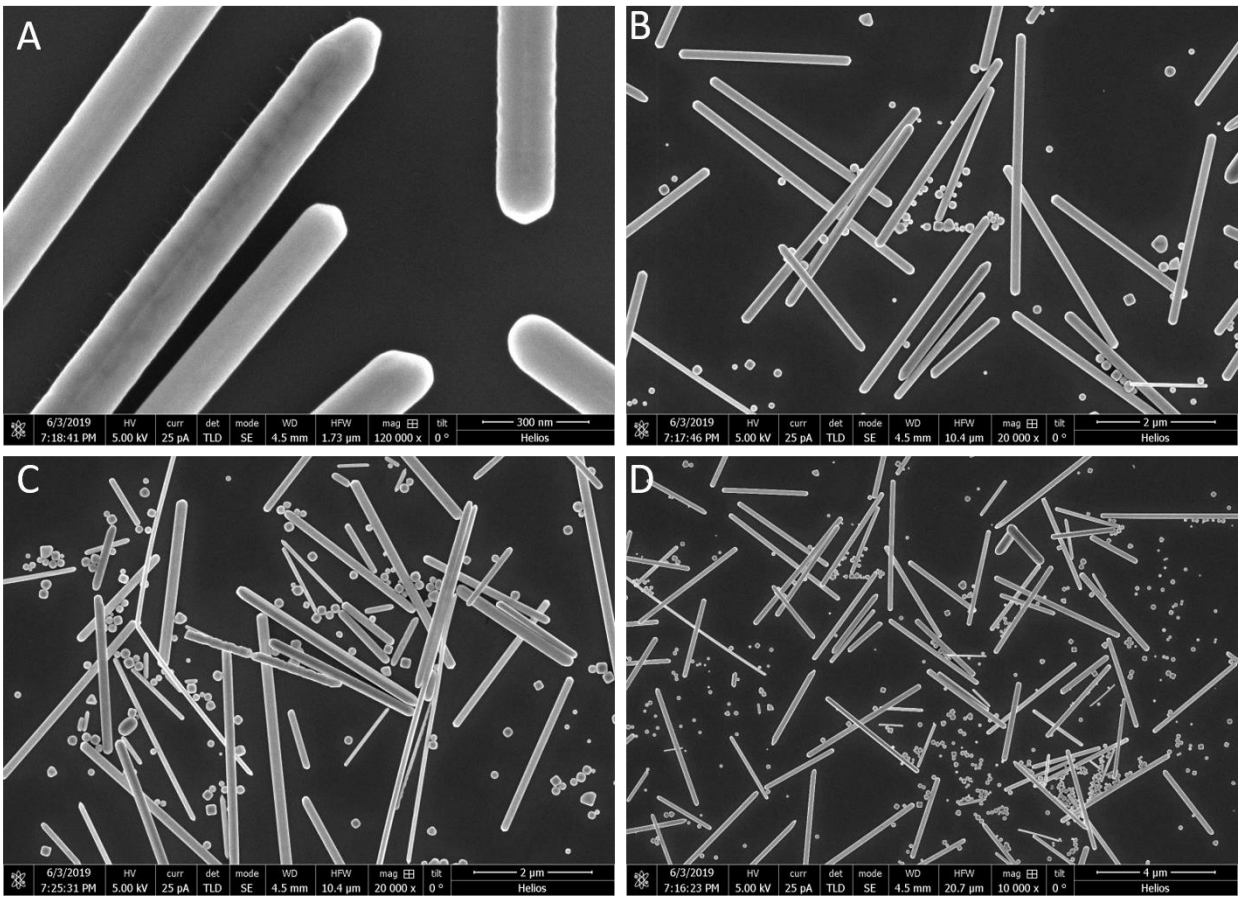

Supplementary Figure SQ. (A-D) Four Representative SEM images of Silver Nanostructures with Nanorod Geometry at Four Different Magnifications. The full reaction condition for the silver nanostructures shown in this Figure is provided in **Supplementary Table SQ** above.

Supplementary Table SR: Silver Nanostructures with Nanorod and Nanocube Geometry. Reaction condition is provided here in this Table for the nanostructures shown in **Supplementary Figure SR** below. Four different SEM images of the same reaction sample are shown in **Supplementary Figure SR** below.

Geometry	**Nanorods + Nanocubes**
Full Reaction Condition	Pure 1,3-Propanediol (5 mL) 0.12 M $AgNO_3$ (3mL) 0.35 M PVP-360,000 MW (3mL) 0.01M Sucrose (1 mL) Temp: 150°C for the first 15 hours and then 170°C.
Note	Pure 1,3-propanediol was heated to 150 °C for 90 minutes followed by the dropwise addition of reactants within 7 minutes. The reaction ran for 15 hours minutes judging from the first addition of $AgNO_3$ to the reaction solution. Color for first 15 hours heating and stirring at 150 °C was light pink. After 15 hours, the temperature increased to 170°C, and immediately yellowish-grey color was obtained and then the reaction continued for 20 minutes.

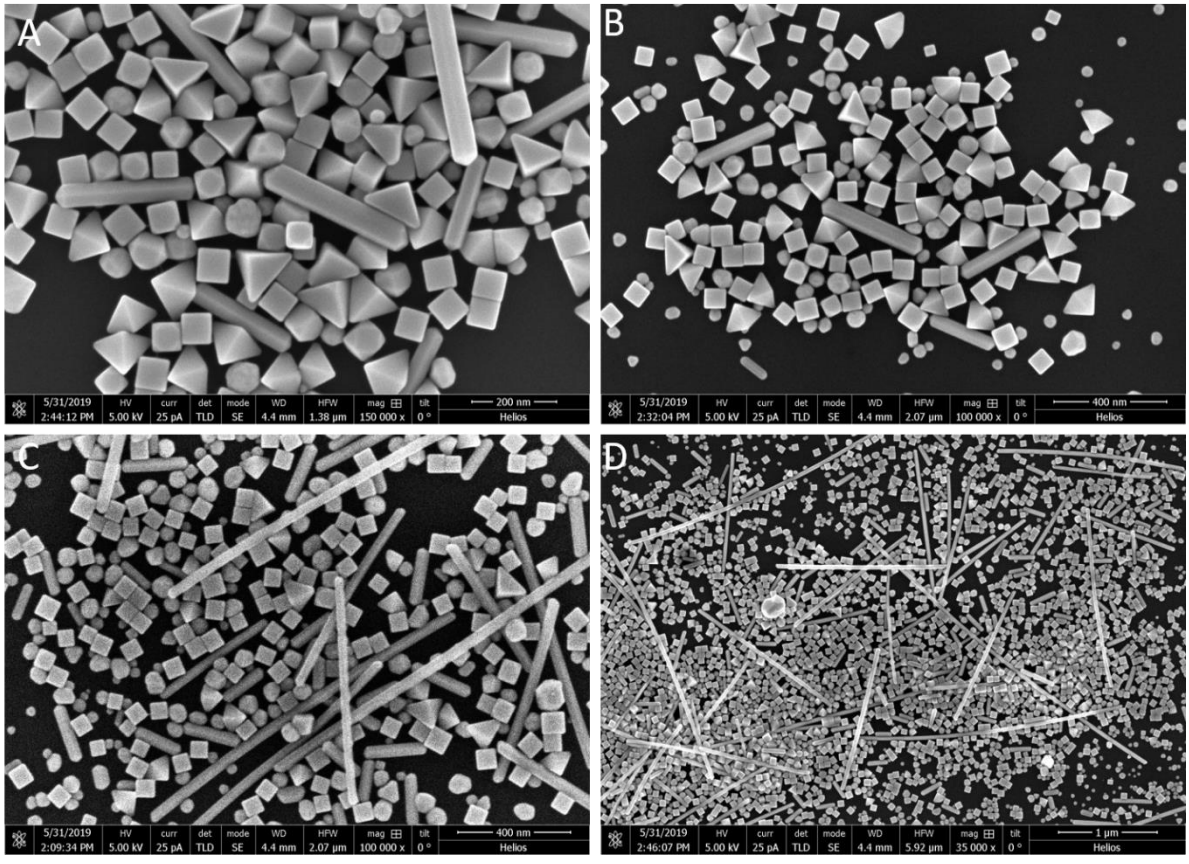

Supplementary Figure SR. (A-D) Four Representative SEM images of Silver Nanostructures with Nanorod and Nanocube Geometry at Four Different Magnifications. The full reaction condition for the silver nanostructures shown in this Figure is provided in **Supplementary Table SR** above.

Supplementary Table SS: Silver Nanostructures with Nanorod Geometry. Reaction condition is provided here in this Table for the nanostructures shown in **Supplementary Figure SS** below. Four different SEM images of the same reaction sample are shown in **Supplementary Figure SS** below.

Geometry	**Nanorods**
Full Reaction Condition	Pure 1,3-Propanediol (5 mL) 0.12 M $AgNO_3$ (3mL) 0.35 M PVP-360,000 MW (3mL) 0.01M Sucrose (1 mL) Temp: 170°C
Note	Pure 1,3-propanediol was heated to 170 °C for 90 minutes followed by the dropwise addition of reactants within 7 minutes. The reaction ran for 120 minutes judging from the first addition of $AgNO_3$ to the reaction solution. The color of the solution was a dark greenish grey at the end of the reaction.

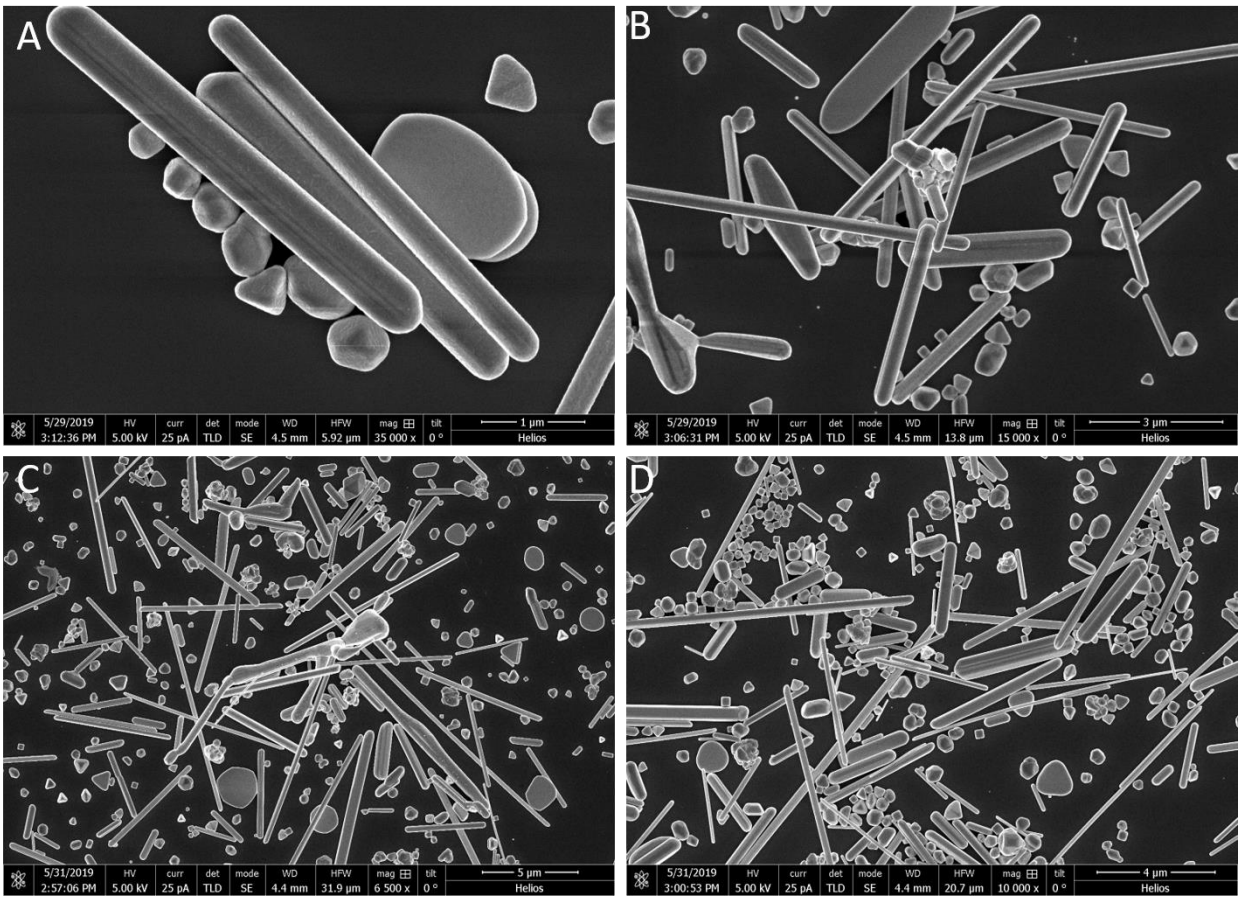

Supplementary Figure SS. (A-D) Four Representative SEM images of Silver Nanostructures with Nanorod Geometry at Four Different Magnifications. The full reaction condition for the silver nanostructures shown in this Figure is provided in **Supplementary Table SS** above.

Supplementary Table ST: Silver Nanostructures with Nanorod Geometry. Reaction condition is provided here in this Table for the nanostructures shown in **Supplementary Figure ST** below. Four different SEM images of the same reaction sample are shown in **Supplementary Figure ST** below.

Geometry	**Nanorods**
Full Reaction Condition	Pure 1,3-Propanediol (5 mL) 0.12 M $AgNO_3$ (3mL) 0.35 M PVP-360,000 MW (3mL) 0.1M CsOH (1 mL) Temp: 150°C
Note	Pure 1,3-propanediol was heated to 150 °C for 90 minutes followed by the dropwise addition of reactants within 7 minutes. The reaction ran for 60 minutes judging from the first addition of $AgNO_3$ to the reaction solution. The color of the solution was a dark greenish grey at the end of the reaction.

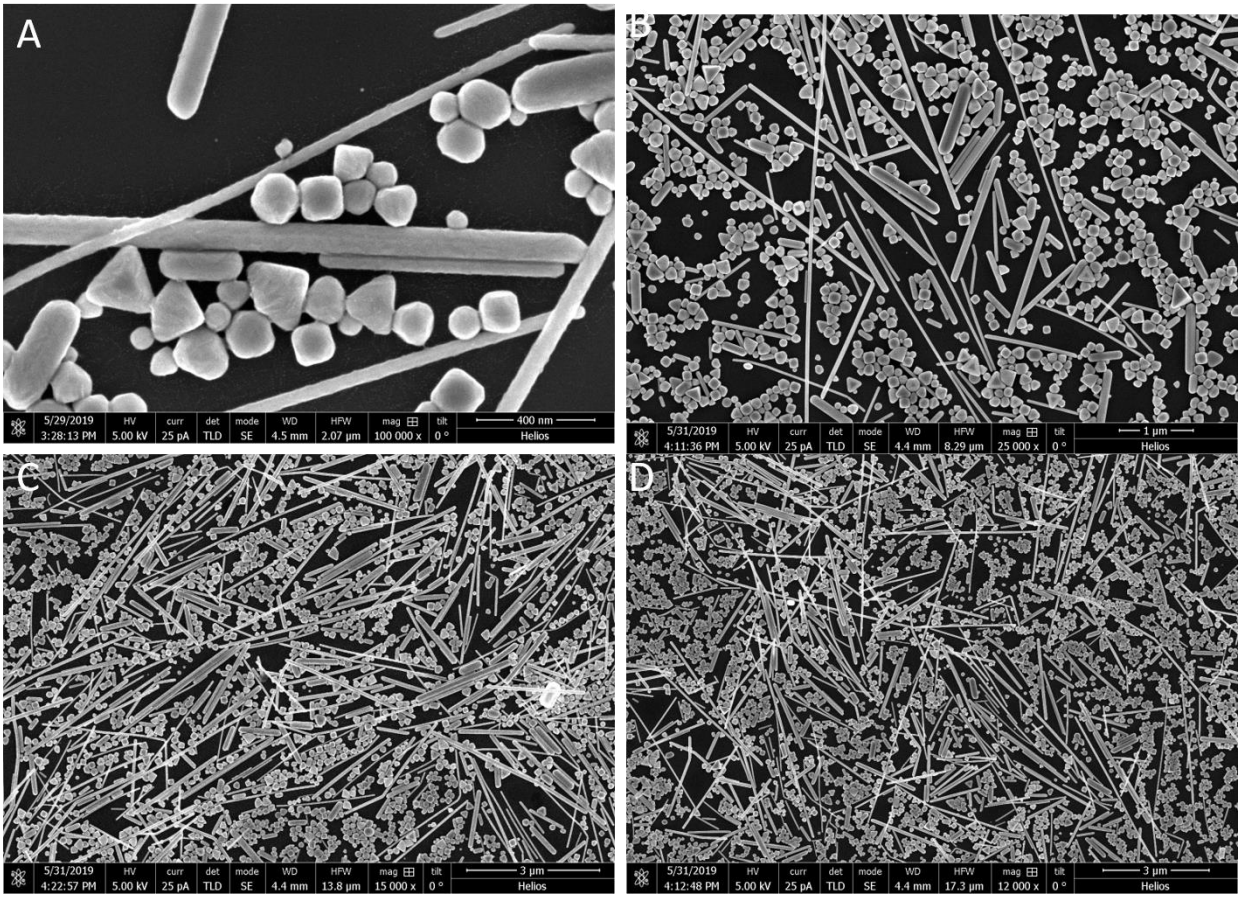

Supplementary Figure ST. (A-D) Four Representative SEM images of Silver Nanostructures with Nanorod Geometry at Four Different Magnifications. The full reaction condition for the silver nanostructures shown in this Figure is provided in **Supplementary Table ST** above.

Supplementary Table SU: Silver Nanostructures with Nanorod Geometry. Reaction condition is provided here in this Table for the nanostructures shown in **Supplementary Figure SU** below. Four different SEM images of the same reaction sample are shown in **Supplementary Figure SU** below.

Geometry	**Nanorods**
Full Reaction Condition	Pure 1,3-Propanediol (5 mL) 0.12 M $AgNO_3$ (3mL) 0.35 M PVP-360,000 MW (3mL) 0.1M KOH (1 mL) Temp: 150°C
Note	Pure 1,3-propanediol was heated to 150 °C for 90 minutes followed by the dropwise addition of reactants within 7 minutes. The reaction ran for 60 minutes judging from the first addition of $AgNO_3$ to the reaction solution. The color of the solution was a dark greenish grey at the end of the reaction.

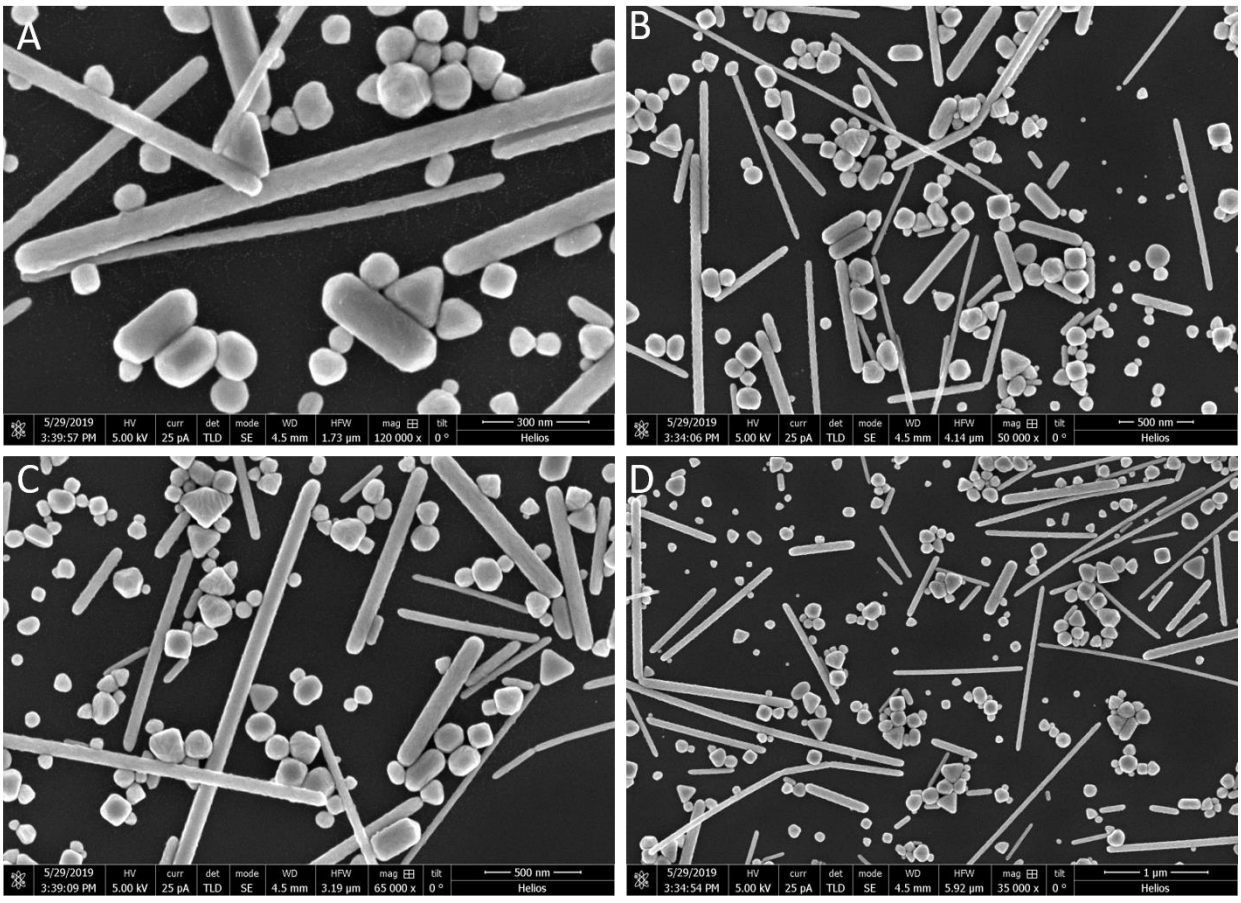

Supplementary Figure SU. (A-D) Four Representative SEM images of Silver Nanostructures with Nanorod Geometry at Four Different Magnifications. The full reaction condition for the silver nanostructures shown in this Figure is provided in **Supplementary Table SU** above.

Supplementary Table SV: Silver Nanostructures with Nanorod Geometry. Reaction condition is provided here in this Table for the nanostructures shown in **Supplementary Figure SV** below. Four different SEM images of the same reaction sample are shown in **Supplementary Figure SV** below.

Geometry	**Nanorods**
Full Reaction Condition	Pure 1,3-Propanediol (5 mL) 0.12 M $AgNO_3$ (3mL) 0.35 M PVP-360,000 MW (3mL) 0.1M NaOH (1 mL) Temp: 150°C
Note	Pure 1,3-propanediol was heated to 150 °C for 90 minutes followed by the dropwise addition of reactants within 7 minutes. The reaction ran for 60 minutes judging from the first addition of $AgNO_3$ to the reaction solution. The color of the solution was a dark greenish grey at the end of the reaction.

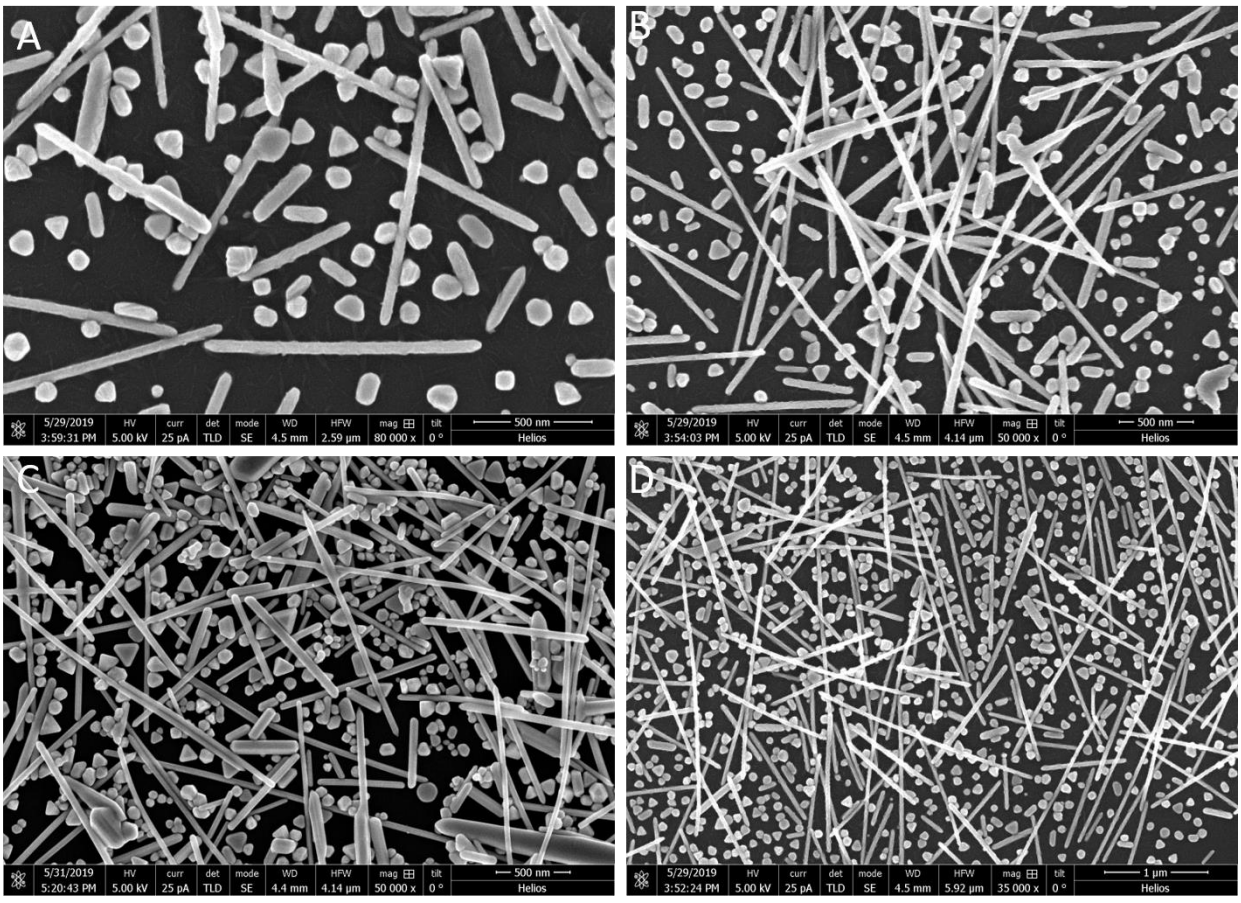

Supplementary Figure SV. (A-D) Four Representative SEM images of Silver Nanostructures with Nanorod Geometry at Four Different Magnifications. The full reaction condition for the silver nanostructures shown in this Figure is provided in **Supplementary Table SV** above.

Supplementary Table SW: Silver Nanostructures with Nanoparticle Geometry. Reaction condition is provided here in this Table for the nanostructures shown in **Supplementary Figure SW** below. Four different SEM images of the same reaction sample are shown in **Supplementary Figure SW** below.

Geometry	**Nanoparticles**
Full Reaction Condition	Pure 1,3-Propanediol (5 mL) 0.12 M $AgNO_3$ (3mL) 0.35 M PVP-55,000 MW (3mL) 0.01M Tannic Acid (1 mL) Temp: 170°C
Note	Pure 1,3-propanediol was heated to 170 °C for 90 minutes followed by the dropwise addition of reactants within 7 minutes. The reaction ran for 60 minutes judging from the first addition of $AgNO_3$ to the reaction solution. The color of the solution was a dark greenish grey at the end of the reaction.

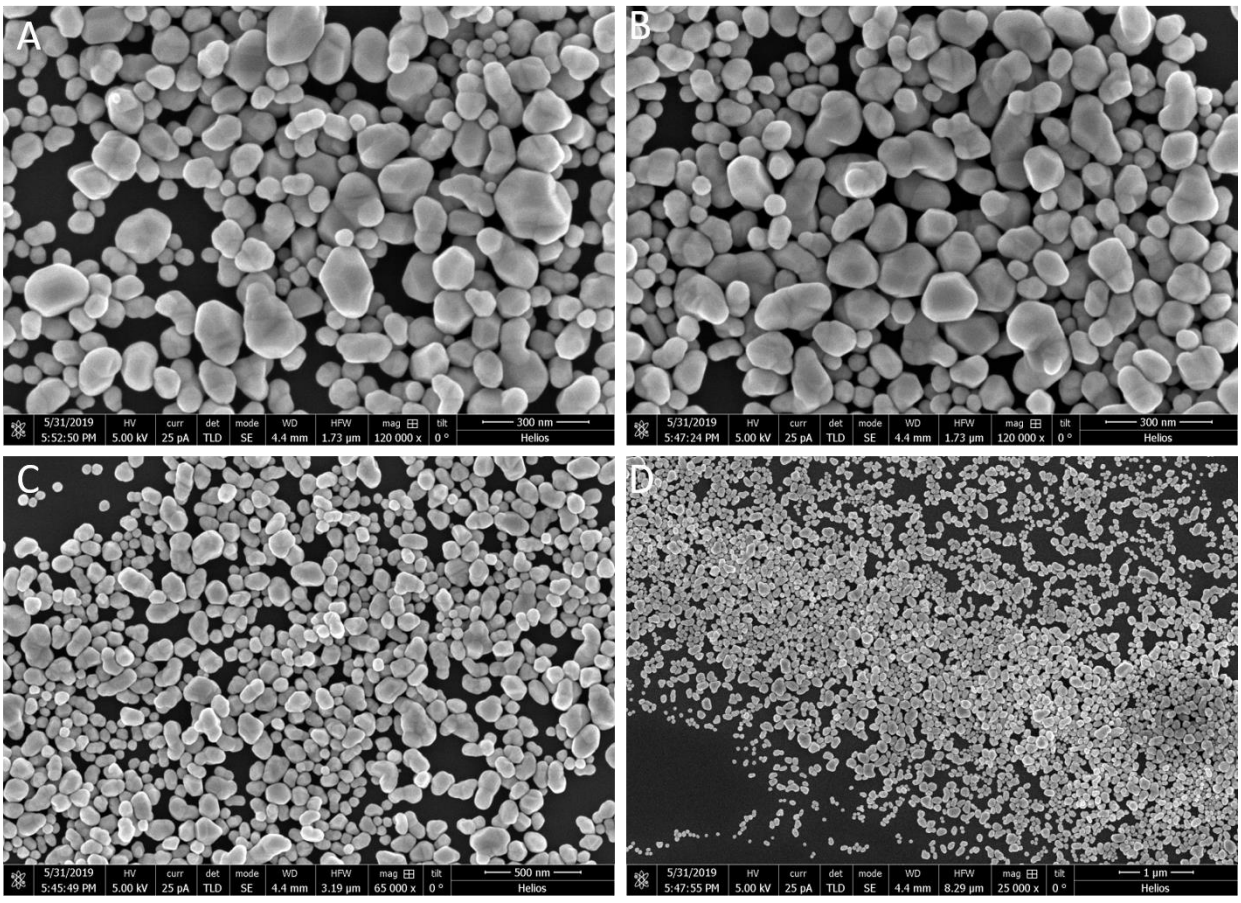

Supplementary Figure SW. (A-D) Four Representative SEM images of Silver Nanostructures with Nanoparticle Geometry at Four Different Magnifications. The full reaction condition for the silver nanostructures shown in this Figure is provided in **Supplementary Table SW** above.

Supplementary Table SX: Silver Nanostructures with Nanoparticle Geometry. Reaction condition is provided here in this Table for the nanostructures shown in **Supplementary Figure SX** below. Four different SEM images of the same reaction sample are shown in **Supplementary Figure SX** below.

Geometry	**Nanoparticles**
Full Reaction Condition	Pure 1,3-Propanediol (5 mL) 0.12 M $AgNO_3$ (3mL) 0.35 M PVP-1,300,000 MW (3mL) 0.01M Tannic Acid (1 mL) Temp: 170°C
Note	Pure 1,3-propanediol was heated to 170 °C for 90 minutes followed by the dropwise addition of reactants within 7 minutes. The reaction ran for 60 minutes judging from the first addition of $AgNO_3$ to the reaction solution. The color of the solution was a dark greenish grey at the end of the reaction.

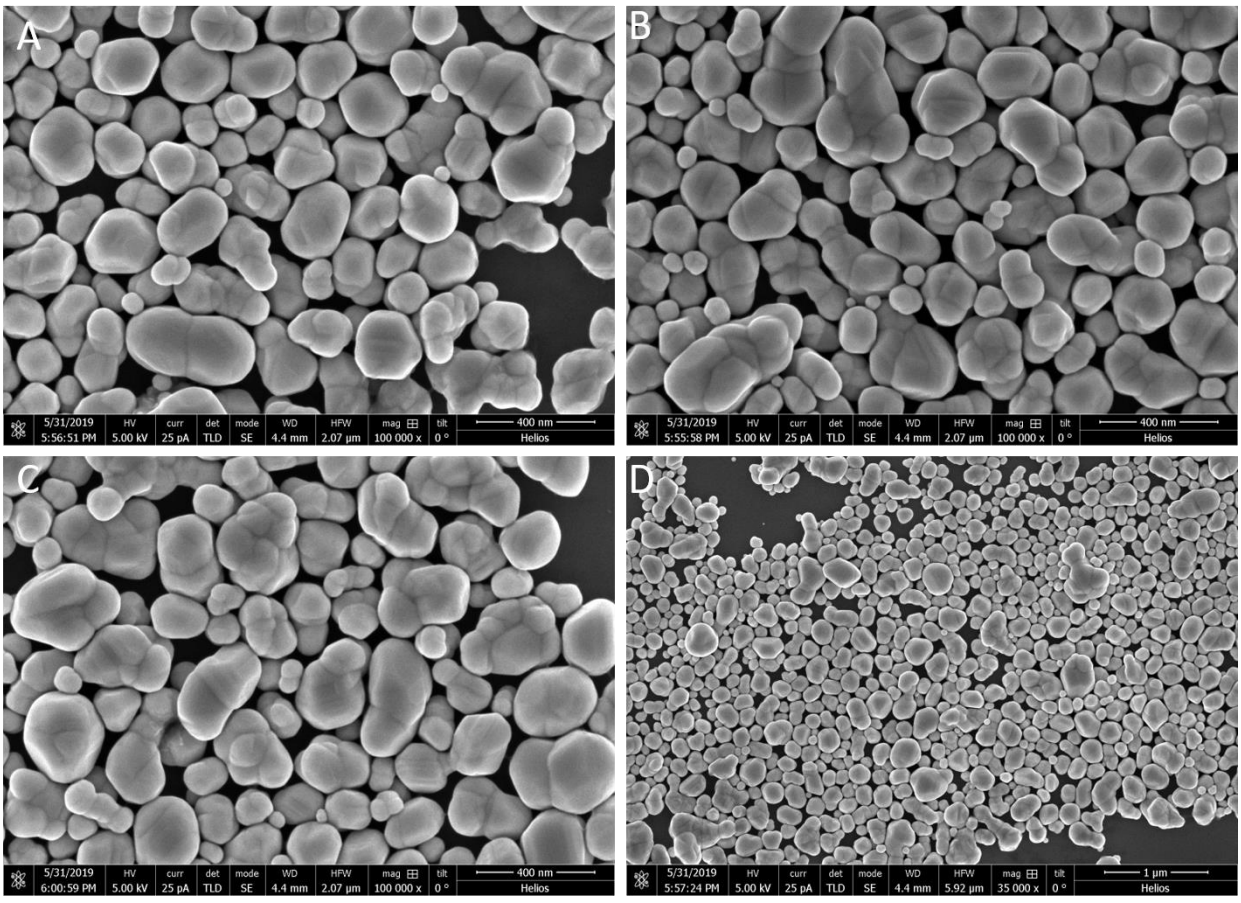

Supplementary Figure SX. (A-D) Four Representative SEM images of Silver Nanostructures with Nanoparticle Geometry at Four Different Magnifications. The full reaction condition for the silver nanostructures shown in this Figure is provided in **Supplementary Table SX** above.

Supplementary Table SY: Silver Nanostructures with Nanoparticle Geometry. Reaction condition is provided here in this Table for the nanostructures shown in **Supplementary Figure SY** below. Four different SEM images of the same reaction sample are shown in **Supplementary Figure SY** below.

Geometry	**Nanoparticles**
Full Reaction Condition	Pure 1,3-Propanediol (5 mL) 0.05 M $AgNO_3$ (3mL) 0.35 M PVP-360,000 MW (3mL) 0.005M Tannic Acid (1 mL) Temp: 167°C
Note	Pure 1,3-propanediol was heated to 167 °C for 90 minutes followed by the dropwise addition of reactants within 7 minutes. The reaction ran for 60 minutes judging from the first addition of $AgNO_3$ to the reaction solution. The color of the solution was a dark greenish grey at the end of the reaction.

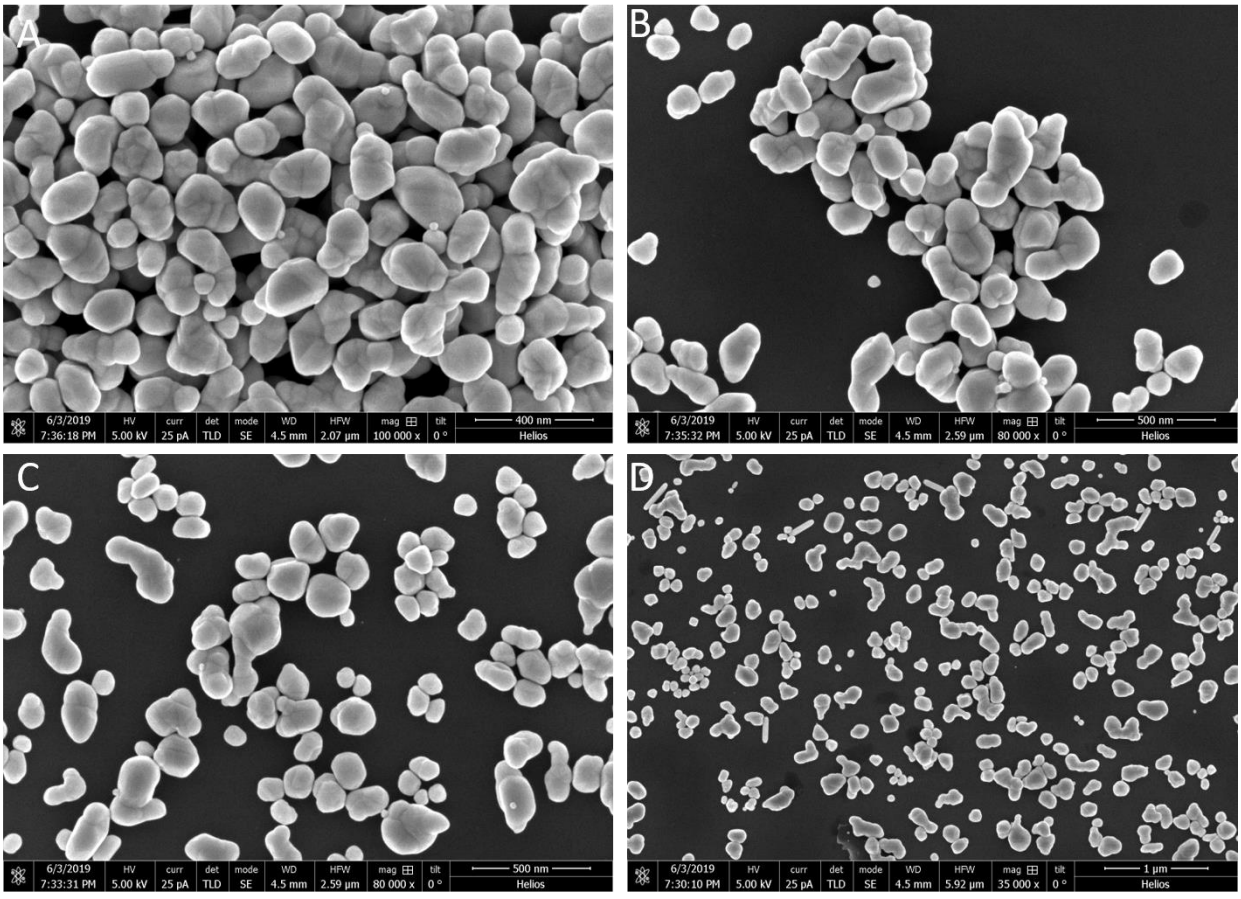

Supplementary Figure SY. (A-D) Four Representative SEM images of Silver Nanostructures with Nanoparticle Geometry at Four Different Magnifications. The full reaction condition for the silver nanostructures shown in this Figure is provided in **Supplementary Table SY** above.

Supplementary Table SZ: Silver Nanostructures with Nanoparticle Geometry. Reaction condition is provided here in this Table for the nanostructures shown in **Supplementary Figure SZ** below. Four different SEM images of the same reaction sample are shown in **Supplementary Figure SZ** below.

Geometry	**Nanoparticles**
Full Reaction Condition	Pure 1,3-Propanediol (5 mL) 0.25 M $AgNO_3$ (3mL) 0.35 M PVP-360,000 MW (3mL) 0.005M Tannic Acid (1 mL) Temp: 167°C
Note	Pure 1,3-propanediol was heated to 167 °C for 90 minutes followed by the dropwise addition of reactants within 7 minutes. The reaction ran for 60 minutes judging from the first addition of $AgNO_3$ to the reaction solution. The color of the solution was a dark greenish grey at the end of the reaction.

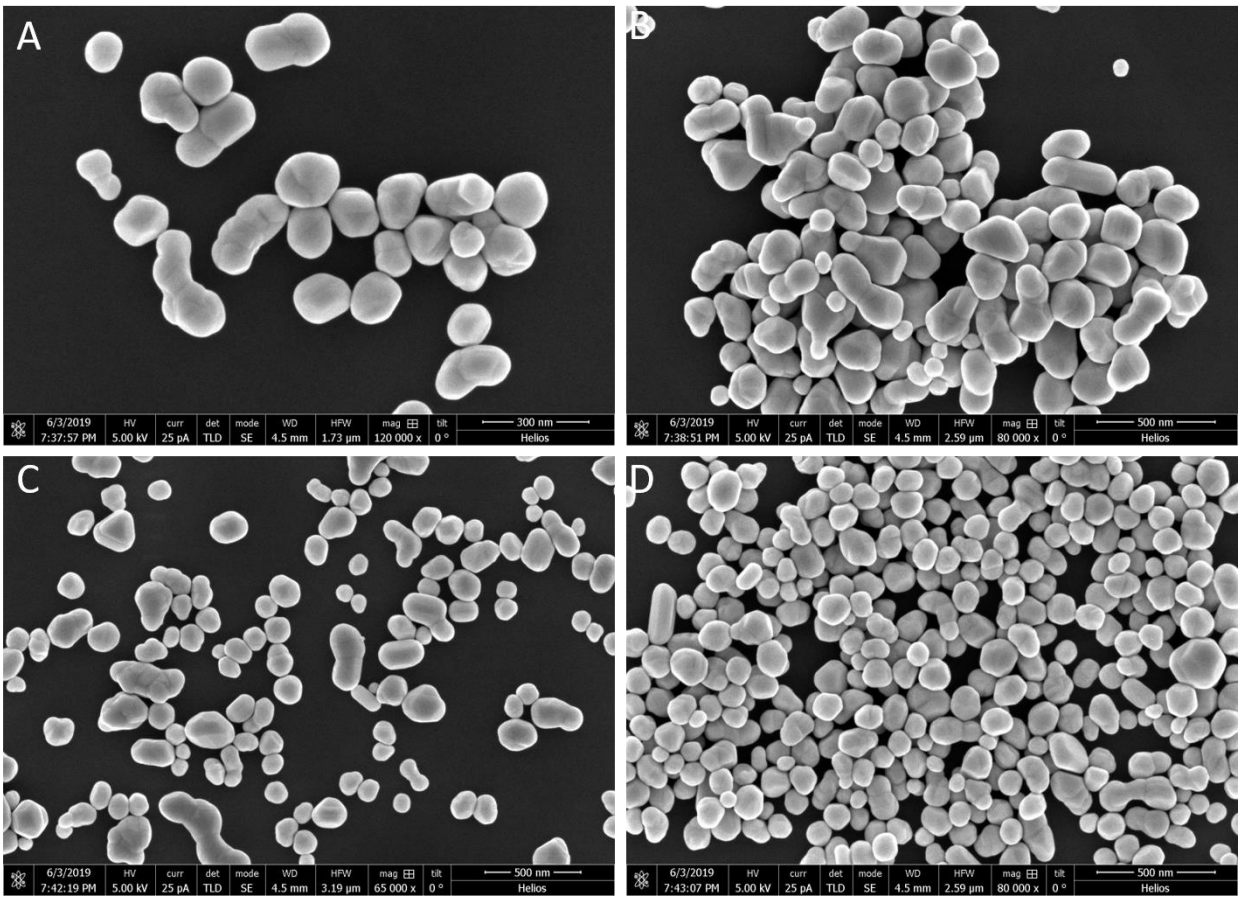

Supplementary Figure SZ. (A-D) Four Representative SEM images of Silver Nanostructures with Nanoparticle Geometry at Four Different Magnifications. The full reaction condition for the silver nanostructures shown in this Figure is provided in **Supplementary Table SZ** above.

Supplementary Table SZA: Silver Nanostructures with Nanorod Geometry. Reaction condition is provided here in this Table for the nanostructures shown in **Supplementary Figure SZA** below. Four different SEM images of the same reaction sample are shown in **Supplementary Figure SZA** below.

Geometry	**Nanorods**
Full Reaction Condition	Pure 1,3-Propanediol (5 mL) 0.15 M $AgNO_3$ (3mL) 0.35 M PVP-360,000 MW (3mL) 0.02M Sodium Borohydride (1 mL) Temp: 167°C
Note	Pure 1,3-propanediol was heated to 167 °C for 90 minutes followed by the dropwise addition of reactants within 7 minutes. The reaction ran for 60 minutes judging from the first addition of $AgNO_3$ to the reaction solution. The color of the solution was a dark greenish grey at the end of the reaction.

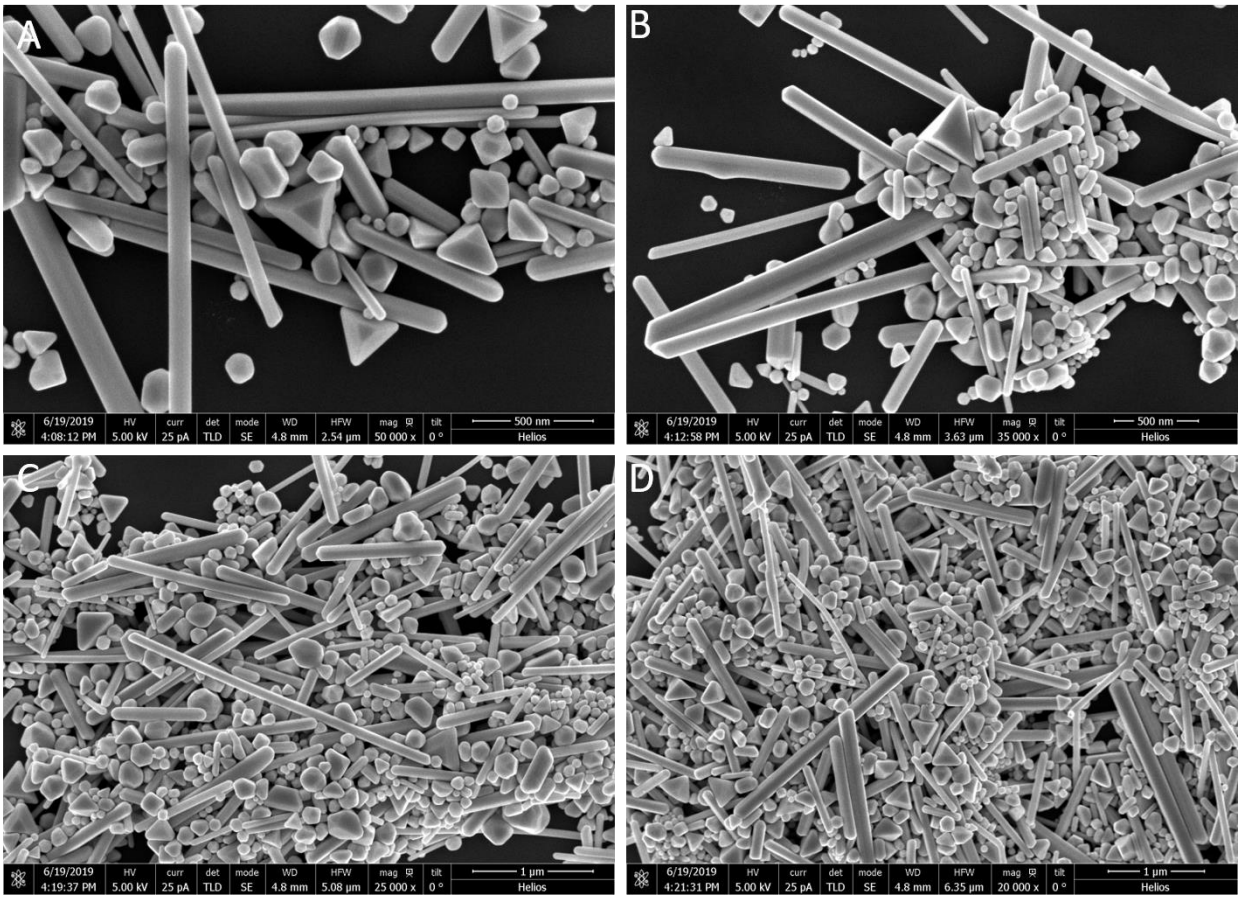

Supplementary Figure SZA. (A-D) Four Representative SEM images of Silver Nanostructures with Nanorod Geometry at Four Different Magnifications. The full reaction condition for the silver nanostructures shown in this Figure is provided in **Supplementary Table SZA** above.

Supplementary Table SZB: Silver Nanostructures with Nanorod Geometry. Reaction condition is provided here in this Table for the nanostructures shown in **Supplementary Figure SZB** below. Four different SEM images of the same reaction sample are shown in **Supplementary Figure SZB** below.

Geometry	**Nanorods**
Full Reaction Condition	Pure 1,3-Propanediol (5 mL) 0.15 M $AgNO_3$ (3mL) 0.35 M PVP-360,000 MW (3mL) 0.01M Ascorbic Acid (1 mL) Temp: 167°C
Note	Pure 1,3-propanediol was heated to 167 °C for 90 minutes followed by the dropwise addition of reactants within 7 minutes. The reaction ran for 60 minutes judging from the first addition of $AgNO_3$ to the reaction solution. The color of the solution was a dark greenish grey at the end of the reaction.

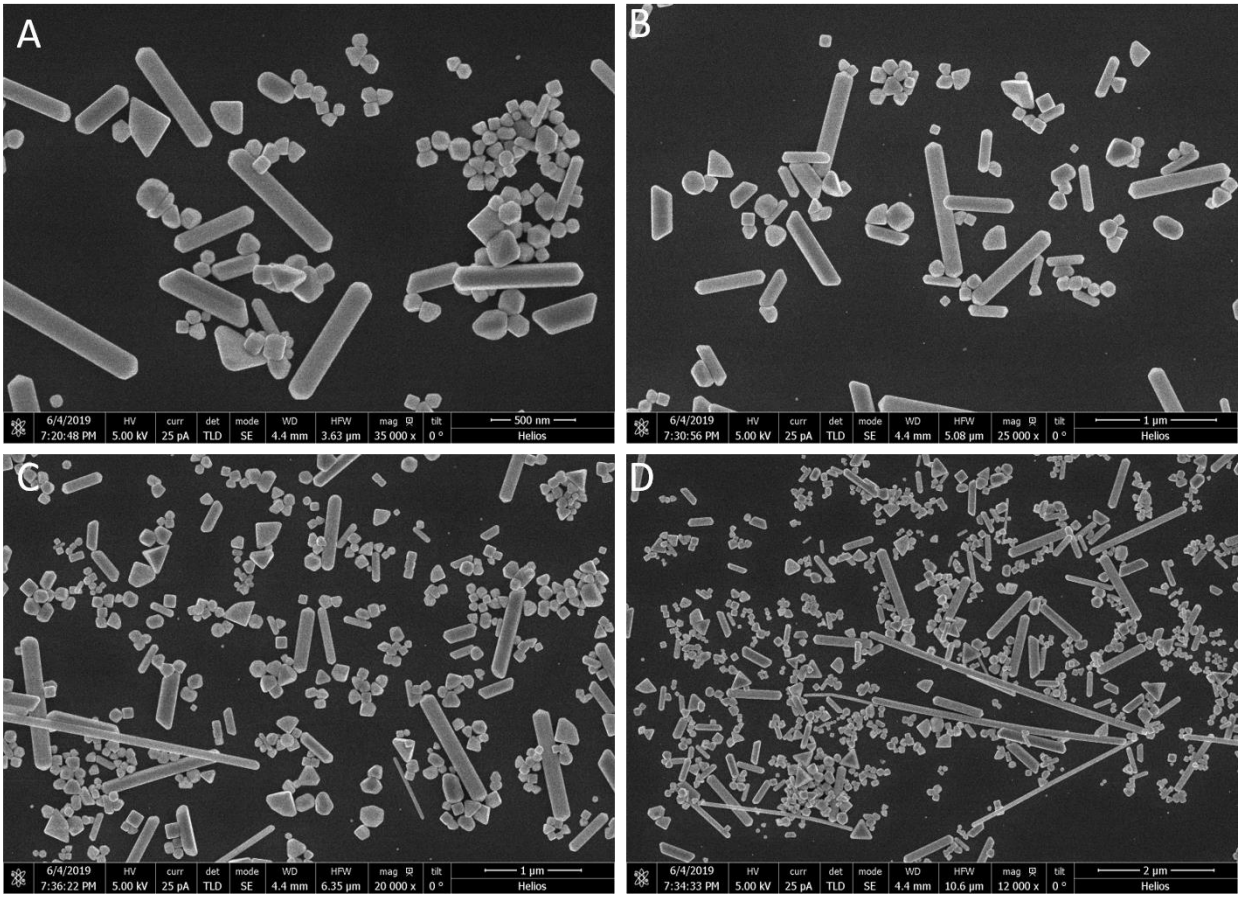

Supplementary Figure SZB. (A-D) Four Representative SEM images of Silver Nanostructures with Nanorod Geometry at Four Different Magnifications. The full reaction condition for the silver nanostructures shown in this Figure is provided in **Supplementary Table SZB** above.

Supplementary Table SZC: Silver Nanostructures with Nanorod Geometry. Reaction condition is provided here in this Table for the nanostructures shown in **Supplementary Figure SZC** below. Four different SEM images of the same reaction sample are shown in **Supplementary Figure SZC** below.

Geometry	**Nanorods**
Full Reaction Condition	Pure 1,3-Propanediol (5 mL) 0.15 M $AgNO_3$ (3mL) 0.35 M PVP-360,000 MW (3mL) 0.05M Ascorbic Acid (1 mL) Temp: 167°C
Note	Pure 1,3-propanediol was heated to 167 °C for 90 minutes followed by the dropwise addition of reactants within 7 minutes. The reaction ran for 60 minutes judging from the first addition of $AgNO_3$ to the reaction solution. The color of the solution was a dark greenish grey at the end of the reaction.

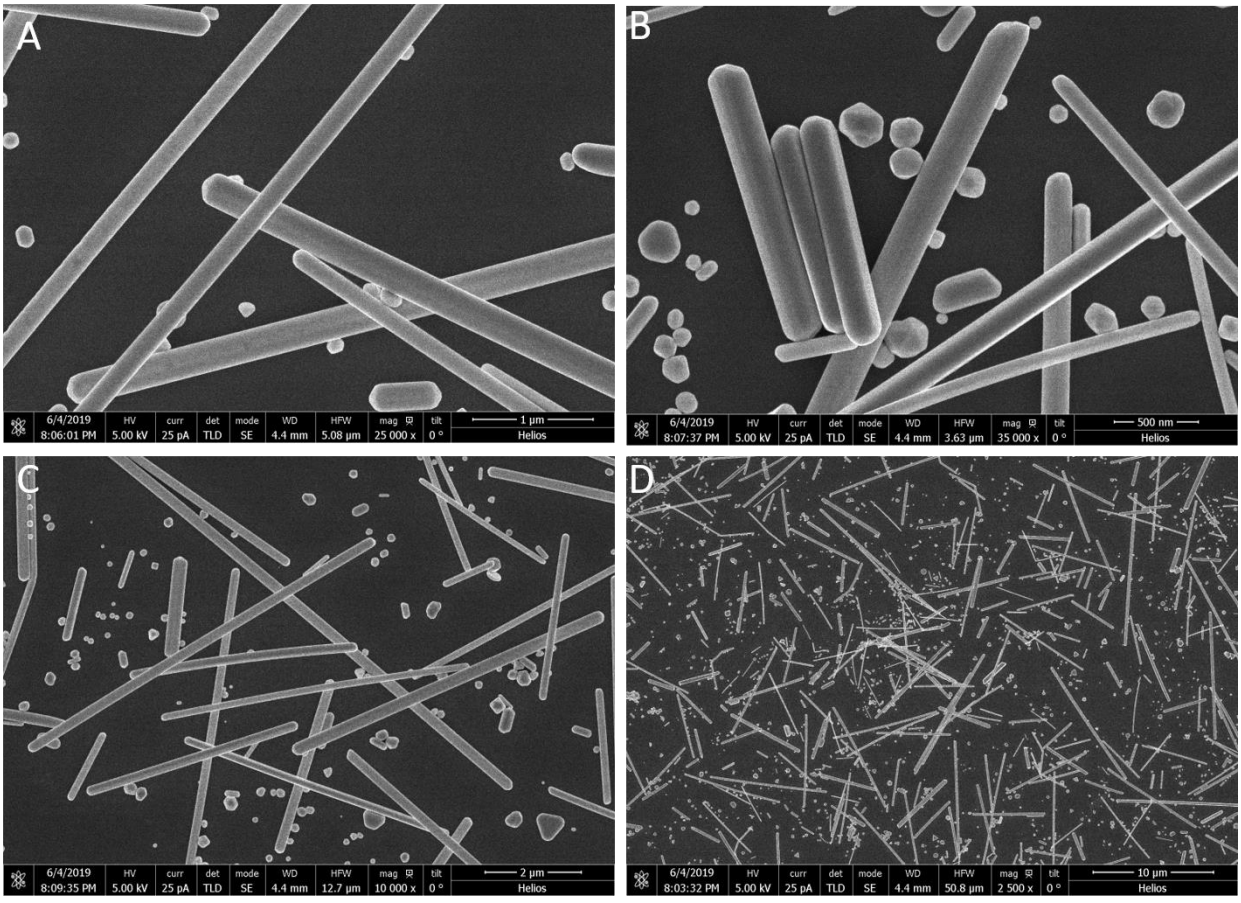

Supplementary Figure SZC. (A-D) Four Representative SEM images of Silver Nanostructures with Nanorod Geometry at Four Different Magnifications. The full reaction condition for the silver nanostructures shown in this Figure is provided in **Supplementary Table SZC** above.

Supplementary Table SZD: Silver Nanostructures with Nanoparticle Geometry. Reaction condition is provided here in this Table for the nanostructures shown in **Supplementary Figure SZD** below. Four different SEM images of the same reaction sample are shown in **Supplementary Figure SZD** below.

Geometry	**Nanoparticles**
Full Reaction Condition	Pure 1,3-Propanediol (5 mL) 0.15 M $AgNO_3$ (3mL) 0.35 M PVP-360,000 MW (3mL) 0.02M Tannic Acid (1 mL) Temp: 167°C
Note	Pure 1,3-propanediol was heated to 167 °C for 90 minutes followed by the dropwise addition of reactants within 7 minutes. The reaction ran for 60 minutes judging from the first addition of $AgNO_3$ to the reaction solution. The color of the solution was a dark greenish grey at the end of the reaction.

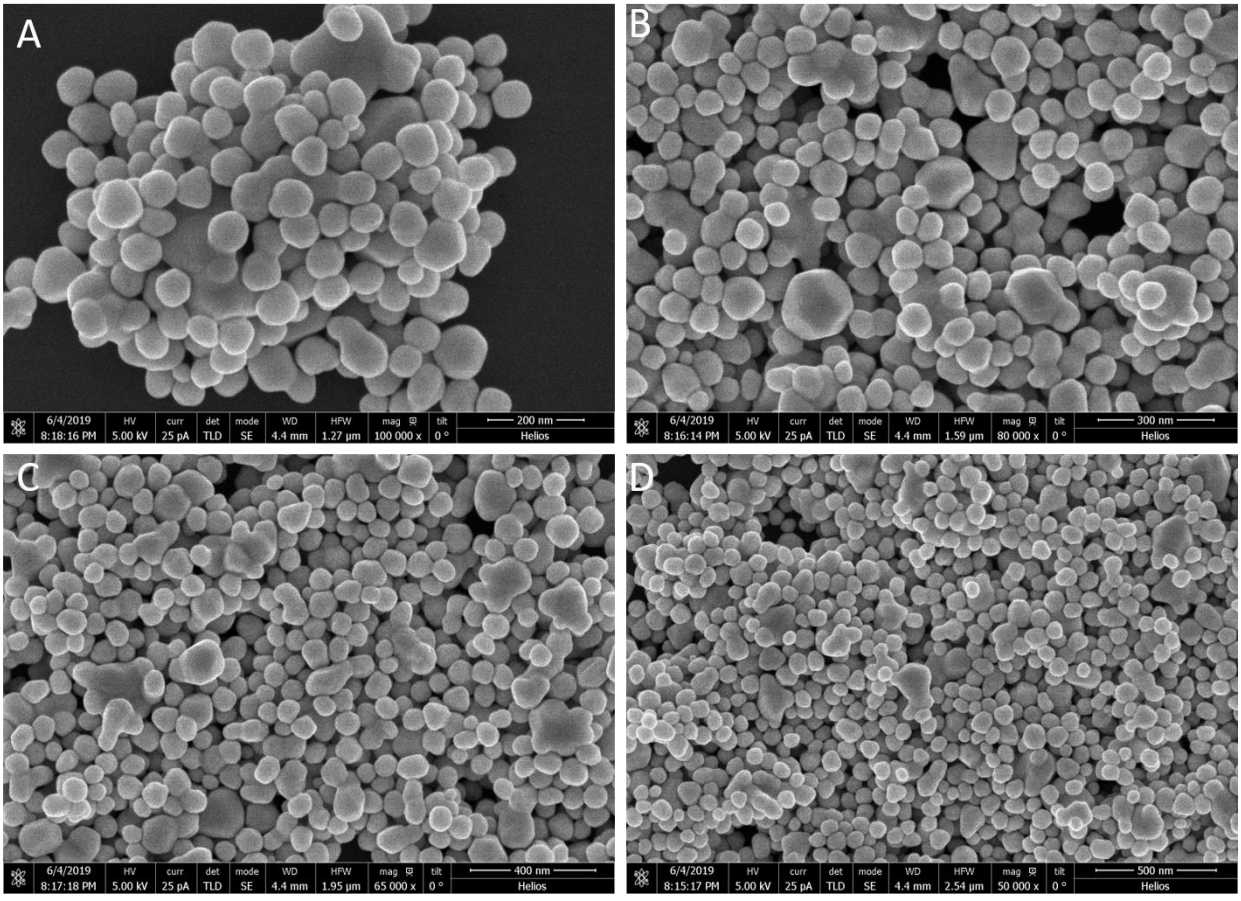

Supplementary Figure SZD. (A-D) Four Representative SEM images of Silver Nanostructures with Nanoparticle Geometry at Four Different Magnifications. The full reaction condition for the silver nanostructures shown in this Figure is provided in **Supplementary Table SZD** above.

Supplementary Table SZE: Silver Nanostructures with Nanoparticle Geometry. Reaction condition is provided here in this Table for the nanostructures shown in **Supplementary Figure SZE** below.

Four different SEM images of the same reaction sample are shown in **Supplementary Figure SZE** below.

Geometry	**Nanoparticles**
Full Reaction Condition	Pure 1,3-Propanediol (5 mL) 0.15 M $AgNO_3$ (3mL) 0.35 M PVP-10,000 MW (3mL) 0.02 M Sucrose(1 mL) Temp: 167°C
Note	Pure 1,3-propanediol was heated to 167 °C for 90 minutes followed by the dropwise addition of reactants within 7 minutes. The reaction ran for 60 minutes judging from the first addition of $AgNO_3$ to the reaction solution. The color of the solution was a dark greenish grey at the end of the reaction.

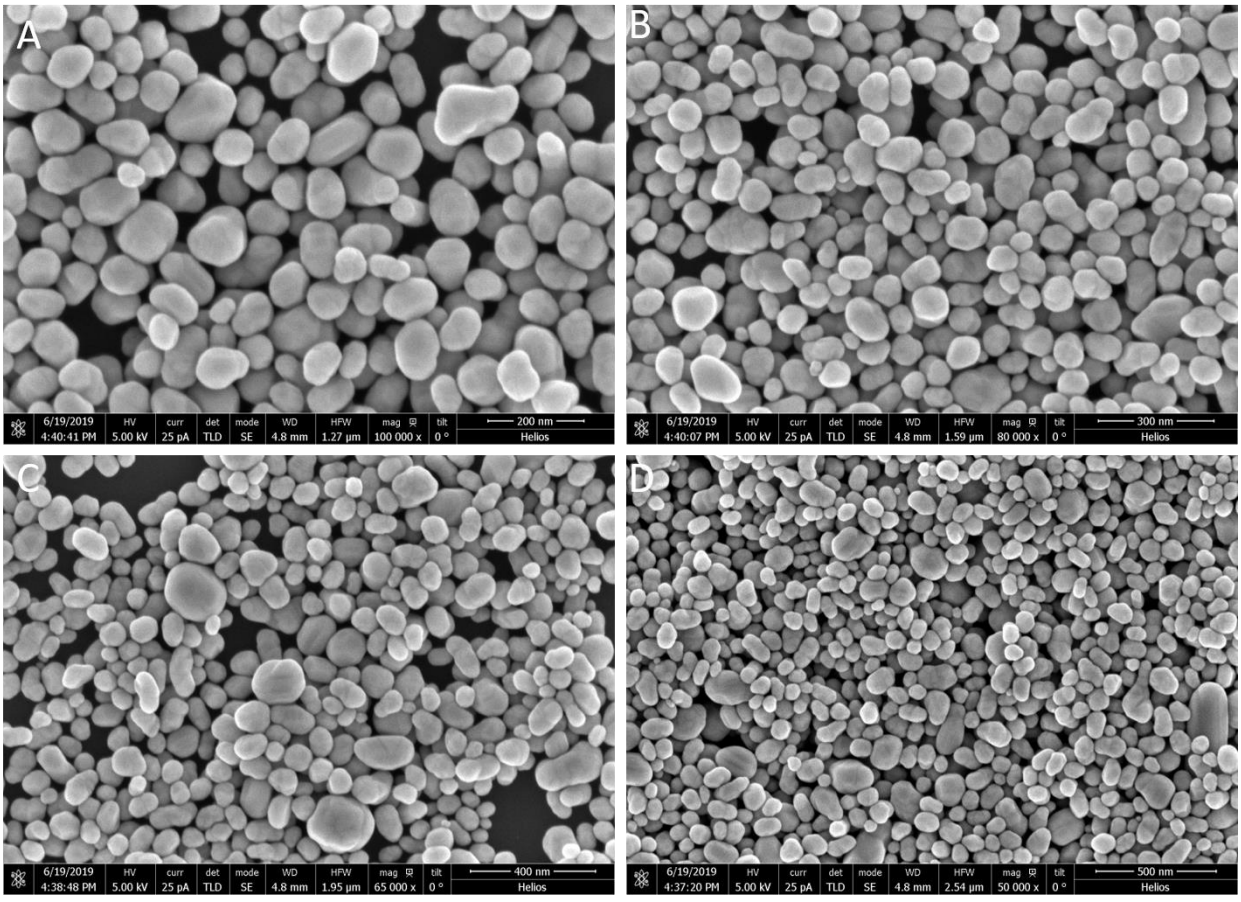

Supplementary Figure SZE. (A-D) Four Representative SEM images of Silver Nanostructures with Nanoparticle Geometry at Four Different Magnifications. The full reaction condition for the silver nanostructures shown in this Figure is provided in **Supplementary Table SZE** above.

Supplementary Table SZF: Silver Nanostructures with Nanorod Geometry. Reaction condition is provided here in this Table for the nanostructures shown in **Supplementary Figure SZF** below. Four different SEM images of the same reaction sample are shown in **Supplementary Figure SZF** below.

Geometry	**Nanorods**
Full Reaction Condition	Pure 1,3-Propanediol (5 mL) 0.15 M $AgNO_3$ (3mL) 0.35 M PVP-29,000 MW (3mL) 0.02 M Sucrose(1 mL) Temp: 167°C
Note	Pure 1,3-propanediol was heated to 167 °C for 90 minutes followed by the dropwise addition of reactants within 7 minutes. The reaction ran for 60 minutes judging from the first addition of $AgNO_3$ to the reaction solution. The color of the solution was a dark greenish grey at the end of the reaction.

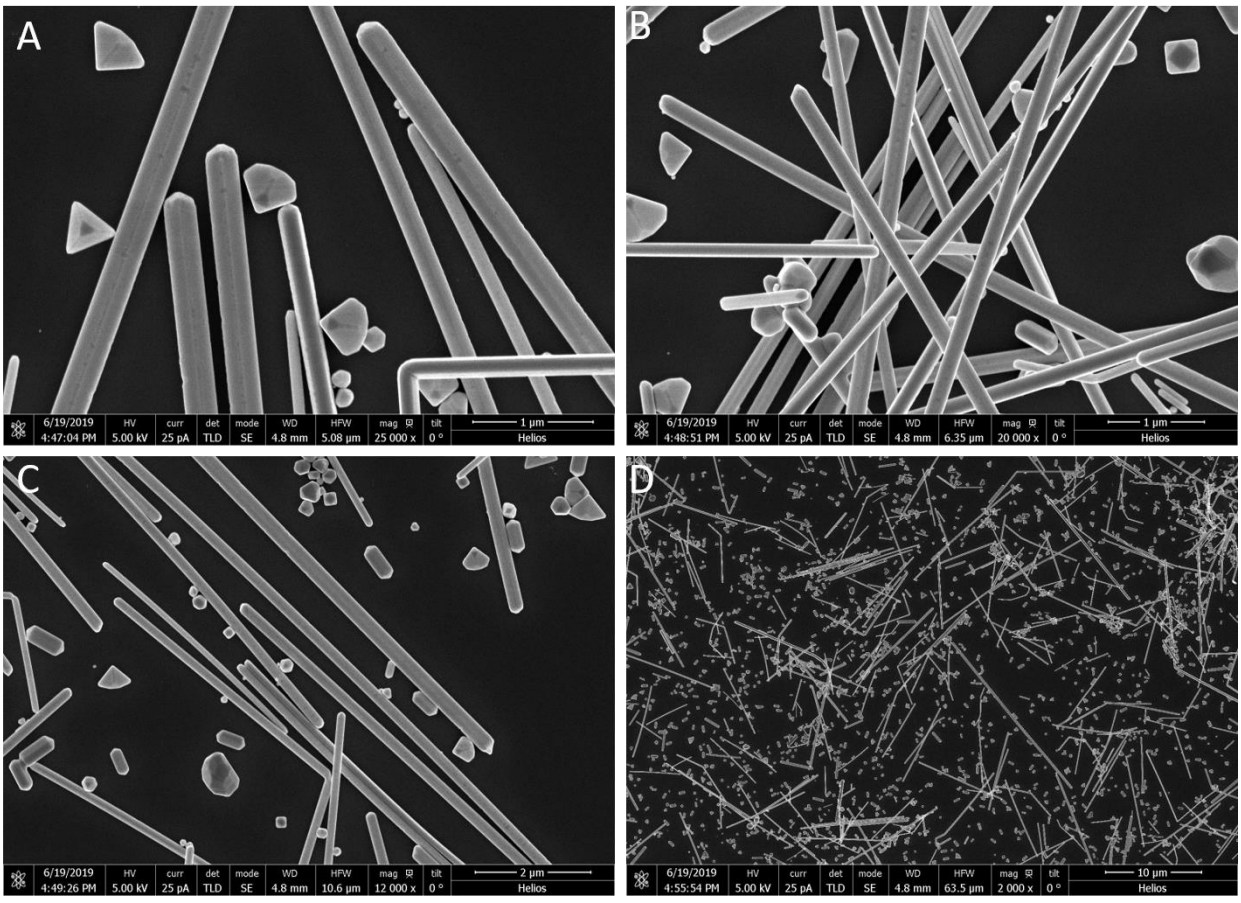

Supplementary Figure SZF. (A-D) Four Representative SEM images of Silver Nanostructures with Nanorod Geometry at Four Different Magnifications. The full reaction condition for the silver nanostructures shown in this Figure is provided in **Supplementary Table SZF** above.

Supplementary Table SZG: Silver Nanostructures with Nanorod and Nanocube Geometry. Reaction condition is provided here in this Table for the nanostructures shown in **Supplementary Figure SZG** below. Four different SEM images of the same reaction sample are shown in **Supplementary Figure SZG** below.

Geometry	**Nanorods + Nanocubes**
Full Reaction Condition	Pure 1,3-Propanediol (5 mL) 0.15 M $AgNO_3$ (3mL) 0.35 M PVP-55,000 MW (3mL) 0.02 M Sucrose(1 mL) Temp: 170°C
Note	Pure 1,3-propanediol was heated to 170 °C for 90 minutes followed by the dropwise addition of reactants within 7 minutes. The reaction ran for 60 minutes judging from the first addition of $AgNO_3$ to the reaction solution. The color of the solution was a dark greenish grey at the end of the reaction.

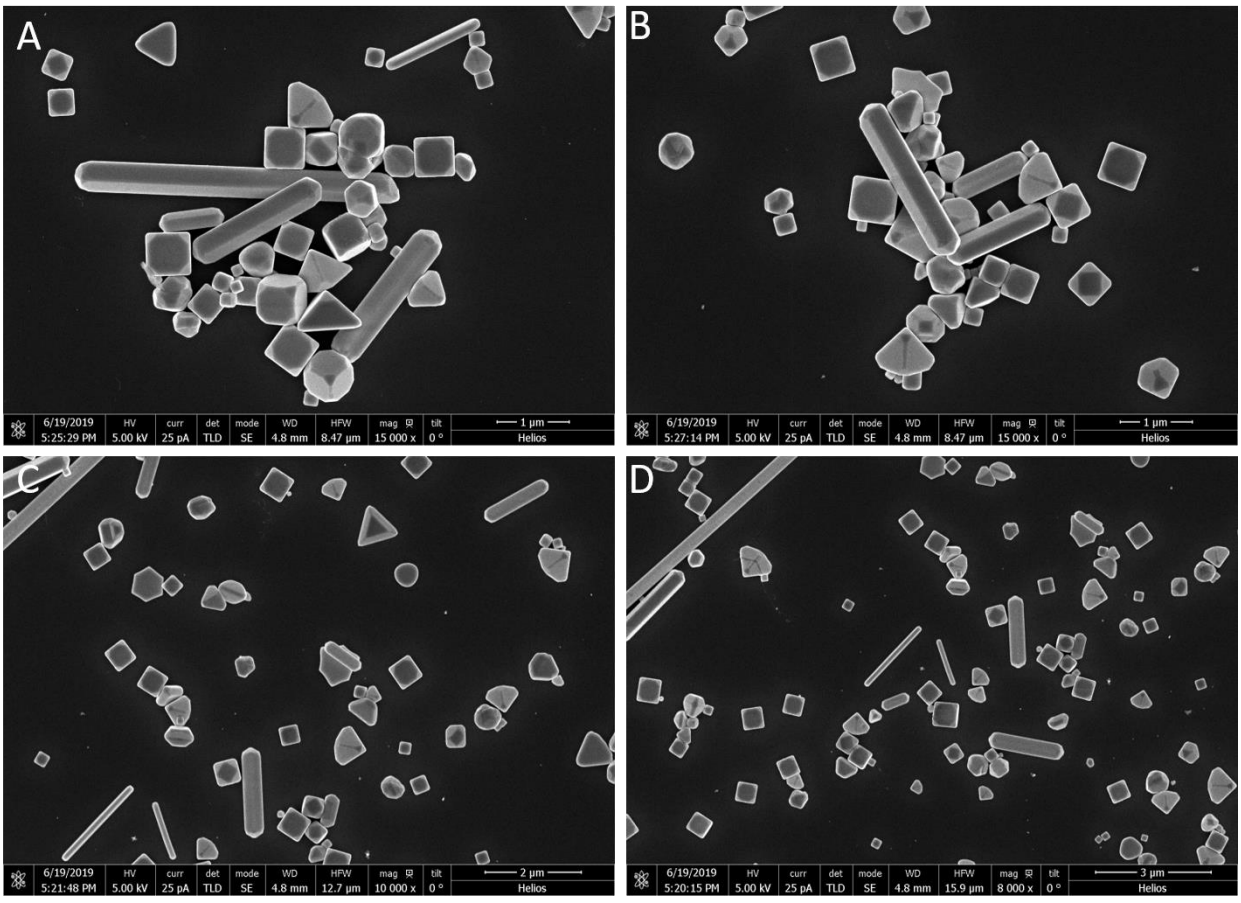

Supplementary Figure SZG. (A-D) Four Representative SEM images of Silver Nanostructures with Nanorod and Nanocube Geometry at Four Different Magnifications. The full reaction condition for the silver nanostructures shown in this Figure is provided in **Supplementary Table SZG** above.

Supplementary Table SZH: Silver Nanostructures with Nanorod Geometry. Reaction condition is provided here in this Table for the nanostructures shown in **Supplementary Figure SZH** below. Four different SEM images of the same reaction sample are shown in **Supplementary Figure SZH** below.

Geometry	**Nanorods**
Full Reaction Condition	Pure 1,3-Propanediol (5 mL) 0.05 M $AgNO_3$ (3mL) 0.35 M PVP-360,000 MW (3mL) 0.02 M Sucrose(1 mL) Temp: 175°C
Note	Pure 1,3-propanediol was heated to 175 °C for 90 minutes followed by the dropwise addition of reactants within 7 minutes. The reaction ran for 60 minutes judging from the first addition of $AgNO_3$ to the reaction solution. The color of the solution was a dark greenish grey at the end of the reaction.

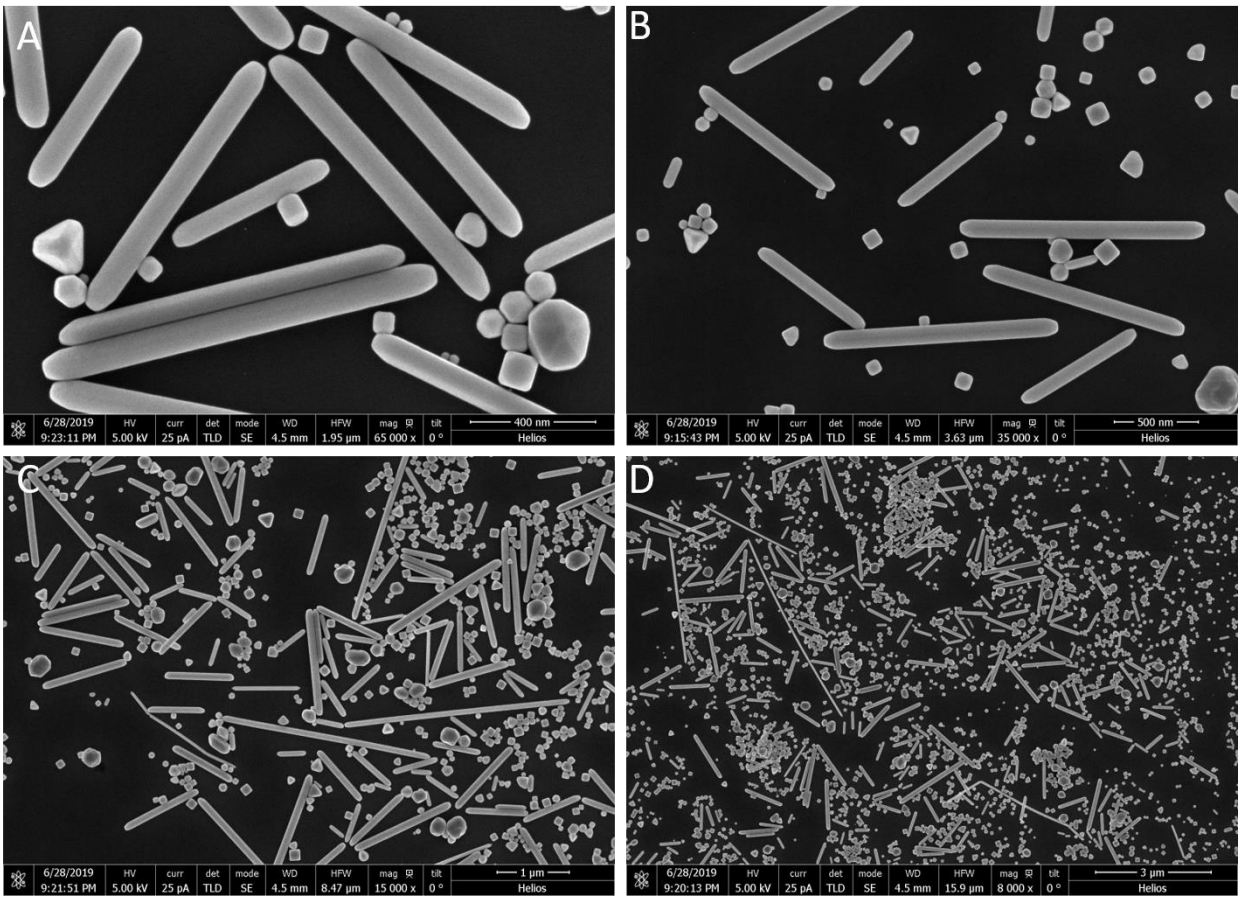

Supplementary Figure SZH. (A-D) Four Representative SEM images of Silver Nanostructures with Nanorod Geometry at Four Different Magnifications. The full reaction condition for the silver nanostructures shown in this Figure is provided in **Supplementary Table SZH** above.

Supplementary Table SZI: Silver Nanostructures with Nanorod Geometry. Reaction condition is provided here in this Table for the nanostructures shown in **Supplementary Figure SZI** below. Four different SEM images of the same reaction sample are shown in **Supplementary Figure SZI** below.

Geometry	**Nanorods**
Full Reaction Condition	Pure 1,3-Propanediol (5 mL) 0.1 M $AgNO_3$ (3mL) 0.35 M PVP-360,000 MW (3mL) 0.02 M Sucrose(1 mL) Temp: 179°C
Note	Pure 1,3-propanediol was heated to 179 °C for 90 minutes followed by the dropwise addition of reactants within 7 minutes. The reaction ran for 60 minutes judging from the first addition of $AgNO_3$ to the reaction solution. The color of the solution was a dark greenish grey at the end of the reaction.

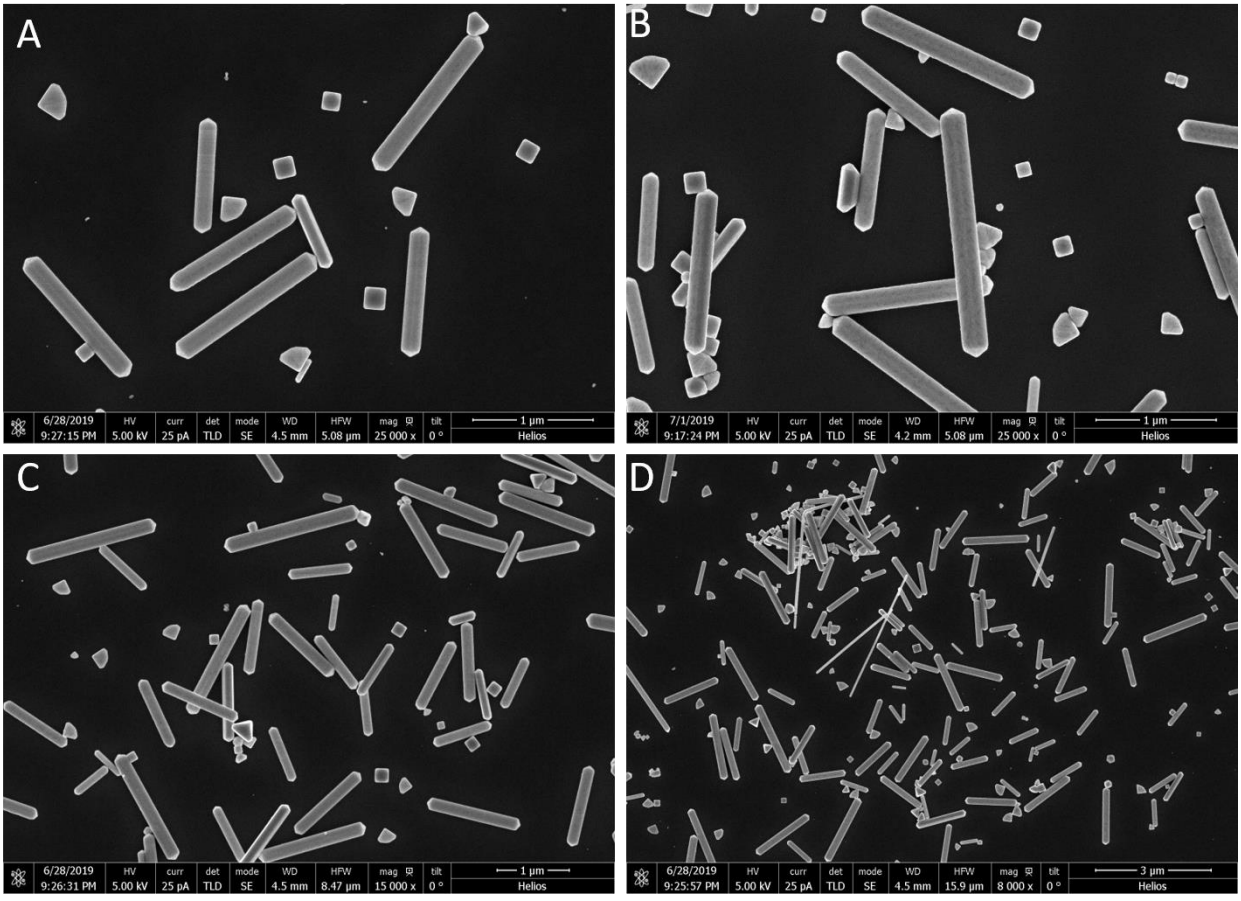

Supplementary Figure SZI. (A-D) Four Representative SEM images of Silver Nanostructures with Nanorod Geometry at Four Different Magnifications. The full reaction condition for the silver nanostructures shown in this Figure is provided in **Supplementary Table SZI** above.

Supplementary Table SZJ: Silver Nanostructures with Nanorod Geometry. Reaction condition is provided here in this Table for the nanostructures shown in **Supplementary Figure SZJ** below. Four different SEM images of the same reaction sample are shown in **Supplementary Figure SZJ** below.

Geometry	**Nanorods**
Full Reaction Condition	Pure 1,3-Propanediol (5 mL) 0.15 M $AgNO_3$ (3mL) 0.35 M PVP-360,000 MW (3mL) 0.02 M Sucrose(1 mL) Temp: 181°C
Note	Pure 1,3-propanediol was heated to 181 °C for 90 minutes followed by the dropwise addition of reactants within 7 minutes. The reaction ran for 60 minutes judging from the first addition of $AgNO_3$ to the reaction solution. The color of the solution was a dark greenish grey at the end of the reaction.

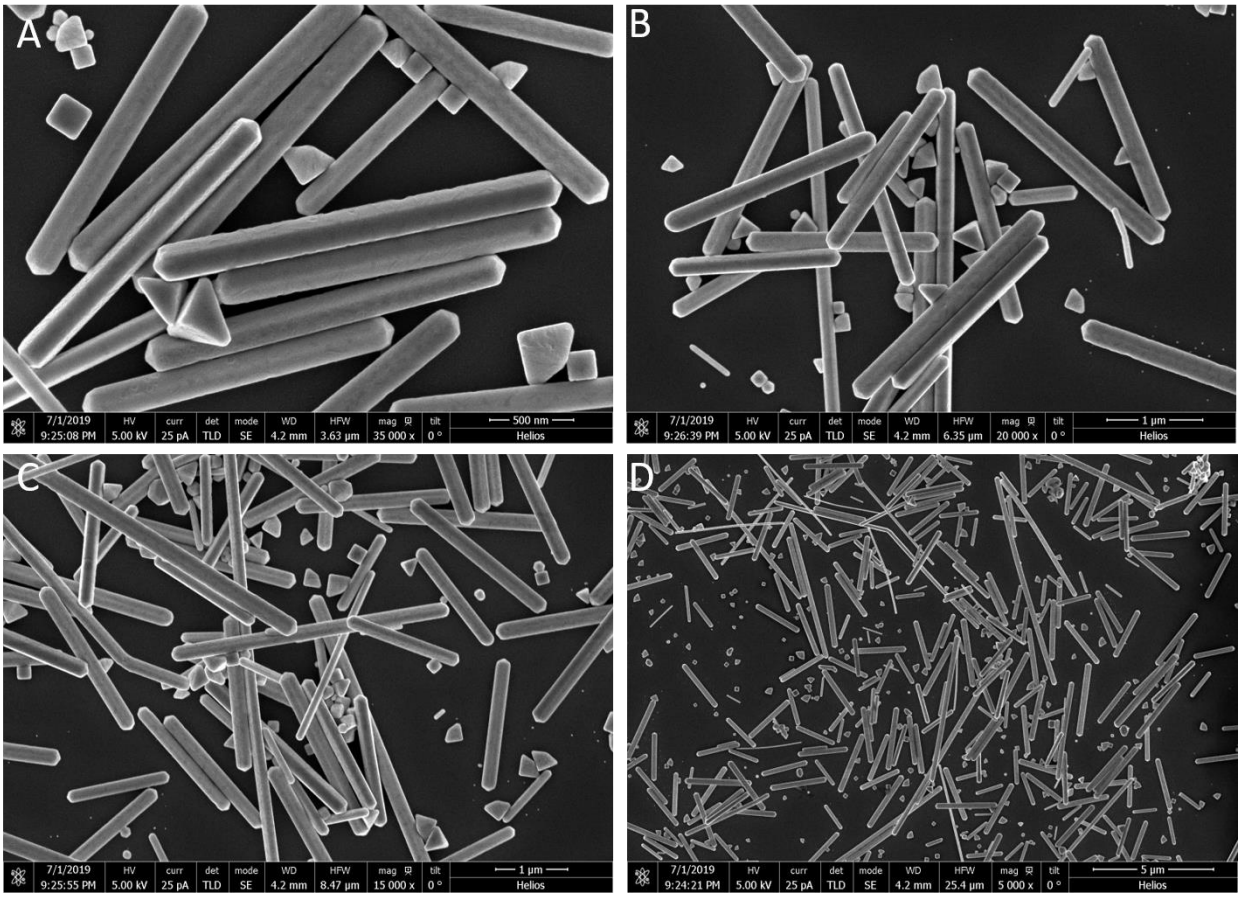

Supplementary Figure SZJ. (A-D) Four Representative SEM images of Silver Nanostructures with Nanorod Geometry at Four Different Magnifications. The full reaction condition for the silver nanostructures shown in this Figure is provided in **Supplementary Table SZJ** above.

Supplementary Table SZK: Silver Nanostructures with Nanorod Geometry. Reaction condition is provided here in this Table for the nanostructures shown in **Supplementary Figure SZK** below. SEM images of the same reaction sample is shown in **Supplementary Figure SZK** below.

Geometry	**Nanorods**
Full Reaction Condition	Pure 1,3-Propanediol (5 mL) 0.08 M $AgNO_3$ (3mL) 0.35 M PVP-360,000 MW (3mL) 0.1 M Ascorbic Acid (1 mL) Temp: 181°C
Note	Pure 1,3-propanediol was heated to 181 °C for 90 minutes followed by the dropwise addition of reactants within 7 minutes. The reaction ran for 60 minutes judging from the first addition of $AgNO_3$ to the reaction solution. The color of the solution was a dark greenish grey at the end of the reaction.

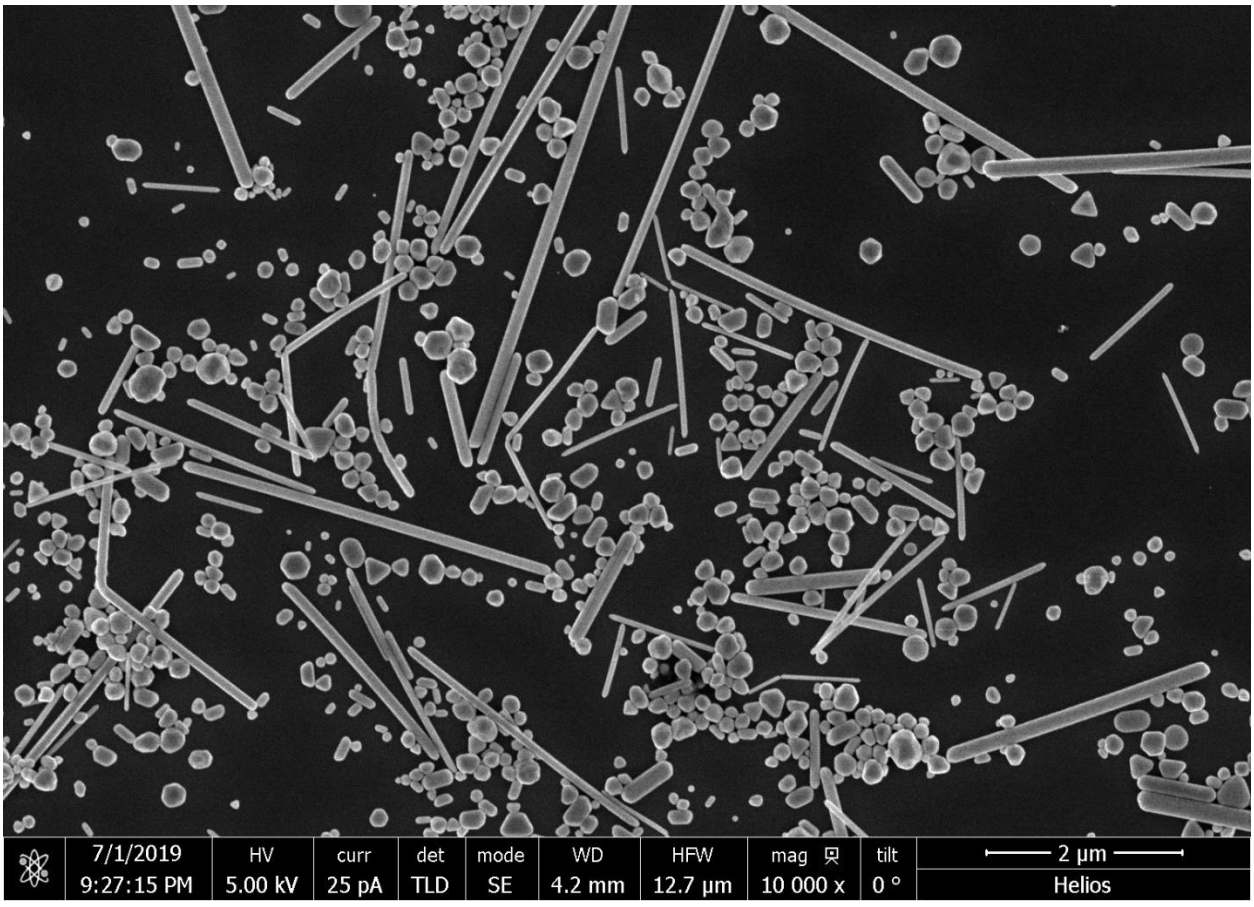

Supplementary Figure SZK. SEM image of Silver Nanostructures with Nanorod Geometry. The full reaction condition for the silver nanostructures shown in this Figure is provided in **Supplementary Table SZK** above.

Supplementary Table SZL: Silver Nanostructures with Nanorod Geometry. Reaction condition is provided here in this Table for the nanostructures shown in **Supplementary Figure SZL** below. Four different SEM images of the same reaction sample are shown in **Supplementary Figure SZL** below.

Geometry	**Nanorods**
Full Reaction Condition	Pure 1,3-Propanediol (5 mL) 0.2 M $AgNO_3$ (3mL) 0.35 M PVP-360,000 MW (3mL) 0.1 M Ascorbic Acid (1 mL) Temp: 172°C
Note	Pure 1,3-propanediol was heated to 172 °C for 90 minutes followed by the dropwise addition of reactants within 7 minutes. The reaction ran for 60 minutes judging from the first addition of $AgNO_3$ to the reaction solution. The color of the solution was a dark greenish grey at the end of the reaction.

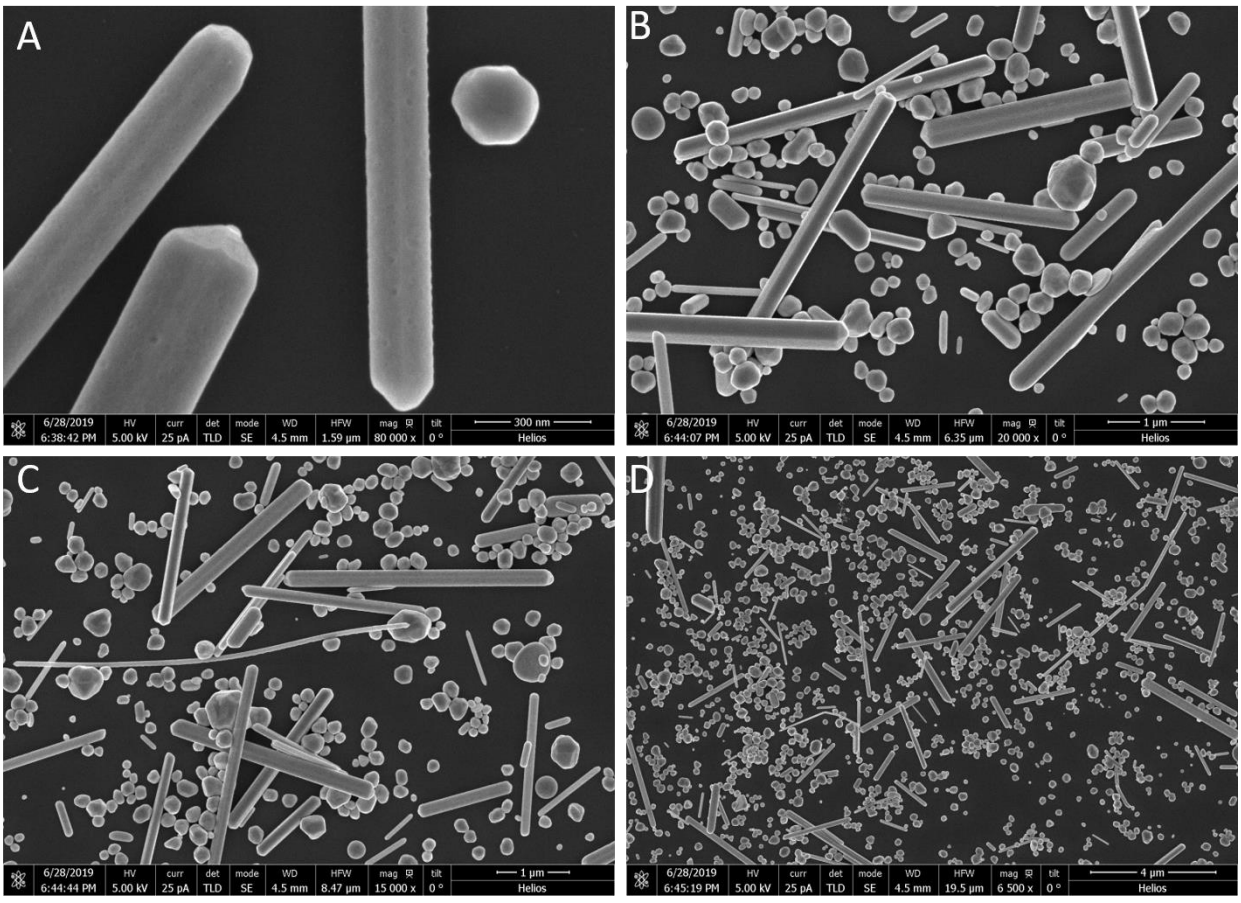

Supplementary Figure SZL. (A-D) Four Representative SEM images of Silver Nanostructures with Nanorod Geometry at Four Different Magnifications. The full reaction condition for the silver nanostructures shown in this Figure is provided in **Supplementary Table SZL** above.

Supplementary Table SZM: Silver Nanostructures with Nanorod Geometry. Reaction condition is provided here in this Table for the nanostructures shown in **Supplementary Figure SZM** below. Four different SEM images of the same reaction sample are shown in **Supplementary Figure SZM** below.

Geometry	**Nanorods**
Full Reaction Condition	Pure 1,3-Propanediol (5 mL) 0.25 M $AgNO_3$ (3mL) 0.35 M PVP-360,000 MW (3mL) 0.1 M Ascorbic Acid (1 mL) Temp: 169°C
Note	Pure 1,3-propanediol was heated to 169°C for 90 minutes followed by the dropwise addition of reactants within 7 minutes. The reaction ran for 60 minutes judging from the first addition of $AgNO_3$ to the reaction solution. The color of the solution was a dark greenish grey at the end of the reaction.

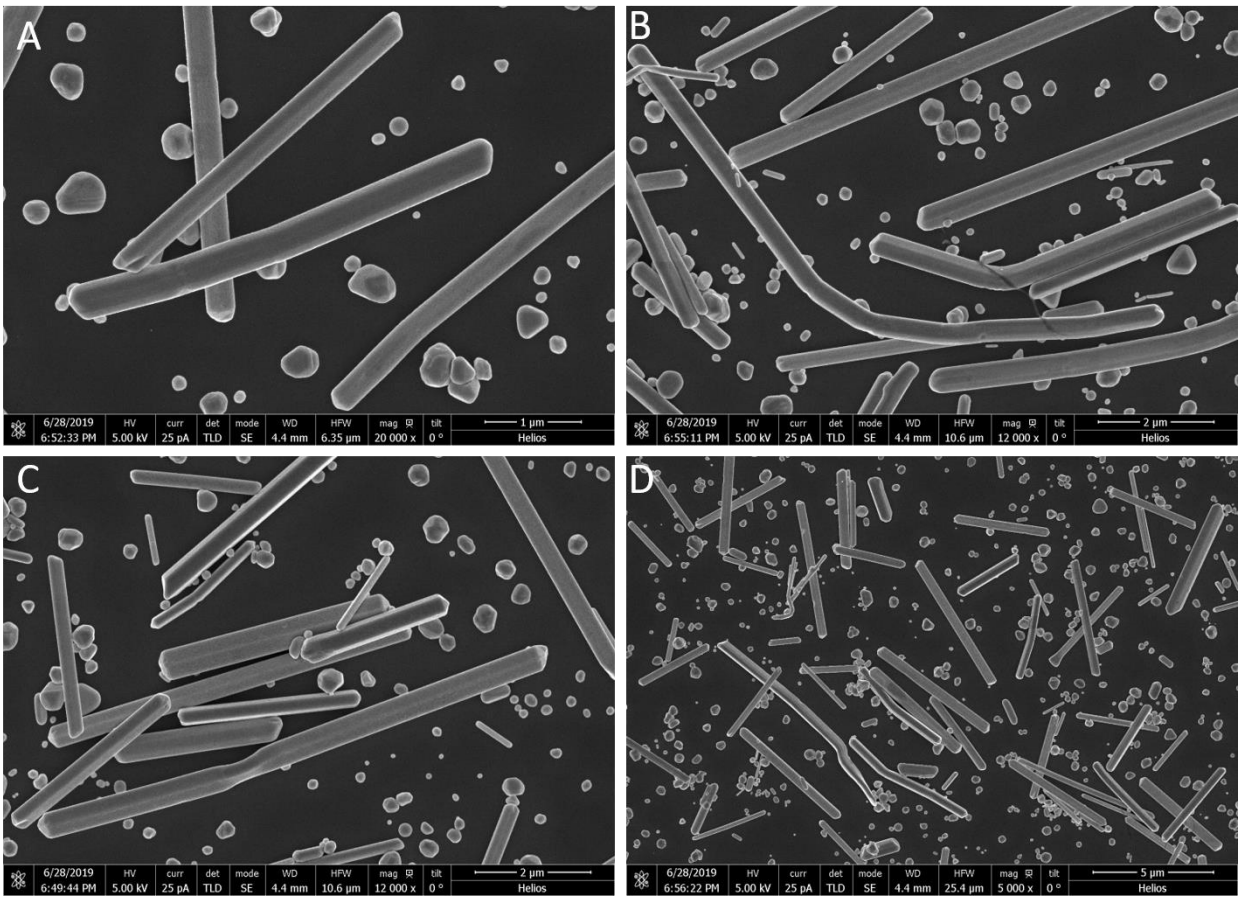

Supplementary Figure SZM. (A-D) Four Representative SEM images of Silver Nanostructures with Nanorod Geometry at Four Different Magnifications. The full reaction condition for the silver nanostructures shown in this Figure is provided in **Supplementary Table SZM** above.

Supplementary Table SZN: Silver Nanostructures with Nanoparticle Geometry. Reaction condition is provided here in this Table for the nanostructures shown in **Supplementary Figure SZN** below. SEM image of the same reaction sample is shown in **Supplementary Figure SZN** below.

Geometry	**Nanoparticles**
Full Reaction Condition	Pure 1,3-Propanediol (5 mL) 0.08 M $AgNO_3$ (3mL) 0.35 M PVP-360,000 MW (3mL) 0.01 M Tannic Acid (1 mL) Temp: 170°C
Note	Pure 1,3-propanediol was heated to 170°C for 90 minutes followed by the dropwise addition of reactants within 7 minutes. The reaction ran for 60 minutes judging from the first addition of $AgNO_3$ to the reaction solution. The color of the solution was a dark greenish grey at the end of the reaction.

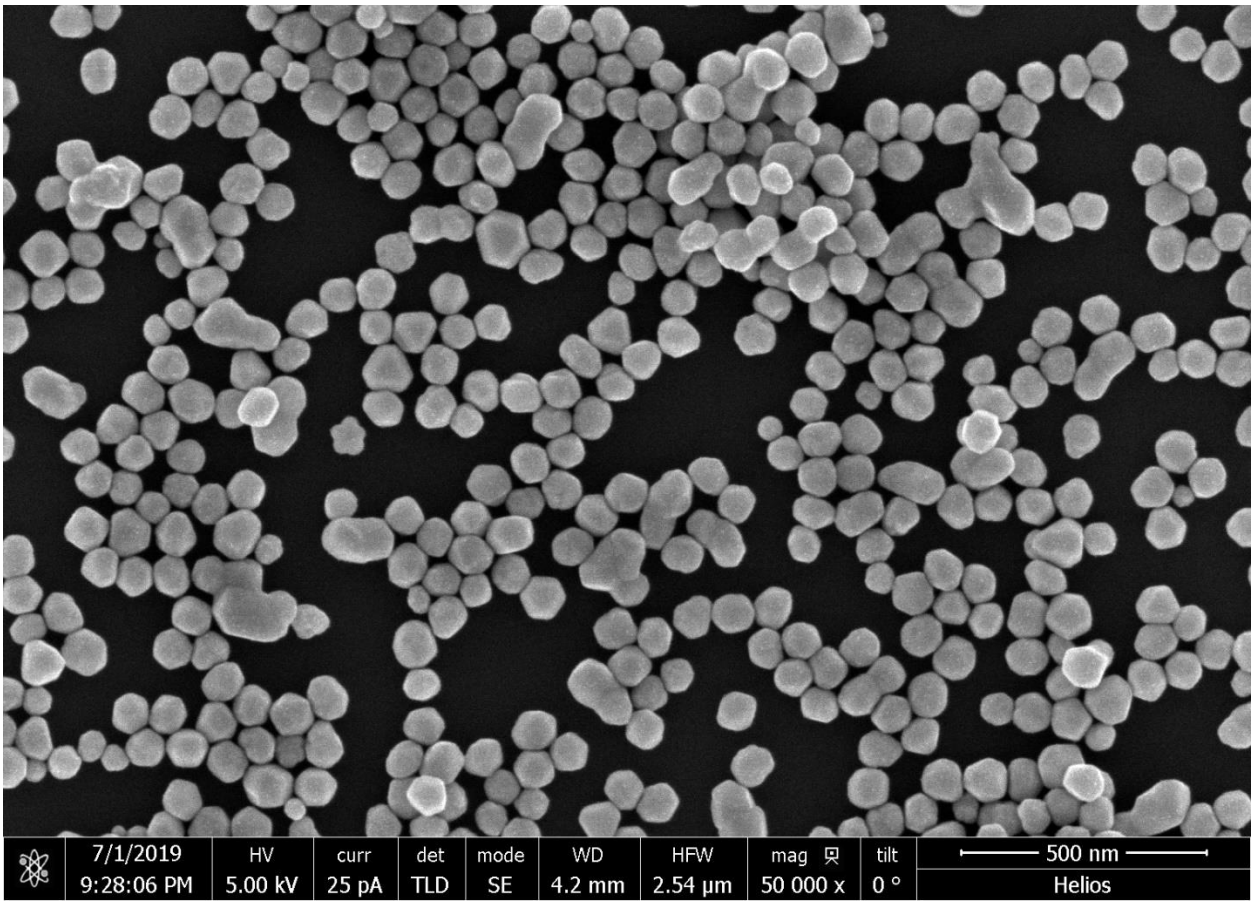

Supplementary Figure SZN. Representative SEM image of Silver Nanostructures with Nanoparticle Geometry. The full reaction condition for the silver nanostructures shown in this Figure is provided in **Supplementary Table SZN** above.

Supplementary Table SZO: Silver Nanostructures with Nanoparticle Geometry. Reaction condition is provided here in this Table for the nanostructures shown in **Supplementary Figure SZO** below. Four different SEM images of the same reaction sample are shown in **Supplementary Figure SZO** below.

Geometry	**Nanoparticles**
Full Reaction Condition	Pure 1,3-Propanediol (5 mL) 0.2 M $AgNO_3$ (3mL) 0.35 M PVP-360,000 MW (3mL) 0.01 M Tannic Acid (1 mL) Temp: 172°C
Note	Pure 1,3-propanediol was heated to 172°C for 90 minutes followed by the dropwise addition of reactants within 7 minutes. The reaction ran for 60 minutes judging from the first addition of $AgNO_3$ to the reaction solution. The color of the solution was a dark greenish grey at the end of the reaction.

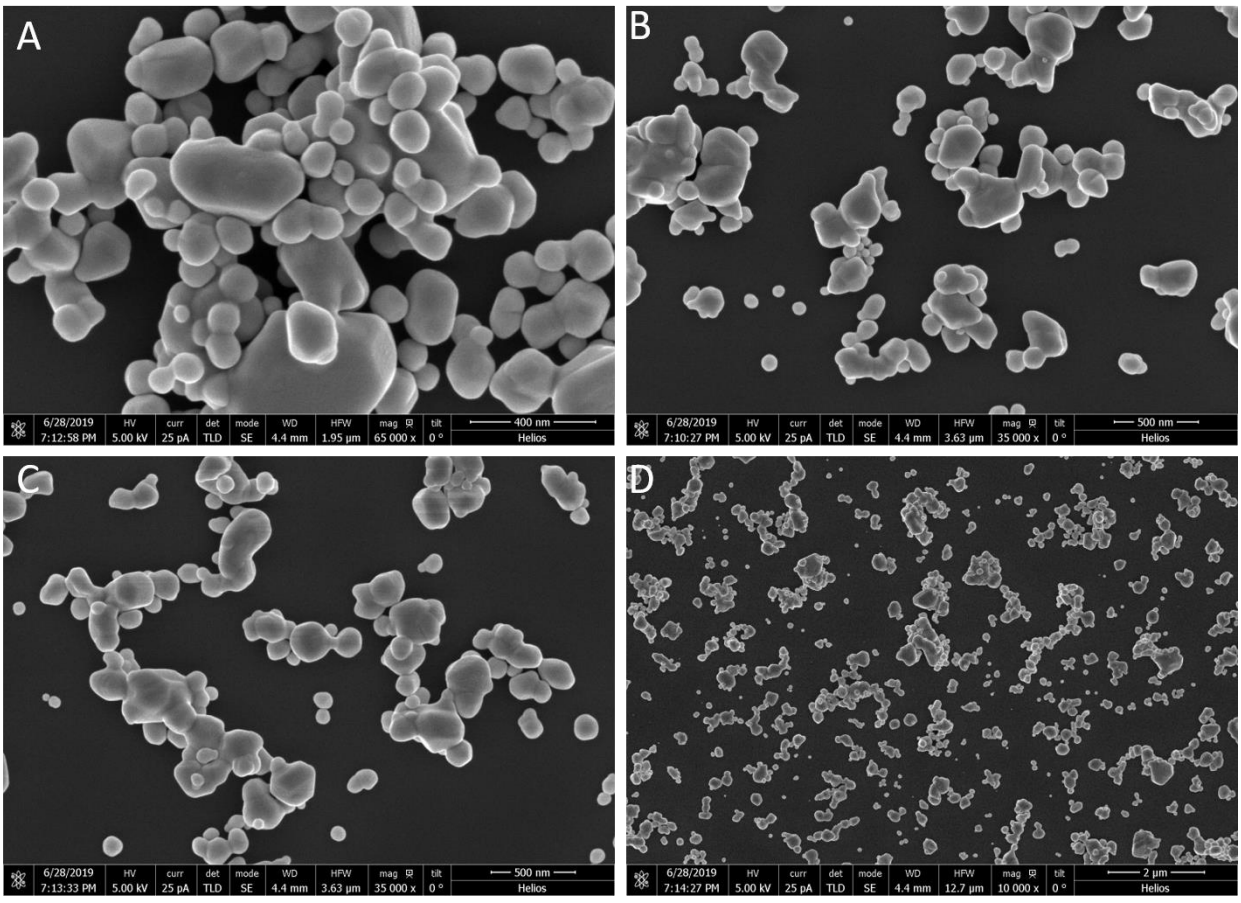

Supplementary Figure SZO. (A-D) Four Representative SEM images of Silver Nanostructures with Nanoparticle Geometry at Four Different Magnifications. The full reaction condition for the silver nanostructures shown in this Figure is provided in **Supplementary Table SZO** above.

Supplementary Table SZP: Silver Nanostructures with Nanoparticle Geometry. Reaction condition is provided here in this Table for the nanostructures shown in **Supplementary Figure SZP** below. Four different SEM images of the same reaction sample are shown in **Supplementary Figure SZP** below.

Geometry	**Nanoparticles**
Full Reaction Condition	Pure 1,3-Propanediol (5 mL) 0.25 M $AgNO_3$ (3mL) 0.35 M PVP-360,000 MW (3mL) 0.01 M Tannic Acid (1 mL) Temp: 172°C
Note	Pure 1,3-propanediol was heated to 172°C for 90 minutes followed by the dropwise addition of reactants within 7 minutes. The reaction ran for 60 minutes judging from the first addition of $AgNO_3$ to the reaction solution. The color of the solution was a dark greenish grey at the end of the reaction.

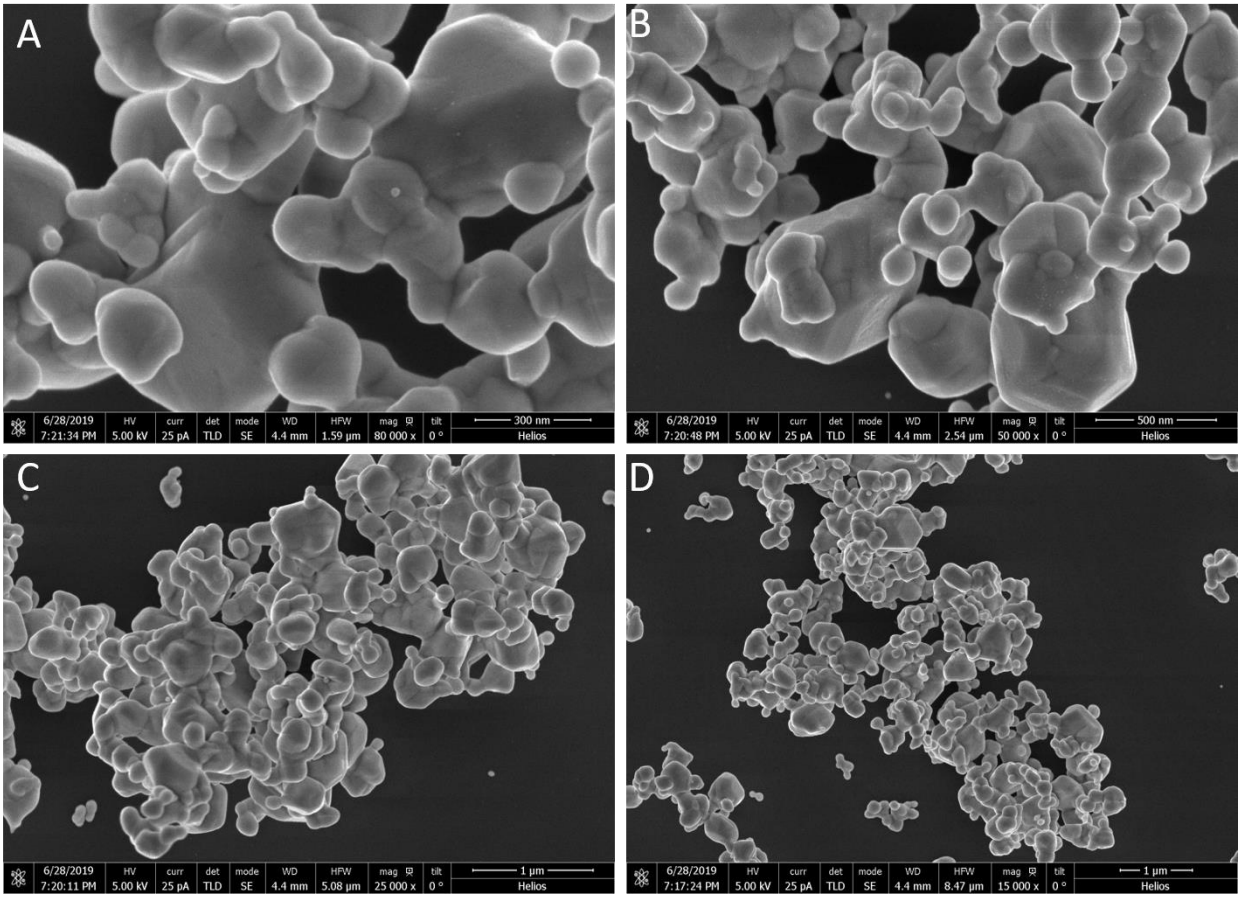

Supplementary Figure SZP. (A-D) Four Representative SEM images of Silver Nanostructures with Nanoparticle Geometry at Four Different Magnifications. The full reaction condition for the silver nanostructures shown in this Figure is provided in **Supplementary Table SZP** above.

Supplementary Table SZQ: Silver Nanostructures with Nanorod Geometry. Reaction condition is provided here in this Table for the nanostructures shown in **Supplementary Figure SZQ** below. Four different SEM images of the same reaction sample are shown in **Supplementary Figure SZQ** below.

Geometry	**Nanorods**
Full Reaction Condition	Pure 1,3-Propanediol (5 mL) 0.15 M $AgNO_3$ (3mL) 0.25 M PVP-360,000 MW (3mL) 0.02M Sucrose (1 mL) Temp: 172°C
Note	Pure 1,3-propanediol was heated to 172 °C for 90 minutes followed by the dropwise addition of reactants within 7 minutes. The reaction ran for 60 minutes judging from the first addition of $AgNO_3$ to the reaction solution. The color of the solution was a dark greenish grey at the end of the reaction.

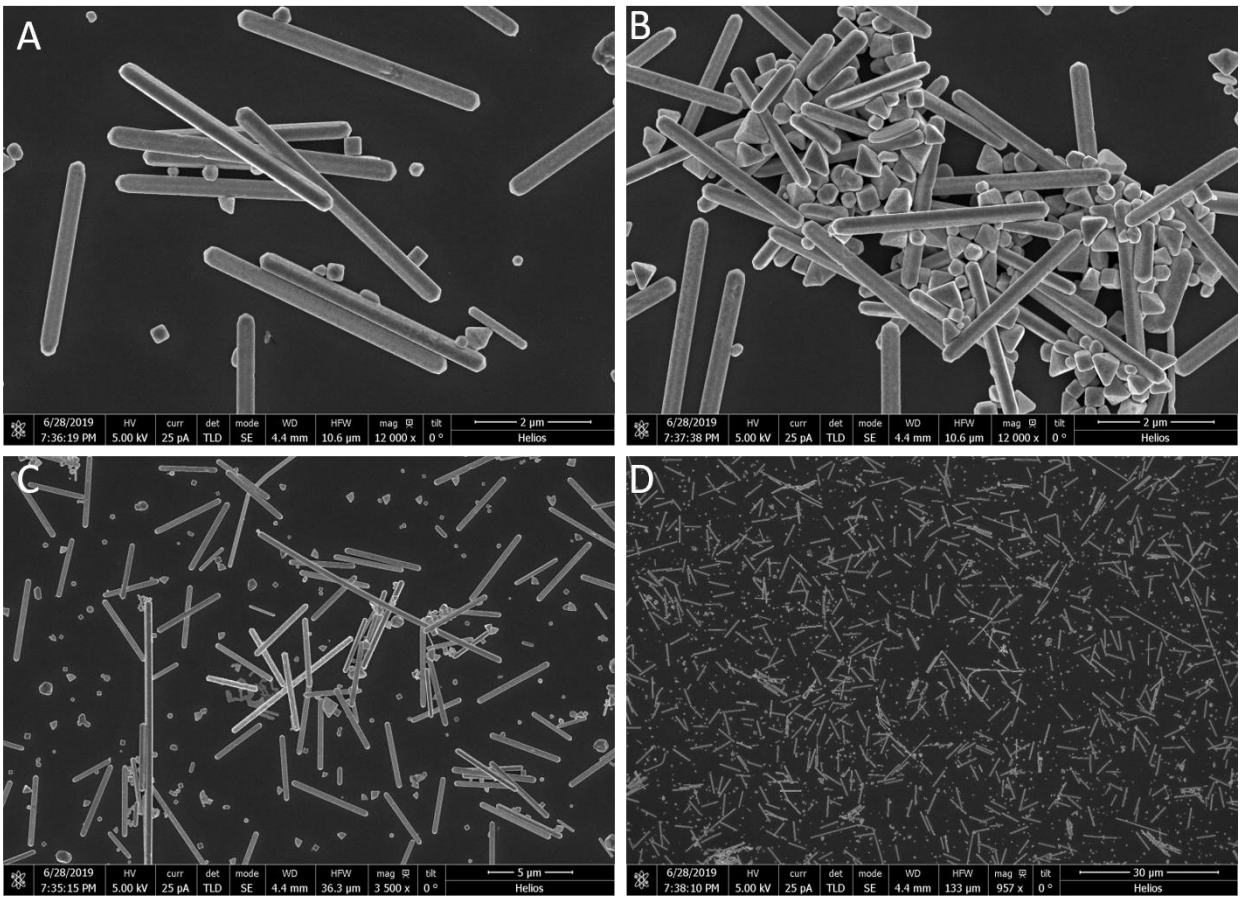

Supplementary Figure SZQ. (A-D) Four Representative SEM images of Silver Nanostructures with Nanorod Geometry at Four Different Magnifications. The full reaction condition for the silver nanostructures shown in this Figure is provided in **Supplementary Table SZQ** above.

Supplementary Table SZR: Silver Nanostructures with Nanorod Geometry. Reaction condition is provided here in this Table for the nanostructures shown in **Supplementary Figure SZR** below. An SEM image of the same reaction sample is shown in **Supplementary Figure SZR** below.

Geometry	**Mixed**
Full Reaction Condition	Pure 1,3-Propanediol (5 mL) 0.15 M $AgNO_3$ (3mL) 0.45 M PVP-360,000 MW (3mL) 0.02M Sucrose (1 mL) Temp: 175°C
Note	Pure 1,3-propanediol was heated to 175 °C for 90 minutes followed by the dropwise addition of reactants within 7 minutes. The reaction ran for 60 minutes judging from the first addition of $AgNO_3$ to the reaction solution. The color of the solution was a dark greenish grey at the end of the reaction.

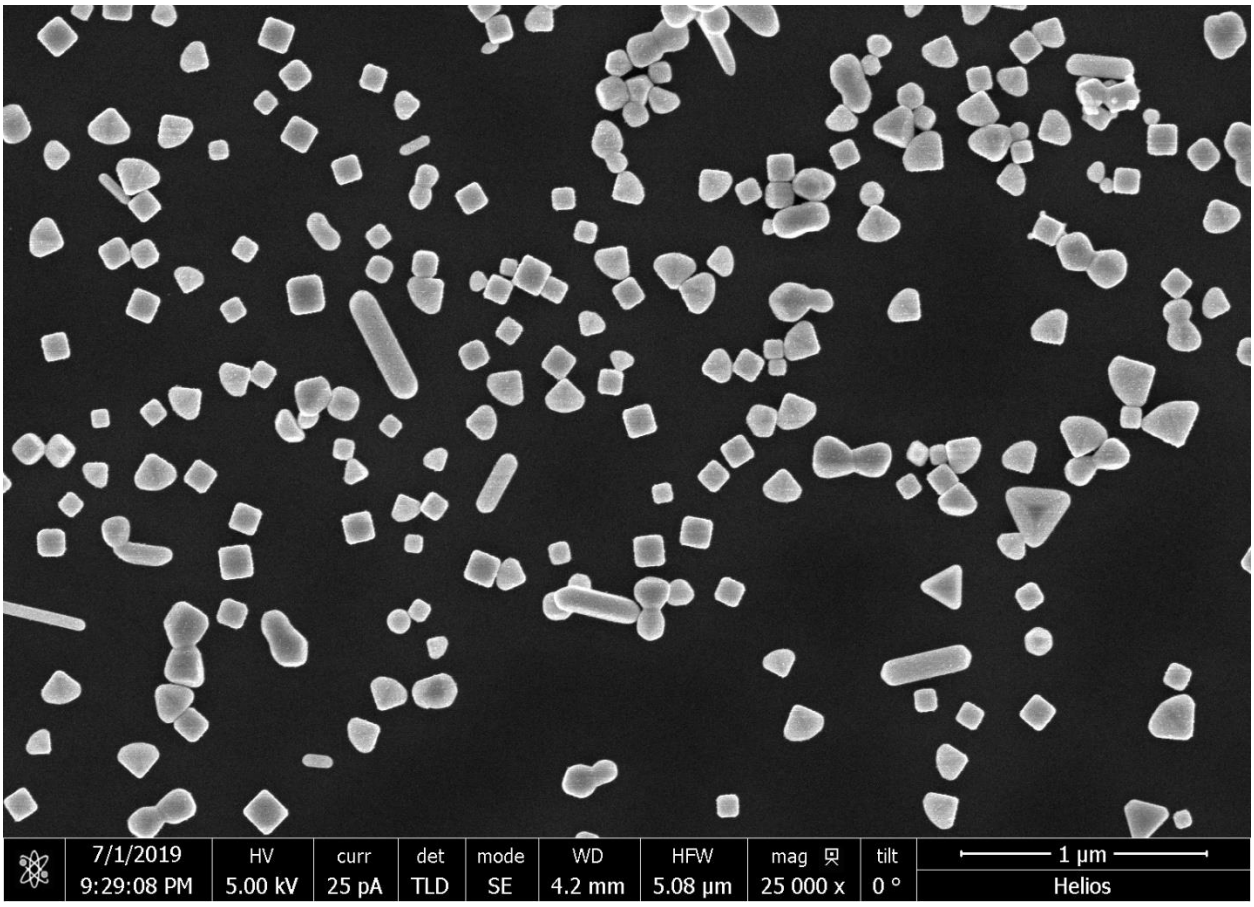

Supplementary Figure SZR. A representative SEM image of Silver Nanostructures with Mix Geometry. The full reaction condition for the silver nanostructures shown in this Figure is provided in **Supplementary Table SZR** above.

Supplementary Table SZS: Silver Nanostructures with Nanorod Geometry. Reaction condition is provided here in this Table for the nanostructures shown in **Supplementary Figure SZS** below. Four different SEM images of the same reaction sample are shown in **Supplementary Figure SZS** below.

Geometry	**Nanorods**
Full Reaction Condition	Pure 1,3-Propanediol (5 mL) 0.15 M $AgNO_3$ (3mL) 0.35 M PVP-360,000 MW (3mL) 0.03M CsOH (1 mL) Temp: 172°C
Note	Pure 1,3-propanediol was heated to 172 °C for 90 minutes followed by the dropwise addition of reactants within 7 minutes. The reaction ran for 60 minutes judging from the first addition of $AgNO_3$ to the reaction solution. The color of the solution was a dark greenish grey at the end of the reaction.

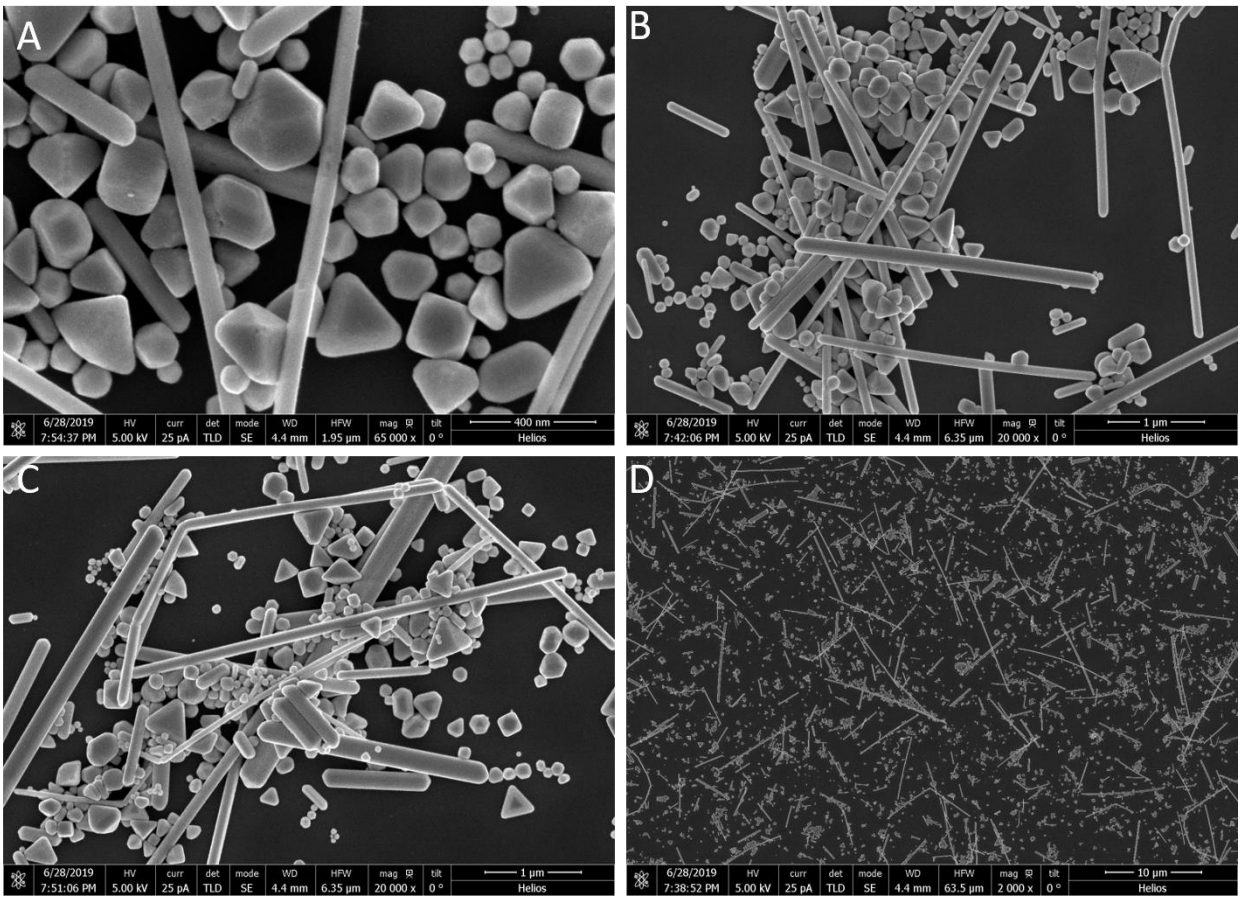

Supplementary Figure SZS. (A-D) Four Representative SEM images of Silver Nanostructures with Nanorod Geometry at Four Different Magnifications. The full reaction condition for the silver nanostructures shown in this Figure is provided in **Supplementary Table SZS** above.

Supplementary Table SZT: Silver Nanostructures with Nanorod Geometry. Reaction condition is provided here in this Table for the nanostructures shown in **Supplementary Figure SZT** below. Four different SEM images of the same reaction sample are shown in **Supplementary Figure SZT** below.

Geometry	**Nanorods**
Full Reaction Condition	Pure 1,3-Propanediol (5 mL) 0.15 M $AgNO_3$ (3mL) 0.35 M PVP-360,000 MW (3mL) 0.03M KOH (1 mL) Temp: 172°C
Note	Pure 1,3-propanediol was heated to 172 °C for 90 minutes followed by the dropwise addition of reactants within 7 minutes. The reaction ran for 60 minutes judging from the first addition of $AgNO_3$ to the reaction solution. The color of the solution was a dark greenish grey at the end of the reaction.

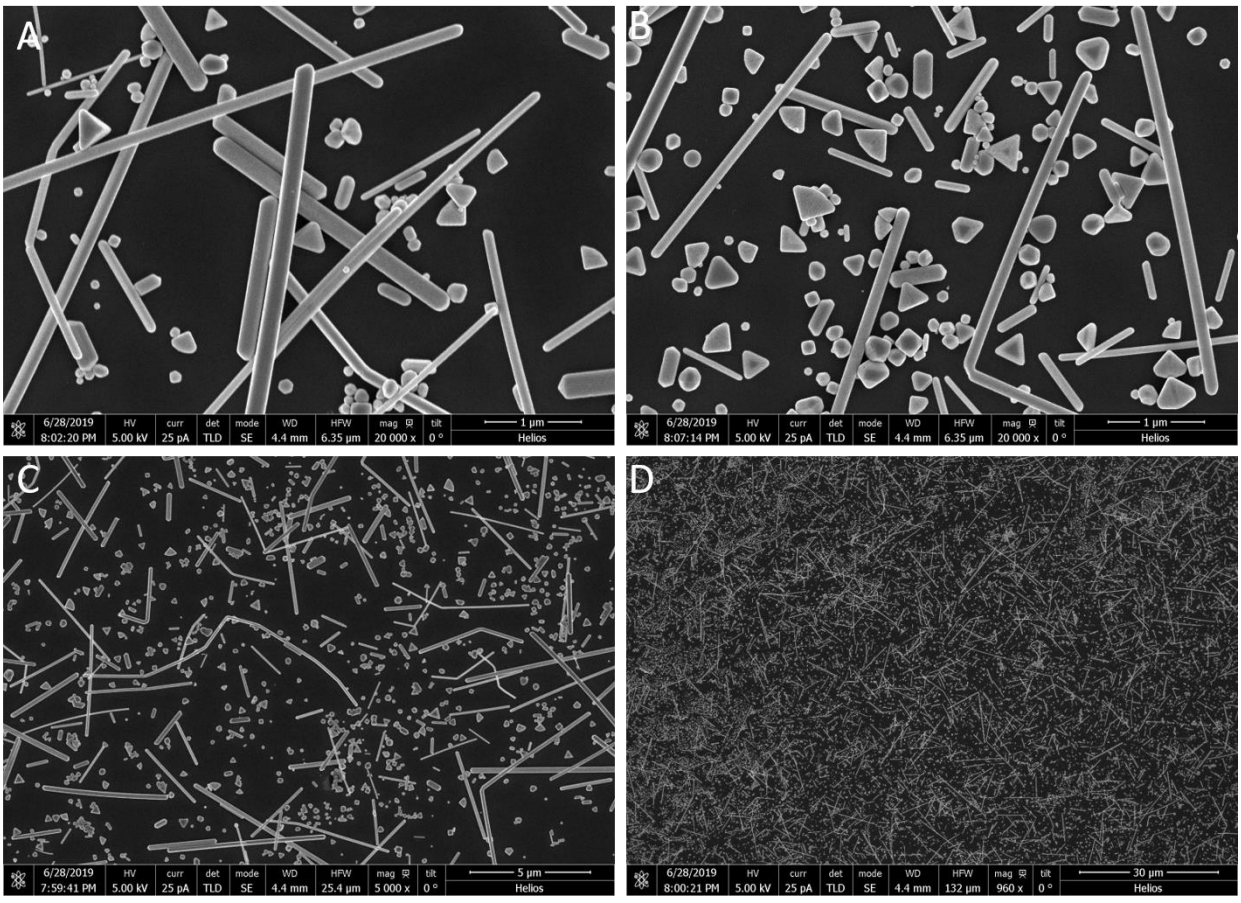

Supplementary Figure SZT. (A-D) Four Representative SEM images of Silver Nanostructures with Nanorod Geometry at Four Different Magnifications. The full reaction condition for the silver nanostructures shown in this Figure is provided in **Supplementary Table SZT** above

Supplementary Table SZU: Silver Nanostructures with Nanorod Geometry. Reaction condition is provided here in this Table for the nanostructures shown in **Supplementary Figure SZU** below. Four different SEM images of the same reaction sample are shown in **Supplementary Figure SZU** below.

Geometry	**Nanorods**
Full Reaction Condition	Pure 1,3-Propanediol (5 mL) 0.15 M $AgNO_3$ (3mL) 0.35 M PVP-360,000 MW (3mL) 0.03M NaOH (1 mL) Temp: 172°C
Note	Pure 1,3-propanediol was heated to 172 °C for 90 minutes followed by the dropwise addition of reactants within 7 minutes. The reaction ran for 60 minutes judging from the first addition of $AgNO_3$ to the reaction solution. The color of the solution was a dark greenish grey at the end of the reaction.

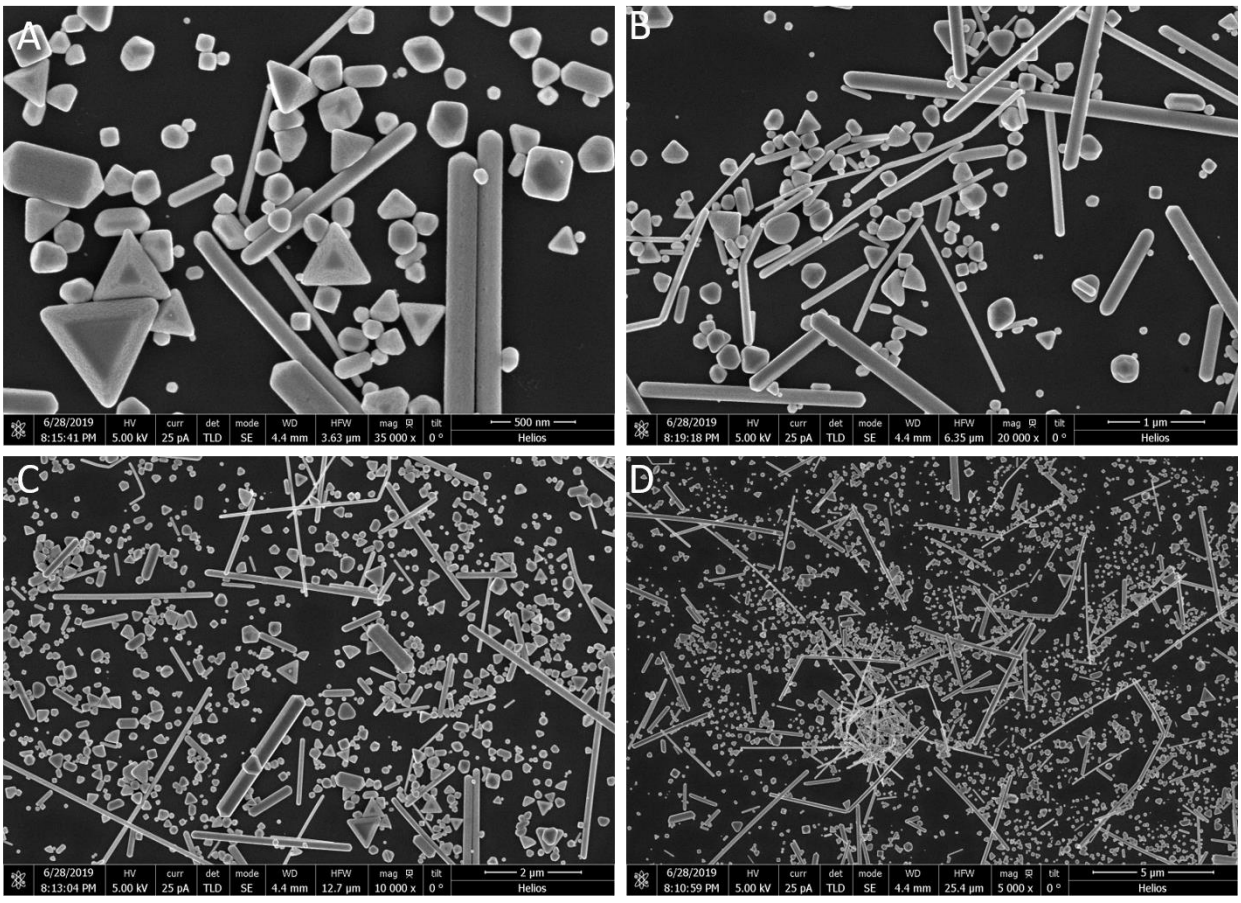

Supplementary Figure SZU. (A-D) Four Representative SEM images of Silver Nanostructures with Nanorod Geometry at Four Different Magnifications. The full reaction condition for the silver nanostructures shown in this Figure is provided in **Supplementary Table SZU** above.

Supplementary Table SZV: Silver Nanostructures with Nanoparticle Geometry. Reaction condition is provided here in this Table for the nanostructures shown in **Supplementary Figure SZV** below. Four different SEM images of the same reaction sample are shown in **Supplementary Figure SZV** below.

Geometry	**Nanoparticles**
Full Reaction Condition	Pure 1,3-Propanediol (5 mL) 0.15 M $AgNO_3$ (3mL) 0.35 M PVP-10,000 MW (3mL) 0.01 M Tannic Acid (1 mL) Temp: 170°C
Note	Pure 1,3-propanediol was heated to 170 °C for 90 minutes followed by the dropwise addition of reactants within 7 minutes. The reaction ran for 60 minutes judging from the first addition of $AgNO_3$ to the reaction solution. The color of the solution was a dark brown at the end of the reaction.

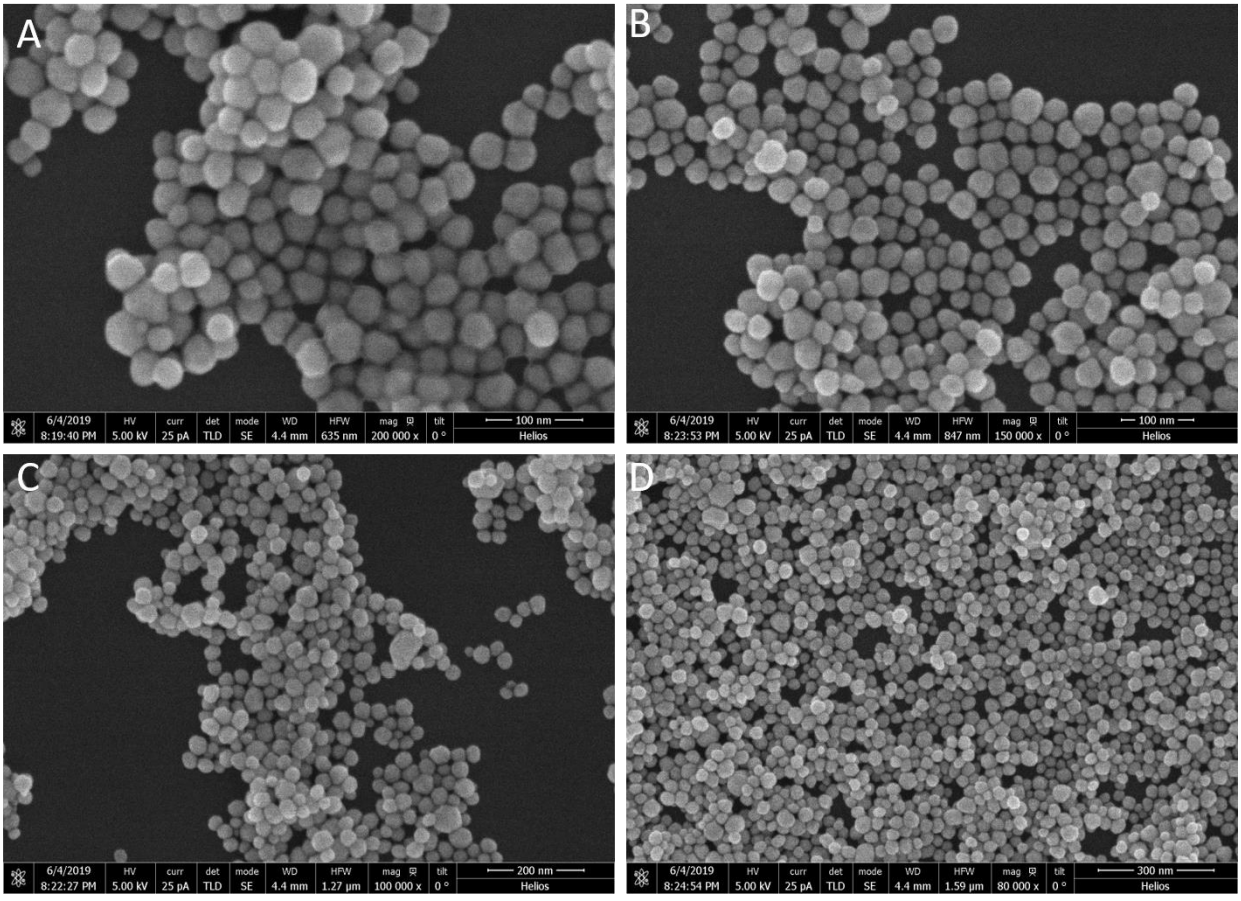

Supplementary Figure SZV. (A-D) Four Representative SEM images of Silver Nanostructures with Nanoparticle Geometry at Four Different Magnifications. The full reaction condition for the silver nanostructures shown in this Figure is provided in **Supplementary Table SZV** above.

Supplementary Table SZW: Silver Nanostructures with Nanoparticle Geometry. Reaction condition is provided here in this Table for the nanostructures shown in **Supplementary Figure SZW** below. Four different SEM images of the same reaction sample are shown in **Supplementary Figure SZW** below.

Geometry	**Nanoparticles**
Full Reaction Condition	Pure 1,3-Propanediol (5 mL) 0.15 M $AgNO_3$ (3mL) 0.35 M PVP-55,000 MW (3mL) 0.01 M Tannic Acid (1 mL) Temp: 170°C
Note	Pure 1,3-propanediol was heated to 170 °C for 90 minutes followed by the dropwise addition of reactants within 7 minutes. The reaction ran for 60 minutes judging from the first addition of $AgNO_3$ to the reaction solution. The color of the solution was a dark brown at the end of the reaction.

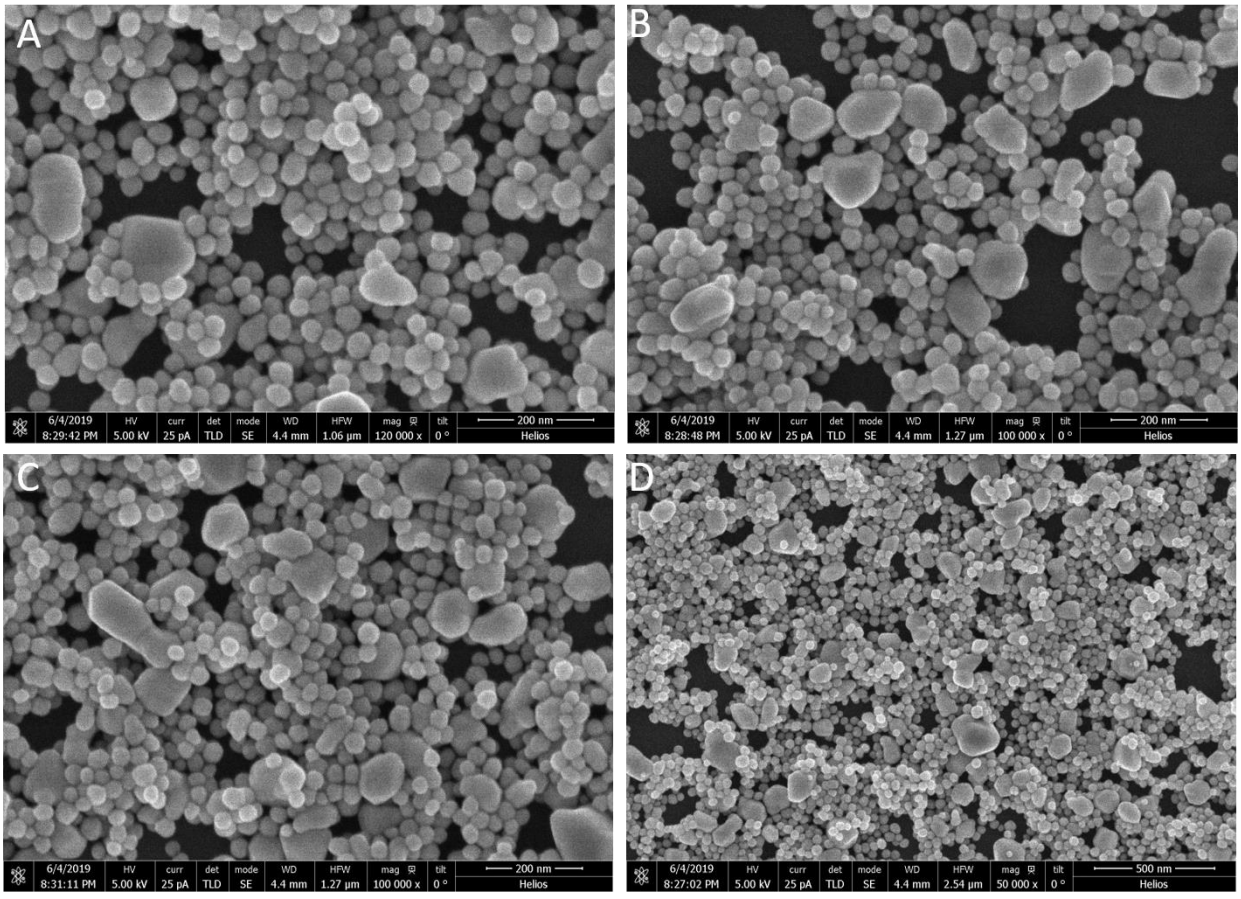

Supplementary Figure SZW. (A-D) Four Representative SEM images of Silver Nanostructures with Nanoparticle Geometry at Four Different Magnifications. The full reaction condition for the silver nanostructures shown in this Figure is provided in **Supplementary Table SZW** above.

Supplementary Table SZX: Silver Nanostructures with Nanoparticle Geometry. Reaction condition is provided here in this Table for the nanostructures shown in **Supplementary Figure SZX** below. Four different SEM images of the same reaction sample are shown in **Supplementary Figure SZX** below.

Geometry	**Nanoparticles**
Full Reaction Condition	Pure 1,3-Propanediol (5 mL) 0.15 M $AgNO_3$ (3mL) 0.35 M PVP-1,300,000 MW (3mL) 0.01 M Tannic Acid (1 mL) Temp: 170°C
Note	Pure 1,3-propanediol was heated to 170 °C for 90 minutes followed by the dropwise addition of reactants within 7 minutes. The reaction ran for 60 minutes judging from the first addition of $AgNO_3$ to the reaction solution. The color of the solution was a dark brown at the end of the reaction.

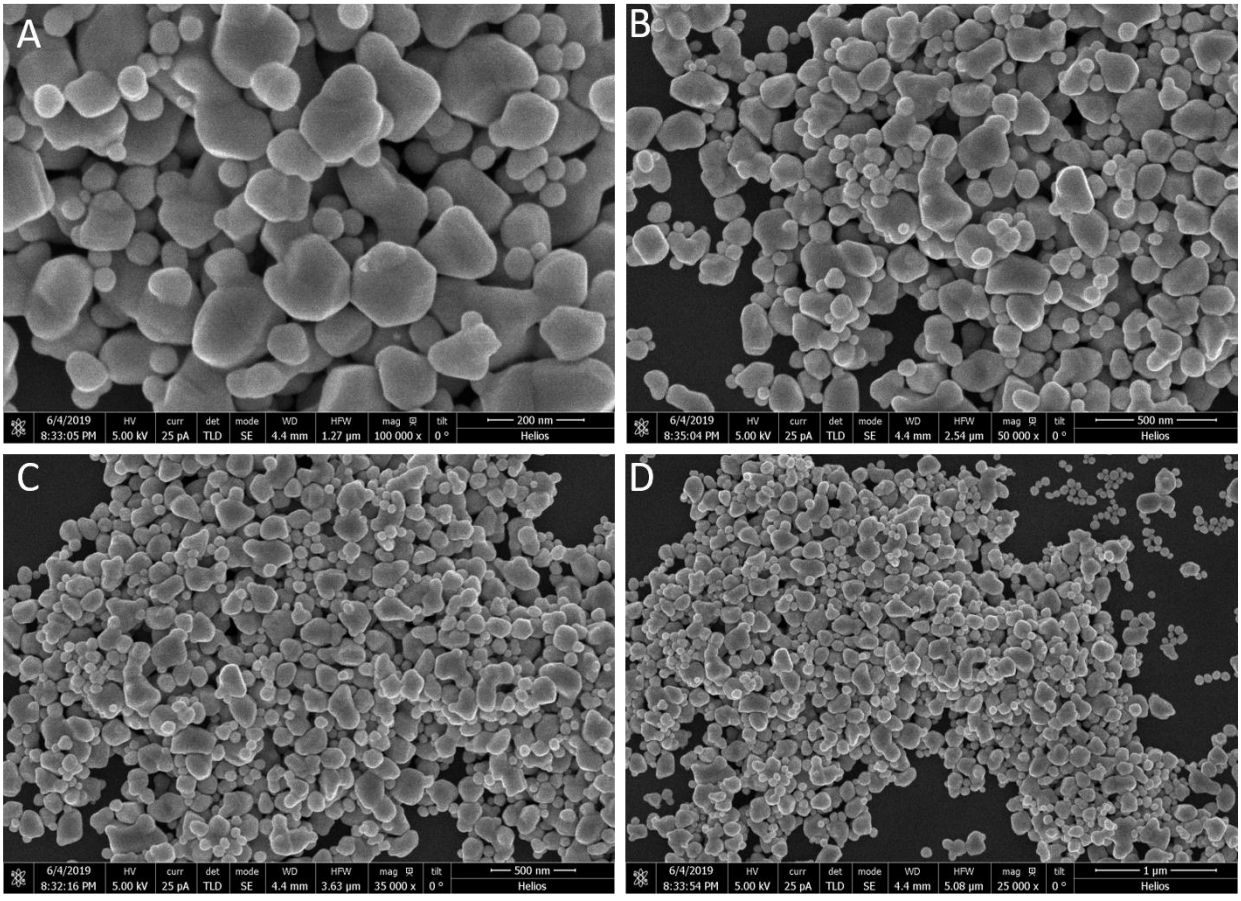

Supplementary Figure SZX. (A-D) Four Representative SEM images of Silver Nanostructures with Nanoparticle Geometry at Four Different Magnifications. The full reaction condition for the silver nanostructures shown in this Figure is provided in **Supplementary Table SZX** above.

Supplementary Table SZY: Silver Nanostructures with Nanorod Geometry. Reaction condition is provided here in this Table for the nanostructures shown in **Supplementary Figure SZY** below. Four different SEM images of the same reaction sample are shown in **Supplementary Figure SZY** below.

Geometry	**Nanorods**
Full Reaction Condition	Pure 1,3-Propanediol (5 mL) 0.15 M $AgNO_3$ (3mL) 0.35 M PVP-1,300,000 MW (3mL) 0.1M Ascorbic Acid (1 mL) Temp: 170°C
Note	Pure 1,3-propanediol was heated to 170 °C for 90 minutes followed by the dropwise addition of reactants within 7 minutes. The reaction ran for 60 minutes judging from the first addition of $AgNO_3$ to the reaction solution. The color of the solution was a greenish-grey at the end of the reaction.

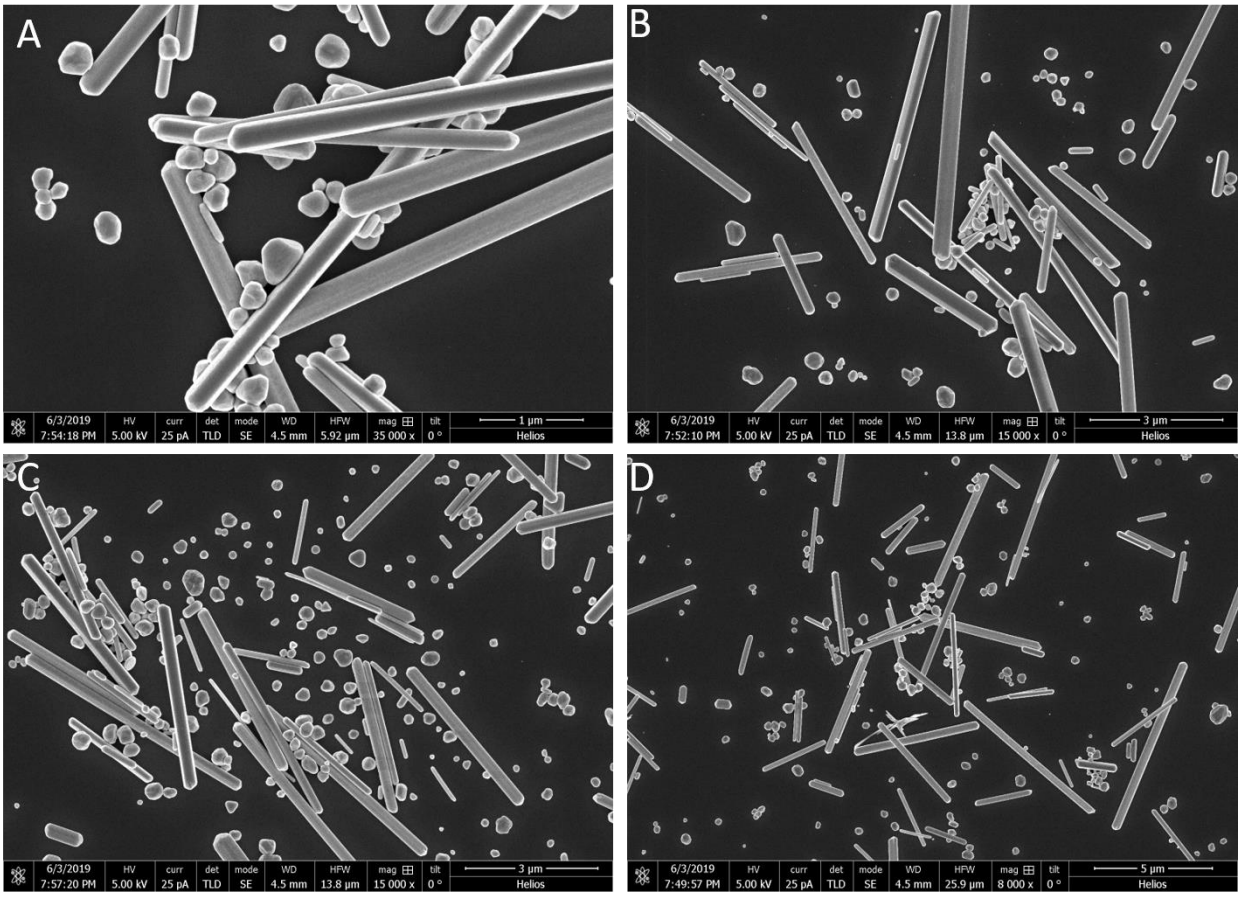

Supplementary Figure SZY. (A-D) Four Representative SEM images of Silver Nanostructures with Nanorod Geometry at Four Different Magnifications. The full reaction condition for the silver nanostructures shown in this Figure is provided in **Supplementary Table SZY** above.

Supplementary Table SZZ: Silver Nanostructures with Nanorod Geometry. Reaction condition is provided here in this Table for the nanostructures shown in **Supplementary Figure SZZ** below. Four different SEM images of the same reaction sample are shown in **Supplementary Figure SZZ** below.

Geometry	**Nanorods**
Full Reaction Condition	Pure 1,3-Propanediol (5 mL) 0.15 M $AgNO_3$ (3mL) 0.35 M PVP-360,000 MW (3mL) 0.1M 3-(N,N-Dimethylmyristylammonio)propanesulfonate (1 mL) Temp: 170°C
Note	Pure 1,3-propanediol was heated to 170 °C for 90 minutes followed by the dropwise addition of reactants within 7 minutes. The reaction ran for 60 minutes judging from the first addition of $AgNO_3$ to the reaction solution. The color of the solution was a yellowish grey at the end of the reaction.

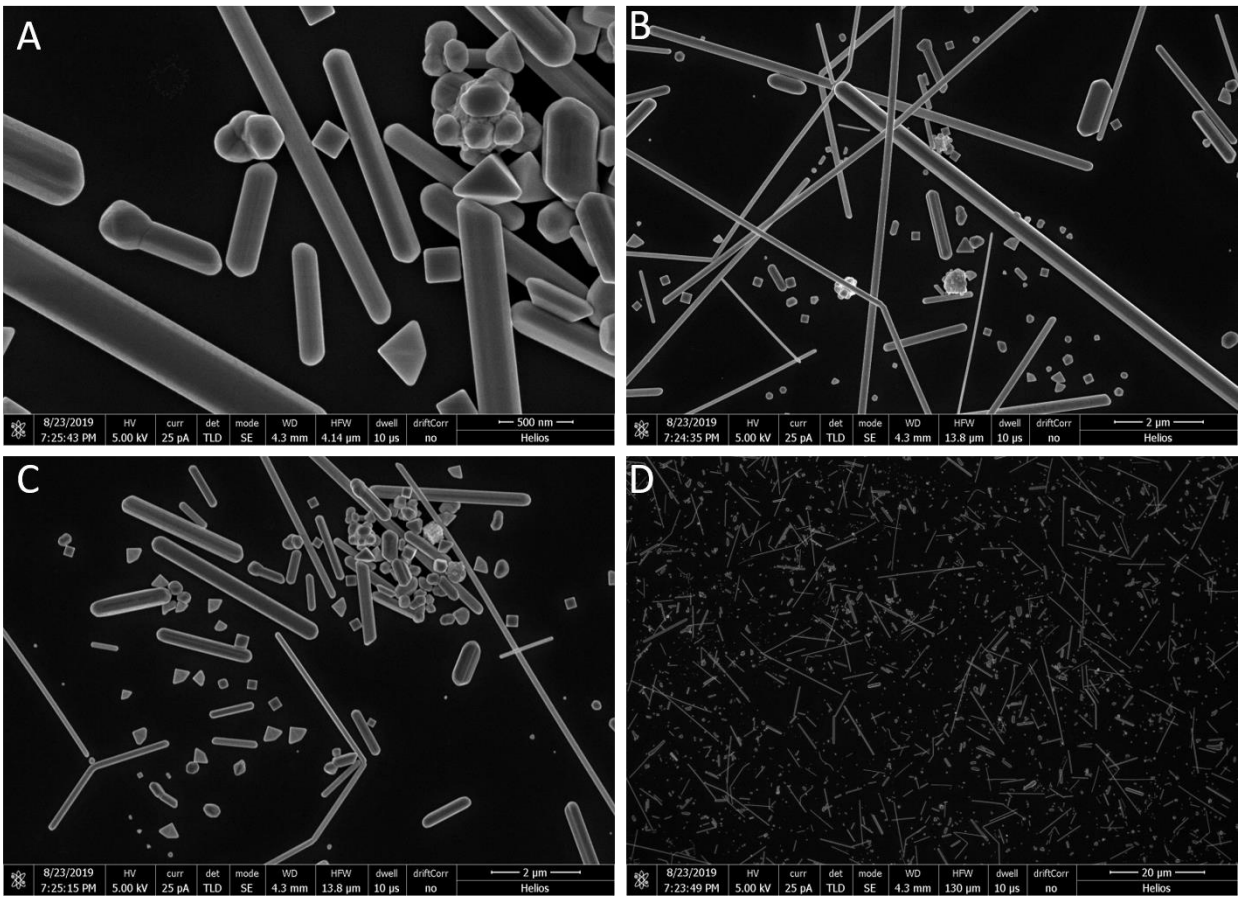

Supplementary Figure SZZ. (A-D) Four Representative SEM images of Silver Nanostructures with Nanorod Geometry at Four Different Magnifications. The full reaction condition for the silver nanostructures shown in this Figure is provided in **Supplementary Table SZZ** above.

Supplementary Table SZZA: Silver Nanostructures with Nanorod Geometry. Reaction condition is provided here in this Table for the nanostructures shown in **Supplementary Figure SZZA** below. Four different SEM images of the same reaction sample are shown in **Supplementary Figure SZZA** below.

Geometry	**Nanorods**
Full Reaction Condition	Pure 1,3-Propanediol (5 mL) 0.15 M $AgNO_3$ (3mL) 0.35 M PVP-360,000 MW (3mL) 0.1M 3-(N,N-Dimethylpalmitylammonio)propanesulfonate (1 mL) Temp: 170°C
Note	Pure 1,3-propanediol was heated to 170 °C for 90 minutes followed by the dropwise addition of reactants within 7 minutes. The reaction ran for 60 minutes judging from the first addition of $AgNO_3$ to the reaction solution. The color of the solution was a yellowish grey at the end of the reaction.

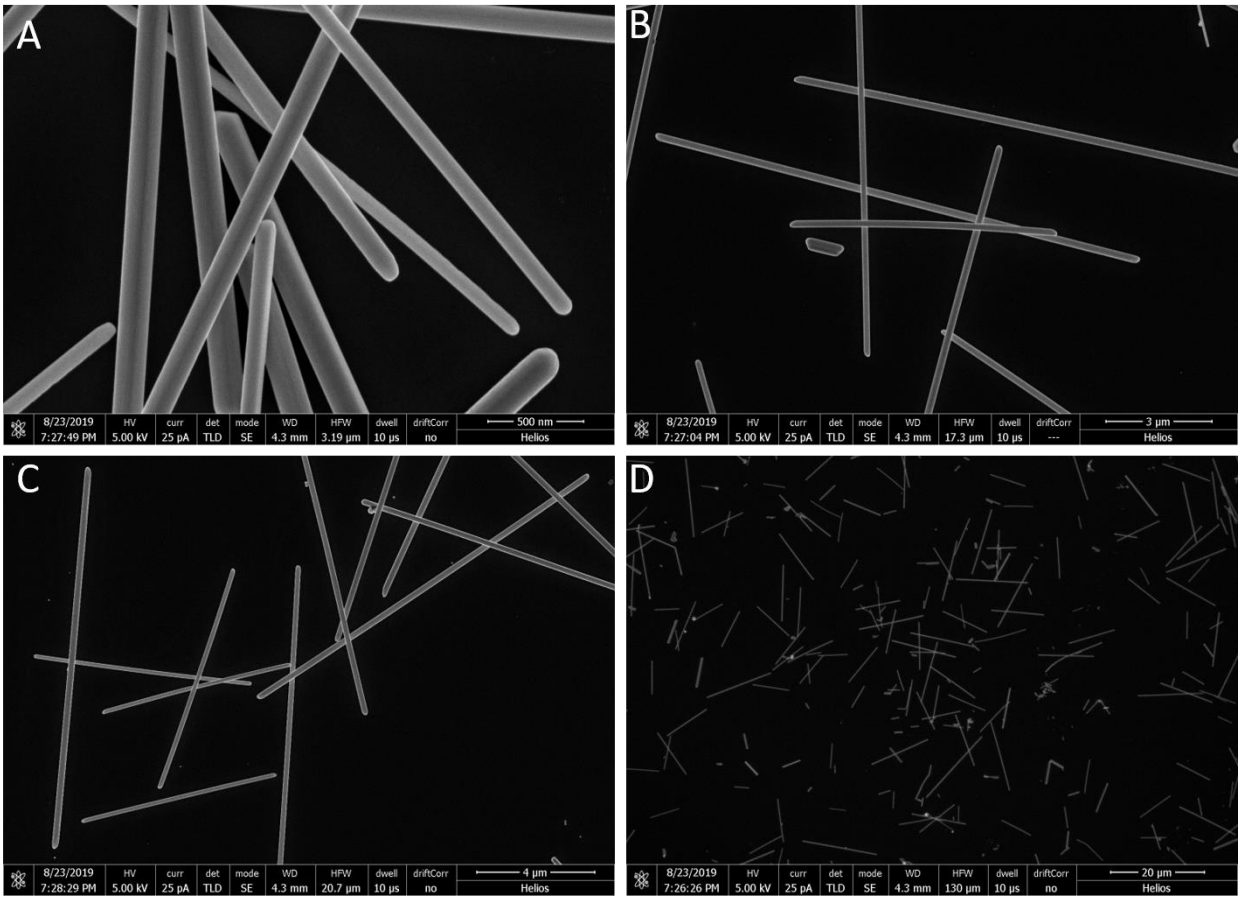

Supplementary Figure SZZA. (A-D) Four Representative SEM images of Silver Nanostructures with Nanorod Geometry at Four Different Magnifications. The full reaction condition for the silver nanostructures shown in this Figure is provided in **Supplementary Table SZZA** above.

Supplementary Table SZZB: Silver Nanostructures with Nanorod Geometry. Reaction condition is provided here in this Table for the nanostructures shown in **Supplementary Figure SZZB** below. Four different SEM images of the same reaction sample are shown in **Supplementary Figure SZZB** below.

Geometry	**Nanorods**
Full Reaction Condition	Pure 1,3-Propanediol (5 mL) 0.15 M $AgNO_3$ (3mL) 0.35 M PVP-360,000 MW (3mL) 0.1M Sodium dodecylbenzenesulfonate (1 mL) Temp: 170°C
Note	Pure 1,3-propanediol was heated to 170 °C for 90 minutes followed by the dropwise addition of reactants within 7 minutes. The reaction ran for 60 minutes judging from the first addition of $AgNO_3$ to the reaction solution. The color of the solution was a greenish-grey at the end of the reaction.

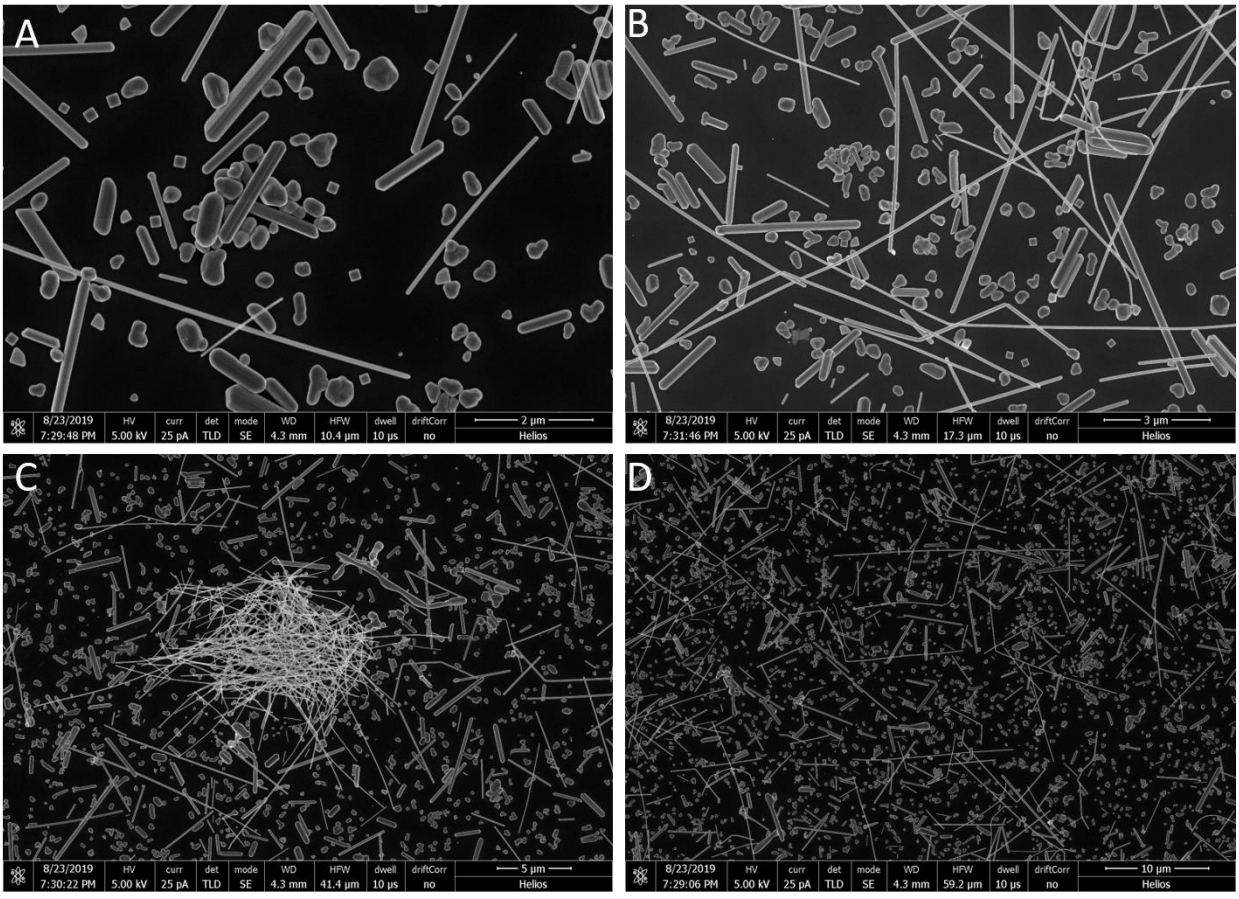

Supplementary Figure SZZB. (A-D) Four Representative SEM images of Silver Nanostructures with Nanorod Geometry at Four Different Magnifications. The full reaction condition for the silver nanostructures shown in this Figure is provided in **Supplementary Table SZZB** above.

Supplementary Table SZZC: Silver Nanostructures with Mixed Geometry. Reaction condition is provided here in this Table for the nanostructures shown in **Supplementary Figure SZZC** below. Four different SEM images of the same reaction sample are shown in **Supplementary Figure SZZC** below.

Geometry	**Mixed**
Full Reaction Condition	Pure 1,3-Propanediol (5 mL) 0.15 M $AgNO_3$ (3mL) 0.35 M PVP-360,000 MW (3mL) 0.1M Sodium 3-mercapto-1-propanesulfonate (1 mL) Temp: 170°C
Note	Pure 1,3-propanediol was heated to 170 °C for 90 minutes followed by the dropwise addition of reactants within 7 minutes. The reaction ran for 60 minutes judging from the first addition of $AgNO_3$ to the reaction solution. The color of the solution was a yellowish grey at the end of the reaction.

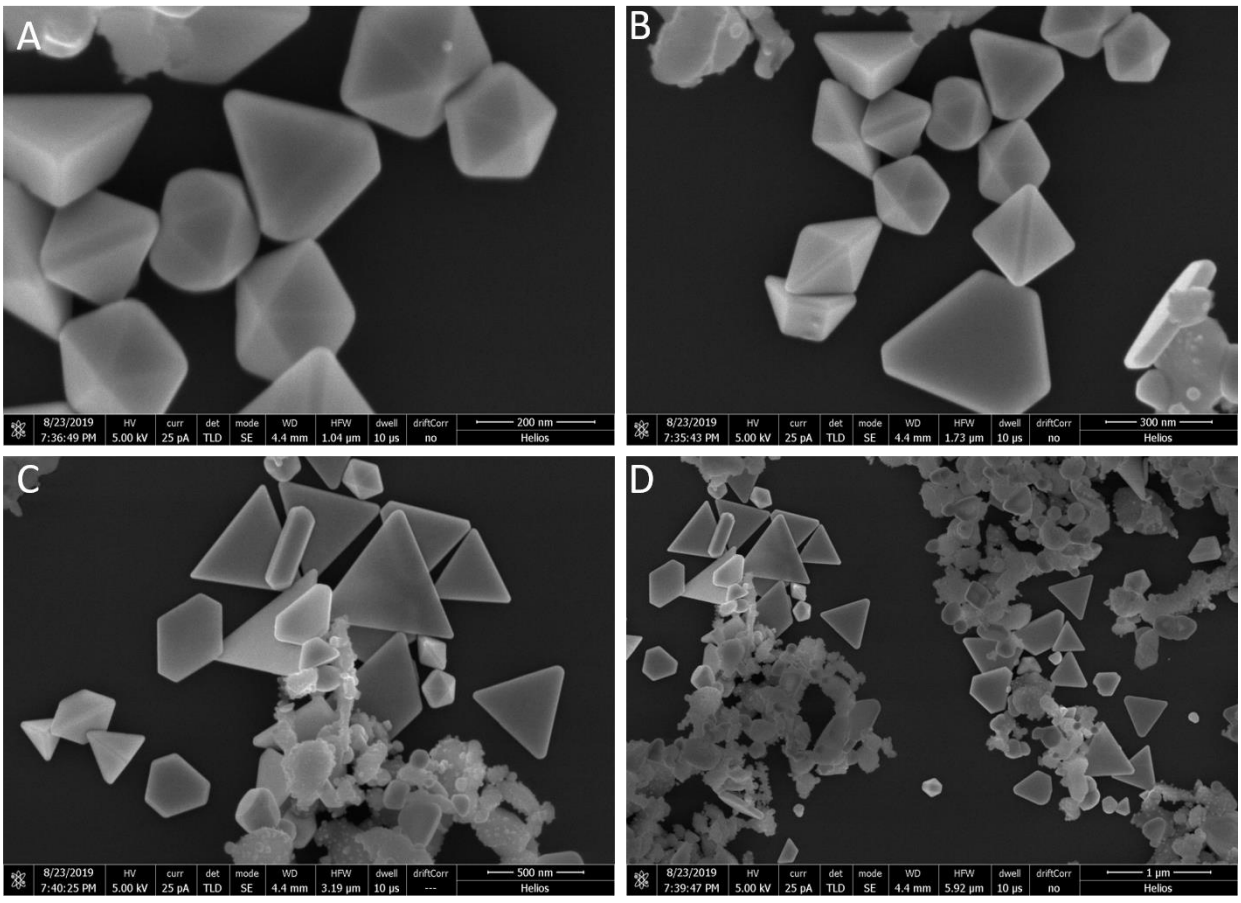

Supplementary Figure SZZC. (A-D) Four Representative SEM images of Silver Nanostructures with mixed Geometry at Four Different Magnifications. The full reaction condition for the silver nanostructures shown in this Figure is provided in **Supplementary Table SZZC** above.

Supplementary Table SZZD: Silver Nanostructures with Nanorod nanocube Geometry. Reaction condition is provided here in this Table for the nanostructures shown in **Supplementary Figure SZZD** below. Four different SEM images of the same reaction sample are shown in **Supplementary Figure SZZD** below.

Geometry	**Nanorods and nanocubes**
Full Reaction Condition	Pure 1,3-Propanediol (5 mL) 0.12 M $AgNO_3$ (3mL) 0.35 M PVP-1,300,000 MW (3mL) 0.02M Sucrose (1 mL) Temp: 170°C
Note	Pure 1,3-propanediol was heated to 170 °C for 90 minutes followed by the dropwise addition of reactants within 7 minutes. The reaction ran for 60 minutes judging from the first addition of $AgNO_3$ to the reaction solution. The color of the solution was a yellowish grey at the end of the reaction.

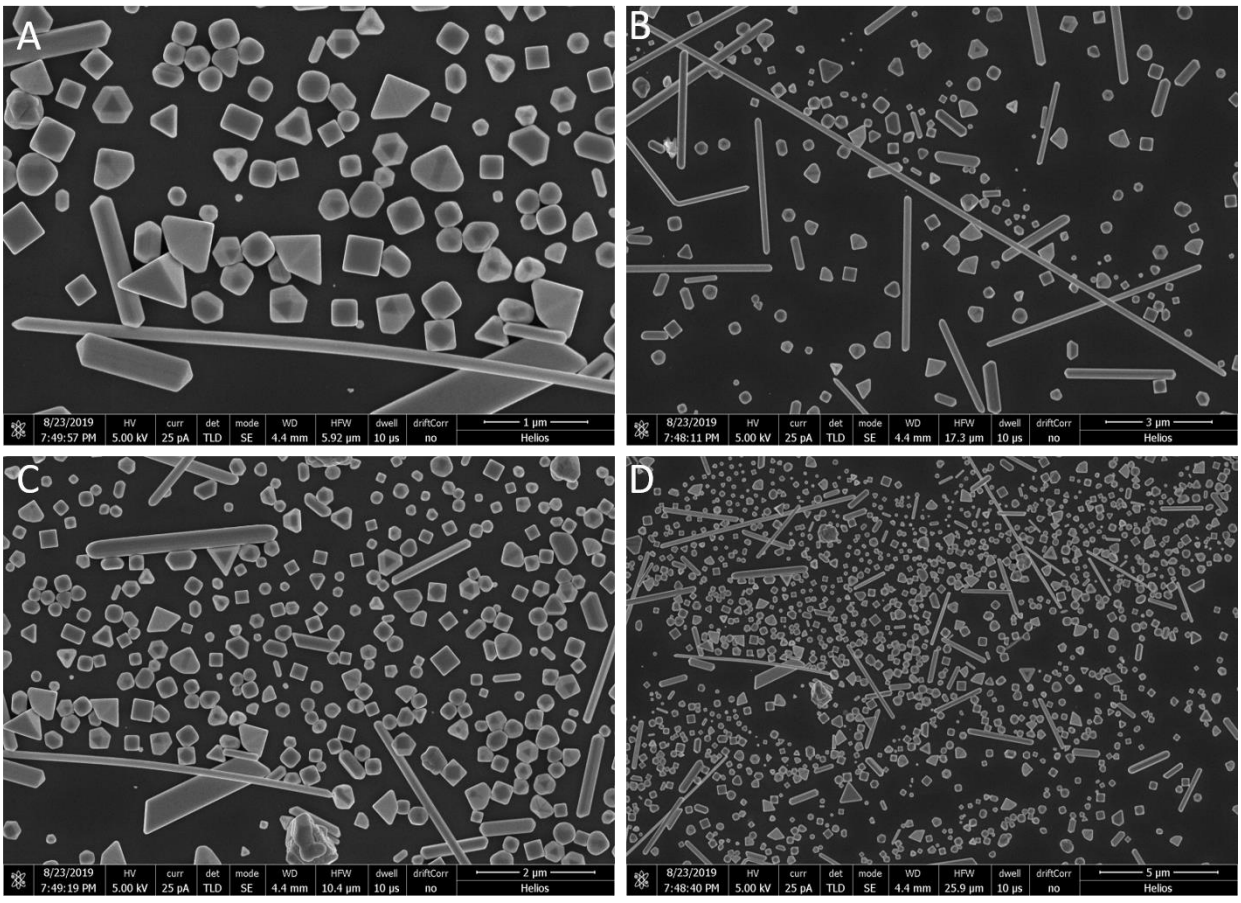

Supplementary Figure SZZD. (A-D) Four Representative SEM images of Silver Nanostructures with Nanorod and nanocube Geometry at Four Different Magnifications. The full reaction condition for the silver nanostructures shown in this Figure is provided in **Supplementary Table SZZD** above.

Supplementary Table SZZE: Silver Nanostructures with Nanorod Geometry. Reaction condition is provided here in this Table for the nanostructures shown in **Supplementary Figure SZZE** below. Four different SEM images of the same reaction sample are shown in **Supplementary Figure SZZE** below.

Geometry	**Nanorods**
Full Reaction Condition	Pure 1,3-Propanediol (5 mL) 0.12 M $AgNO_3$ (3mL) 0.25 M PVP-1,300,000 MW (3mL) 0.02M Sucrose (1 mL) Temp: 170°C
Note	Pure 1,3-propanediol was heated to 170 °C for 90 minutes followed by the dropwise addition of reactants within 7 minutes. The reaction ran for 60 minutes judging from the first addition of $AgNO_3$ to the reaction solution. The color of the solution was a yellowish grey at the end of the reaction.

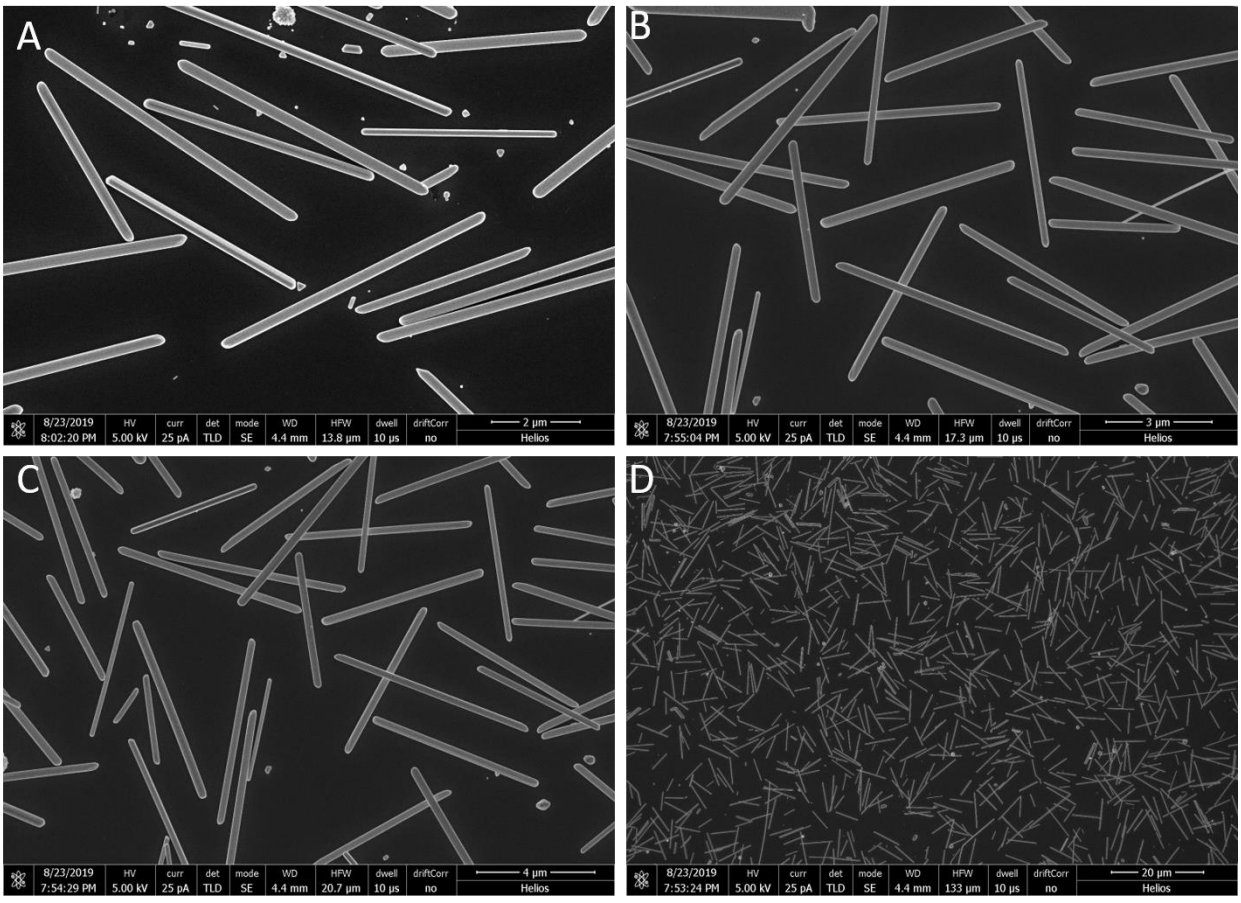

Supplementary Figure SZZE. (A-D) Four Representative SEM images of Silver Nanostructures with Nanorod Geometry at Four Different Magnifications. The full reaction condition for the silver nanostructures shown in this Figure is provided in **Supplementary Table SZZE** above.

Supplementary Table SZZF: Silver Nanostructures with Nanorod and nanocubes Geometry. Reaction condition is provided here in this Table for the nanostructures shown in **Supplementary Figure SZZF** below. Four different SEM images of the same reaction sample are shown in **Supplementary Figure SZZF** below.

Geometry	**Nanorods and Nanocubes**
Full Reaction Condition	Pure 1,3-Propanediol (5 mL) 0.12 M $AgNO_3$ (3mL) 0.15 M PVP-1,300,000 MW (3mL) 0.02M Sucrose (1 mL) Temp: 170°C
Note	Pure 1,3-propanediol was heated to 170 °C for 90 minutes followed by the dropwise addition of reactants within 7 minutes. The reaction ran for 60 minutes judging from the first addition of $AgNO_3$ to the reaction solution. The color of the solution was a yellowish grey at the end of the reaction.

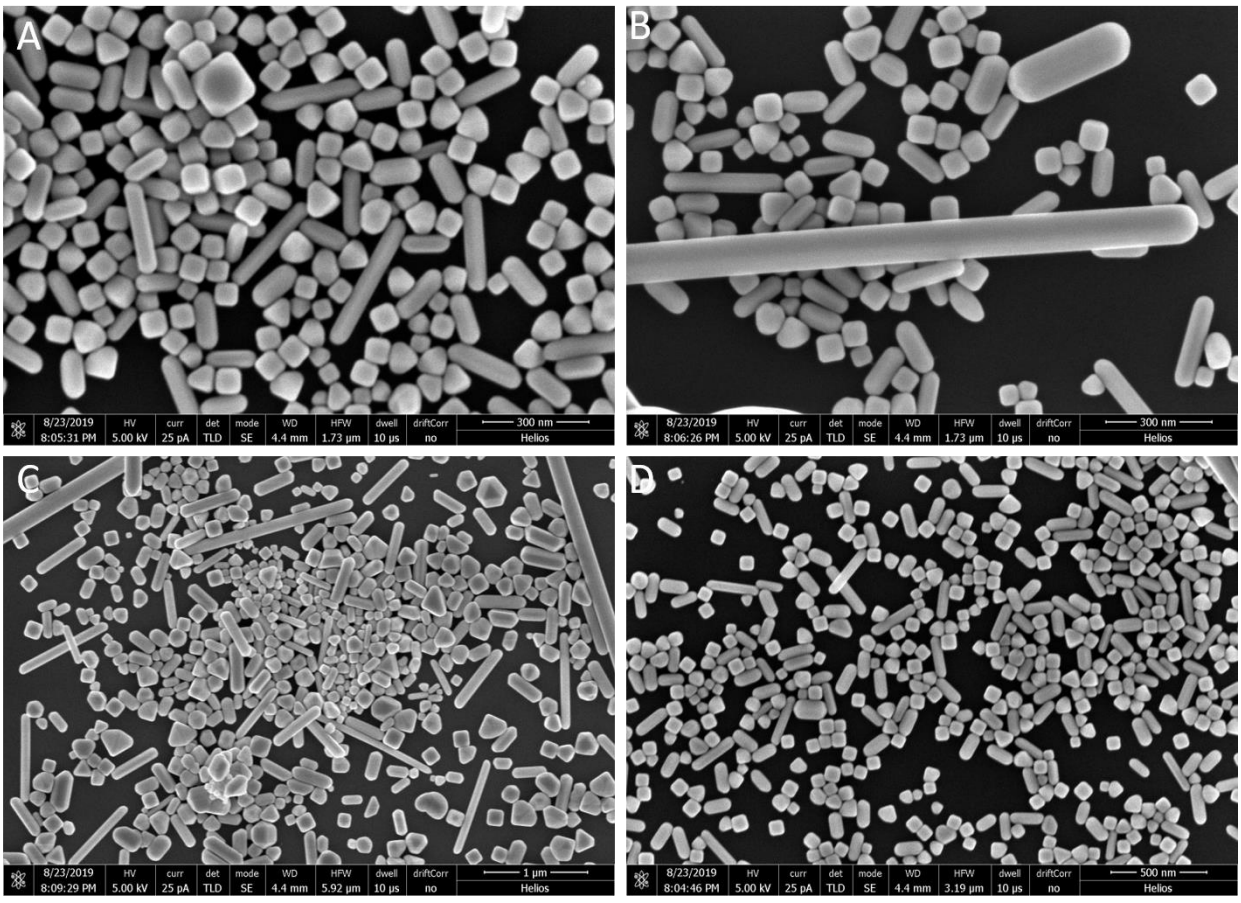

Supplementary Figure SZZF. (A-D) Four Representative SEM images of Silver Nanostructures with Nanorod and nanocubes Geometry at Four Different Magnifications. The full reaction condition for the silver nanostructures shown in this Figure is provided in **Supplementary Table SZZF** above.

Supplementary Table SZZG: Silver Nanostructures with Nanorod Geometry. Reaction condition is provided here in this Table for the nanostructures shown in **Supplementary Figure SZZG** below. Four different SEM images of the same reaction sample are shown in **Supplementary Figure SZZG** below.

Geometry	**Nanorods**
Full Reaction Condition	Pure 1,3-Propanediol (5 mL) 0.12 M $AgNO_3$ (3mL) 0.45 M PVP-1,300,000 MW (3mL) 0.02M Sucrose (1 mL) Temp: 170°C
Note	Pure 1,3-propanediol was heated to 170 °C for 90 minutes followed by the dropwise addition of reactants within 7 minutes. The reaction ran for 60 minutes judging from the first addition of $AgNO_3$ to the reaction solution. The color of the solution was a yellowish grey at the end of the reaction.

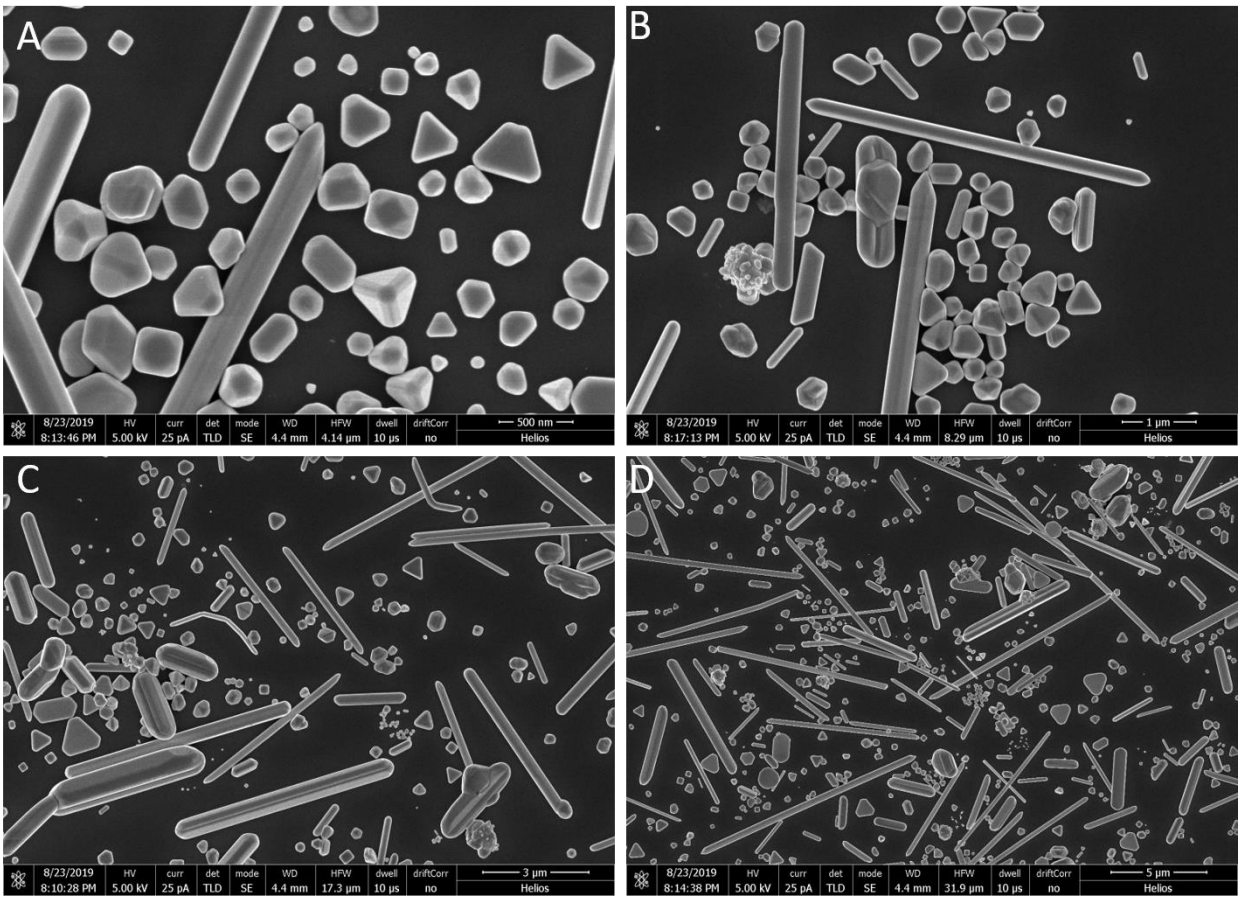

Supplementary Figure SZZG. (A-D) Four Representative SEM images of Silver Nanostructures with Nanorod Geometry at Four Different Magnifications. The full reaction condition for the silver nanostructures shown in this Figure is provided in **Supplementary Table SZZG** above.

Supplementary Table SZZH: Silver Nanostructures with Nanorod Geometry. Reaction condition is provided here in this Table for the nanostructures shown in **Supplementary Figure SZZH** below. Four different SEM images of the same reaction sample are shown in **Supplementary Figure SZZH** below.

Geometry	**Nanorods**
Full Reaction Condition	Pure 1,3-Propanediol (5 mL) 0.15 M $AgNO_3$ (3mL) 0.15 M PVP-1,300,000 MW (3mL) 0.02M Sucrose (1 mL) Temp: 170°C
Note	Pure 1,3-propanediol was heated to 170 °C for 90 minutes followed by the dropwise addition of reactants within 7 minutes. The reaction ran for 60 minutes judging from the first addition of $AgNO_3$ to the reaction solution. The color of the solution was a yellowish grey at the end of the reaction.

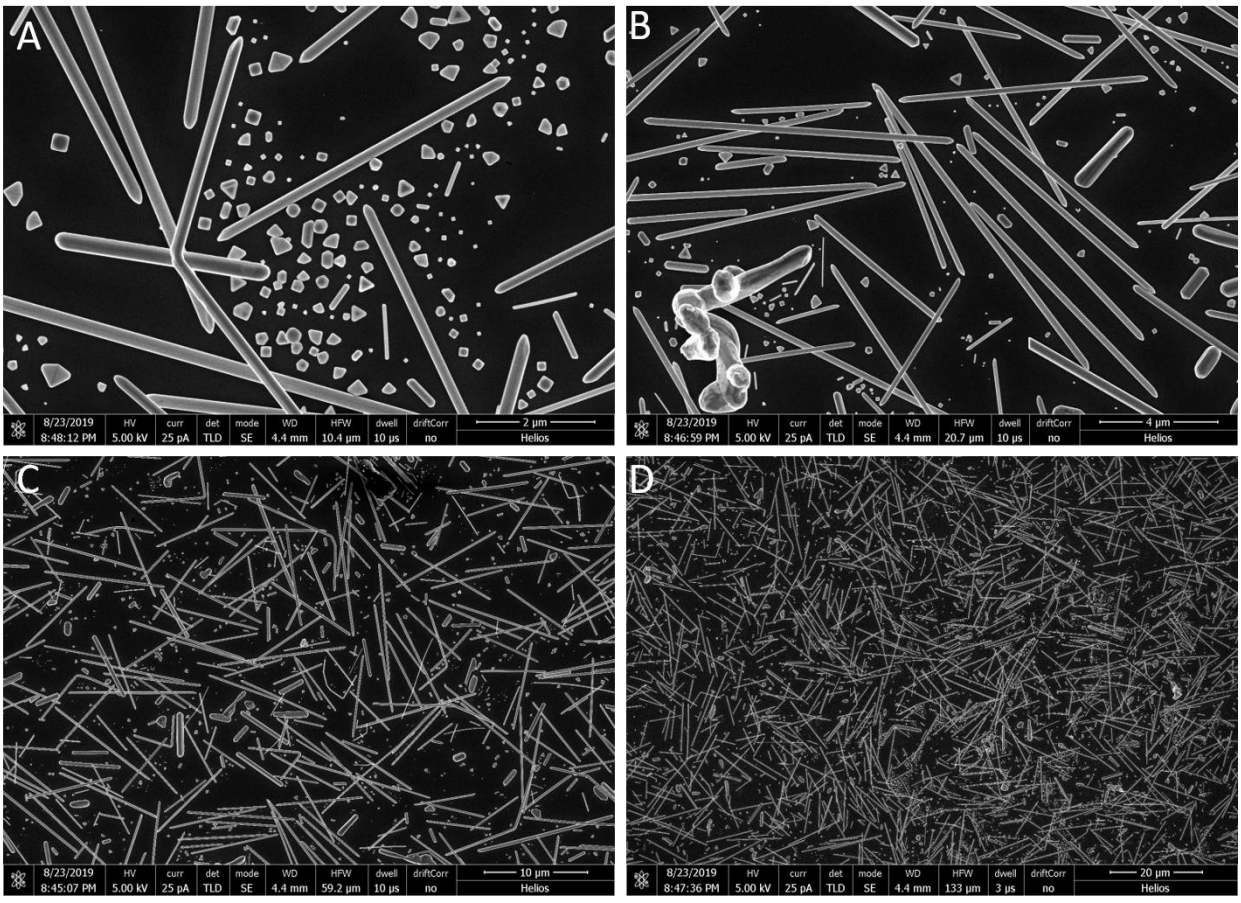

Supplementary Figure SZZH. (A-D) Four Representative SEM images of Silver Nanostructures with Nanorod Geometry at Four Different Magnifications. The full reaction condition for the silver nanostructures shown in this Figure is provided in **Supplementary Table SZZH** above.

Supplementary Table SZZI: Silver Nanostructures with Nanorod Geometry. Reaction condition is provided here in this Table for the nanostructures shown in **Supplementary Figure SZZI** below. Two different SEM images of the same reaction sample are shown in **Supplementary Figure SZZI** below.

Geometry	**Nanorods**
Full Reaction Condition	Pure 1,3-Propanediol (5 mL) 0.15 M $AgNO_3$ (3mL) 0.25 M PVP-1,300,000 MW (3mL) 0.02M Sucrose (1 mL) Temp: 170°C
Note	Pure 1,3-propanediol was heated to 170 °C for 90 minutes followed by the dropwise addition of reactants within 7 minutes. The reaction ran for 60 minutes judging from the first addition of $AgNO_3$ to the reaction solution. The color of the solution was a yellowish grey at the end of the reaction.

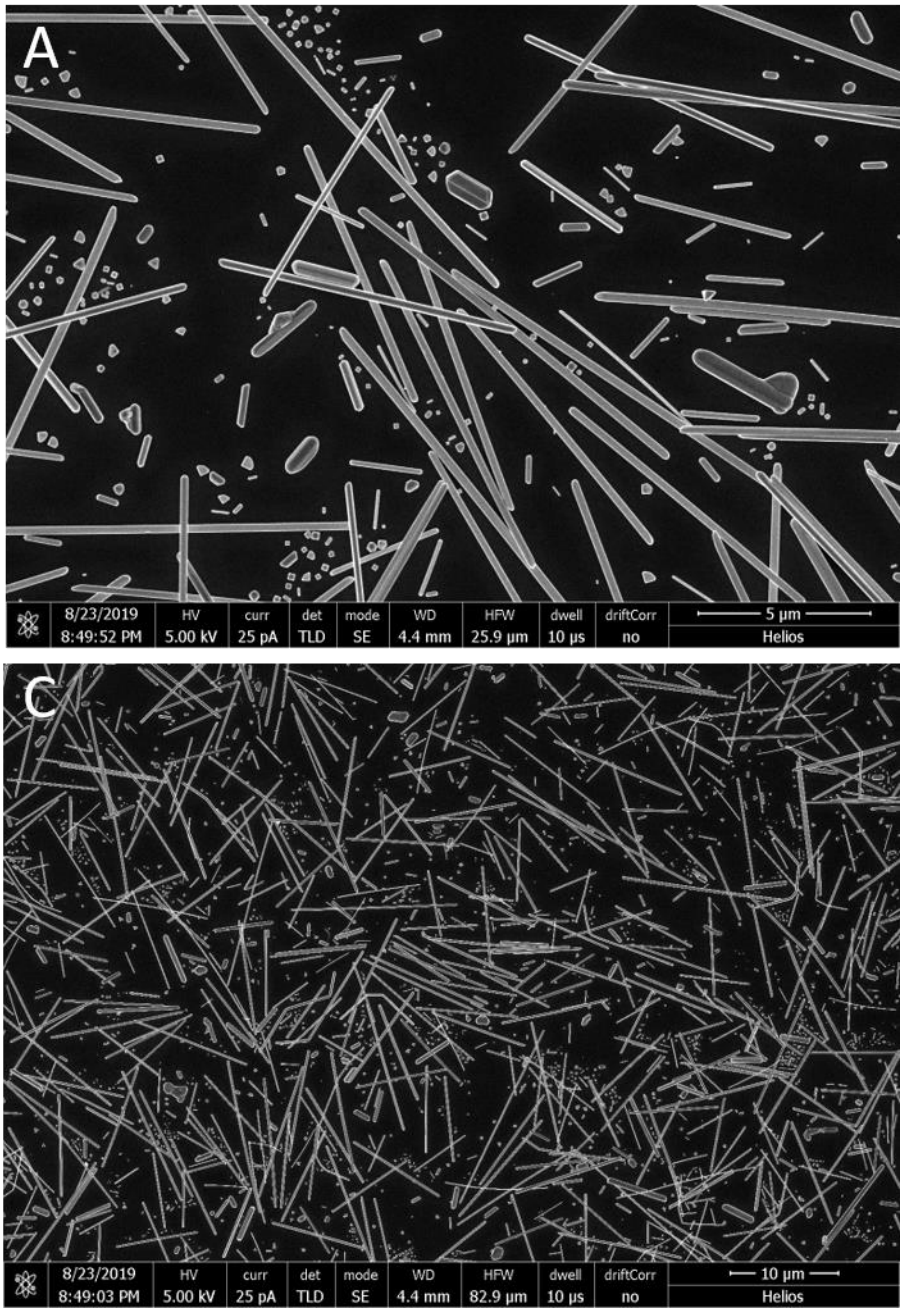

Supplementary Figure SZZI. Two Representative SEM images of Silver Nanostructures with Nanorod Geometry at Two Different Magnifications. The full reaction condition for the silver nanostructures shown in this Figure is provided in **Supplementary Table SZZI** above.

Supplementary Table SZZJ: Silver Nanostructures with Nanorod Geometry. Reaction condition is provided here in this Table for the nanostructures shown in **Supplementary Figure SZZJ** below. Four different SEM images of the same reaction sample are shown in **Supplementary Figure SZZJ** below.

Geometry	**Nanorods**
Full Reaction Condition	Pure 1,3-Propanediol (5 mL) 0.15 M $AgNO_3$ (3mL) 0.35 M PVP-1,300,000 MW (3mL) 0.02M Sucrose (1 mL) Temp: 170°C
Note	Pure 1,3-propanediol was heated to 170 °C for 90 minutes followed by the dropwise addition of reactants within 7 minutes. The reaction ran for 60 minutes judging from the first addition of $AgNO_3$ to the reaction solution. The color of the solution was a yellowish grey at the end of the reaction.

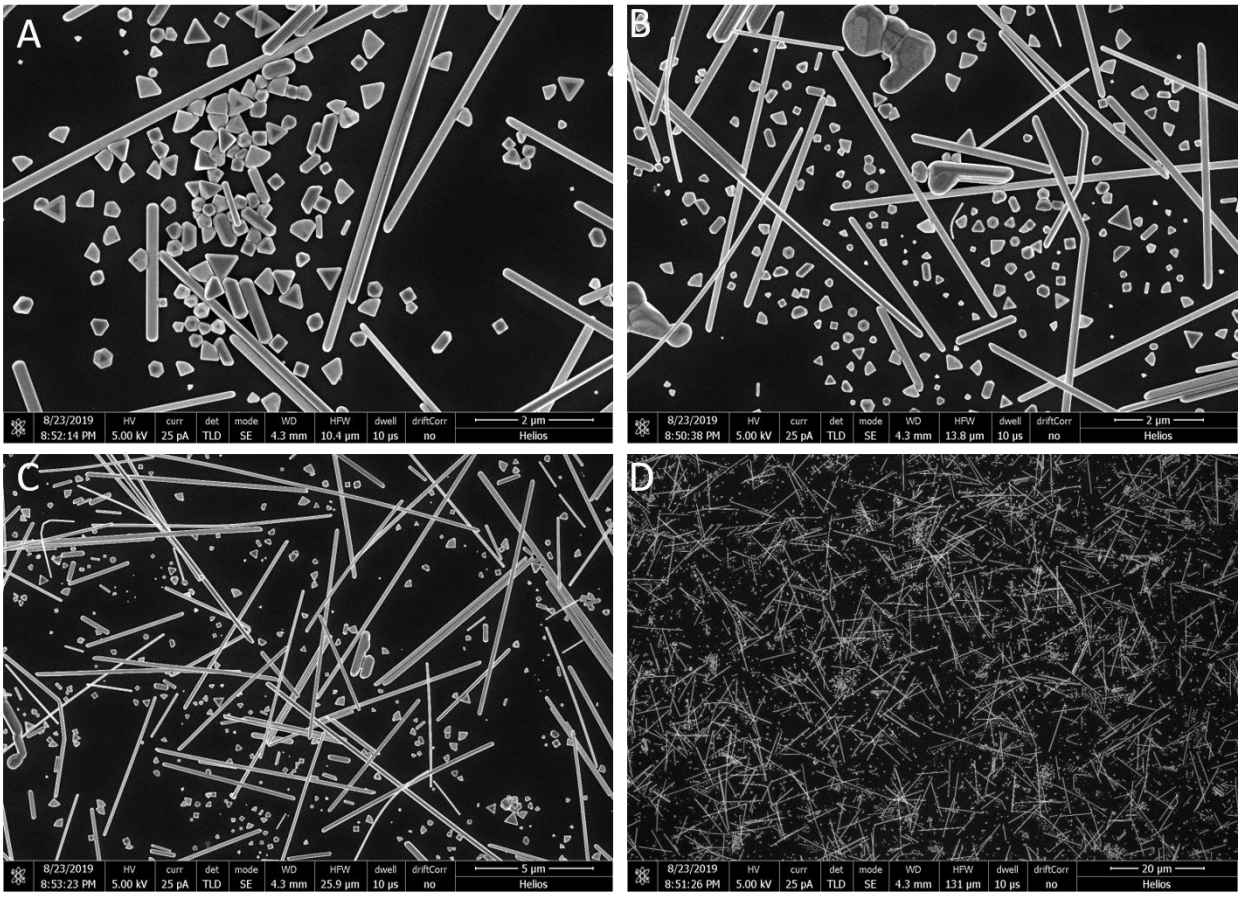

Supplementary Figure SZZJ. (A-D) Four Representative SEM images of Silver Nanostructures with Nanorod Geometry at Four Different Magnifications. The full reaction condition for the silver nanostructures shown in this Figure is provided in **Supplementary Table SZZJ** above.

Supplementary Table SZZK: Silver Nanostructures with Nanorod Geometry. Reaction condition is provided here in this Table for the nanostructures shown in **Supplementary Figure SZZK** below. Four different SEM images of the same reaction sample are shown in **Supplementary Figure SZZK** below.

Geometry	**Nanorods**
Full Reaction Condition	Pure 1,3-Propanediol (5 mL) 0.15 M $AgNO_3$ (3mL) 0.15 M PVP-1,300,000 MW (3mL) 0.02M Sucrose (1 mL) Temp: 170°C
Note	Pure 1,3-propanediol was heated to 170 °C for 90 minutes followed by the dropwise addition of reactants within 7 minutes. The reaction ran for 60 minutes judging from the first addition of $AgNO_3$ to the reaction solution. The color of the solution was a yellowish grey at the end of the reaction.

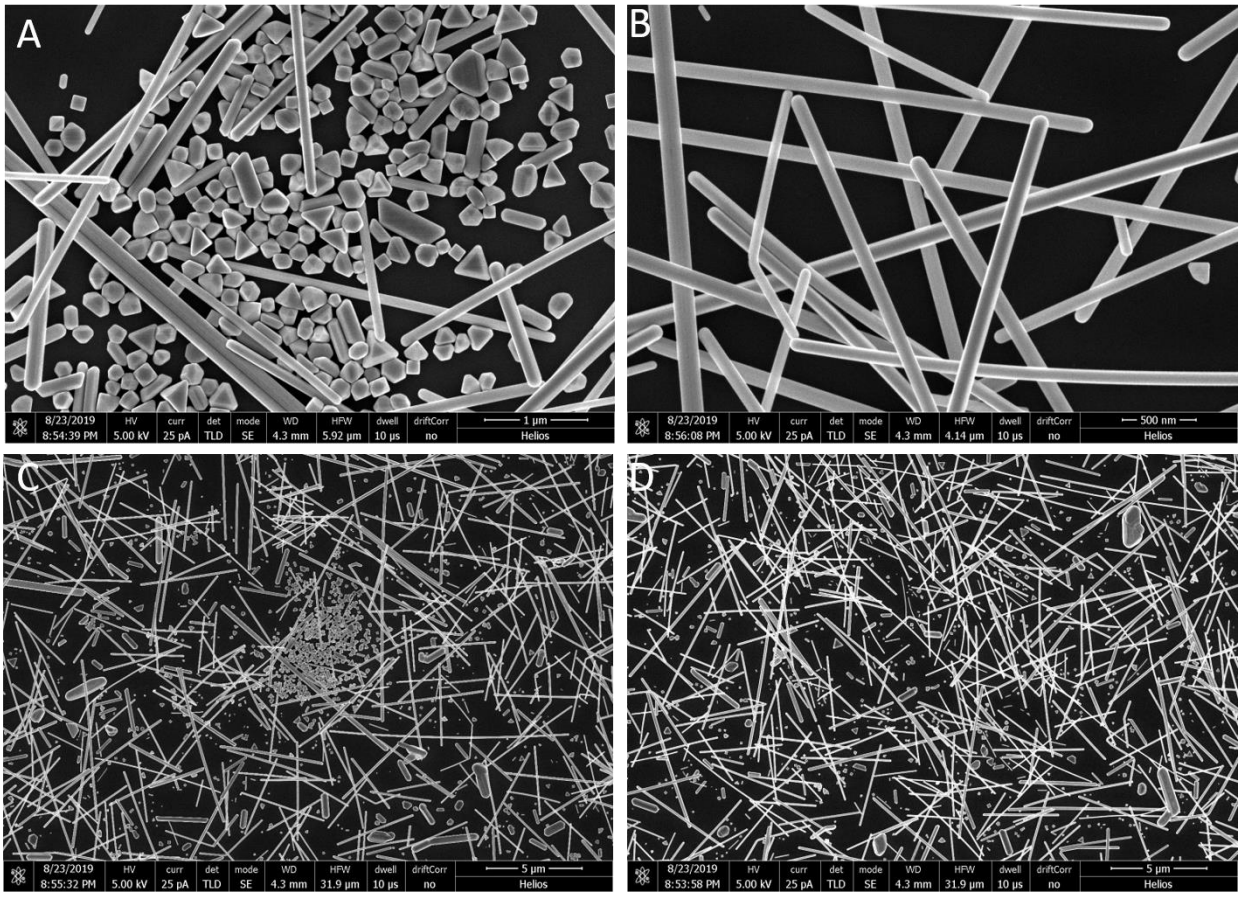

Supplementary Figure SZZK. (A-D) Four Representative SEM images of Silver Nanostructures with Nanorod Geometry at Four Different Magnifications. The full reaction condition for the silver nanostructures shown in this Figure is provided in **Supplementary Table SZZK** above.

Supplementary Table SZZL: Silver Nanostructures with Nanorod Geometry. Reaction condition is provided here in this Table for the nanostructures shown in **Supplementary Figure SZZL** below. Four different SEM images of the same reaction sample are shown in **Supplementary Figure SZZL** below.

Geometry	**Nanorods**
Full Reaction Condition	Pure 1,3-Propanediol (5 mL) 0.2 M $AgNO_3$ (3mL) 0.15 M PVP-1,300,000 MW (3mL) 0.02M Sucrose (1 mL) Temp: 170°C
Note	Pure 1,3-propanediol was heated to 170 °C for 90 minutes followed by the dropwise addition of reactants within 7 minutes. The reaction ran for 60 minutes judging from the first addition of $AgNO_3$ to the reaction solution. The color of the solution was a yellowish grey at the end of the reaction.

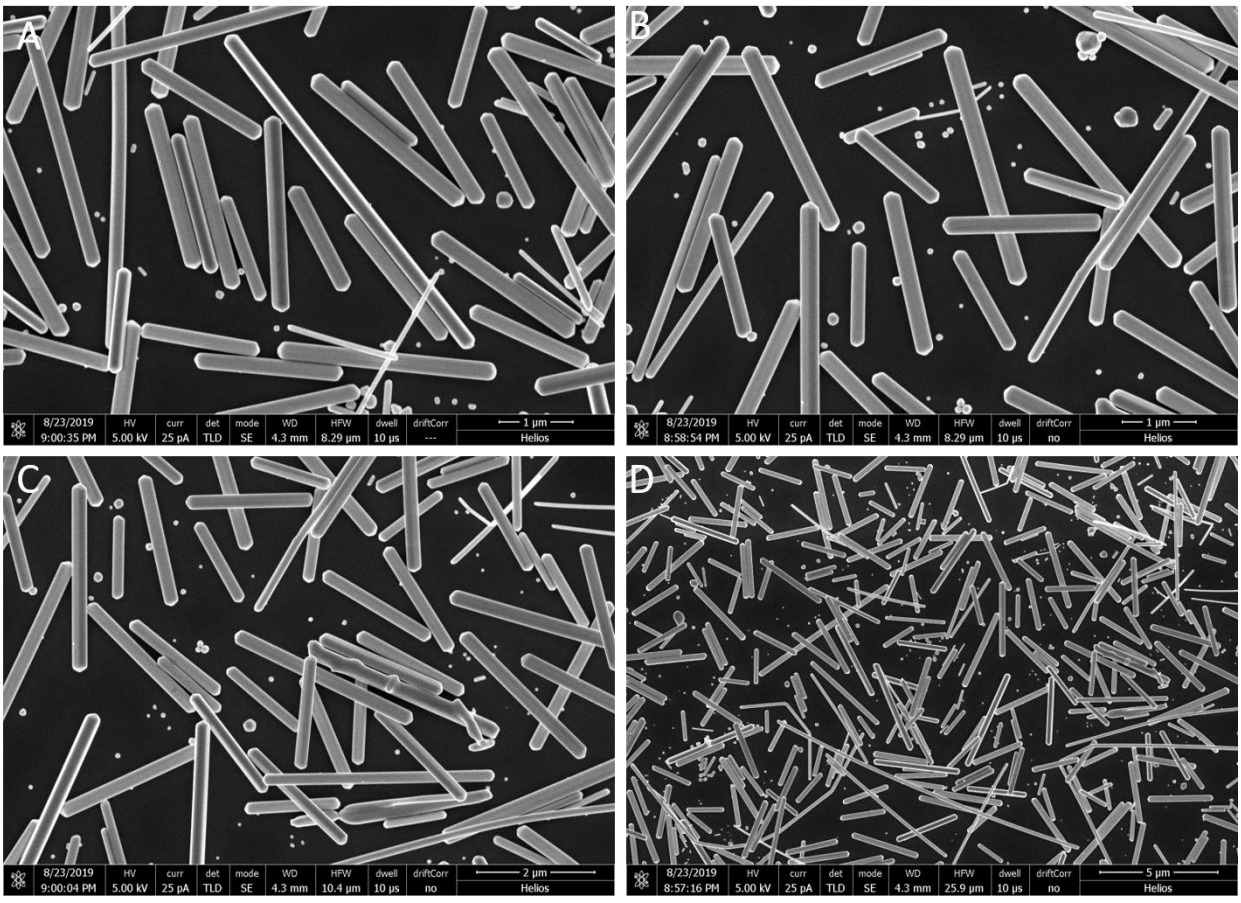

Supplementary Figure SZZL. (A-D) Four Representative SEM images of Silver Nanostructures with Nanorod Geometry at Four Different Magnifications. The full reaction condition for the silver nanostructures shown in this Figure is provided in **Supplementary Table SZZL** above.

Supplementary Table SZZM: Silver Nanostructures with Nanorod and nanocubes Geometry. Reaction condition is provided here in this Table for the nanostructures shown in **Supplementary Figure SZZM** below. Four different SEM images of the same reaction sample are shown in **Supplementary Figure SZZM** below.

Geometry	**Nanocubes and nanorods**
Full Reaction Condition	Pure 1,3-Propanediol (5 mL) 0.2 M $AgNO_3$ (3mL) 0.25 M PVP-1,300,000 MW (3mL) 0.02M Sucrose (1 mL) Temp: 170°C
Note	Pure 1,3-propanediol was heated to 170 °C for 90 minutes followed by the dropwise addition of reactants within 7 minutes. The reaction ran for 60 minutes judging from the first addition of $AgNO_3$ to the reaction solution. The color of the solution was a yellowish grey at the end of the reaction.

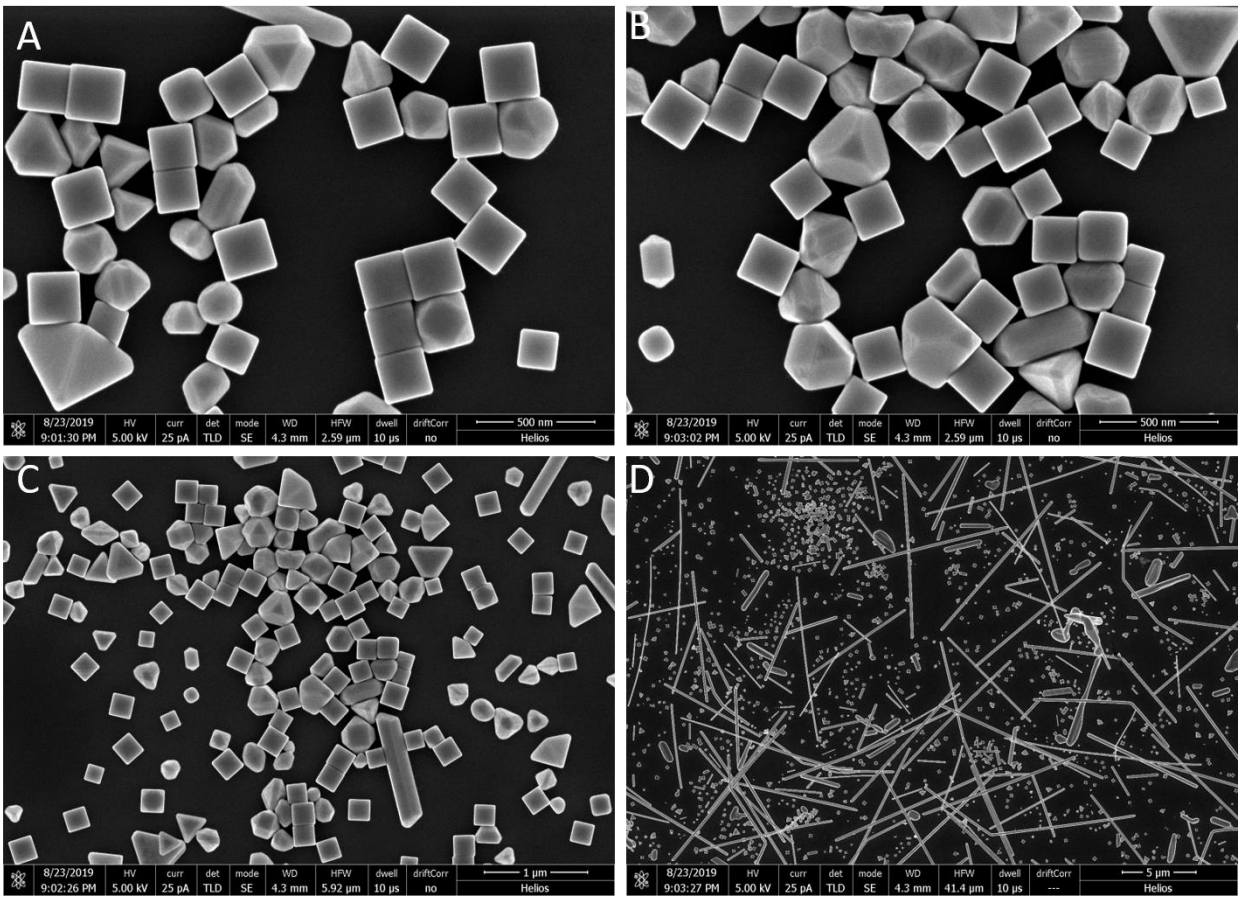

Supplementary Figure SZZM. (A-D) Four Representative SEM images of Silver Nanostructures with Nanorod and nanocube Geometry at Four Different Magnifications. The full reaction condition for the silver nanostructures shown in this Figure is provided in **Supplementary Table SZZM** above.

Supplementary Table SZZN: Silver Nanostructures with Nanorod Geometry. Reaction condition is provided here in this Table for the nanostructures shown in **Supplementary Figure SZZN** below. Two different SEM images of the same reaction sample are shown in **Supplementary Figure SZZN** below.

Geometry	**Nanorods**
Full Reaction Condition	Pure 1,3-Propanediol (5 mL) 0.2 M $AgNO_3$ (3mL) 0.35 M PVP-1,300,000 MW (3mL) 0.02M Sucrose (1 mL) Temp: 170°C
Note	Pure 1,3-propanediol was heated to 170 °C for 90 minutes followed by the dropwise addition of reactants within 7 minutes. The reaction ran for 60 minutes judging from the first addition of $AgNO_3$ to the reaction solution. The color of the solution was a yellowish grey at the end of the reaction.

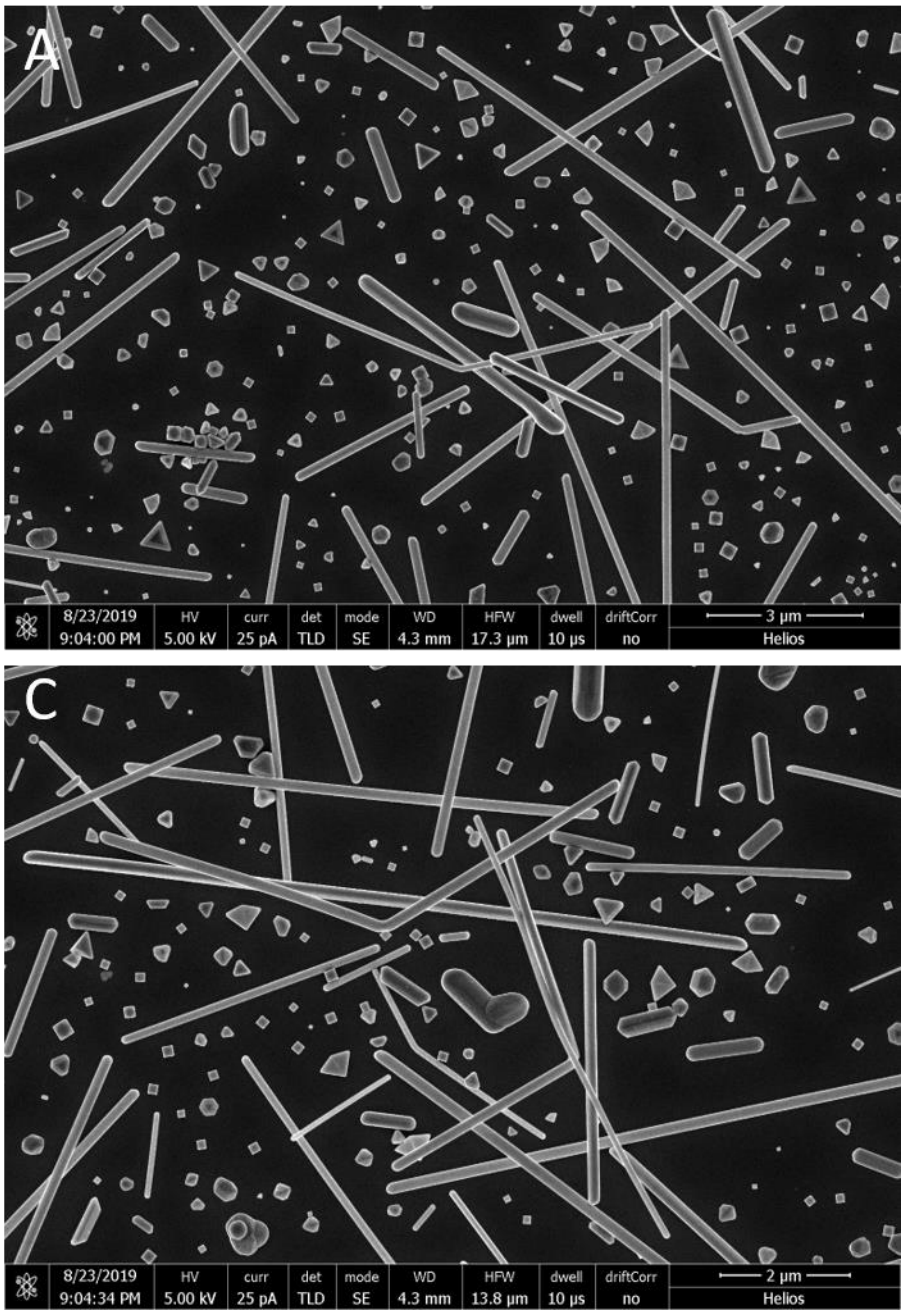

Supplementary Figure SZZN. Two Representative SEM images of Silver Nanostructures with Nanorod Geometry at Two Different Magnifications. The full reaction condition for the silver nanostructures shown in this Figure is provided in **Supplementary Table SZZN** above.

Supplementary Table SZZO: Silver Nanostructures with Nanorod Geometry. Reaction condition is provided here in this Table for the nanostructures shown in **Supplementary Figure SZZO** below. A representative SEM image of the same reaction sample is shown in **Supplementary Figure SZZO** below.

Geometry	**Nanorods**
Full Reaction Condition	Pure 1,3-Propanediol (5 mL) 0.2 M $AgNO_3$ (3mL) 0.45 M PVP-1,300,000 MW (3mL) 0.02M Sucrose (1 mL) Temp: 170°C
Note	Pure 1,3-propanediol was heated to 170 °C for 90 minutes followed by the dropwise addition of reactants within 7 minutes. The reaction ran for 60 minutes judging from the first addition of $AgNO_3$ to the reaction solution. The color of the solution was a yellowish grey at the end of the reaction.

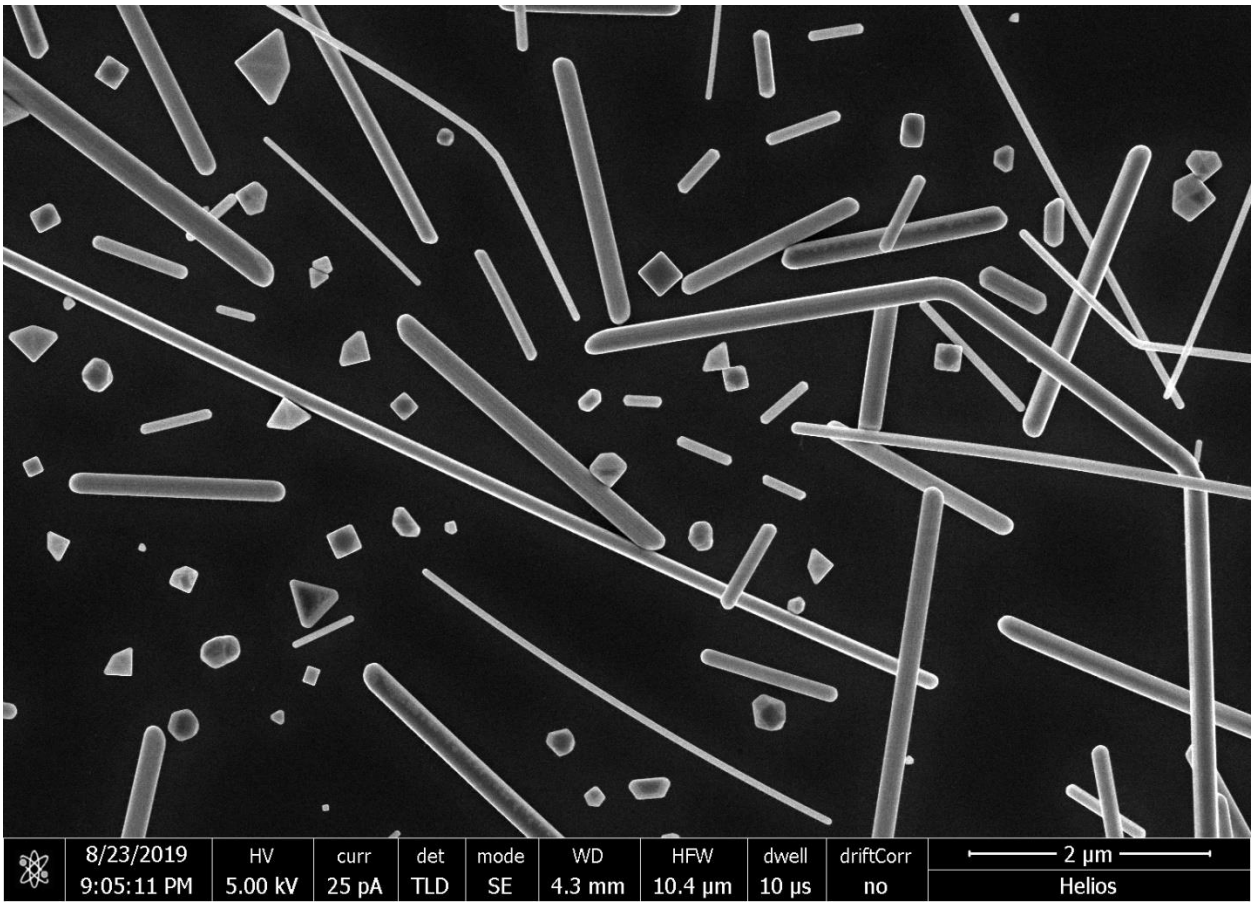

Supplementary Figure SZZO. A representative SEM image of Silver Nanostructures with Nanorod Geometry. The full reaction condition for the silver nanostructures shown in this Figure is provided in **Supplementary Table SZZO** above.

6. Plasmonic Building-block Geometries: *Nanostructure's Surface Charge by Zeta Potential Measurements*

Characterization: *Zeta Potential*

Interfacial agents on the surface of metallic nanostructures help to stabilize the nanostructures against agglomeration in the solution.[3,4] The presence of interfacial agents such as surfactants, polyelectrolytes, or charged ligands promotes interfacial interactions that drive the assembly of nanoparticles into structures with different properties. The surface charge of different nanostructures was measured herein using a Zetasizer Malvern instrument (Zetasizer Nano Series: Nano ZS). For the measurement, 1/20 dilutions of silver nanostructures were filled into the zeta potential cell (Malvern: DTS1070) and measured at room temperature with 1/100 runs over three repeated measurement cycles. All silver nanostructures show a negative charge on the surface. In general, PVP is a non-ionic polymer. However, in solution, a keto-enol transformation may occur that presents the outer negative charge surface of the nanostructure.[1]

Here, representative samples are shown with their obtained zeta potential value. The number (from P-136-A to P-140-F) indicates the experiment number.

Supplementary Table S28: Zeta potential measurements of silver nanostructures.

(Sample Name) Silver Nanostructures	**Measured Zeta Potential**
P-136-A (Rods)	-13.6 mV ± 4.1 mV
P-136-B (Cubes)	-11.8 mV ± 2.6 mV
P-136-C (Particles)	-12.9 mV ± 5.6 mV
P-134-A (Bars)	-10.4 mV ± 3.2 mV
P-134-B (Rods)	-28.5 mV ± 4 mV
P-134-C (Cubes)	-21.4 mV ± 7.2 mV
P-140-D (Particles)	-11.1 mV ± 3.8 mV
P-140-E (Cubes)	-20.6 mV ± 5.2 mV
P-140-F (Rods)	-14.2 mV ± 4.9 mV

7. Plasmonic Building-block Surface Characteristics: *Nanostructure's Layer-By-Layer Surface Modification*

The zeta potential of the as-synthesized silver nanorods *via* 1,3-propanediol-based polyol synthesis is -13.6 mV ± 4.1 mV. A positively charged poly(diallyldimethyl ammonium chloride) (polyDADMAC) has been applied, therefore, electrostatically on the surface of negatively-charged silver nanorods. After electrostatic interaction within 15 minutes of room temperature stirring, the obtained zeta potential of the nanostructures was +78 mV. Similarly, a negatively charged polystyrene sodium sulfonate (PSSS) layer was successfully applied as a second layer. The zeta potential value after the successful interaction with PSSS has obtained -48 mV. A third layer has been applied again with polyDADMAC and the zeta potential of the final layer was +65 mV (**Supplementary Figure S38)**.

Specifically, for the model layer-by-layer surface modification process, 0.8% cationic poly(diallyldimethylammoniumbromide) (polyDADMAC) (average Mw 200,000-350,000, Sigma-Aldrich) was applied on the as-synthesized negatively charged silver nanorods (measured zeta potential -13.6 mV ± 1.8 mV). The zeta potential value after the modification with polyDADMAC was obtained +78mV ± 7mV. Similarly, the second and third layers were applied by 0.4% anionic poly(styrene sodium sulfonate) (PSSS) (average Mw ~1,000,000, Sigma-Aldrich) and 0.8% cationic polyDADMAC (average Mw 400,000-500,000, Sigma Aldrich), respectively. The zeta potential after the second and third layer modification was obtained as -48mV ± 4.8mV and +65mV ± 6mV, respectively.

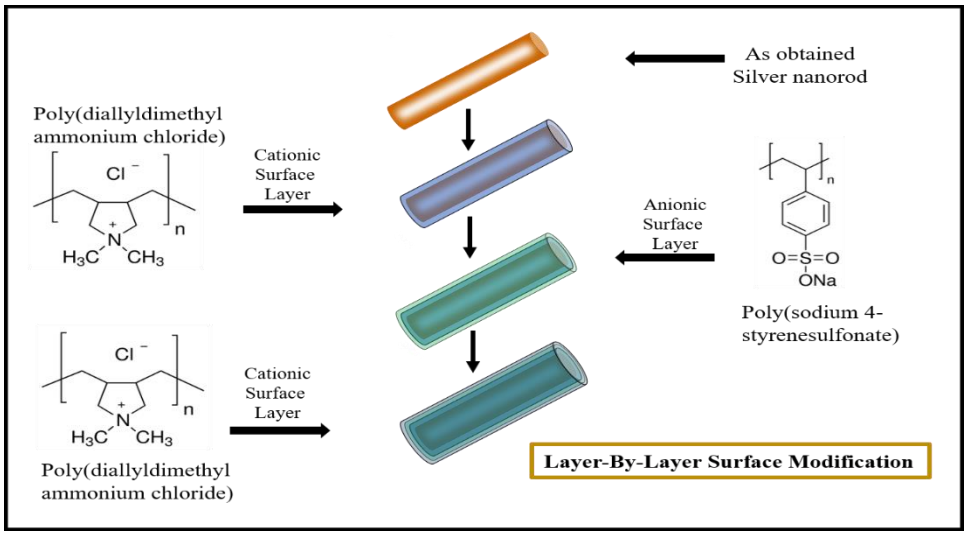

Supplementary Figure S38: Layer-by-layer (LBL) surface modification of the silver rods *via* alternatively charged polyelectrolytes. A schematic drawing for the layer-by-layer surface functionalization of the silver nanostructures *via* oppositely charged polyelectrolytes (cationic poly(diallyldimethylammonium chloride) and anionic poly(sodium 4-styrenesulfonate)).

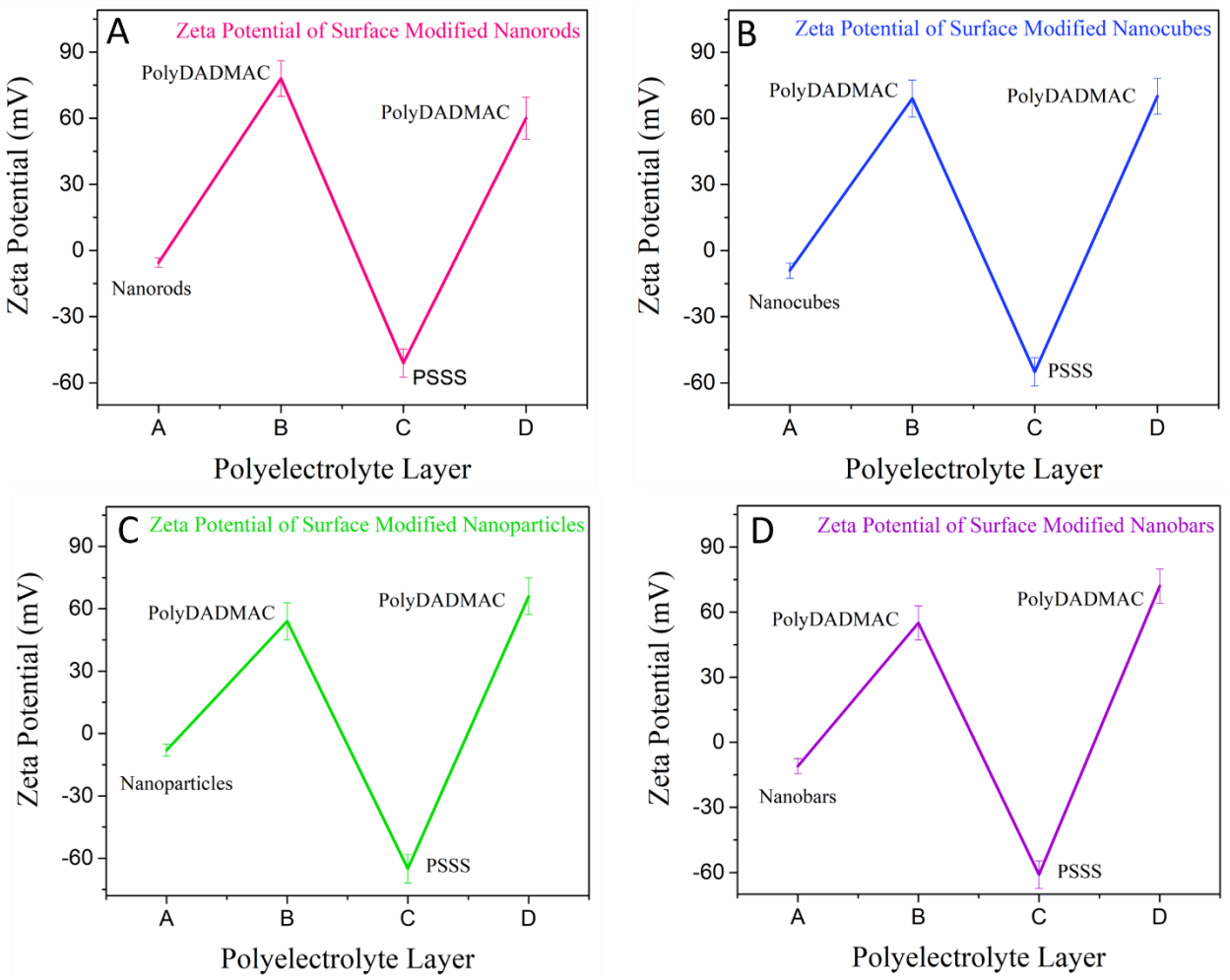

Supplementary Figure S39: Surface charge measurements of the silver nanostructures after layer-by-layer (LBL) surface modification *via* alternatively charged polyelectrolytes. (A-D) Three layers of cationic poly(diallydimethyl ammonium chloride) (polyDADMAC), anionic polystyrene sodium sulfonate (PSSS), and cationic polyDADMAC polyelectrolytes were applied on the surface of the silver nanostructures (A) nanorods, (B) nanocubes, (C) nanobars, and (D) nanoparticles after repeatedly washing and centrifuging the samples.

9. Solution-based Plasmonic Nanoassembling: *Showcasing Metal-Metal Electrostatic Nanoassembling*

Overview: Plasmon-plasmon nanoassemblies—coupled systems of metal nanoparticles—are promising for their remarkable efficiency in sensing, optoelectronics, and catalysis applications.[9-14] Random coagulation is a significant challenge during the formation of plasmonic nanoassemblies because the strong attraction between oppositely charged plasmonic nanoparticles causes rapid aggregation. Precise control over the structure and interface of the nanoparticles can address the issue of uncontrolled aggregation.

Our Finding: A synthetic approach was applied for plasmonic nanoassembling aimed at fulfilling four key conditions; (1) controllable surface-charge, (2) specific surface functionalities, (3) homogeneous reaction environment for nanoparticle interactions, and (4) well-defined ratio of nanoparticle suspension. We observed that the surface modification of silver nanostructures with poly(acrylamide-co-diallyl dimethyl ammonium chloride) was crucial for highly controlled interactions with citrate-stabilized gold nanoparticles to form silver-gold assembling nanostructures. For sensing applications, the requirement is to have a roughened surface (present high surface area) and a ligand-free metallic surface (for direct interaction with analytes). For creating a ligand-free surface, we applied a metal-catalyzed metal deposition approach where silver-gold nanoassembling structures allow the deposition of a free silver layer at the surface. These structures are metal-rich, ligand-free, and have roughened surfaces with large numbers of hotspots (a basic requirement for potential SERS sensing application).

In general, we applied the electrostatic interfacial interaction approach for binding the negatively charged gold nanoparticles on the surface-modified silver nanostructures. We observed that the efficient uptakes of the incoming guest nanoparticles (gold nanoparticles) on the surface of host silver nanostructures can be realized when the silver nanostructures were modified with poly(acrylamide-co-diallyl dimethyl ammonium chloride).

Method: For a model electrostatic plasmonic assemblies, primarily, silver nanorods (prepared via 1,3-propanediol mediated polyol synthesis as explained in **Supplementary Section 2**) have been functionalized with 0.8 % cationic poly(acrylamide-co-diallyldimethylammonium chloride) (poly(AAm-co-DADMAC)) by adding 1 mL poly(AAm-co-DADMAC) to 150 µL of silver nanorods dispersion at room temperature under stirring. Afterward, three repeated washing cycles were applied with ultrapure water to remove the unreacted polyelectrolyte molecules, and finally, nanorods were re-dispersed in pure water. For silver-gold nanoassembling, gold nanoparticles were prepared following the synthesis protocol from ref[15]. Briefly, 20 ml of 1.2 mM of gold chloride (99%, Sigma-Aldrich) were heated at boiling temperature, and subsequently, 2 ml of 1% trisodium citrate dihydrate (>99%, Sigma-Aldrich) were added to the boiling gold chloride solution. Within two minutes, the color has been changed from light yellow to dark red indicating the formation of gold nanoparticles. Later, freshly prepared citrate-capped anionic gold nanoparticles were mixed with poly(AAm-co-DADMAC)-functionalized silver nanorods under the stirring condition in a 1:2 (silver:gold) solution ratio. The ratio of the silver rods to gold nanoparticles can be varied in order to obtain the variable density of the gold nanoparticles on the surface of silver rods. Because of the strong surface charge, the solution changed its color to dark purple immediately upon the addition of gold nanoparticles indicating the successful assembling reaction. After the silver-gold assembling, an additional metal layer was deposited on its surface to obtain a ligand-free metal surface useful for potential catalysis and sensing applications. Initially, 150 µL 0.1 M ascorbic acid solution was added to 100 µL dispersion of silver-gold nanoassembly, and then 150 µL $AgNO_3$ solution has been added under a strong stirring condition at room temperature. Upon deposition of the metal layer, the color becomes dark brown (reaction time is less than 10 seconds). For all the experiments, all chemicals were used as received without further purification.

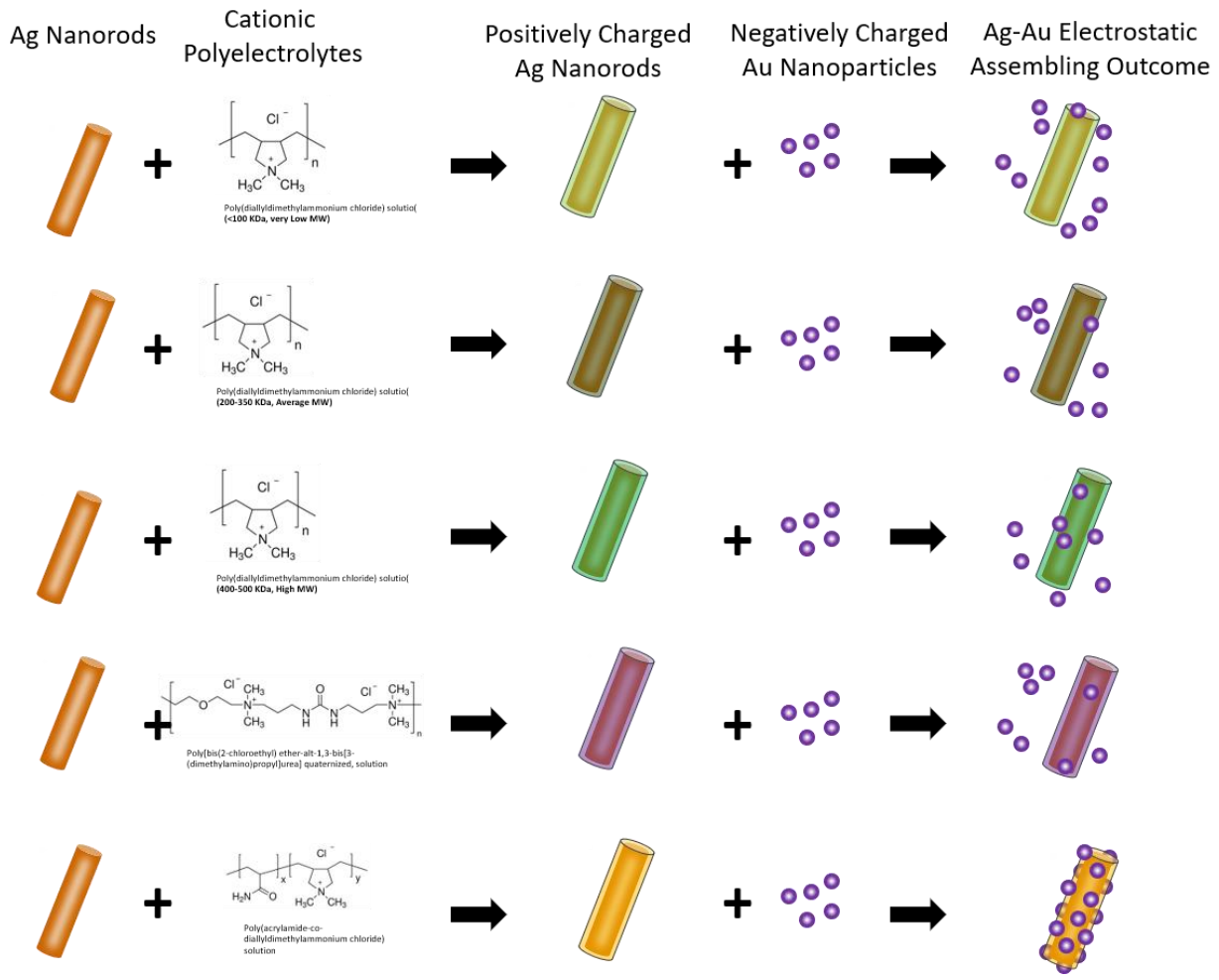

Supplementary Figure S40: Electrostatic nanoassembling of metal nanoparticles after the application of various polyelectrolytes on the surface. Electrostatic assembling scheme between silver nanorods and gold nanoparticles in which only PAA-co-PDADMAC shows strong and homogeneous assembling in a reproducible manner. Modifications with other polyelectrolytes create a positively charged silver nanorod surface but do not initiate electrostatic interaction with anionic gold nanoparticles at all.

The obtained results of the plasmonic nanoassembling structures with surface modification with five different polyelectrolytes are shown in five Tables below with details of the reaction conditions.

Supplementary Table S29: Yield of Au-Ag electrostatic assembling when PolyDADMAC (<100,000 MW) was used for the surface modification of the Ag nanorods.

Product	**Au-Ag Assembly did not realize**	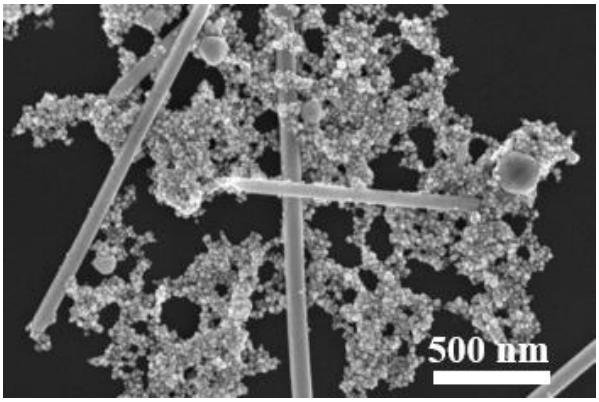
Yield Approx. %	< 5 %	
Homogeneity	Electrostatic assembly NOT happening.	
Best Ag:Au Ratio for homogeneous assembling	• 1:2 solution ratio of Ag nanorods:Au nanoparticles • No assembling was realized	
Polyelectrolyte	PolyDADMAC <100,000 MW	
Concentration of Polyelectrolyte	0.8 Volume %	
Note	Even after extended stirring for 24 hours, the assembling reaction between citrate-capped negatively charged gold nanoparticles and polyDADMAC (<100,000 molecular weight)-functionalized silver nanorods did not materialize.	

Supplementary Table S30: Yield of Au-Ag electrostatic assembling when PolyDADMAC (200,000-350,000 MW) was used for the surface modification of the Ag nanorods.

Product	**Au-Ag Assembly did not realize**	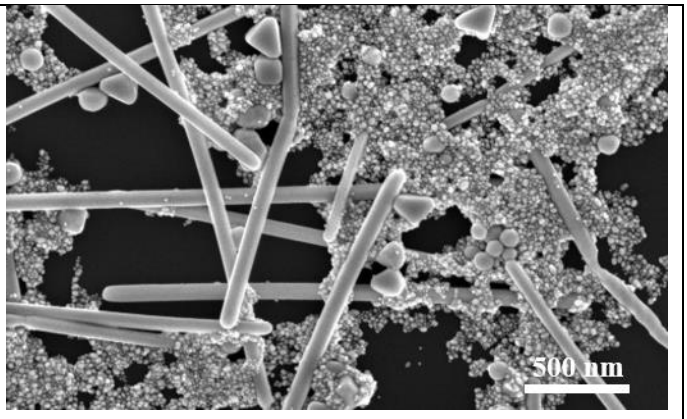
Yield Approx. %	< 5 %	
Homogeneity	Electrostatic assembly NOT happening.	
Best Ag:Au Ratio for homogeneous assembling	• 1:2 solution ratio of Ag nanorods:Au nanoparticles • No assembling realized	
Polyelectrolyte	PolyDADMAC 200,000-350,000 MW	
Concentration of Polyelectrolyte	0.8 Volume %	
Note	Even after extended stirring for 24 hours, the assembling reaction between citrate-capped negatively charged gold nanoparticles and polyDADMAC (200,000-300,000 molecular weight)-functionalized silver nanorods did not materialize.	

Supplementary Table S31: Yield of Au-Ag electrostatic assembling when PolyDADMAC (400,000-500,000 MW) was used for the surface modification of the Ag nanorods.

Product	**Au-Ag Assembly did not realize**	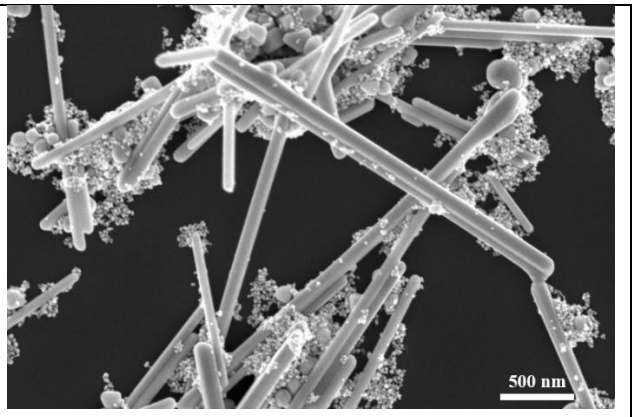
Yield Approx. %	< 5 %	
Homogeneity	Electrostatic assembly NOT happening.	
Best Ag:Au Ratio for homogeneous assembling	• 1:2 solution ratio of Ag nanorods:Au nanoparticles • No assembling realized	
Polyelectrolyte	PolyDADMAC 400,000-500,000 MW	
Concentration of Polyelectrolyte	0.8 Volume %	
Note	Even after extended stirring for 24 hours, the assembling reaction between citrate-capped negatively charged gold nanoparticles and polyDADMAC (400,000-500,000 molecular weight)-functionalized silver nanorods did not materialize.	

Supplementary Table S32: Yield of Au-Ag electrostatic assembling when Poly[bis(2-chloroethyl) ether-alt-1,3-bis[3-(dimethylamino)propyl]urea] quaternized solution was used for the surface modification of the Ag nanorods.

Product	**Au-Ag Assembly did not realize**	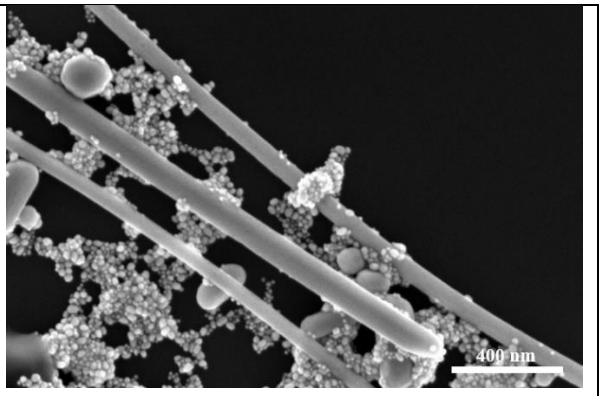
Yield Approx. %	< 5 %	
Homogeneity	Electrostatic assembly NOT happening.	
Best Ag:Au Ratio for homogeneous assembling	1:2 solution ratio of Ag nanorods:Au Nanoparticles No assembling was obtained.	
Polyelectrolyte	Poly[bis(2-chloroethyl) ether-alt-1,3-bis[3-(dimethylamino)propyl]urea] quaternized, solution	
Concentration of Polyelectrolyte	0.8 Volume %	
Note	Even after extended stirring for 24 hours, the assembling reaction between citrate-capped negatively charged gold nanoparticles and Poly[bis(2-chloroethyl) ether-alt-1,3-bis[3-(dimethylamino)propyl]urea] quaternized-functionalized silver nanorods did not materialize.	

Supplementary Table S33: Yield of Au-Ag electrostatic assembling when poly(acrylamide-co-diallyldimethylammonium chloride) (P(AAm-co-DADMAC)) was used for the surface modification of the Ag nanorods.

Product	**Au-Ag Assembly**	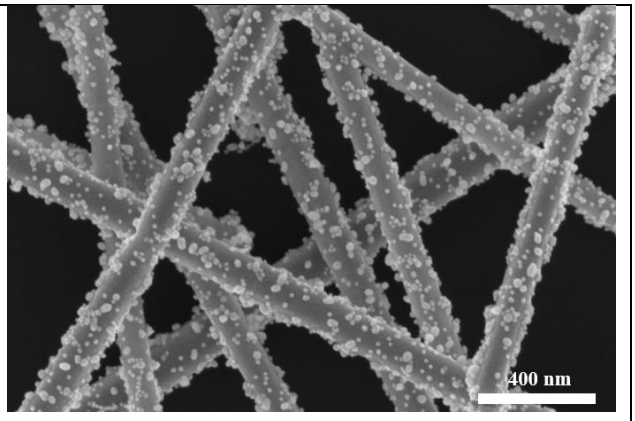
Yield Approx. %	~ 100 %	
Homogeneity	Systematically distributed Au nanoparticles on Ag rods without any coagulation were observed	
Best Ag:Au Ratio for homogeneous assembling	1:2 solution ratio of Ag nanorods:Au Nanoparticles	
Polyelectrolyte	poly(acrylamide-co-diallyldimethylammonium chloride) (P(AAm-co-DADMAC))	
Concentration of Polyelectrolyte	0.8 Volume %	
Note	The systematic Au-Ag nanoaseembly was obtained in a short stirring of 22 minutes when silver nanorods were functionalized with poly(acrylamide-co-diallyldimethylammonium chloride) (P(AAm-co-DADMAC)).	

After the successful silver-gold nanoassembly, the ligand-free silver layer has been applied on the surface of the nanoassembly. The overall results are shown in SEM images in **Supplementary Figure S42.**

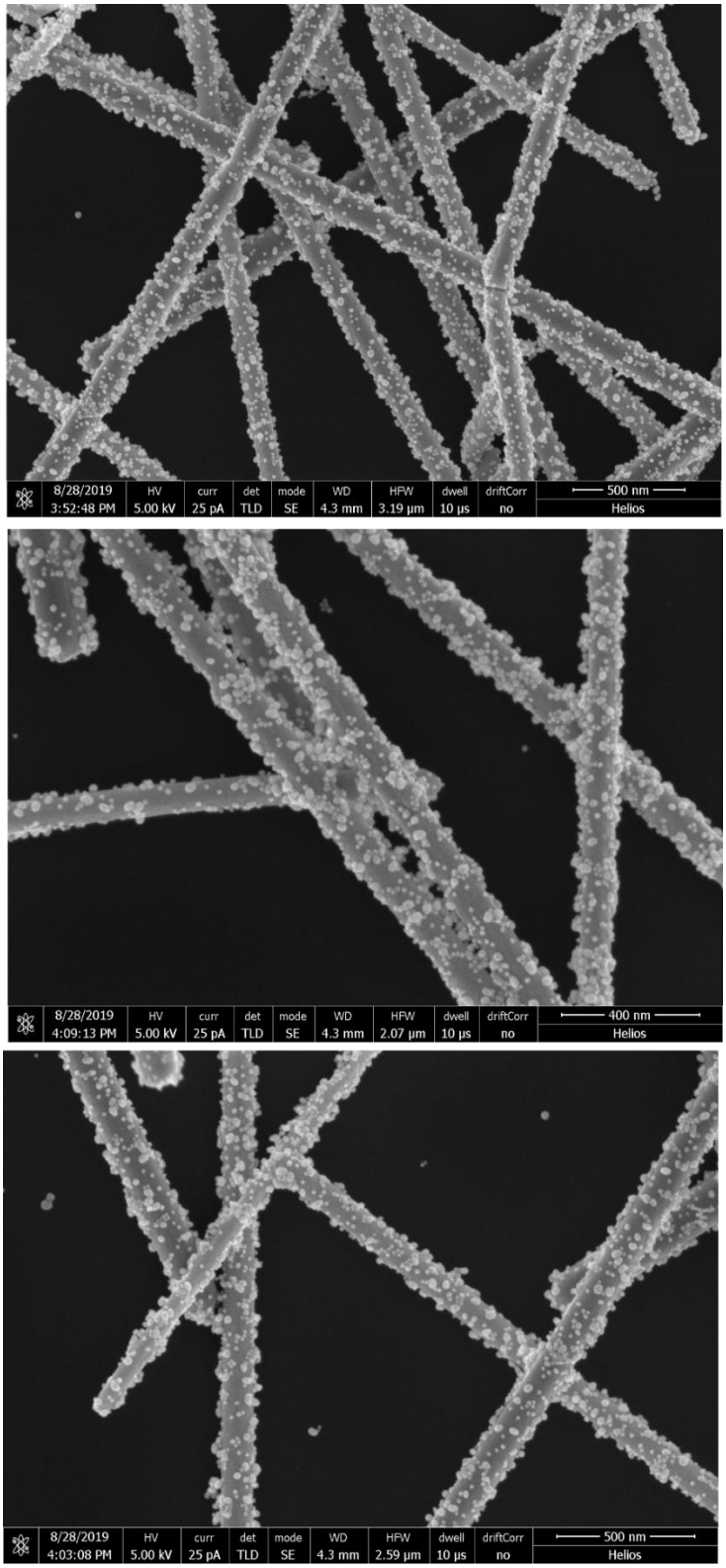

Supplementary Figure S41: Electrostatic nanoassembling of gold nanoparticles/silver nanorods. Three different SEM images of the same sample of silver-gold nanoassembling structures where silver rods were first functionalized with cationic poly(AAm-co-DADMAC) and subsequently assembled with anionic gold nanoparticles.

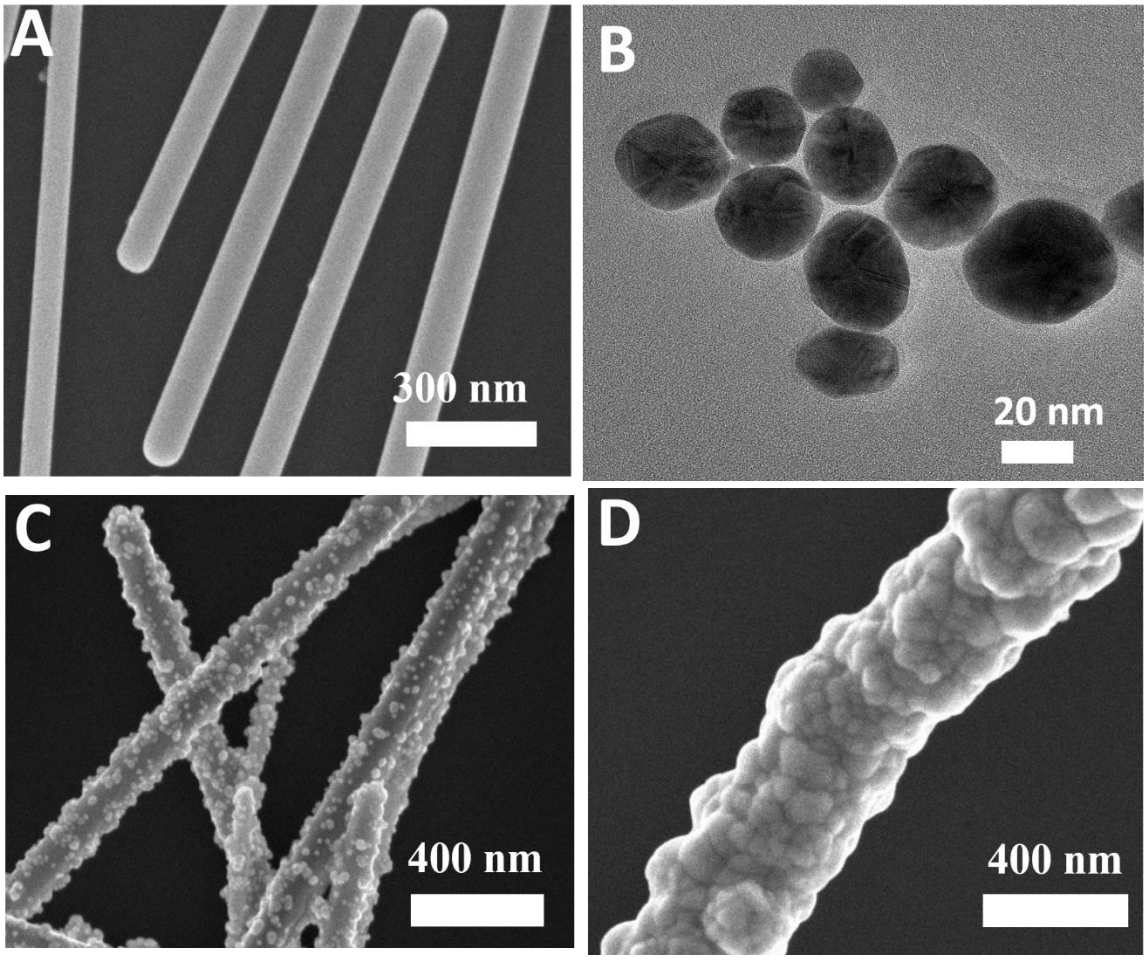

Supplementary Figure S42: Electrostatic nanoassembling of gold nanoparticles/silver nanorods and their ligand-free surface. (A-D) metal-catalyzed metal deposition reaction on the nanoassembling structures for obtaining a ligand-free outer surface: SEM images of (A) pure silver rods obtained by using 0.02 M sucrose as a reducing agent in 1,3-propanediol-based polyol synthesis, (B) citrate-capped gold nanoparticles, (C) silver-gold nanoassembling structures where silver rods were first functionalized with cationic poly(AAm-co-DADMAC) and subsequently assembled with anionic gold nanoparticles, and (D) ligand-free metal layer deposition on the silver-gold nanoassembling structure *via* metal-catalyzed metal deposition process.

10. References

1 Gao, Y. *et al.* Growth mechanism of silver nanowires synthesized by polyvinylpyrrolidone-assisted polyol reduction. *J. Phys. D-Appl. Phys.* **38**, 1061-1067 (2005).

2 Molleman, B. & Hiemstra, T. Size and shape dependency of the surface energy of metallic nanoparticles: unifying the atomic and thermodynamic approaches. *Physical Chemistry Chemical Physics* **20**, 20575-20587 (2018).

3 Koczkur, K. M., Mourdikoudis, S., Polavarapu, L. & Skrabalak, S. E. Polyvinylpyrrolidone (PVP) in nanoparticle synthesis. *Dalton Transactions* **44**, 17883-17905 (2015).

4 Al-Johani, H. *et al.* The structure and binding mode of citrate in the stabilization of gold nanoparticles. *Nature Chemistry* **9**, 890-895 (2017).

5 Heuer-Jungemann, A. *et al.* The Role of Ligands in the Chemical Synthesis and Applications of Inorganic Nanoparticles. *Chemical Reviews* **119**, 4819-4880 (2019).

6 Herricks, T., Chen, J. & Xia, Y. Polyol Synthesis of Platinum Nanoparticles: Control of Morphology with Sodium Nitrate. *Nano Letters* **4**, 2367-2371 (2004).

7 Wiley, B., Herricks, T., Sun, Y. & Xia, Y. Polyol Synthesis of Silver Nanoparticles: Use of Chloride and Oxygen to Promote the Formation of Single-Crystal, Truncated Cubes and Tetrahedrons. *Nano Letters* **4**, 1733-1739 (2004).

8 Cho, G., Park, Y., Hong, Y.-K. & Ha, D.-H. Ion exchange: an advanced synthetic method for complex nanoparticles. *Nano Convergence* **6**, 17 (2019).

9 Barrow, S. J., Wei, X., Baldauf, J. S., Funston, A. M. & Mulvaney, P. The surface plasmon modes of self-assembled gold nanocrystals. *Nature Communications* **3**, 1275 (2012).

10 Deng, D. *et al.* Catalysis with two-dimensional materials and their heterostructures. *Nature Nanotechnology* **11**, 218 (2016).

11 Fan, J. A. *et al.* Self-Assembled Plasmonic Nanoparticle Clusters. *Science* **328**, 1135-1138 (2010).

12 Li, J. *et al.* Hierarchical Assembly of Plasmonic Nanoparticle Heterodimer Arrays with Tunable Sub-5 nm Nanogaps. *Nano Letters* **19**, 4314-4320 (2019).

13 Nie, Z., Petukhova, A. & Kumacheva, E. Properties and emerging applications of self-assembled structures made from inorganic nanoparticles. *Nature Nanotechnology* **5**, 15-25 (2010).

14 Yu, H., Peng, Y., Yang, Y. & Li, Z.-Y. Plasmon-enhanced light–matter interactions and applications. *npj Computational Materials* **5**, 45 (2019).

15 Kimling, J. *et al.* Turkevich Method for Gold Nanoparticle Synthesis Revisited. *The Journal of Physical Chemistry B* **110**, 15700-15707 (2006).

REFERENCES

1. Halas, N.J., Lal, S., Chang, W.-S., Link, S. & Nordlander, P. Plasmons in Strongly Coupled Metallic Nanostructures. *Chem. Rev.* **111**, 3913-3961 (2011).
2. Li, J. et al. Hierarchical Assembly of Plasmonic Nanoparticle Heterodimer Arrays with Tunable Sub-5 nm Nanogaps. *Nano Lett.* **19**, 4314-4320 (2019).
3. Wu, X. et al. Environmentally responsive plasmonic nanoassemblies for biosensing. *Chem. Soc. Rev.* **47**, 4677-4696 (2018).
4. Yu, H., Peng, Y., Yang, Y. & Li, Z.-Y. Plasmon-enhanced light–matter interactions and applications. *Npj Comput. Mater.* **5**, 45 (2019).
5. Anker, J.N. et al. Biosensing with plasmonic nanosensors. *Nat. Mater.* **7**, 442-453 (2008).
6. Xia, Y., Xiong, Y., Lim, B. & Skrabalak, S.E. Shape-Controlled Synthesis of Metal Nanocrystals: Simple Chemistry Meets Complex Physics? *Angew. Chem. Int. Ed.* **48**, 60-103 (2009).
7. Seeman, N.C. & Sleiman, H.F. DNA nanotechnology. *Nat. Rev. Mater.* **3**, 17068 (2017).
8. Edwardson, T.G.W., Lau, K.L., Bousmail, D., Serpell, C.J. & Sleiman, H.F. Transfer of molecular recognition information from DNA nanostructures to gold nanoparticles. *Nat. Chem.* **8**, 162-170 (2016).
9. Yao, G. et al. Programming nanoparticle valence bonds with single-stranded DNA encoders. *Nat. Mater.* **19**, 781-788 (2020).
10. Fan, J.A. et al. Self-Assembled Plasmonic Nanoparticle Clusters. *Science* **328**, 1135-1138 (2010).
11. Molleman, B. & Hiemstra, T. Size and shape dependency of the surface energy of metallic nanoparticles: unifying the atomic and thermodynamic approaches. *Phys. Chem. Chem. Phys.* **20**, 20575-20587 (2018).
12. Ha, M. et al. Multicomponent Plasmonic Nanoparticles: From Heterostructured Nanoparticles to Colloidal Composite Nanostructures. *Chem. Rev.* **119**, 12208-12278 (2019).
13. Schirato, A. et al. Transient optical symmetry breaking for ultrafast broadband dichroism in plasmonic metasurfaces. *Nat. Photonics* **14**, 723-727 (2020).
14. Tan, S.J., Campolongo, M.J., Luo, D. & Cheng, W. Building plasmonic nanostructures with DNA. *Nat. Nanotechnol.* **6**, 268-276 (2011).
15. Aldaye, F.A. & Sleiman, H.F. Sequential Self-Assembly of a DNA Hexagon as a Template for the Organization of Gold Nanoparticles. *Angew. Chem. Int. Ed.* **45**, 2204-2209 (2006).
16. Sun, S. et al. Valence-programmable nanoparticle architectures. *Nat. Commun.* **11**, 2279 (2020).
17. Zhang, H., Kinnear, C. & Mulvaney, P. Fabrication of Single-Nanocrystal Arrays. *Adv. Mater.* **32**, 1904551 (2020).
18. Lin, Q.-Y. et al. Building superlattices from individual nanoparticles via template-confined DNA-mediated assembly. *Science* **359**, 669-672 (2018).
19. Fan, J.A. et al. DNA-Enabled Self-Assembly of Plasmonic Nanoclusters. *Nano Lett.* **11**, 4859-4864 (2011).
20. Eisele, D.M. et al. Utilizing redox-chemistry to elucidate the nature of exciton transitions in supramolecular dye nanotubes. *Nat. Chem.* **4**, 655-62 (2012).

21. Ng, K. et al. Frenkel excitons in heat-stressed supramolecular nanocomposites enabled by tunable cage-like scaffolding. *Nat. Chem.* **12**, 1157-1164 (2020).

22. Grommet, A.B., Feller, M. & Klajn, R. Chemical reactivity under nanoconfinement. *Nat. Nanotechnol.* **15**, 256-271 (2020).

23. Du, J.S. et al. Galvanic Transformation Dynamics in Heterostructured Nanoparticles. *Adv. Funct. Mater.* **31**, 2105866 (2021).

24. Fiévet, F. et al. The polyol process: a unique method for easy access to metal nanoparticles with tailored sizes, shapes and compositions. *Chem. Soc. Rev.* **47**, 5187-5233 (2018).

25. Sun, Y.G., Yin, Y.D., Mayers, B.T., Herricks, T. & Xia, Y.N. Uniform silver nanowires synthesis by reducing AgNO3 with ethylene glycol in the presence of seeds and poly(vinyl pyrrolidone). *Chem. Mater.***14**, 4736-4745 (2002).

26. Lu, F. et al. Unusual packing of soft-shelled nanocubes. *Sci. Adv.* **5**, eaaw2399 (2019).

27. Li, Q. et al. Structural distortion and electron redistribution in dual-emitting gold nanoclusters. *Nat. Commun.* **11**, 2897 (2020).

28. Hendricks, M.P., Campos, M.P., Cleveland, G.T., Jen-La Plante, I. & Owen, J.S. NANOMATERIALS. A tunable library of substituted thiourea precursors to metal sulfide nanocrystals. *Science* **348**, 1226-30 (2015).

29. Jayant, K. et al. Targeted intracellular voltage recordings from dendritic spines using quantum-dot-coated nanopipettes. *Nat. Nanotechnol.* **12**, 335-342 (2017).

30. Zhou, L. et al. Hot carrier multiplication in plasmonic photocatalysis. *Proc. Natl. Acad. Sci.* **118**, e2022109118 (2021).

31. Dong, H., Chen, Y.C. & Feldmann, C. Polyol synthesis of nanoparticles: status and options regarding metals, oxides, chalcogenides, and non-metal elements. *Green Chem.* **17**, 4107-4132 (2015).

32. Biacchi, A.J. & Schaak, R.E. The Solvent Matters: Kinetic versus Thermodynamic Shape Control in the Polyol Synthesis of Rhodium Nanoparticles. *ACS Nano* **5**, 8089-8099 (2011).

33. Ducrot, É., He, M., Yi, G.-R. & Pine, D.J. Colloidal alloys with preassembled clusters and spheres. *Nat. Mater.* **16**, 652-657 (2017).

34. Liu, M. et al. Two-Dimensional (2D) or Quasi-2D Superstructures from DNA-Coated Colloidal Particles. *Angew. Chem. Int. Ed.* **60**, 5744-5748 (2021).

35. Wang, S. et al. The emergence of valency in colloidal crystals through electron equivalents. *Nat. Mater.* (2022) doi.org/10.1038/s41563-021-01170-5.

36. Nagaoka, Y. et al. Superstructures generated from truncated tetrahedral quantum dots. *Nature* **561**, 378-382 (2018).

37. Liz-Marzán, L.M. & Grzelczak, M. Growing anisotropic crystals at the nanoscale. *Science* **356**, 1120-1121 (2017).

38. Wu, Z., Yang, S. & Wu, W. Shape control of inorganic nanoparticles from solution. *Nanoscale* **8**, 1237-1259 (2016).

39. Chen, Z., Balankura, T., Fichthorn, K.A. & Rioux, R.M. Revisiting the Polyol Synthesis of Silver Nanostructures: Role of Chloride in Nanocube Formation. *ACS Nano* **13**, 1849-1860 (2019).

40. Heuer-Jungemann, A. et al. The Role of Ligands in the Chemical Synthesis and Applications of Inorganic Nanoparticles. *Chem. Rev.* **119**, 4819-4880 (2019).

41. Koczkur, K.M., Mourdikoudis, S., Polavarapu, L. & Skrabalak, S.E. Polyvinylpyrrolidone (PVP) in nanoparticle synthesis. *Dalton Trans.* **44**, 17883-17905 (2015).

42. Al-Johani, H. et al. The structure and binding mode of citrate in the stabilization of gold nanoparticles. *Nat. Chem.* **9**, 890-895 (2017).

43. Nie, Z., Petukhova, A. & Kumacheva, E. Properties and emerging applications of self-assembled structures made from inorganic nanoparticles. *Nat. Nanotechnol.* **5**, 15-25 (2010).

44. Reinhard, I., Miller, K., Diepenheim, G., Cantrell, K. & Hall, W.P. Nanoparticle Design Rules for Colorimetric Plasmonic Sensors. *ACS Appl. Nano Mater.* **3**, 4342-4350 (2020).

45. Howes, P.D., Chandrawati, R. & Stevens, M.M. Colloidal nanoparticles as advanced biological sensors. *Science* **346** (2014).

46. Decher, G. Fuzzy nanoassemblies: Toward layered polymeric multicomposites. *Science* **277**, 1232-1237 (1997).

47. Budy, S.M., Hamilton, D.J., Cai, Y., Knowles, M.K. & Reed, S.M. Polymer mediated layer-by-layer assembly of different shaped gold nanoparticles. *J. Colloid Interface Sci.* **487**, 336-347 (2017).

48. Zhang, Y., Lu, F., Yager, K.G., van der Lelie, D. & Gang, O. A general strategy for the DNA-mediated self-assembly of functional nanoparticles into heterogeneous systems. *Nat. Nanotechnol.* **8**, 865-72 (2013).

49. Tian, Y. et al. Ordered three-dimensional nanomaterials using DNA-prescribed and valence-controlled material voxels. *Nat. Mater.* **19**, 789-796 (2020).

50. Kimling, J. et al. Turkevich Method for Gold Nanoparticle Synthesis Revisited. *J. Phys. Chem. B* **110**, 15700-15707 (2006).